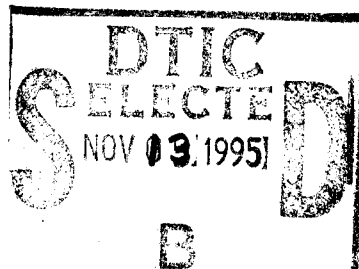
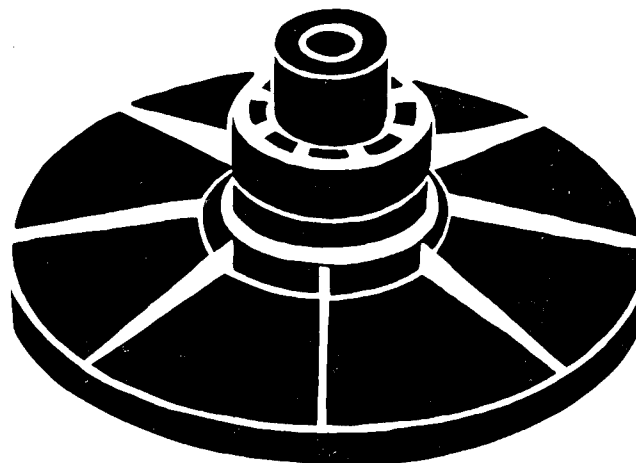


Proceedings of the 1975 Flywheel Technology Symposium



19951107 117



DTIC QUALITY INSPECTED 5

LAWRENCE HALL OF SCIENCE
BERKELEY, CALIFORNIA
NOV. 10-12, 1975

DEPARTMENT OF DEFENSE
PLASTICS TECHNICAL EVALUATION CENTER
PICATINNY ARSENAL, DOVER, N. J.



DISTRIBUTION STATEMENT A

Approved for public release;
Distribution Unlimited

**LAWRENCE
LIVERMORE
LABORATORY**
University of California - Livermore

PLASTICS

NOTICE

This report was prepared as an account of work sponsored by the United States Government. Neither the United States nor the United States Energy Research and Development Administration, nor any of their employees, nor any of their contractors, subcontractors, or their employees, makes any warranty, express or implied, or assumes any legal liability or responsibility for the accuracy, completeness or usefulness of any information, apparatus, product or process disclosed, or represents that its use would not infringe privately owned rights.

*MSG DI4 DROLS PROCESSING-LAST INPUT IGNORED

-- 6 OF 12

OTIC DOES NOT HAVE THIS ITEM

-- 1 - AD NUMBER: D422603
-- 5 - CORPORATE AUTHOR: CALIFORNIA UNIV LIVERMORE LAWRENCE LIVERMORE LAB
-- 6 - UNCLASSIFIED TITLE: 1975 FLYWHEEL TECHNOLOGY SYMPOSIUM,
--10 - PERSONAL AUTHORS: CHANG, G. C.; STONE, R. G.;
--11 - REPORT DATE: NOV 10, 1975
--12 - PAGINATION: 238P
--14 - REPORT NUMBER: ERDA 76-85, UC948
--20 - REPORT CLASSIFICATION: UNCLASSIFIED
--21 - SUPPLEMENTARY NOTE: PROCEEDINGS: '1975 FLYWHEEL TECHNOLOGY
-- SYMPOSIUM', HELD 10-12 NOV 75, BERKELEY, CALIF. SPONSORED BY
-- ENERGY RESEARCH AND DEVELOPMENT ADMINISTRATION AND LAWRENCE
-- LIVERMORE LABORATORY. (SEE PL-26204 - PL-26217).
--22 - LIMITATIONS (ALPHA): APPROVED FOR PUBLIC RELEASE; DISTRIBUTION
-- UNLIMITED. ~~AVAILABILITY: SUPERINTENDENT OF DOCUMENTS, U.S.~~
-- ~~GOVERNMENT PRINTING OFFICE, WASHINGTON, D. C. 20540.~~
--33 - LIMITATION CODES: 1

-- END Y FOR NEXT ACCESSION END

Alt-Z FOR HELP3 ANSI 3 HDX 3 3 LOG CLOSED 3 PRINT OFF 3 PARITY

UC 94b

PROCEEDINGS

1975 FLYWHEEL TECHNOLOGY SYMPOSIUM

Co-Chairmen & Editors

G. C. Chang - U.S. Energy Research & Development Administration

R. G. Stone - Lawrence Livermore Laboratory

Program Chairman

T. T. Chiao - Lawrence Livermore Laboratory

Local Arrangements

J. A. Rinde, LLL
 R. L. Moore, LLL
 C. F. Miller, LLL
 J. E. Jens, LLL
 S. A. Busey, LLL

Lawrence Hall of Science
 Berkeley, California

November 10-12, 1975

DTIC QUALITY INSPECTED 5

Accession For	
NTIS GRA&I	<input checked="" type="checkbox"/>
DTIC TAB	<input type="checkbox"/>
Unannounced	<input type="checkbox"/>
Justification	<i>per</i>
<i>Printed and used</i>	
<i>DTIC memo,</i>	
<i>By 2 Nov 75</i>	
Distribution/	
Availability Codes	
Dist	Avail and/or Special
<i>A-1</i>	

TABLE OF CONTENTS

	Page
FOREWORD G. C. Chang and R. G. Stone	1
WELCOME TO THE SYMPOSIUM K. Street	2
KEYNOTE ADDRESS G. F. Pezdirtz	3
FLYWHEEL SYSTEMS APPLICATIONS J. E. Notti, Jr.	16
ALL-SERVICE ELECTRIC TRANSIT VEHICLE J. F. Campbell	18
POSTAL VEHICLE MISSIONS T. Norman	26
THE BROAD RANGE OF FLYWHEEL APPLICATIONS D. W. Rabenhorst	34
SYSTEMS ASPECTS OF ENERGY WHEELS E. W. Sclieben	40
PROGRAM FOR COMPOSITE FLYWHEELS T. T. Chiao and R. G. Stone	53
DESIGN, CONSTRUCTION AND TESTING OF ADVANCED COMPOSITE FLYWHEELS AT THE U.S. NAVAL ACADEMY R. A. McCoy	56
KEVLAR/EPOXY FLYWHEELS: AN EXPERIMENTAL STUDY M. Moss and F. P. Gerstle, Jr.	59
GARRETT'S OUTLOOK ON VEHICLE FLYWHEELS J. A. Friedericy and A. E. Raynard	62
IMPROVED FUEL ECONOMY IN AUTOMOBILES BY USE OF A FLYWHEEL ENERGY MANAGEMENT SYSTEM A. A. Frank and N. Beachley	76
POLAR WEAVE COMPOSITE FLYWHEELS A. M. Garber	89
BEARING AND ELECTRICAL INPUT-OUTPUT FOR FLYWHEEL ENERGY STORAGE SYSTEMS A. F. Veneruso	91
DESIGN AND TEST OF A SPACECRAFT ENERGY MOMENTUM FLYWHEEL J. E. Notti, Jr.	105

	Page
FLYWHEEL-POWERED AUTOMOBILES P. M. Newgard	106
RIM-SPOKE COMPOSITE FLYWHEELS: DETAILED STRESS VIBRATION ANALYSIS C. C. Chamis and L. J. Kiraly	26204 110
THE USA-MERDC HIGH ENERGY STORAGE HOMOGENEOUS FLYWHEEL MODULE D. E. Davis	117
IDEAS AND EXPERIMENTS IN MAGNETIC INTERFACING K. Aaland and J. E. Lane	123
APPROACH TO FLYWHEEL DEVELOPMENT G. B. Andeen	26205 133
ON EFFECTIVE USE OF FILAMENTARY COMPOSITES IN FLYWHEELS F. P. Gerstle, Jr. and F. Biggs	146
FIBER EVALUATION FOR FLYWHEEL APPLICATIONS L. Penn and T. T. Chiao	26206 151
EPOXY RESINS FOR FLYWHEEL APPLICATIONS J. A. Rinde	26207 153
STRESS REDISTRIBUTION DUE TO RADIAL DISPLACEMENTS AND ITS EFFECTS ON ENERGY STORAGE CAPABILITY E. J. Brunelle	157
LONG-TERM PERFORMANCE OF FIBER COMPOSITES C. C. Chiao	26208 160
POTENTIAL MERITS OF THERMOPLASTIC COMPOSITE MATERIALS FOR MODULAR RIM FLYWHEELS J. H. Laakso	26209 164
ENGINEERING PROPERTIES OF ELASTOMER/ADVANCED COMPOSITE LAMINAR STRUCTURES A. F. Lewis and R. T. Natarajan	185
MECHANICAL PROPERTIES OF COMPOSITES T. J. Reinhart, Jr.	194
MOMENTUM WHEELS R. Torossian	195
FIBER GLASS FOR COMPOSITE FLYWHEELS S. N. Loud	26210 198
"SCOTCHPLY" PREPREGS FOR FLYWHEEL APPLICATIONS J. B. Snell and J. N. Schurb	26211 203

POTENTIAL ADVANTAGES OF KEVLAR ^R 49 IN FLYWHEEL APPLICATIONS D. L. G. Sturgeon	26212	210
ENGINEERING DESIGN DATA FOR COMPOSITE MATERIALS L. L. Clements	26213	229
FRACTURE MECHANICS ASPECTS OF FILAMENTARY COMPOSITE FLYWHEELS G. A. Vroman	26214	234
TRANSFER MATRIX ANALYSIS OF COMPOSITE FLYWHEELS WITH RELIABILITY APPLICATIONS R. H. Toland	26215	243
HYBRID CAR PROJECT BY LEMMENS ENTERPRISES J. Lemmens		257
FABRICATION AND THERMAL STRESS IN COMPOSITE FLYWHEELS R. C. Reuter, Jr.	26216	261
DESIGN AND MANUFACTURING CONSIDERATIONS FOR COMPOSITE FLYWHEELS W. E. Dick	26217	276
PANEL DISCUSSION		288
LIST OF ATTENDEES AND SPEAKERS		289

PROCEEDINGS
1975 FLYWHEEL TECHNOLOGY SYMPOSIUM

FORWORD

Although flywheels, such as the potter's wheel can be dated back several thousand years, there has been a great resurgence of interest recently in the flywheel as an energy storage mechanism. The reasons are both economic and technological -- economic because the growing costs and potential scarcity of energy have increased the importance of energy storage as a conservation measure, and technological because improvements in materials and mechanics make flywheel energy storage more and more attractive.

The United State Energy Research and Development Administration in its Office of Conservation is responsible for research and development promoting energy storage systems in the national interest. To this end a gathering of leaders in flywheel technology from industry, government and universities was conceived. Thus, the Energy Research and Development Administration and the Lawrence Livermore Laboratory sponsored the 1975 Flywheel Technology Symposium at Lawrence Hall of Science, Berkeley, California, November 10-12, 1975. The Symposium was designed as a forum where these leaders of flywheel technology and research could exchange information and ideas on advances, potential applications, and research needs of the flywheel technology. The symposium was also designed to provide a seminar at which interested people could update their understanding of flywheels.

The Symposium was expected to be quite informal, and no written papers were requested. However, there has been such widespread interest in the Symposium that we decided to prepare this Proceedings. It is a compilation of the papers and summaries submitted by the speakers, presented in the order of the program.

WELCOME TO THE SYMPOSIUM

Kenneth Street, Jr.
Associate Director for Energy Programs
Lawrence Livermore Laboratory

It is a great pleasure to welcome you to the 1975 Flywheel Technology Symposium sponsored by the Lawrence Livermore Laboratory of the University of California for the U. S. Energy Research and Development Administration. We hope that you will find the program both informative and enjoyable.

This symposium is a historical first. It is the first time that researchers and engineers working with flywheels have come together specifically for the purpose of presenting their results, exchanging information and talking about the future. Let us hope that this will be the first of many such gatherings.

The titles of the more than thirty papers on the program cover a wide range of subjects. Some papers will discuss the testing of new design flywheels. Others will present information about the properties of materials of construction and suggest ways of using these materials in flywheels. Still other papers will tell us how to select flywheel design criteria and how to fit flywheels into their total environment. And the voices of some who use the end products containing flywheels will also be heard.

We here owe a very great debt to George Chang and Richard Stone, symposium committee co-chairmen; to T. T. Chiao and to other members of the committee who shared the task of organizing this symposium.

We hope that your visit here will be both pleasant and profitable and that you will return home stimulated by the progress being made in the field of flywheel energy storage.

Keynote Address
of
Dr. George F. Pezdirtz
for
Office of Conservation
U.S. ERDA
before
The 1975 Flywheel Technology Conference
Sponsored by U.S. ERDA
Coordinated by Lawrence Livermore Laboratory
Berkeley, California

November 10, 1975

It gives me a great deal of pleasure to give an overview of the 1975 Flywheel Technology Conference. I am especially pleased in that this is the first meeting of its kind and is thus bringing together many experts in the field for a very meaningful discussion. Because of the tremendous potential for the utilization of flywheel energy storage systems and the development necessary prior to their use, I would like to suggest that you all have before you great opportunities as well as challenges in the years to come.

I would like to take the next few minutes to acquaint you with the outline of this address. I will begin with a brief discussion of the purpose of this conference and how it and flywheel storage in general fit into the overall mission of ERDA. It will be profitable to spend time here to convey to you the ERDA philosophy of the flywheel energy storage program. We have several questions here. What potential applications do we see? What benefits do we see in those applications? What is the current state of flywheel technology? Finally, what are ERDA's near term goals for developing this technology?

I hope to answer those questions to your satisfaction this morning. In addition, I will provide a brief history of flywheel utilization from Biblical times to the present. This will lead to a discussion of the current government programs in this area including those sponsored by ERDA. Finally, I would like to present our point of view on the research and development necessary to implement the use of flywheel energy storage systems as conservation measures in critical applications.

Purpose of Conference

First, I would like to briefly touch upon the purpose of this conference.

This conference could be properly called the First National Flywheel Technology Conference. We have invited leading industry, research laboratory, and university contributors to the concept of flywheel energy storage systems to discuss and evaluate the state-of-the-art of this concept, and to peek into the future to examine the promise of the concept to energy conservation. It is, in essence, and open forum for review of the state-of-the-art of flywheels and an evaluation of possible benefits.

We are also using this conference to publicize research funded by ERDA. Other government research efforts will also be highlighted. We wish to obtain the maximum return from our projects by maximizing the exposure of our studies. ERDA has several projects in the flywheel energy storage area and has established a program for further development of flywheels. By publicizing our activity, we hope to provide a stimulus to the industry efforts in this area. We want to make certain that our plan for future activities in the area of flywheel energy storage systems is correct with respect to: What ERDA goals should be? What can industry do? How much research and development is necessary? What the best government and industry approach which lead ultimately to demonstration and utilization of the concept should be? In fact, this is one technology in which ERDA is truly interested in "re-inventing the wheel" - the energy flywheel built with advanced technology.

ERDA Mission

Before discussing our program in flywheel energy storage, I would like to make a few general remarks on the mission of ERDA.

ERDA was created to bring together into a single federal agency the major energy research and development programs aimed at determining means of conserving current sources of energy, finding ways of optimizing the utilization of these sources, examining methods for increasing the supply of present sources, and developing new sources of energy. To effect this, ERDA's mission is to speed-up the advance of state-of-the-art technology in all promising energy areas. The basic objective is to develop and demonstrate a broad spectrum of promising technologies as early as possible through accelerated evolutionary growth, conceptual breakthroughs, and comprehensive planning.

ERDA has been chartered by Congress to use science and technology to make vital and fundamental contributions to the energy needs of both the present and the future, and to make the nation energy self-sufficient. At the same time, ERDA will strive to protect and enhance the environment, and assure public health and safety.

Due to the long range nature of producing new energy technologies, ERDA's only near-term option is energy conservation. We consider conservation research and development as that which leads to more efficient use of energy, use of alternate, less critical, less expensive sources of energy, and more efficient use of capital and other variables within our energy systems.

Within conservation, one of the essential elements is energy storage systems. Energy storage is a key concept of efficient energy

utilization. Large scale use of energy storage systems will save the nation hundreds of millions of barrels of oil annually and will result in direct savings for the consumer.

A number of energy storage technologies have evolved, albeit slowly, through the years. ERDA's goal is to accelerate the development of these technologies for demonstration in the near-term. One specific concept, which shows a tremendous potential and one which has been known and used for several thousand years, is flywheel energy storage. The use of flywheel energy storage technology could contribute significantly to energy conservation. Our direction is to bring into realization this concept as soon as it is technically and economically possible. To bring this about, we have established goals and programs in flywheel energy storage.

Goals and Programs in Flywheel Energy Storage

The research programs in flywheel energy storage are part of broadly scoped programs in conservation research and technology that are directed to advancing technology applicable to several applications sectors. Continued advancements in flywheel technology are expected to provide benefits in at least four sectors -- electric power utilities, industries, buildings and transportation.

The particular benefits expected from the accomplishment of this program support two of the major goals of the ERDA National Plan for RD&D. The goals are:

- Increase the efficiency and reliability of the processes used in energy conversion and delivery systems;
- Transform consumptive patterns to improve energy use;

These goals are supported by a corresponding ERDA plan to develop and demonstrate technology for energy storage applications, to increase capital efficiency in energy generation, and to effect the use of alternate energy sources.

The concept of flywheel energy storage has a number of attributes which could contribute to the overall ERDA goals. Flywheel energy storage can

- Provide peaking power for electric utilities using base power for spin-up during off-peak hours;
- Serve as a back-up, on-site, or emergency power source for industrial and institutional applications;
- Conserve petroleum in transportation applications;
- Provide a non-polluting power source with no environmental debits.

The benefits resulting from implementations of flywheels are significant. For example, implementation of flywheel energy storage plants at a level where they supply 20% of the nation's average daily load delivered by peaking plants would save an estimated 70,000,000 to 100,000,000 barrels of oil per year in the late 1980's. This would be done by replacing conventional peaking equipment, primarily gas turbines, and using base-load power for spin-up energy during off-peak hours.

The transportation sector promises even greater benefits in use of flywheel energy storage systems. Assuming a fleet of vehicles with a mixture that includes about 15% flywheel-electric and flywheel-heat engine propulsion systems by the year 2000, the petroleum savings could reach 300,000,000 to 500,000,000 barrels per year. The vehicles that employ flywheels as a power source achieve petroleum savings through at least three major mechanisms:

- Reduction of demand in power supplied by conventional internal combustion engines;
- Using off-peak power to spin up flywheels;
- Regenerative braking --- using energy normally dissipated during braking for flywheel spinup.

In addition to the foregoing, flywheel systems are non-polluting and, in fact, could lead to a decrease in overall pollution levels in cities if they gain broad acceptance in the utility and transportation sectors.

Flywheel energy storage systems can also have significant impact on solar and wind energy technology development. These potential energy sources are intermittent in nature and any practical system

designed for use with these sources must provide a guarantee of a reliable, continuous power supply. This requires efficient energy storage methods such as flywheel to level their output for continuous use.

In the development of the flywheel energy storage program, it is the goal of ERDA energy storage program to stimulate the industry, especially electric utilities and transportation industry, into participating in this program with a high level of activity. These industries can contribute to future success of our national flywheel program by:

- assisting in stating the need and requirements for technology development;
- pursuing the development of promising new technologies that are economically viable;
- performing ERDA-sponsored RD&D projects identified in the ERDA program plan.

In particular, industrial support of the flywheel demonstration projects is mandatory. Term of agreements for such joint ventures will, of course, be negotiated.

And now I will briefly discuss the flywheel energy storage program at ERDA. The program was initiated by starting the following:

a. Technical and economic feasibility study

The result of this study will help us formulate a detailed long range plan in the flywheel area. It will be presented at this conference by Rockwell International, the ERDA study contractor.

b. Establish a data base for the design of flywheels made of composite materials.

- c. Develop economical and reliable manufacturing processes for composite rotors;
- d. Study critical component areas such as rotor configuration, rotor dynamics and control, bearings, seals, input and output systems;
- e. Demonstrate small regenerative systems for battery-flywheel and heat engine-flywheel power systems for automobiles;
- f. Develop primary flywheel packages for automobiles, particularly commuter cars;
- g. Demonstrate an energy storage flywheel unit for electric power stations and other industrial uses.

If the results of these component demonstrations are successful, the technology will be transferred to the appropriate ERDA energy system organization for the system development-to-demonstration phases.

If the results are unfavorable, decisions will be made whether to discontinue that portion of the program or to perform additional R&D. The results will be measured in terms of both technical and economic feasibility as well as promise of commercial marketability.

At this time, we are confident that within ten years, practical flywheel units designed for energy missions will become a reality. Naturally this will come about only as a result of serious national effort involving the government, the industry, and the universities.

Flywheel Energy System Background

Now let us look at the concept of flywheel energy storage and its potential as a practical system for everyday use. It is not a concept beyond our immediate grasp and, in fact as I mentioned previously it is a concept which has been with us for many centuries.

Flywheels have long ago made their mark in history with their energy storage characteristics. One of the first known use of flywheel energy was in connection with the inertial mechanism of the potter's wheel. This application was revealed by archeological evidence unearthed at the site of the biblical city of Ur. The Chinese Mandarins applied a similar principle to maintain the rotation of a weighted, wind-powered water wheel during low periods of wind activity while pumping water for irrigation. The flywheel-powered bow drill and child's yo-yo were also early applications of flywheel energy storage properties.

During the last 200 years, large shaft-mounted flywheels have been used to stabilize the output of steam engines used in the mills and factories of the Industrial Revolution period. Today, automobiles, trucks, and diesel locomotives use the flywheel to maintain continuity between power strokes of their piston-driven IC engines.

Other flywheel applications have emerged over the last 200 years, the most notable of which was the Howell torpedo built in 1884. This torpedo incorporated two "firsts": flywheel propulsion, with the flywheel spun-up by an external steam turbine; and gyroscopic stabilization by means of a flywheel.

The most extensive use of flywheels in the transportation field

during the last 25 years was the vehicle propulsion system used by the Oerlikon Engineering Company of Switzerland. In developing a small flywheel-powered railroad engine for switchyard work, it saw the possibility of using flywheels in public transportation. This led to the development of the Gyrobus in the early 1950's. This 35-passenger bus with about 3 kilowatt-hours of stored energy operated between electrical charging sites located about 1/2 miles apart. It went into service in 1953 and remained in service for 10 years. Several of these buses were also tried in the Belgian Congo. Routing limitations, the 1-2 minute spin-up charge period at each stop, and the convenience of conventional diesel buses limited more widespread acceptance of this bus. Economics might have played a role detrimental to the metal-flywheel powered buses.

The convenience of alternate systems and other restrictions have limited more modern applications of flywheels to gyroscopic stabilization and guidance functions. However, new technological demands and technical advancements have resulted in a large number of studies and applications over the recent years. I shall discuss some of the highlights of these efforts.

At the 1963 International Meeting of the Society for Automotive Engineers, Mr. R.C. Clerk presented a paper entitled "The Utilization of Flywheel Energy". It was pointed out that a flywheel built with advanced materials and bearings could be efficiently used as an energy storage.

Since late 1960, the Applied Physics Laboratory at Johns Hopkins University has established the fact that energy densities of certain fiber-reinforced flywheels can match those of advanced batteries now

undergoing development. Lawrence Livermore Laboratory, Stanford Research Institute, Lockheed Corporation, NASA and COMSAT are among those that have done significant amount of work in this area.

The Lockheed Corporation also studied the feasibility of flywheels and hybrid combinations as propulsion systems for passenger cars, vans, and buses. In addition, Lockheed participated in a program to develop a full scale flywheel system to power San Francisco trolley cars.

Garrett is currently installing flywheel systems on some experimental New York City subway cars. These have been used primarily to assess regenerative braking benefits.

TRW and General Motors have studied the use of the flywheel in both pure flywheel and hybrid configurations to power personal vehicles.

In 1970, EPRI and the San Diego Gas and Electric Company jointly sponsored work to investigate possible flywheel resonance problems. It was established that no problems existed at the operating speed investigated. This effort marked the beginning of utility interest in the concept of energy flywheels.

Although flywheels have recieved attention in the past primarily for transportation uses, there have been other applications that are equally important. Flywheels are in use now at Lawrence Livermore Laboratory as a back-up power source, in Europe as small scale load regulators, and in some university plasma physics laboratories (e.g., Princeton University for plasma physics experiments) to provide very high power peaks for plasma physics experiments.

Since 1970, a good deal of attention has been directed to development of flywheel materials. The emphasis is on **high** strength, filament-reinforced composite material which could double and triple the best energy densities possible with steel alloys. Among these are

fiberglass composites and fibers made of boron and graphite. One very promising fiber that is receiving considerable evaluation is the organic fiber known as Kevlar.

This brings us to today. The Rockwell International Corporation has just completed a technical and economic feasibility study of the flywheel as an energy storage device for utilities, transportation, and industry under our sponsorship. This is just one of a number of government-sponsored activities in this area. The others, including the previously-mentioned study are:

- a. ERDA--technical and economic feasibility;
- b. ERDA--flywheel technology development;
- c. MERDC--special power unit;
- d. MERDC--composite materials development;
- e. NSF--bearing development;
- f. NSF--advanced rotor design.

Discussions are in progress to transfer the NSF activities in bearing development and rotor design to ERDA. In the near future we hope to initiate a number of other studies related to our flywheel energy storage program. We at ERDA appreciate your attendance and contribution to this meeting. We hope this will be the first stepping-stone of a continuing effort in the pursuit of achieving our national flywheel program objectives. Lastly, we are looking forward to meeting with you, and many others, at the next conference on flywheel technology two years from now.

FLYWHEEL SYSTEMS APPLICATIONS

J. E. Notti, Jr.
Rockwell International Corporation
Downey, California 90241

ABSTRACT

Flywheel energy storage systems (FESS) were studied within the framework of both the near term and projected 1985-1995 technology for their applicability to the residential, commercial, industrial, transportation and utility sectors.

RESULTS

From the study, the following fundamental findings emerged:

The cost of the energy storage flywheel dominates technical considerations to appear as the major determining factor in the broad based application of FESS.

The development of high energy density composite rotors is the dominant factor in lowering the cost of FESS energy storage.

The development of composite rotors with densities in the range of 40 to 60 watt-hours per pound will significantly broaden applicability of FESS in the transportation sector and is essential to the use of FESS in utility energy storage applications.

Advanced technology FESS employing composite rotors can extend hybrid and all-electric transportation applications to smaller vehicles and provide significant oil savings. A moderate scenario depicting growth of flywheel hybrid vehicles to eleven percent of the projected 1995 vehicle population could conserve 100 million barrels of oil per year (MBOPY).

Advanced technology FESS utilizing large composite rotors offer the potential for replacing combustion turbines for utility peak power storage when combined with nuclear or coal fired electric generating facilities. In addition to oil savings from deleting combustion turbines, total power send-out costs could be lowered significantly. A moderate scenario would predict cumulative oil savings of 570 MBO by 1995 with a yearly conservation potential of nearly 100

MBOPY. The cost of generation may be decreased during the period 1985 to 1995 by \$1 to 2 billion.

Composite rotor developments are presently in progress at a low funding level. With additional funding the question of feasibility of the high energy densities may be established within two to three years. Kevlar appears a promising candidate for high energy density low cost composites.

Even though FESS were found to be technically feasible they were not found to be cost effective in residential, commercial, or industrial applications for the near or far term assuming current utility rate structures. Conceivably, altered rate structures which more severely penalize peak power demands combined with lower projected flywheel capital costs, could make some industrial applications effective.

Flywheel energy storage systems of the current technology employing metallic rotors could have near term (1978-1980) application in short range electric commercial vehicles and hybrid heat engine commuter automobiles. Fuel savings are expected to be moderate with essentially no change in vehicle cost of ownership for hybrid vehicles and moderate increase for electric vehicles.

Safety need be no more severe a problem for properly designed FESS rotors than any of several other high stress elements commonly used in commercial applications today. Rotors must, and can be, derated for generous burst safety margins.

A small mechanically coupled regenerative FESS for the heat engine urban auto is a near term (1980) application which

can result in moderate savings in oil for the urban transportation vehicle. With small increase in vehicle cost of ownership, the unit would store the braking energy of urban stops and return energy to the wheels upon acceleration. Primary power would be developed by a less powerful heat engine. Early introduction could occur as an optional equipment offering for the family urban commuter, taxis and urban delivery vehicles.

A small motor-generator driven FESS could also be developed in the near term (1970-1980) to be used in conjunction with a battery driven electric drive vehicle. At least one prototype has been developed and demonstrated. The battery electric drive accrues the credits for oil savings. The vehicle cost savings attributed to this unit come about through the increased battery life which accrues as a result of FESS absorbing peak power demands and protecting the battery from damaging discharge cycles.

From an institutional standpoint, the introduction of the above systems could not be expected to significantly impact our current transportation industry. Increased electrical equipment demands could be well serviced by the current industry.

Any significant transportation systems impact upon oil consumption by 1990 will require more comprehensive and more costly developments than are currently in progress.

Metallic rotors do not appear candidates for general large fixed base installations because of their low energy density and high cost of storage.

The major findings of the study have effectively dictated the development strategy upon which the proposed FESS Research and Development plan is predicated. Briefly stated the strategy is as follows:

Noting the importance of rotor energy density to FESS costs and general application, begin immediately a comprehensive program for development of composite material rotors. Since no single design has a demonstrated superiority, several designs should be pursued concurrently. Development work should stress actual rotor fabrication and test since the analytical techniques for composite rotors are emerging and their results must be considered only indicative. Emphasis should be given

large rotor technology. Concurrently, the development of metallic rotor systems should be accelerated by a) augmenting current transportation programs with the development of smaller hybrid power packs and b) establishing test facilities for rotor burst testing, multiple rotor life cycle testing and c) establishing a vehicle simulator which will reproduce road and impact shocks for testing complete FESS including housing and suspension systems. Continued systems design and effectiveness and user application studies are necessary, especially in the utility sector, to develop advanced concepts and to define the impact of user requirements upon the design. Continual re-evaluation of applications in light of emerging technology and evolving economics is considered essential.

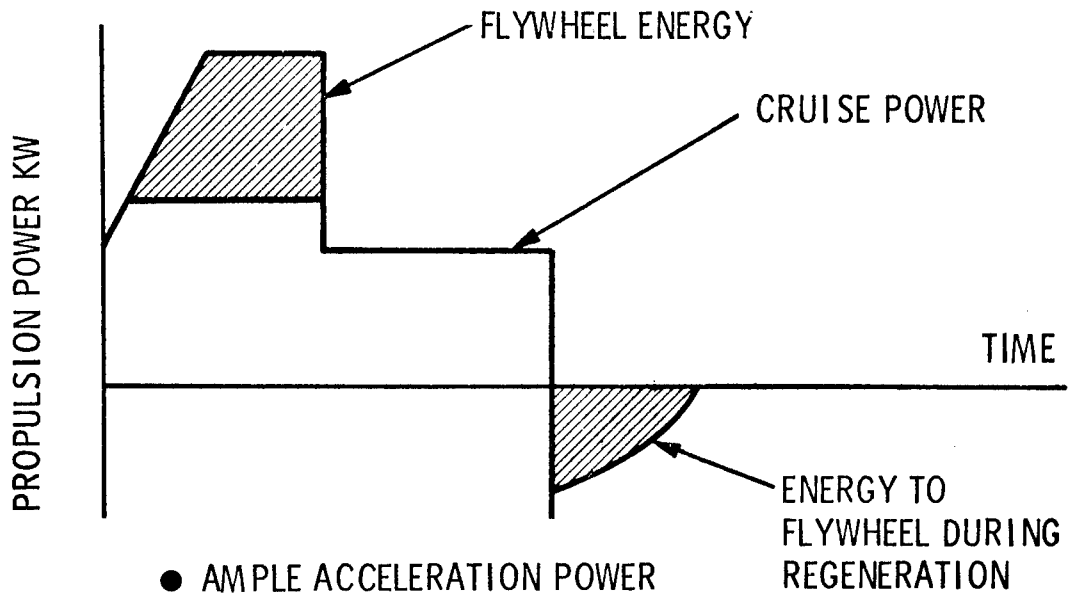
ALL-SERVICE ELECTRIC TRANSIT VEHICLE

J. F. Campbell
Room 6104F
U. S. Department of Transportation
2100 Second Street, S.W.
Washington, D. C. 20590

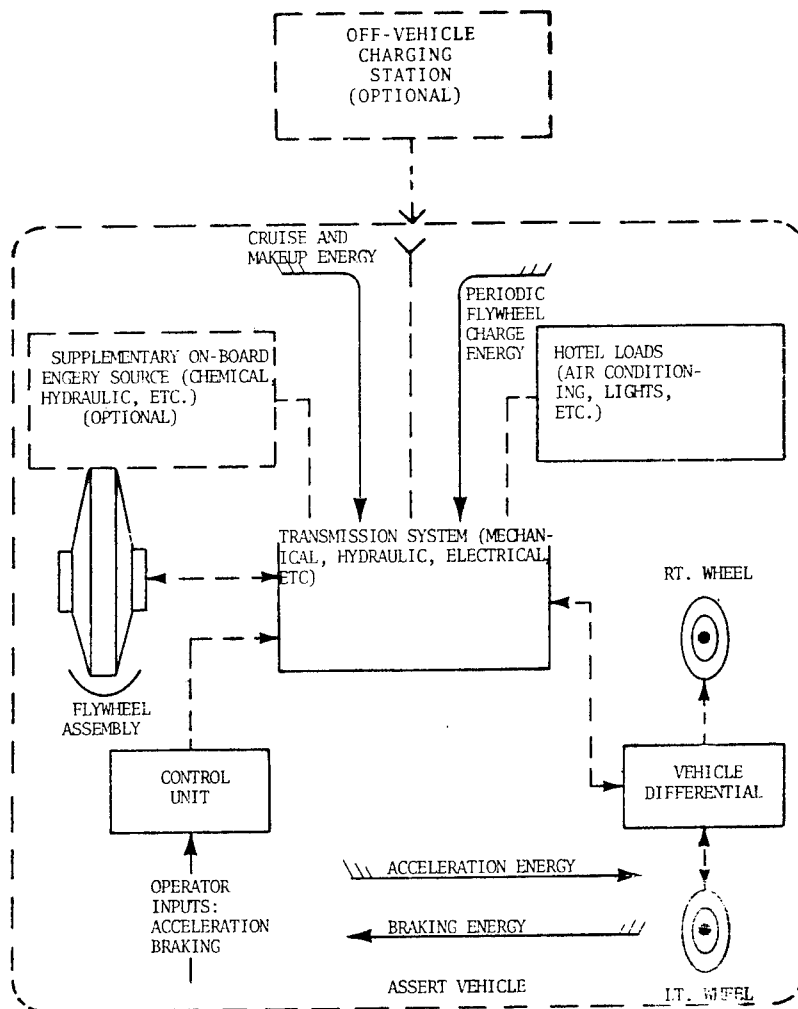
ABSTRACT

Electric transit vehicles powered by flywheels have many advantages on predetermined, multi-stop routes. More than fifty such Oerlikon buses that stored 9 kwh of energy served for twenty years in Switzerland. This paper examined the general characteristics of flywheel-powered vehicles and the performance of a hypothetical vehicle on three bus routes in San Francisco.

ATTRACTIVE FEATURES OF FLYWHEELS



- AMPLE ACCELERATION POWER
- RECOVERY OF BRAKING ENERGY
- LONG LIFE
- QUICK RECHARGE



KEY CHARACTERISTICS

- SYSTEM APPROACH
- MODULARITY
- SAFETY
- SHORT CHARGE TIME
- CHARGING STATION MOBILITY
- EMERGENCY RECHARGE

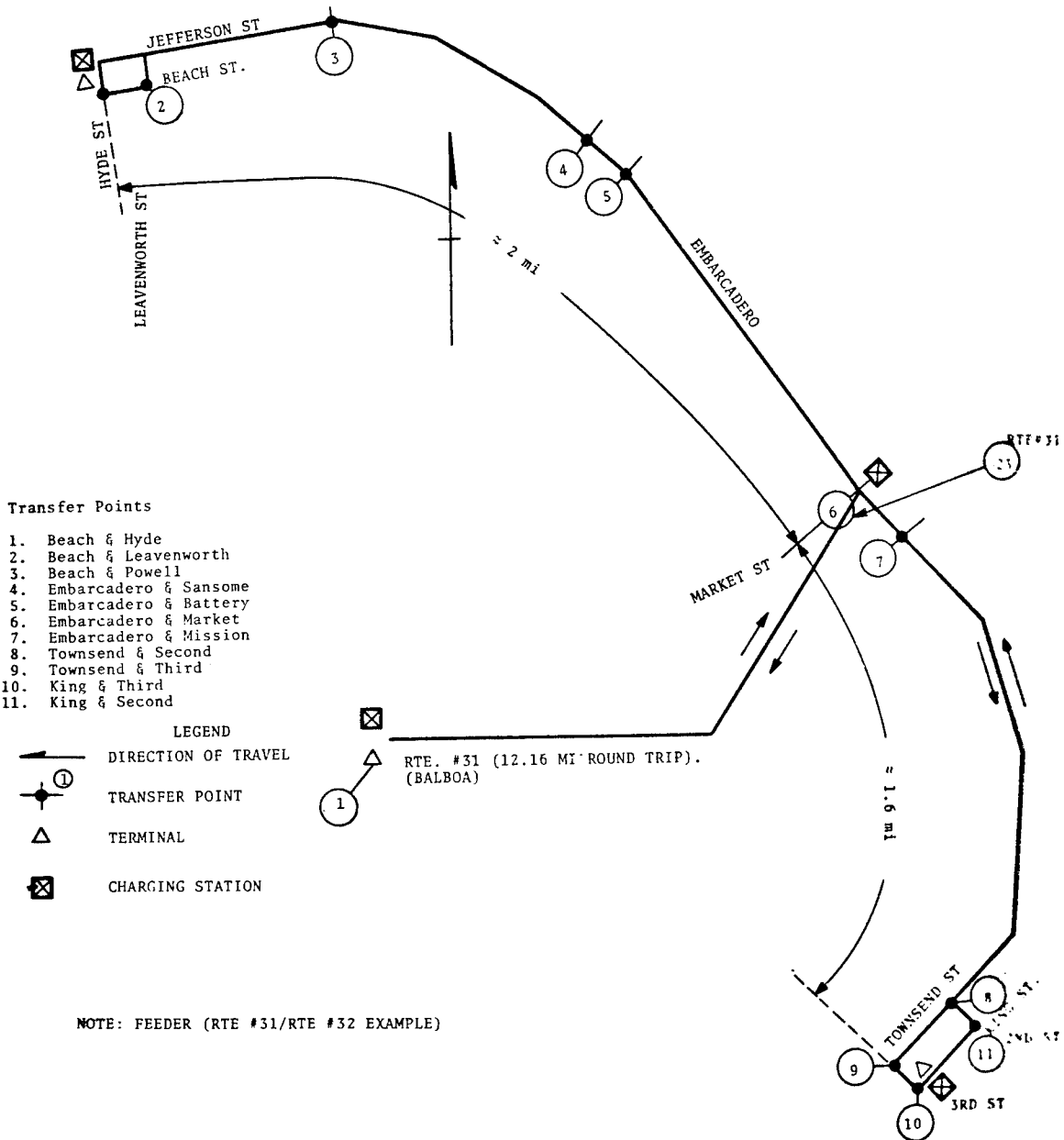
#32 EMBARCADERO

Motor Coach

Round Trip Mileage 7.19 Miles

Regular Route: From King & 3rd (S. P. Depot) via King, 2nd, Townsend, Embarcadero, Jefferson (Fisherman's Wharf) Leavenworth, Beach to Hyde.

Return: Via Hyde, Jefferson, Embarcadero, Townsend, 3rd to King.



02 CLEMENT EXPRESS Round Trip Mileage 12.14 Miles

Motor Coach

Regular Route: Outbound P.M. from Pine and Montgomery via Pine, Masonic, Euclid, Argucillo, Clement, 33rd Ave., Geary, P. Lobos to 48th Ave. or Geary, 42nd Ave. to Fort Miley.
 Regular Route: Inbound A.M. from 48th Ave., and Pt. Lobos via 48th Ave., Geary, 33rd Ave. or Ft. Miley, 43rd Ave., Geary, 33rd Ave., Clement, Argucillo, Euclid, Bush to Sansome.

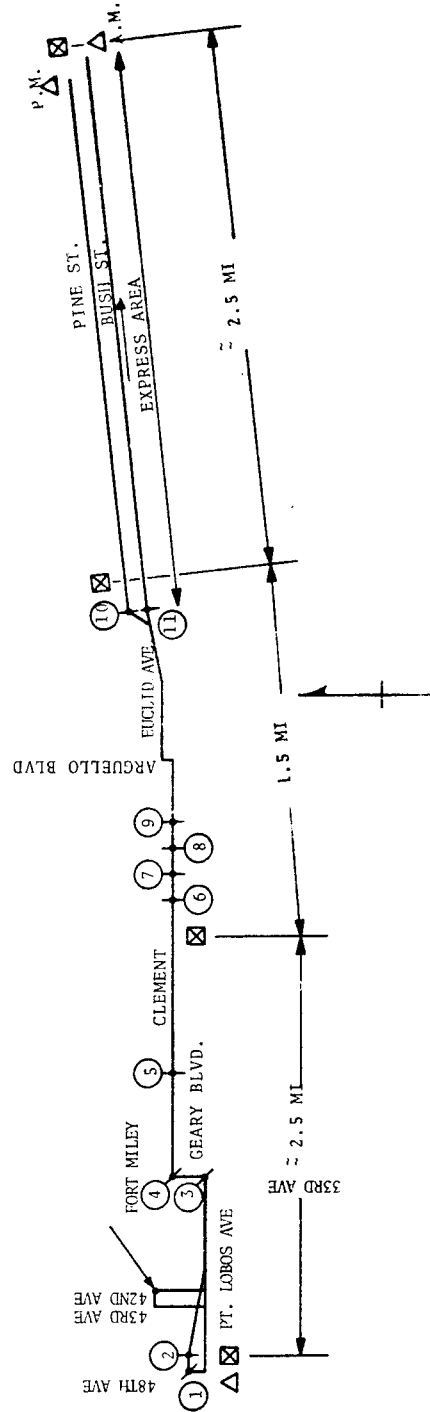
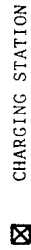
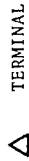
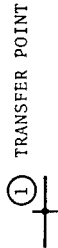
Transfer Points

1. 48th Ave. & Pt. Lobos
2. 47th Ave. & Pt. Lobos
3. 33rd Ave. & Geary
4. 33rd Ave. & Clement
5. 25th Ave. & Clement
6. 12th Ave. & Clement
7. 10th Ave. & Clement
8. 8th Ave. & Clement
9. 5th Ave. & Clement
10. Presidio Ave. & Pine
11. Presidio Ave. & Bush

Note: Local/Express Example.

Scale 1"=4000 FT

DIRECTION OF TRAVEL



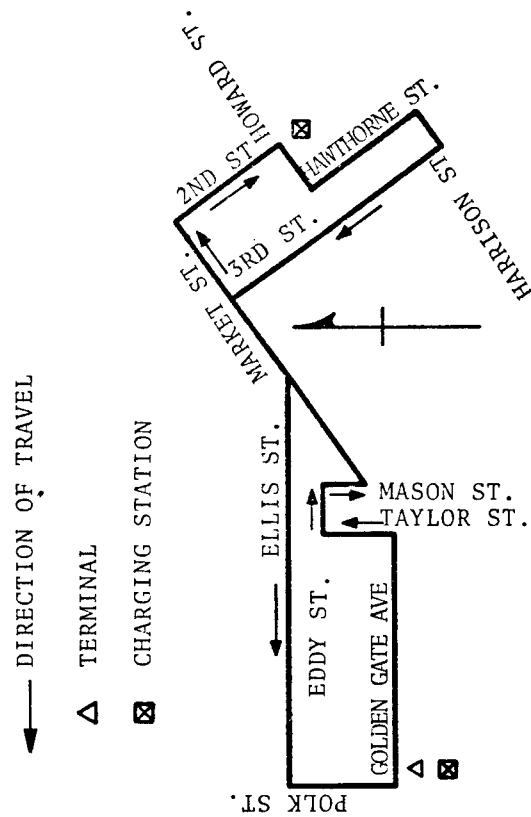
#84 DOWNTOWN SHOPPERS' SHUTTLE Motor Coach Round Trip Mileage 3.94 Miles

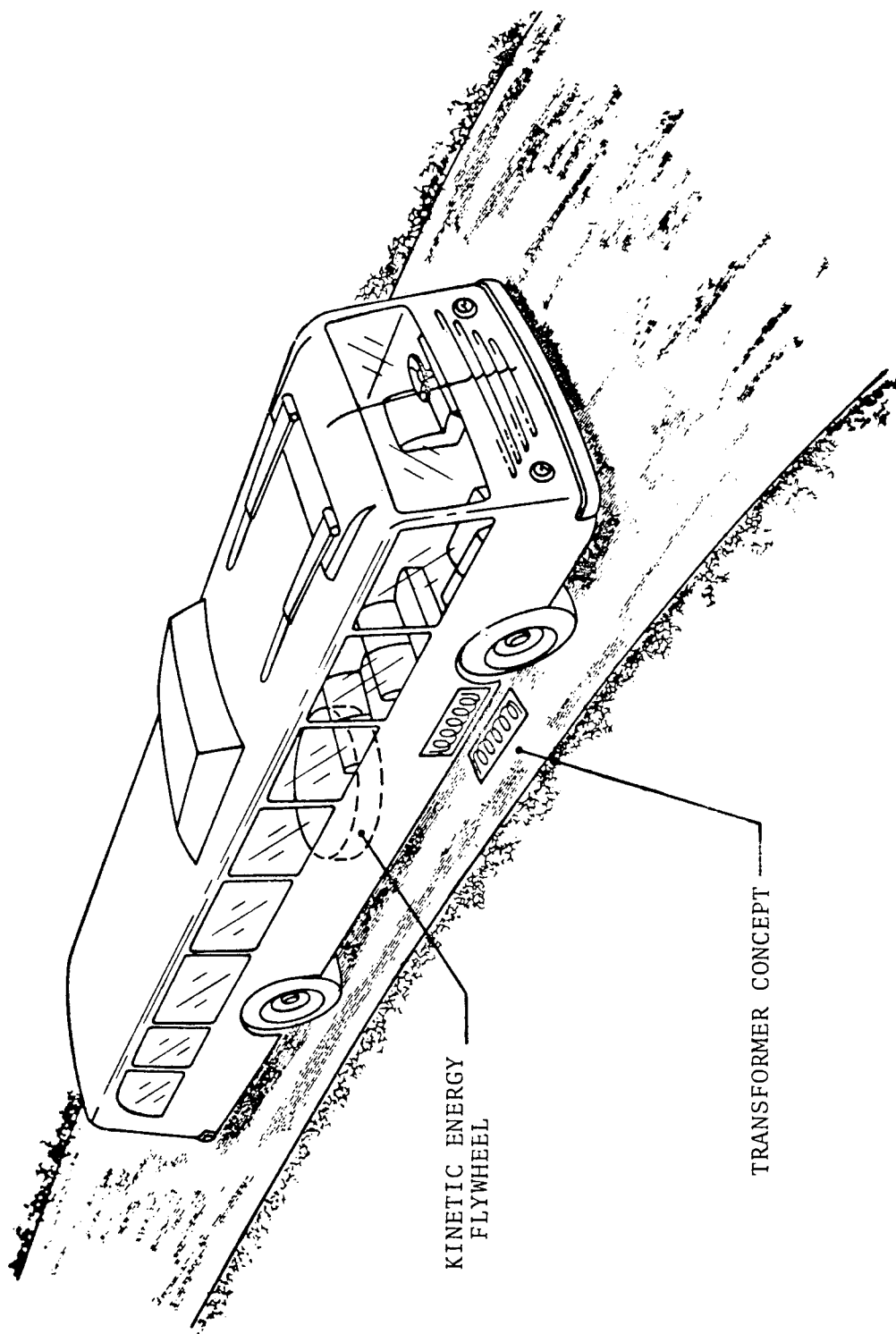
Regular Route: From Hawthorne & Folsom via Hawthorne, Harrison, 3rd, Market, Ellis, Polk, to Golden Gate Avenue.
Return: Via Golden Gate Avenue, Taylor, Eddy, Mason, Market, 2nd, Howard, Hawthorne to Folsom.

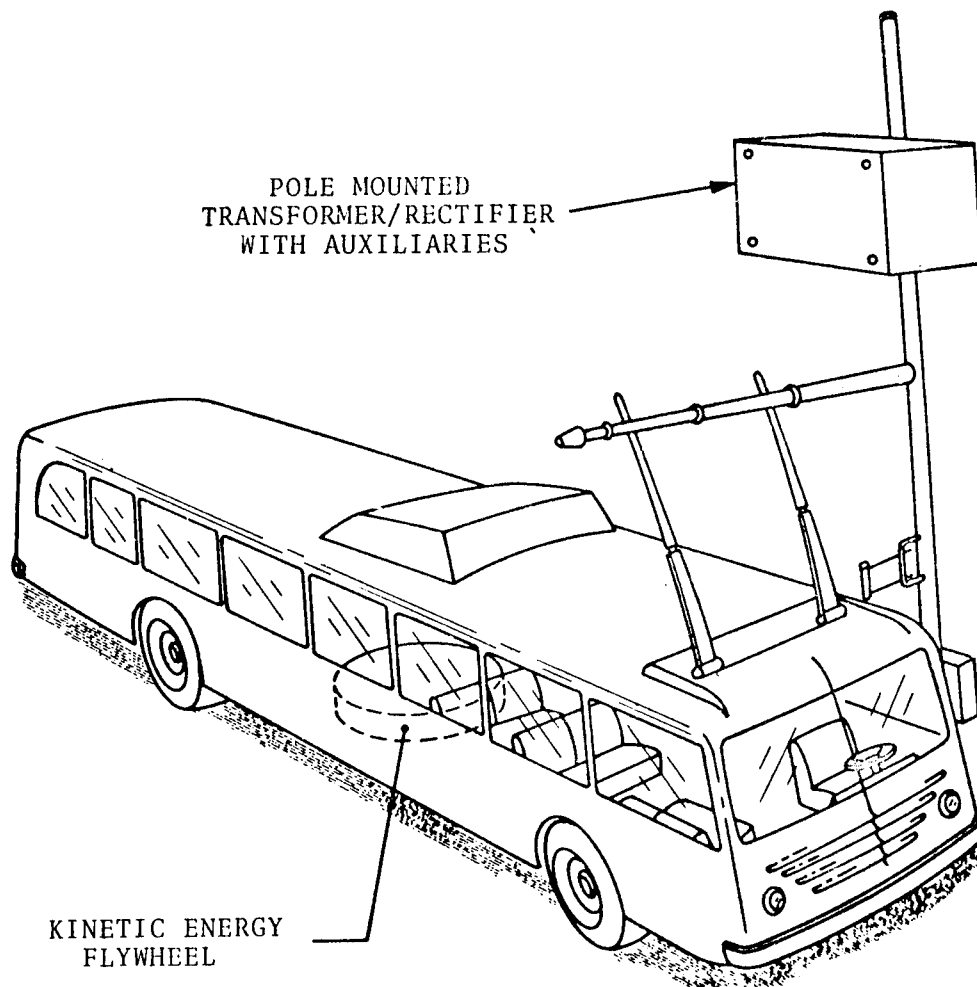
*Distance Between Charging Stations ~ 2 miles.

Note: Circulator/Shuttle Example.

Scale 1"=1500 FT







POSTAL VEHICLE MISSIONS

T. Norman
U. S. Postal Service
11711 Parklawn Drive
Rockville, Maryland 20852

ABSTRACT

The Postal Service has a program under way to reduce the operating cost, the dependence on oil-based fuel and the pollution characteristics of its vehicle fleet. At present, more than 90,000 relatively inefficient gasoline-powered vehicles are in use on postal routes requiring 100 to 600 stops per day. After extensive testing of three developmental all-electric trucks on simulated postal routes, the Service bought 352 trucks for operational use. Other efforts are being made to develop efficient specialized vehicles. A contract will be let soon for development of a flywheel electric vehicle. A hybrid electric truck with a small internal combustion engine is ready for evaluation, and four small diesel trucks are under test. Other approaches are being considered.

INTRODUCTION

The U.S. Postal Service operates one of the largest vehicle fleets in the country. My purpose here today is to provide you with an appreciation of the magnitude of this fleet, the operational missions of the vehicles and our plans for vehicle propulsion system improvement. It is hoped that from this presentation you will recognize, as we in the Postal Service do, the application of the flywheel propulsion system concept to the postal vehicles. It is also hoped that it will stimulate interest within the industry to develop flywheel systems directly applicable to the Postal Service needs.

THE POSTAL SERVICE FLEET

Slide 1. The Postal Service operates a fleet of approximately 130,000 vehicles. This includes leased vehicles. Of this total, 106,000 are owned by the Postal Service. There are 9,000 1-ton vehicles, 28,000 1/2-ton vehicles and 65,000 1/4-ton vehicles. During FY 74, we used 89,678,271 gallons of gasoline at a cost of \$31,118,104. We have found that since FY 73 the cost of gasoline has increased by about 60%.

Slide 2. The 1-ton vehicles are used primarily for collection of mail from the corner mailboxes. The 1/2 and 1/4-ton vehicles are used for delivery of mail to individual patrons. There are basically two types of delivery routes. First, there is the park and loop route which

consists of driving the vehicle to pre-established locations from which the mail is delivered, on foot, to the individual patrons. The second type is the mounted delivery route. This type of route consists of driving the vehicle to each patron's house or office to deliver the mail.

The characteristics of the many delivery routes vary widely and, as such, it would be difficult to define a typical route. However, we can, in general, define the range of these characteristics. The distance of a route may vary from seven to 60 miles. The number of stops may range from 100 to 600. It is interesting to note that the vehicle engine may idle up to 60% of the time during a delivery route. The routes may be level or very hilly, while the temperature may range from very hot to very cold. Because of the variation of these routes, the vehicles may get from four to 13 miles per gallon. It is not unusual for a 1/4-ton delivery vehicle to get four miles per gallon.

IMPROVED VEHICLE PROPULSION PROGRAM

Slide 3. We have established an improved vehicle propulsion system program with the objectives of reducing operating cost, dependence on oil-based fuel and pollution.

Slide 4. This program consists of developing, testing and evaluating a number of

different propulsion systems. The systems divide into internal combustion engines and electric propulsion systems.

We have four diesel engines being installed in a like number of 1/4-ton vehicles. Diesel engines have the potential advantage of high efficiency during idling. We will test these engines and establish their potential for postal application.

We have also contracted for the installation of four stratified charge engines in 1/4-ton delivery vehicles. Stratified charge engines have been advertised to reduce pollution while increasing engine efficiency. Again, we will evaluate these engines for their potential application to postal vehicles.

We are also planning to contract for further development of a hydrogen engine, which we will test and evaluate. Hydrogen engines require no gasoline, produce essentially no pollution and are highly efficient at low performance levels. Hydrogen must be maintained in a liquid form at a temperature of -276°F. This, of course, causes problems in storage and handling. Hydrogen also is not readily available.

The Postal Service had three different electric vehicles developed by Otis, Electromotion and Battronic for test and evaluation. These vehicles performed relatively well on limited delivery routes. As a result, we purchased 352 American General electric vehicles for operational use. The two vehicles assigned for engineering tests have not yet been received. Electric vehicles have the advantage of not polluting or requiring oil-based fuel, however, they are presently limited in their application.

In order to increase their application, we have investigated improved batteries. It has been found that production batteries, with significant improvements, appear to be some years away. However, we do plan to test and evaluate a nickel zinc battery during the next few months. Nickel zinc batteries have the potential advantage of producing twice the energy as the lead acid batteries for the same weight, but this double energy capacity requires double the volume. The life cycle is projected as approximately 1/2 that of the lead acid batteries.

We are planning to evaluate the hybrid electric propulsion system concept by testing a system which has been installed in a 1/4-ton postal delivery vehicle. This system consists of a small internal combustion engine operating in conjunction with an electrical propulsion system. It is considered that additional development effort is necessary before this type of system could be used operationally.

The flywheel electric vehicle appears to have all the advantages we are seeking. However, such a system has not been developed for our type of vehicles. Therefore, we are planning in the near future, to contract for the development of such a system.

TESTS OF ALL-ELECTRIC VEHICLES

Slide 5. In order to effectively develop and evaluate improved propulsion systems for electric vehicles, it is first necessary to establish the capabilities and limitations of the existing electric vehicles. We have conducted a number of tests on the three electric vehicles to support this requirement. The next two slides will show some of these test results. The accelerations, as shown, are considered acceptable, but since these tests were performed on level terrain, improvements may be considered necessary to improve the performance on grades. The top speed should be increased to 50 or 55 mph to allow for safe operation on highways.

Slide 6. We tested each of the three vehicles on simulated routes to determine the range of routes over which these vehicles could satisfactorily perform. This slide shows the results of these tests. If we take the Otis vehicle, as an example, it can be seen that it could perform over routes that have up to 350 stops provided that the total distance does not exceed 10 miles. It can also be seen that it could perform on routes with distances up to 24 miles, provided that the number of stops does not exceed 100. These tests were all performed on flat terrain during mild temperatures. Additional tests will be performed to establish the effect of grades and low temperatures.

Slide 7. In addition to establishing the electric vehicle delivery route capabili-

ties, it is also necessary to establish the potential application of the electric vehicles to the actual operational routes. We plan to do this by sampling routes throughout the country and determining their characteristics in terms of number of stops, total distance, type of grades and energy consumed. Instrumentation packages are being developed to record this type of data. From the information obtained, we can then classify the routes, on a statistical basis, in accordance with their characteristics. We can then establish the number of electric vehicles, with any given capability, that could be utilized throughout the country on postal delivery routes.

U.S. POSTAL SERVICE VEHICLE FLEET

130,000 TOTAL VEHICLES (Including leased)

106,000 VEHICLES OWNED & OPERATED

9,000	1 Ton Vehicles
28,000	1/2 Ton Vehicles
65,000	1/4 Ton Vehicles
<hr/>	
102,000	

89,678,271 GALS./FY-74

\$31,118,104 /FY-74

60% COST INCREASE/GALS. SINCE FY-73

FIGURE I

DELIVERY & COLLECTION ROUTES

(1, 1/2, 1/4 TON VEHICLES)

CHARACTERISTICS

Distance - 70 to 60 miles/day

Stops - 100 to 600/day

Total Engine Idle Time - Up To 60%

Terrain - Level to Very Hilly

Temperature - Very Hot to Very Cold

ENERGY CONSUMPTION

Miles/Gal - 4 to 13

FIGURE II

IMPROVED PROPULSION SYSTEMS

OBJECTIVES

REDUCE OPERATING COSTS
REDUCE DEPENDENCE ON OIL BASED FUEL
REDUCE POLLUTION

FIGURE III

IMPROVED PROPULSION SYSTEM PROGRAM

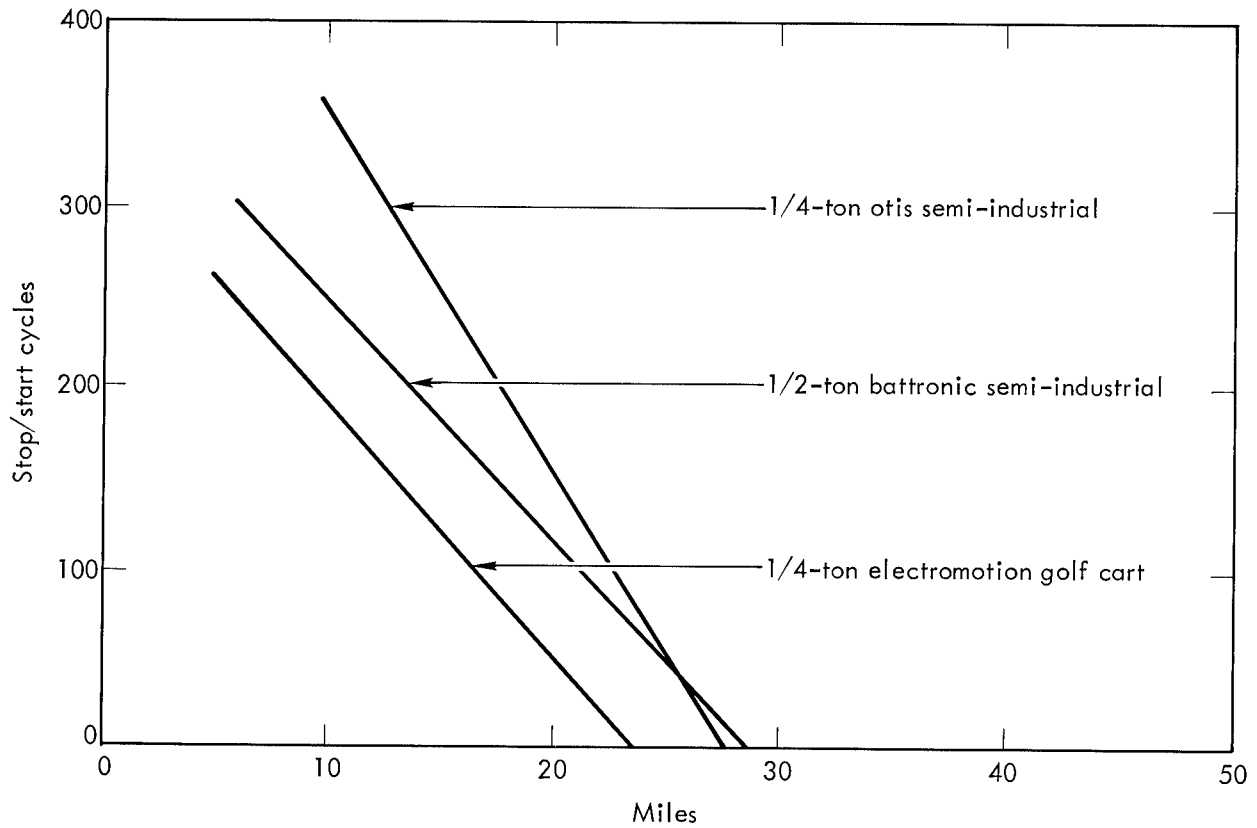
<u>INTERNAL COMBUSTION ENGINES</u>	<u>PROBLEMS</u>
Diesel Engine	Requires Oil Based Fuel
Stratified Charge Engine	Requires Oil Based Fuel
Hydrogen Engine	Availability & Storage of Hydrogen
 <u>ELECTRIC PROPULSION SYSTEMS</u>	
Electric	Limited Application
Improved Batteries	Limited Application - Not Developed
Hybrid-Electric	Requires Oil Based Fuel - Not Developed
Flywheel-Electric	Not Developed

FIGURE IV

ELECTRIC VEHICLE PERFORMANCE CHARACTERISTICS

<u>PERFORMANCE PARAMETERS</u>	<u>OTIS</u>	<u>ELECTROMOTION</u>	<u>BATTRONIC</u>
Acceleration (Sec)			
0-15 MPH	4.6	4.2	4.8
0-30 MPH	13.5	13.4	14.5
Top Speed (MPH)			
Level	40.5	38.5	42
5% Grade	28	28	28
15% Grade	-	13	-

FIGURE V



POTENTIAL APPLICATION OF ELECTRIC VEHICLES

DETERMINE NUMBER OF ROUTES SERVICEABLE BY ELECTRIC
VEHICLES AND FLYWHEEL/ELECTRIC VEHICLES

SAMPLE ROUTES USING INSTRUMENTATION TO OBTAIN

Number of Stops

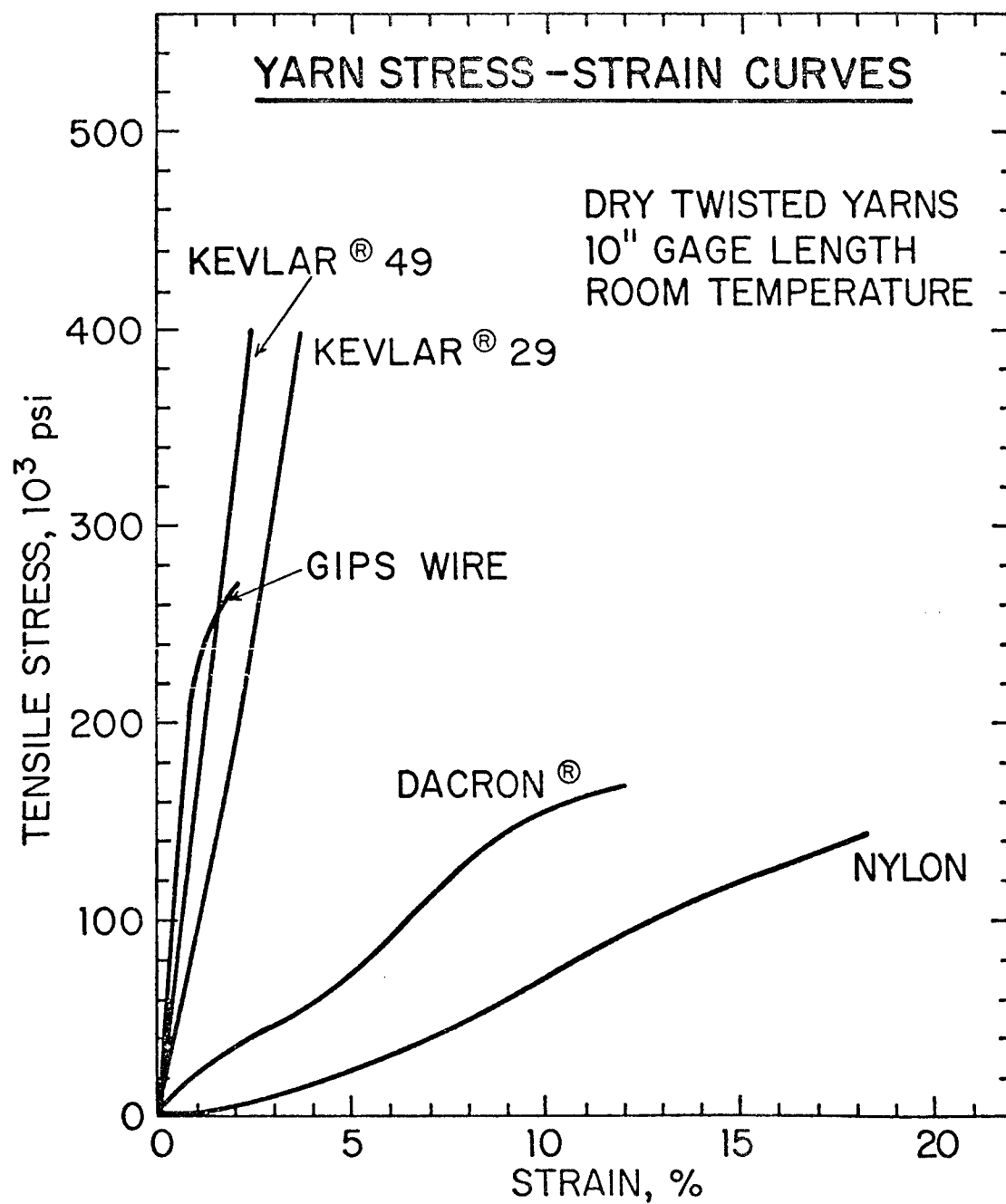
Total Distance

Percent Grades

Energy Consumed

CLASSIFY ROUTES BY THEIR CHARACTERISTICS

FIGURE VII



THE BROAD RANGE OF FLYWHEEL APPLICATIONS

D. W. Rabenhorst
Applied Physics Laboratory
Johns Hopkins University
Johns Hopkins Road
Laurel, Maryland 20810

ABSTRACT

This paper considers flywheels of three basic types, depending on their cost and their capability in meeting performance requirements. Each type is discussed in terms of materials, energy inputs and outputs and fields of application.

INTRODUCTION

It is the opinion of an increasing number of flywheel proponents that practical applications of the modern flywheel number in the hundreds, with the business potential running well into the multi-billion dollar bracket. Ideally, a hypothetical flywheel capable of storing 100 watt-hours per pound and 10,000 watt-hour per ft³ and costing 10¢ per pound would satisfy the requirements of all of these applications.

Unfortunately, there is no known material from which a single flywheel configuration could be made which could meet these requirements. On the other hand, there are few, if any, of the applications in which ALL of the optimum requirements are mandatory at the same time.

DISCUSSION

This discussion will be concerned with the definition of basic types of flywheels which will be respectively capable of meeting the applications requirements. As one might expect, the most basic category breakdown is in the area of materials cost. The performance of the flywheels will vary categorically with the materials cost, although this is not true in every case. For this reason it is convenient to define both performance and cost in each case simultaneously. The three basic cost vs performance classes are shown in Figure 1, together with the other functional categories which may pertain to each.

The typical maximum performance types and their applicable materials are listed

in Figure 2. It can be seen that these are all cases where minimum weight and volume are of paramount importance. Also, these flywheels are all relatively small compared to those in the other two cost categories, and only a moderate amount of relatively exotic material is required. The detailed requirements of two of these applications are covered in Figures 3 and 4.

It would appear that the category of flywheels involving the greatest number of units, and, in some cases, the largest size units is that of the moderate performance, low cost types listed in Figure 5. These include most of the road, off-road and rail vehicles, as well as a wide variety of stationary applications. Typical examples of this category, together with their requirements are shown in Figures 6, 7 and 8.

While nearly all of the current R & D flywheel activity is aimed at the moderate performance flywheel development, there is another important category which is receiving virtually no attention, even though it represents a multi-billion dollar market potential. This is the category of very low cost flywheels, as described in Figure 9. In addition to their enormous market potential, the low cost flywheels represent a considerably less severe development problem than either of the other types. This is because their relatively low performance requires correspondingly low rotational speeds, which, in turn, reduces the severity of bearing, seal, transmission and aerodynamic problems by about an order of magnitude compared to the other types. The characteristics of this type are shown in Figure 10.

FLYWHEEL APPLICATIONS PARAMETERS

ENVIRONMENT	INPUT/OUTPUT	PERFORMANCE VS COST
STATIONARY	ELECTRIC MECHANICAL	① VERY HIGH PERFORMANCE VERY HIGH COST
MOVING		② HIGH PERFORMANCE LOW COST
PORTABLE		③ LOW PERFORMANCE VERY LOW COST

MAXIMUM PERFORMANCE FLYWHEELS

PARAMETER

VERY HIGH PERFORMANCE
VERY HIGH COST

RANGE

50-100 WATT-HR/POUND
> \$ 300/POUND

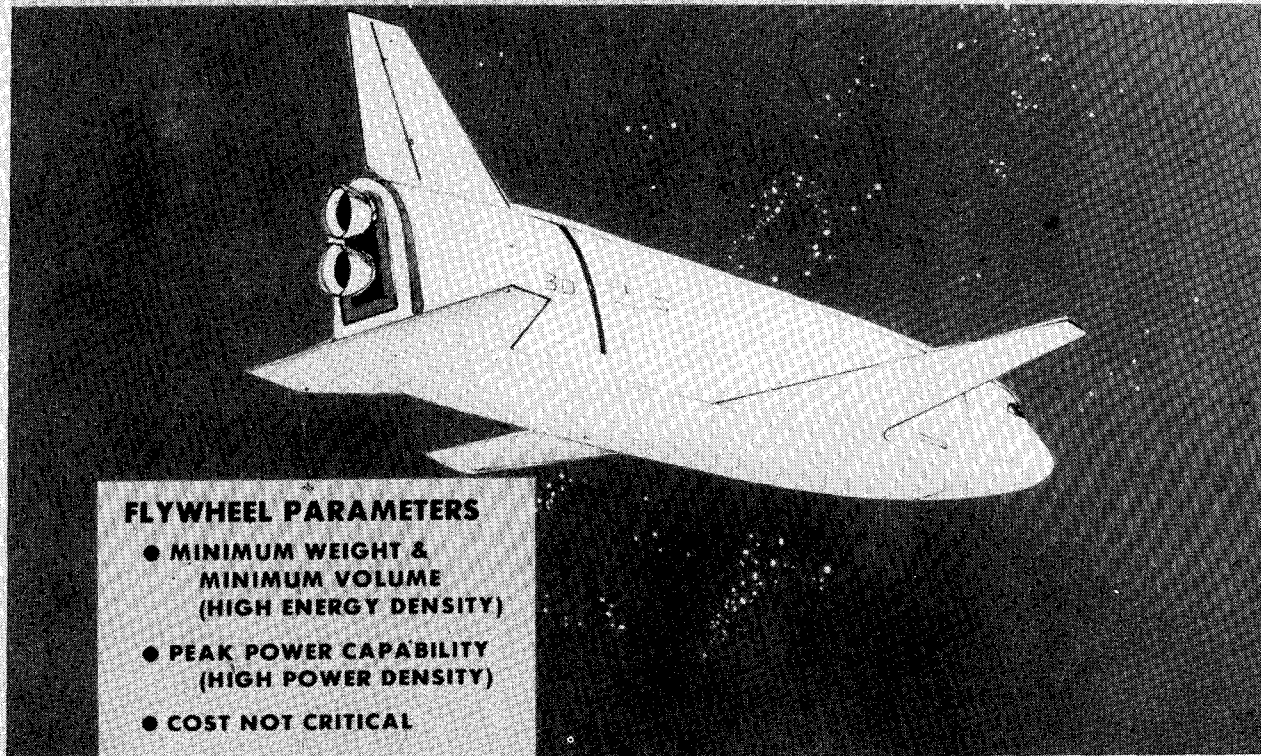
TYPICAL MATERIALS

BORON
KEVLAR
BULK GLASS
FUSED SILICA
FUTURE WHISKERS
RUBY/SAPPHIRE
FIBERGLASS WIRE

TYPICAL FIELDS OF APPLICATION

AIRCRAFT
★ SPACECRAFT
WEAPONS
TOOLS
★ UNDERWATER SURVEILLANCE

TYPICAL MAXIMUM PERFORMANCE APPLICATION (SPACECRAFT)



TYPICAL MAXIMUM PERFORMANCE APPLICATION

(UNDERWATER)



MODERATE PERFORMANCE FLYWHEELS

PARAMETER

HIGH PERFORMANCE
LOW COST

RANGE

20-50 WATT-HR/POUND
\$ 1-3/POUND

TYPICAL MATERIALS

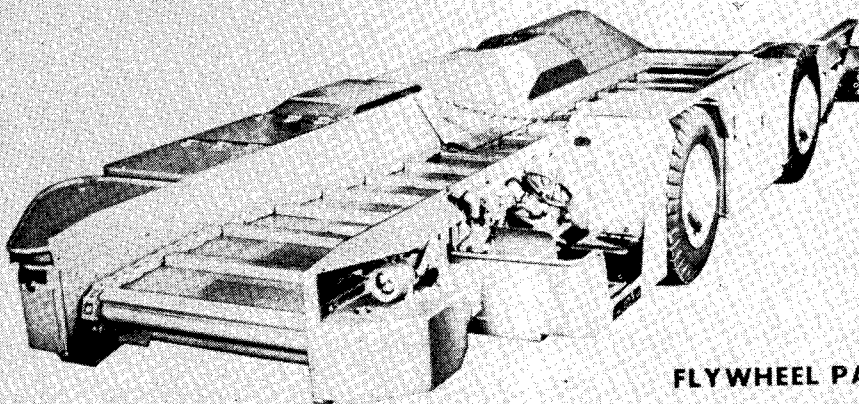
E-GLASS
S-GLASS
Kevlar (POSSIBLE)
GRAPHITE (POSSIBLY)
WIRE
NEW MATERIALS

TYPICAL FIELDS OF APPLICATION

HIGH POWER LOAD LEVELING
★ UTILITIES PEAKING
USER SITE LOAD LEVELING
SOLAR ENERGY STORAGE
WIND ENERGY STORAGE
ROAD VEHICLES
★ OFF ROAD VEHICLES
RAIL VEHICLES
TOOLS
NO-BREAK POWER
★ EMERGENCY POWER

TYPICAL MODERATE PERFORMANCE APPLICATION

(OFF-ROAD VEHICLE)

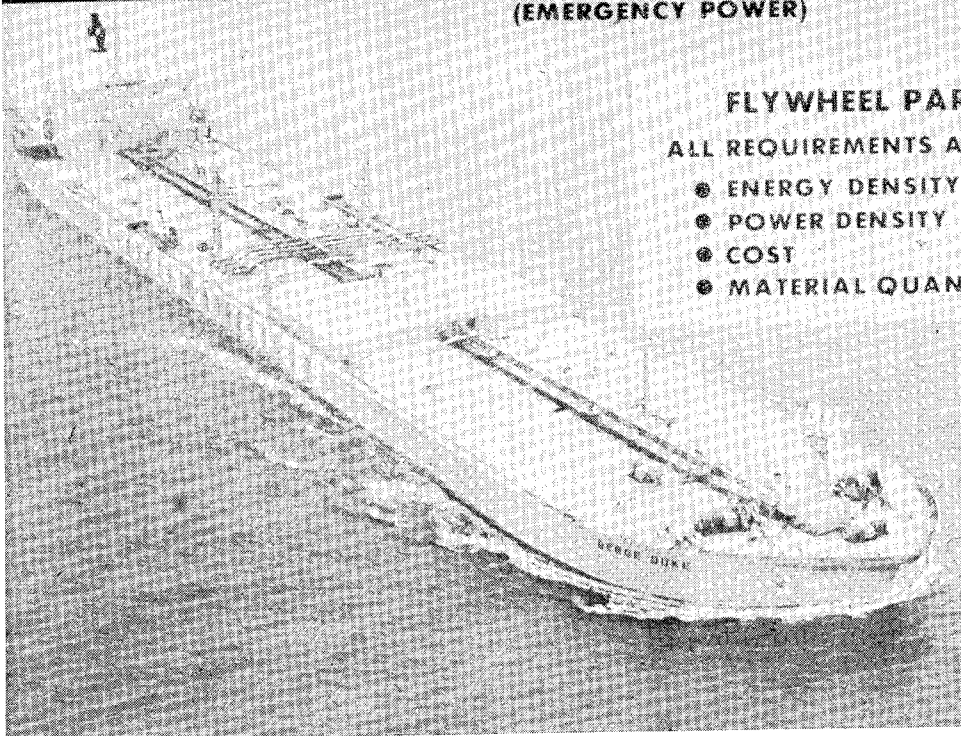


FLYWHEEL PARAMETERS

- VERY RAPID CHARGING
(HIGH POWER DENSITY)
- LOW VOLUME
- LOW COST

TYPICAL MODERATE PERFORMANCE APPLICATION

(EMERGENCY POWER)



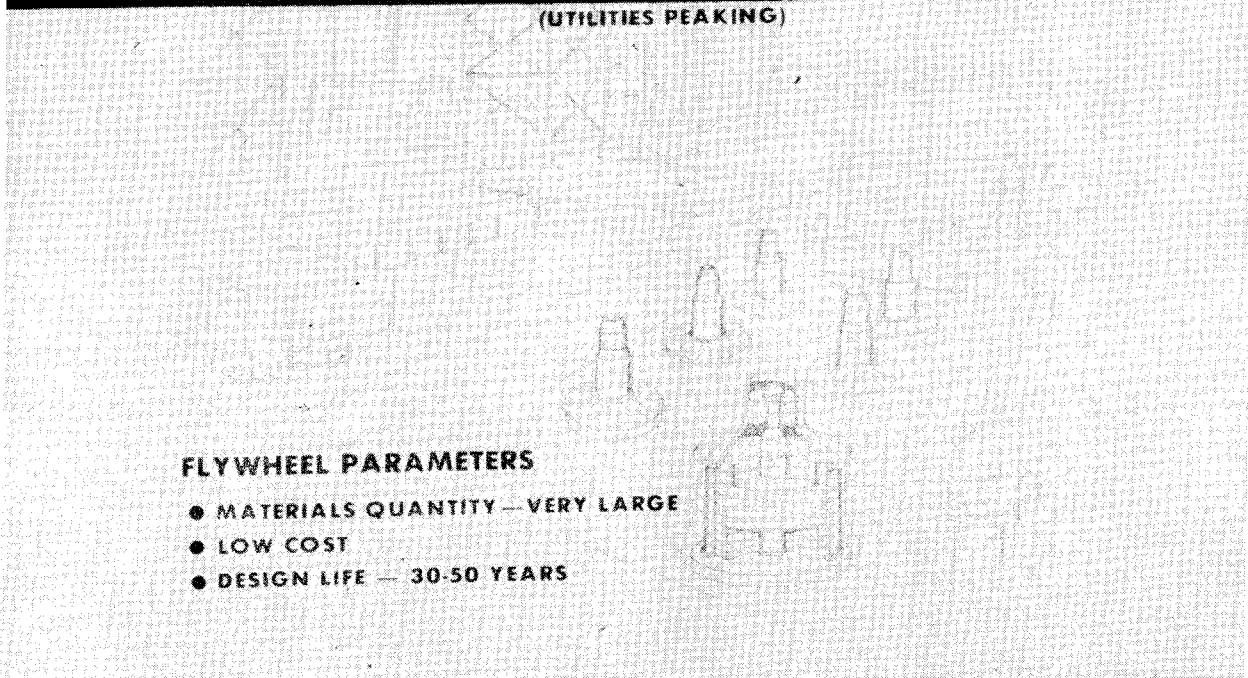
FLYWHEEL PARAMETERS

ALL REQUIREMENTS ARE MODERATE

- ENERGY DENSITY
- POWER DENSITY
- COST
- MATERIAL QUANTITY

TYPICAL MODERATE PERFORMANCE APPLICATION

(UTILITIES PEAKING)



FLYWHEEL PARAMETERS

- MATERIALS QUANTITY — VERY LARGE
- LOW COST
- DESIGN LIFE — 30-50 YEARS

LOW COST FLYWHEELS

PARAMETER

LOW PERFORMANCE
VERY LOW COST

RANGE

< 1-20 WATT-HOUR/POUND
< 1¢ — 1¢/POUND

TYPICAL MATERIALS

STEEL
STEEL FOIL & WIRE
METGLASS
PLANT FIBERS
MANY MATERIAL
COMBINATIONS

TYPICAL FIELDS OF APPLICATION

LIMITED USER SITE STORAGE
★ SOLAR ENERGY
WIND ENERGY
NO-BREAK POWER
EMERGENCY POWER
LIMITED HIGH POWER LOAD LEVELING

TYPICAL LOW COST APPLICATION

FLYWHEEL PARAMETERS

- VERY LOW COST
- OPTIONAL INPUT/OUTPUT
- 20-30 YEAR LIFE
- WEIGHT, VOLUME AND POWER DENSITY — NON-CRITICAL

SYSTEMS ASPECTS OF ENERGY WHEELS

Ernest W. Schlieben
Radio Corporation of America
Box 800
Princeton, New Jersey 08540

ABSTRACT

Energy wheels (flywheels) are not just wheels. They are components of a system, and system requirements dictate their design. Other components, such as the motor/generator and controls, suspension system, vacuum and safety housings, support structures, gimbals and power conditioner unit, are also major parts of the system. This paper discusses some flywheel system considerations: shelf life, safety, system weight, energy density per pound of system, system dynamics, life and cost. Rim-only, magnetically-supported fiber energy wheels have great potential. With further development they should have high, stored-energy density (up to 60 watts/lb), good durability at high stresses, long life (up to 20 years) with almost unlimited recharging, long shelf life (wheel rundown time) with low bearing energy losses and good intrinsic safety characteristics. We are considering these aspects in our design.

INTRODUCTION

The Astro-Electronics Division of RCA has been developing flywheels for fifteen years as part of its spacecraft development and production effort. These wheels are used for momentum exchange on spacecraft in the attitude control system and are referred to as momentum wheels, reaction wheels and control moment gyros. By way of emphasis that flywheels are always components of a system and that system requirements dictate their design, Figure 1 shows the installation at Princeton University's Plasma Physics Laboratory for supplying pulse power needed to produce magnetic confinement fields for the ionized plasma used in fusion reaction experiments. The installation consists of three sets of generators, each set comprising a 7000 hp, 350 rpm motor, a 96-ton flywheel and four generators. The total energy requirement is 440 megawatt-seconds for a power pulse of 1 second at maximum current and the equivalent of about 1.2 seconds at maximum current for current rise and fall time.

I thought you might like to see a picture of a real flywheel (Figure 2). This is the flywheel used in the Plasma Physics Laboratory pulse power system and is a good example of a classic flywheel configuration. Energy storage density is less than one watt-hour/lb.

Flywheels are always used as a buffer store for energy in power systems between a prime power source and the load. Figure 3 illustrates this point. The prime source may be a wind generator, a portable generator or a photovoltaic source and the load may be a spacecraft momentum wheel, a compact car or other device. In all cases the flywheel and its subsystem components, including housing, controller and power converter functions, is a secondary energy source.

SOME SYSTEM CHARACTERISTICS OF RIM-ONLY, COMPOSITE FLYWHEELS

In my company, we are considering flywheels incorporating advanced technology to obtain maximum energy density or some other characteristic. Figure 4 shows a wheel concept which has the best potential for storing the maximum energy per pound of wheel. The wheel comprises a rim as the only moving part. The rim is magnetically supported at several points. The supports are part of a fixed structure. There is no physical contact between the rotating rim and the support "bearings".

The supports contain linear motor/generators which act as transducers in accelerating or decelerating the rim, therefore storing or extracting energy.

This rim-only concept is unique and can be compared to the Stodola wheel. The Stodola wheel, we know, is the ideal configuration for materials with isotropic physical strength characteristics. The material is usually high strength steel. Well-designed Stodola wheels can store about 12-14 watt-hours per pound.

The thin rim, rim-only, magnetically-supported wheel that incorporates high strength, circumferentially-wound fibers can store 60 watt-hours/lb. or more, depending on the life time desired. This wheel configuration can exploit fully the properties of anisotropic materials and possesses other attributes that I will touch upon.

Energy wheels are in competition with other devices. Figure 5 shows the rim-only energy wheel domain superimposed on a plot showing the domains of other devices. This plot has been extracted from an article titled "Batteries Power Urban Autos" by Drs. Elton J. Cairns and James McBreen of General Motors Research Laboratories, that appeared in the June, 1975 issue of Industrial Research. It can be seen that flywheels have the potential to compete in the energy and power domains.

Energy wheel system characteristics must be compared with those of other energy storage devices if one wishes to be realistic. Shown in Figure 6 are some of the main components of a flywheel (energy wheel) system. Some of these components must appear in all systems and all in some systems, depending on the application. Although ideal energy wheels may store >60 watt-hours/lb. of wheel, system energy density may be a small fraction of this number, if considerable weight must be allocated to housings, support structure and so on.

From a systems point of view then, we are interested in a number of considerations. Figure 7 lists some of these.

Shelf life must be considered if one is called upon to compare energy wheels with batteries. In Figure 8 we list three recently developed Stodola type wheels, supported on shafts equipped with ball bearings, and three magnetically supported wheels, one of which is a thin rim-only fiber wheel.

It can be seen that the torque/lb. of supported wheel weight is lower for

magnetically-supported wheels. The power to overcome bearing torque must come from the stored energy in a quiescent wheel. Wheel B, a carefully-designed metal wheel with very low friction bearings, will lose all its stored energy in 34 hours or less (if windage and other losses are considered).

Magnetically-supported fiber wheels, on the other hand, have the potential for much longer shelf life because they are subject to lower bearing losses and contain more energy/unit mass. One caveat, however--magnetically-supported wheels require power for suspension and this is another loss or drain on the stored energy. Wheel F rundown time is reduced, as shown, if this loss is included. It is anticipated that suspension power loss can be minimized.

Referring back to the system considerations list in Figure 7, we note that safety is a highly desirable characteristic. All metal wheels fail violently (usually in three pieces) and the debris must be contained by heavy crash barriers or housings. A fiber-magnetic wheel should fail more gracefully by shredding of the composite, heating of the composite, and probably some burst effects. It is likely that a low weight Kevlar cloth belt can be developed to contain all debris with little hazard to people and the wheel system support structure.

Systems dynamics is another area that must be addressed, particularly for mobile system applications--such as energy wheels for cars, trucks, buses, etc.

Energy wheels must be fail-safe if the vehicle overturns and wheel bearings must not experience high loads due to vehicle dynamics. Wheel systems may be compliantly mounted on springs or gimbal mounted as shown in Figure 9. In any event, the energy wheel has to be designed into the system and must meet the requirements involving inertial loading.

Energy wheel life is of considerable importance if wheels are to compete with other energy stores. A fiber rim-only, magnetically-supported wheel has the potential for long life. This type of wheel does not experience bearing wear. Life is ultimately determined by the sustained load rupture stress and fatigue stress properties of the composite rim. It is not unreasonable to anticipate life-

times of 10 to 20 years and an almost unlimited number of charge cycles. These attributes, plus the high power density that energy wheels can be designed for, would suggest that these devices will have a good future.

Incidentally, you may be interested in seeing a toroidal high vacuum enclosure which can be used to house a rim-only, magnetically-supported energy wheel (Figures 10 and 11). This enclosure was built for another purpose. However, it is interesting to note that this eight-foot, nominal diameter enclosure is made of aluminum with a thin wall section. Vacuum enclosures for rim-only wheels can therefore be built to meet minimum weight requirements.

Finally, there is the everpresent problem of designing to cost. A rim-only energy wheel is not likely to be less costly than a conventional wheel for the same performance. Both must show cost advantages over storage batteries and must meet economic criteria when used in different systems as indicated on this vu-graph (Figure 7). In my company we are developing cost models for energy wheels and their subsystems, using the highly successful RCA PRICE cost modeling technique of top-down cost estimating which permits rapid estimation of the effect of changes in system characteristics and manufacturing techniques on product cost. It would appear that energy wheels will be cost effective for many applications.

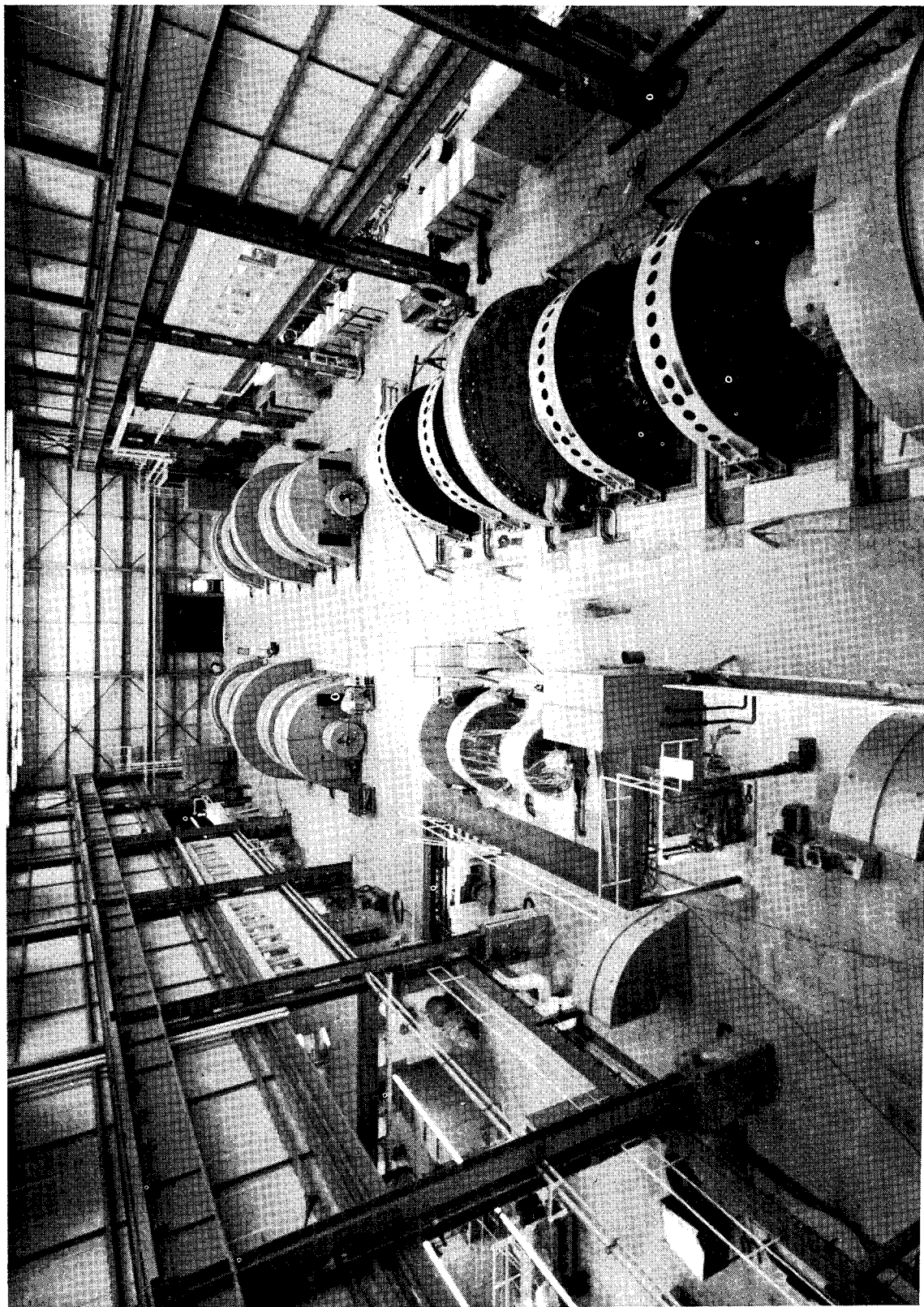


Fig. 1. Princeton University's Plasma Physics Laboratory Pulse Power Installation.

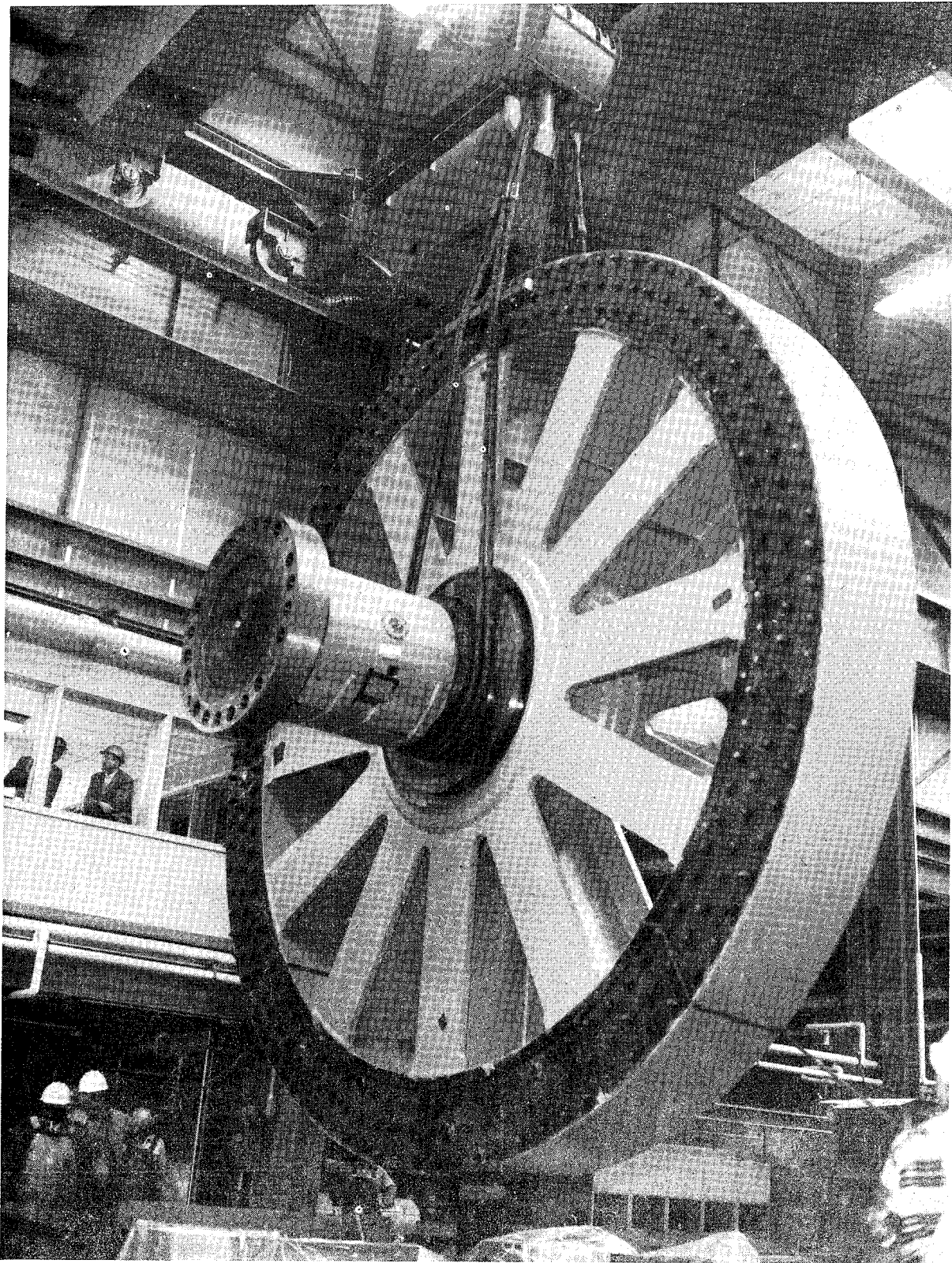
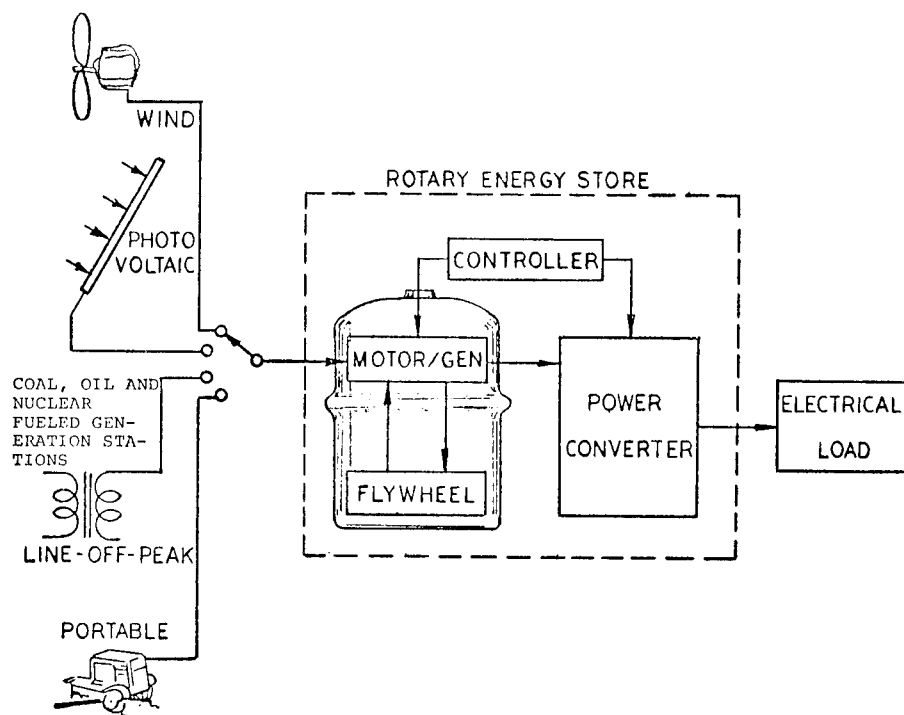


Fig. 2. 96 Ton Flywheel - One of Three
Used in Pulse Power Installation.

ROTARY ENERGY STORE



CIVIL

HOME
25 - 75 kw hr.
HOSPITAL
1500 - 3000 kw hr.
INDUSTRIAL PARK
1000 - 3000 kw hr.
SHOPPING MALL
3000 - 8000 kw hr.
GENERATION STATIONS
100 mw hr.
COMPUTER CENTERS

MILITARY

TACTICAL - PORTABLE
25 - 100 kw hr.
UNDERSEA TOOL AND LIGHTS
10 - 50 kw hr.
AIRCRAFT
1 - 5 kw hr.

SPACE

0.5 - 1.0 kw hr.

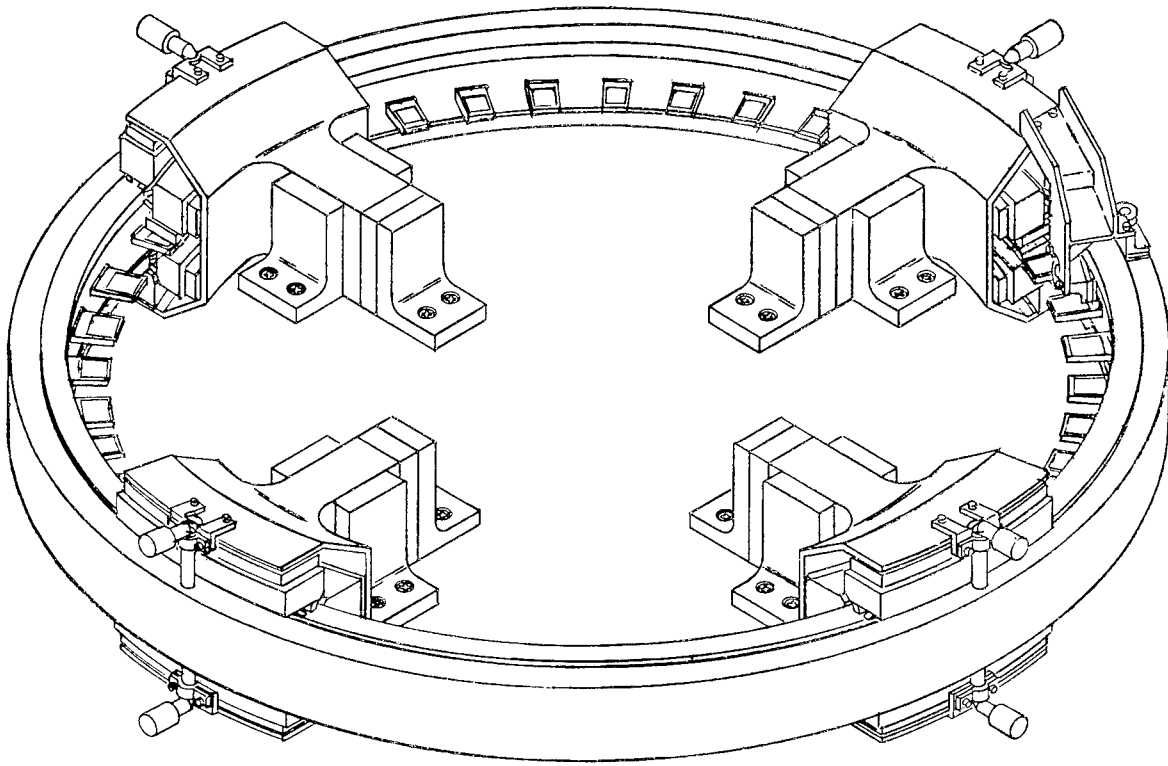
VEHICULAR

COMPACT CAR (100 mi)
30 kw hr.
INDUSTRIAL HANDLING
10 kw hr.
BUSES, VANS, ETC.
50 - 100 kw hr.

Figure 3. Rotary Energy Store.

Energy Wheel

Configuration



THE COMPOSITE STRUCTURE RIM IS THE ONLY MOVING PART IN THIS ENERGY STORAGE SYSTEM. THE RIM IS STABLY SUPPORTED RADIALY AND AXIALLY BY SERVOED ELECTROMAGNETS. BACKUP HYDROSTATIC GAS BEARINGS MAY ALSO BE BROUGHT INTO PLAY. LINEAR MOTOR/GENERATORS, MOUNTED IN THE SUPPORT ASSEMBLIES PROVIDE TORQUE FOR RIM SPEED UP AND SLOW DOWN, AND EXCHANGE OF ELECTRICAL AND MECHANICAL KINETIC ENERGY.

Fig. 4.

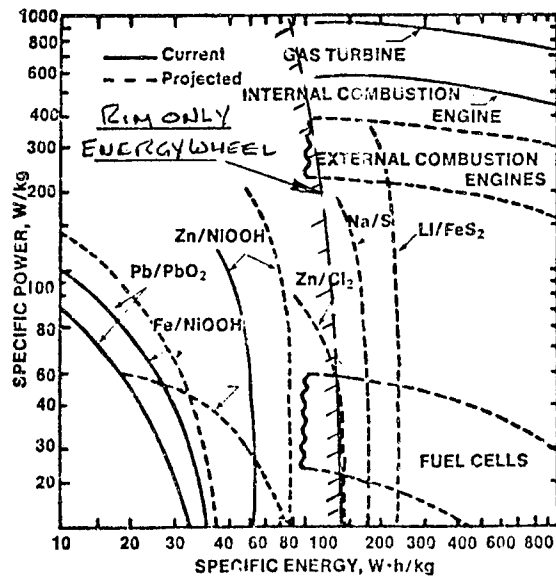


Fig. 5. The domains of competitive advanced battery and advanced energy wheel.

ENERGY WHEEL SYSTEM

-
- o WHEEL
 - o MOTOR/GENERATOR AND CONTROLS
 - o SUSPENSION SYSTEM AND CONTROLS
 - o HOUSING (VACUUM)
 - o HOUSING (SAFETY)
 - o SUPPORT STRUCTURE
 - o GIMBALS
 - o POWER CONDITIONER UNIT

Fig. 6. Energy Wheel System.

	<u>CONVENTIONAL</u>	<u>FIBER-MAGNETIC</u>
1. SHELF LIFE		✓
2. SAFETY		✓
3. SYSTEM WEIGHT AND ENERGY DENSITY/LB OF SYSTEM		✓
4. SYSTEM DYNAMICS		✓
5. LIFE		✓
6. COST*	?	?

*\$.16-.25/PEAK WATT - TO COMPETE WITH LEAD ACID BATTERIES.

GOAL OF \$.05/PEAK WATT TO COMPETE WITH PUMPED STORAGE FACILITIES
FOR UTILITIES.

Fig. 7. An Energy Wheel is not Just a Wheel.



SHELF LIFE AND FRICTION TORQUE OF WHEELS

	MECHANICALLY SUPPORTED			MAGNETICALLY SUPPORTED		
	A	B	C	D	E	F*
WT, LB	7.88	118.80	13.99	33	64	9.1
TORQUE, IN-OZ	2.68	20.39	1.98	.25	.8	.413
TORQUE/LB	.34	.17	.14	.0075	.0125	.0450
POWER LOSS, WTS/LB		.37				.08 (.1255)**
STORED ENERGY, WT HRS/LB		12.5				60
MAXIMUM SHELF LIFE, HRS		34				750 (480)

* FIBER WHEEL

**INCLUDES GOAL OF 5 WTS/1000 LB OF SUSPENDED WT

(REF. SAMSO PROGRAM ELEMENT 65806F)

Fig. 8. Shelf Life and Friction Torque
of Wheels.

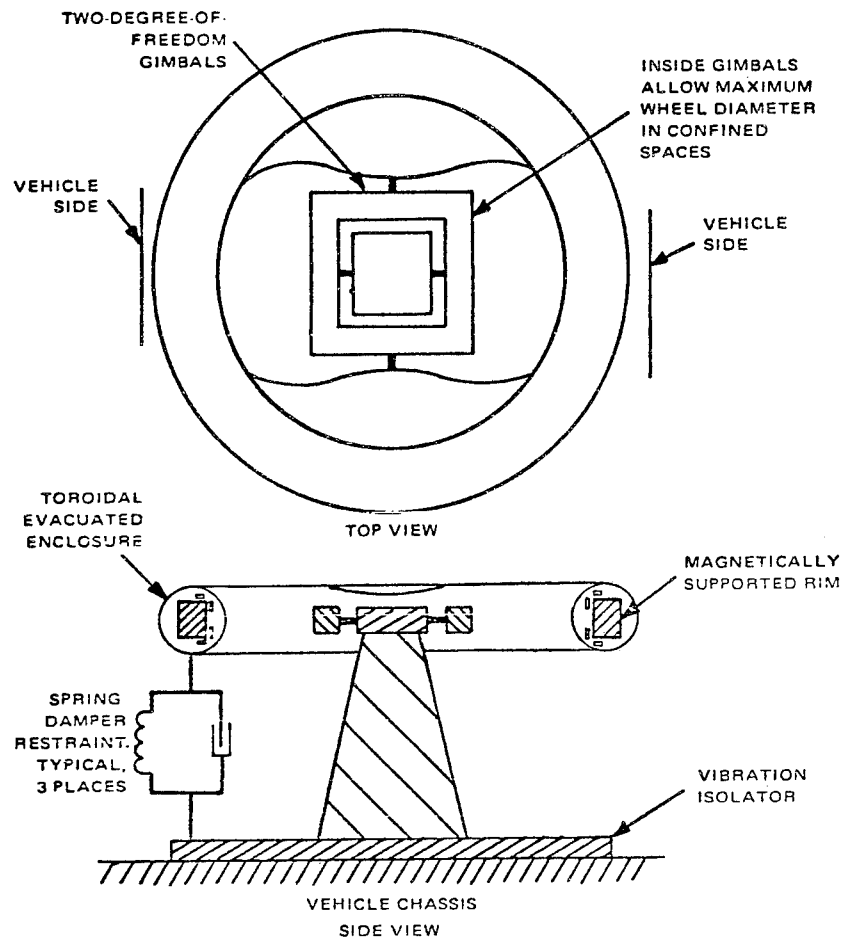


Fig. 9. Energy Wheel Suspension

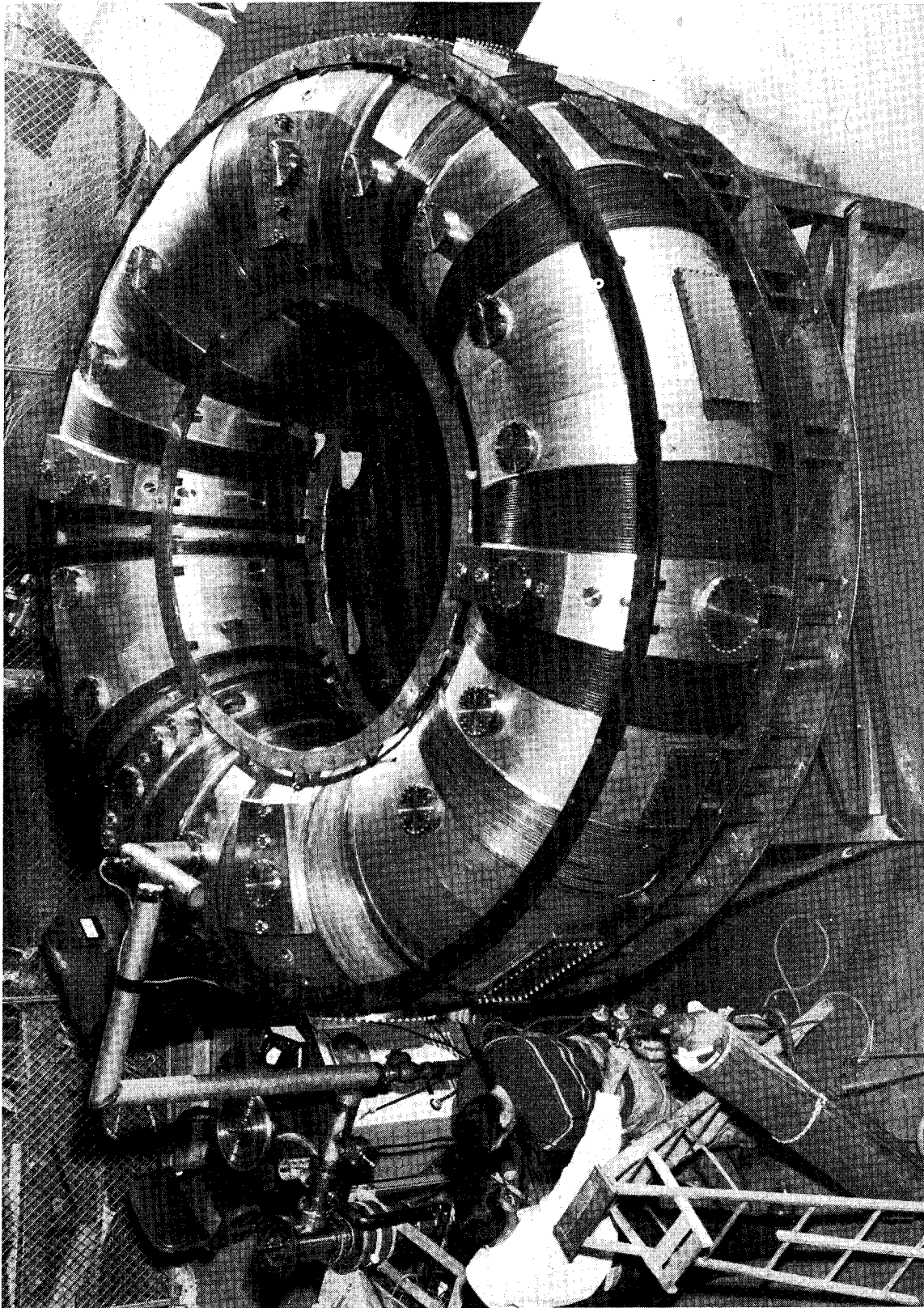


Fig. 10. Toroidal High Vacuum Enclosure.

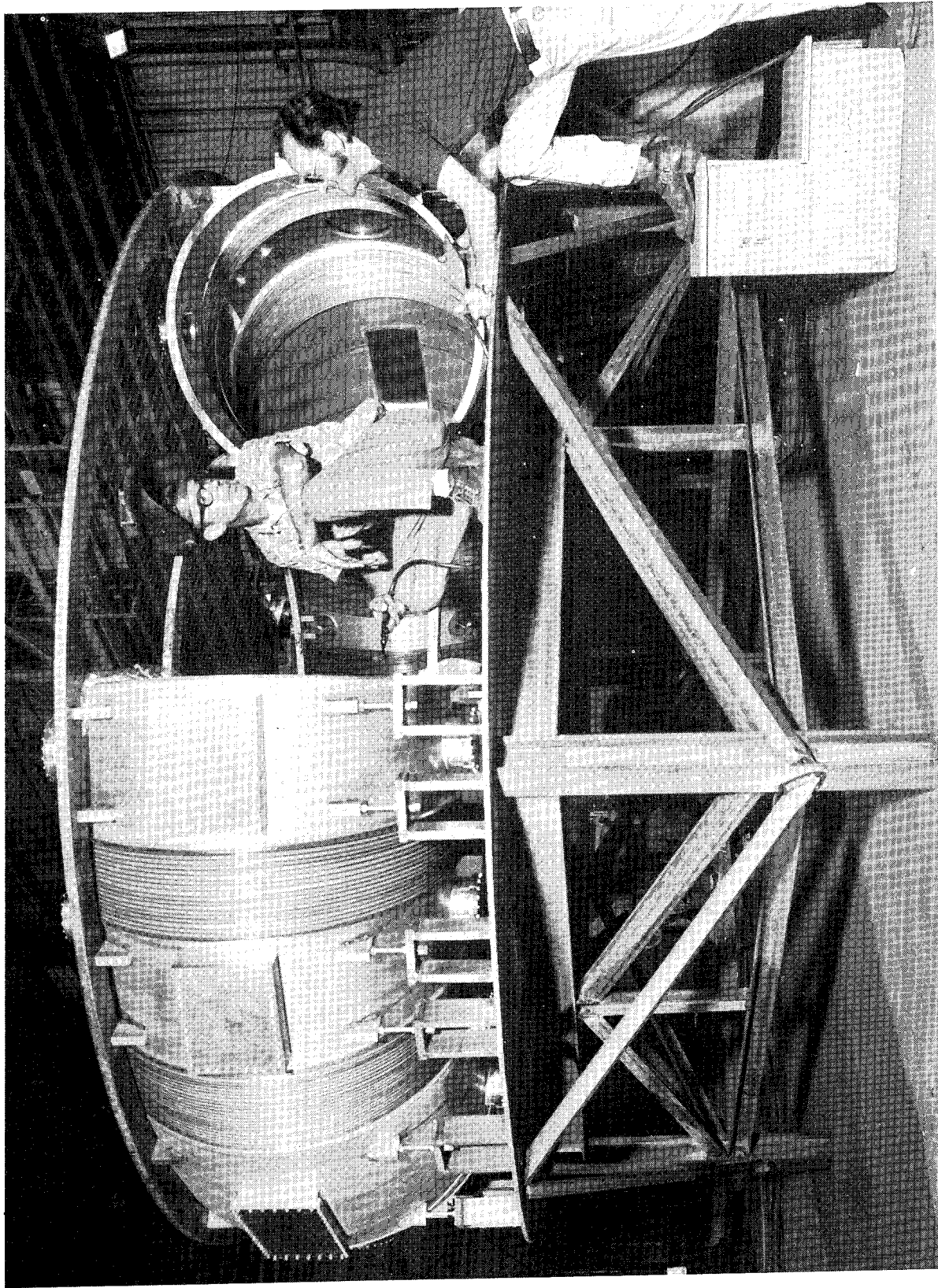


Fig. 11. Interior View of Vacuum Enclosure
Made of Thin Aluminum Plate.

PROGRAM FOR COMPOSITE FLYWHEELS*

T.T. Chiao and R.G. Stone
Lawrence Livermore Laboratory, University of California
Livermore, California 94550

ABSTRACT

The Lawrence Livermore Laboratory has mapped out a flywheel development program intended to 1) provide a data base for engineering design, 2) solve some long-standing problems of composites and 3) develop flywheel manufacturing processes. Information generated will be disseminated promptly to industry.

In our studies of composites we will characterize fiber-resin matrices, measure their static engineering properties, including those that are time-dependent, examine failure criteria, reliability and fatigue resistance and study hybrid fiber resin constructions.

We plan to build model flywheels and to evaluate techniques for their mass production.

INTRODUCTION

As a unit of the U.S. Energy Research and Development Administration, LLL is interested in many types of energy utilization, including solar power, geothermal steam, nuclear power, underground mining and coal conservation and wind power. Our mission also includes development of techniques for energy storage and withdrawal, as in flywheels.

Studies of fiber composites suitable for flywheels have been underway in our laboratory for some time. Some of the results available so far will be described by members of our staff during this symposium.

This paper describes plans for the enlarged flywheel development program now starting at LLL.

APPROACHES

1. We plan to map out an overall composite program and divide it into logical pieces, which can then be selectively studied according to relative priority and available funding.

2. Data generated from this program should be basic data and should be useable generally for a composite flywheel of any design.
3. To avoid confusion, experimental data from simple composite specimens will be used to rank material systems. Thus, the engineering data developed will be based on realistic specimens.
4. We will disseminate credible information to industry promptly through formal meetings, personal contact, technical reports and consultations.

SCOPE

1. Characterization of Material Systems
The candidate matrices are epoxies and polyesters. The candidate ** fibers are S2-glass, Kevlar 29, Kevlar 49, E-glass and low cost graphites. We plan to use matrix-impregnated fiber strands to evaluate the fiber strength distribution, density, and cost. Approximately three composite systems will be selected for in-depth study in the program.

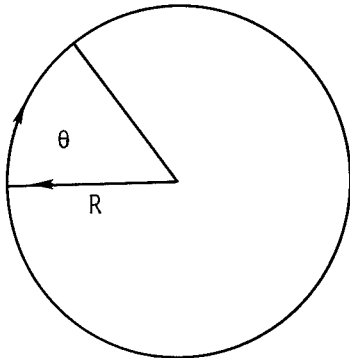
*This work was performed under the auspices of the U.S. Energy Research & Development Administration under contract no. W-7405-Eng-48.

**Reference to a company or product name does not imply approval or recommendation of the product by the University of California or the U.S. Energy Research and Development Administration to the exclusion of others that may be suitable.

2. Static Engineering Composite Properties for Preliminary Design

In a centrifugal field, the non-zero stresses are:

σ_θ , circumferential; σ_R , radial; and $\sigma_{R\theta}$, shear.



In testing composite materials, it is more convenient to replace the cylindrical coordinates, θ - Z - R , with rectangular coordinates, 1-2-3. Using simple composite test specimens, we will measure the elastic properties, such as moduli (E_{11} , E_{22} , E_{33} , G_{12} = G_{13} and G_{23}) and Poisson's ratios (ν_{12} = ν_{13} , ν_{22} , and ν_{23}) and strength properties in tension (X_1 , X_2 = X_3) and in shear (X_5 and X_6).¹ Initially, these engineering design allowables will be measured using composites that have a volumetric fiber content in the range of 75-80%.

3. Time-Dependent Engineering Properties of Composites

Time-dependent properties such as stress-rupture and creep are important in considering long-term performance of composites. We plan to study this subject using matrix impregnated fiber strands. Stress-rupture experiments can be carried out in our existing facilities.

4. Failure Criteria and Reliability of Composites

Failure criteria and the reliability of composites are areas that require

major study if composites are to be used in long term applications. To use flywheels safely in cars, for example, we must be able to recognize signs of impending flywheel failure and have assurance that the wheel will pulverize itself if it fails.

5. Composite Flywheel Manufacturing Process Development

Mass production techniques and variational limits need to be evaluated to bring the cost of the composite flywheel down. We also plan to fabricate some flywheel models for testing.

6. Hybrid Composites

The weakest property of any fiber composite is in shear, particularly in the thickness direction. Hybrid construction that combines two or more fibers in a common matrix is a very attractive concept that would insure strain compatibility and minimize radial growth of a composite flywheel under stress. We plan to develop material and preliminary engineering design data on several such systems.

7. Fatigue Resistance of Composites

Cyclic tension-tension (5 to 100% of design load) fatigue to simulate actual applications of a flywheel is also important. Depending on the design of the fatigue machine, ring specimens can be used. Data can be obtained at a room temperature initially.

For some flywheel designs, fatigue under shear or combined stresses may be particularly important. In this case ring specimens under cyclic flexural loading is preferred.

PLANS FOR THE FISCAL YEAR 1976

This year we are concentrating on raw materials characterization, static composite properties and improved government-industry interaction. However, we will make a limited effort to study time-dependent properties, such as stress-rupture, and to improve the filament winding process.

CURRENT PROGRAM STATUS

1. For long term technical program planning, LLL has a team of distinguished consultants to provide guidance:

Dr. C. Chamis, NASA - Lewis
Dr. R. Christensen, Washington University
Dr. T. Toland, Drexel University
Dr. E. Wu, Washington University

2. In the area of the epoxy matrix, we have recommended several formulations for flywheel winding. Mr. J. Rinde will summarize the details in a separate presentation.
3. The key candidate fibers are E-glass, S2-glass, Kevlar 29 and Kevlar 49. They will be evaluated in terms of strength, density and cost using both epoxy-coated strands and NOL lab scale rings. Dr. L. Penn will be reporting data available to date in this area.
4. Static composite properties are important for preliminary engineering design. Our data to date on Kevlar 49/epoxy and E-glass/epoxy will be reported by Dr. L. Clements.
5. Long term performance of fiber composites is vital for flywheel applications. LLL has already amassed up to 6 years of stress

rupture data on a couple of composites. We have just begun to study creep in the matrix. Ms. C. Chiao will summarize these data later in this symposium.

6. Bearings are key components in a fly-wheel system. LLL has been studying the magnetic system and performing some experimental work. K. Aaland and J. Lane will be presenting their results.

CONCLUSIONS

LLL is anxious to help industry develop flywheels as successful energy storage devices. We are:

1. Providing basic data which can be used in any flywheel design.
2. Working to solve problems that cannot be solved by any one company.
3. Screening and disseminating information useful for flywheel design and construction.

NOTICE

"This report was prepared as an account of work sponsored by the United States Government. Neither the United States nor the United States Energy Research & Development Administration, nor any of their employees, nor any of their contractors, subcontractors, or their employees, makes any warranty, express or implied, or assumes any legal liability or responsibility for the accuracy, completeness or usefulness of any information, apparatus, product or process disclosed, or represents that its use would not infringe privately-owned rights."

DESIGN, CONSTRUCTION AND TESTING OF ADVANCED COMPOSITE FLYWHEELS
AT THE U. S. NAVAL ACADEMY

Dr. Robert A. McCoy
Naval Systems Engineering Department
U. S. Naval Academy
Annapolis, Maryland 21402

ABSTRACT

Flywheels based on two configurations, an optimized disc and an optimized bar, will be built by layup techniques from high strength E-glass/epoxy tape. The 25-lb. models will be tested in an evacuated chamber.

INTRODUCTION

One hundred years ago the U. S. Navy was using flywheel energy to propel its Howell torpedo. Today there are numerous naval applications of flywheels as energy storage devices and for gyroscopic control associated with the operation of ships, submarines, aircraft, aircraft catapults, rockets, and missiles. Thus the U. S. Navy, like most other technically oriented segments of today's society, is keenly interested in technological advancement in the area of flywheels.

In recent years the very high specific strengths (strength to density ratio) of advanced filamentary composite materials have led to the design and construction of flywheels having new and highly efficient configurations. The next logical step is the design development of such flywheels leading to the fabrication, testing, and evaluation of promising designs. These are the technical objectives of this project being performed at the U. S. Naval Academy.

FLYWHEEL CONFIGURATIONS AND MATERIALS

In optimizing the design of flywheels, the selection of both the flywheel configuration and the materials used in their construction are of vital importance. Much literature has recently been published surveying the most promising configurations and materials along with their associated parameters, (References 1-5). Tradeoffs among the flywheel parameters of specific energy (energy stored per unit weight of flywheel), specific volume (energy stored per unit volume of fly-

wheel), and specific cost (energy stored per unit cost of flywheel) must often be performed.

For this project two configurations were selected for further design development: the optimized disc and the optimized bar (Figures 1 and 2). Design calculations are being based upon what appears to be one of the most promising materials available today for the construction of advanced composites--Kevlar 49/epoxy filamentary composites. The two flywheel models to be built will weigh approximately 25 pounds each and should be able to store up to 1 kWh if rotated at the maximum allowable speed.

FABRICATION AND TESTING

The first models will be fabricated of Scotchply SP-250 unidirectional prepreg tape. This tape is a high-strength moldable E-glass/epoxy tape that will cure at temperatures as low as 250°F and at mold pressures of 50 to 100 psi. Initially several layup techniques will be attempted to build up the desired configurations before the best technique is selected.

The chamber for testing the flywheel models is shown in Figure 3. Tests will be conducted in a vacuum of 10^{-2} torr and a maximum rotational speed of 5000 rpm.

The objectives of the tests will be to verify the following:

1. structural integrity of the models
2. shape factors

3. energy storage capacities

SUMMARY

A research project is now underway at the U. S. Naval Academy to design, fabricate, and test advanced composite flywheels. The project is now emerging from the design phase and entering the model fabrication phase. Models up to 25 pounds in weight will be tested in an evacuated chamber at speeds up to 5000 rpm.

So the Navy's future looks bright with both advanced flywheels and women Naval Academy officers to keep it running smoothly and efficiently.

Acknowledgment

This project is being performed as part of the Energy Environment Study Group of the U. S. Naval Academy and is being funded by the Naval Material Command.

References

1. Fullman, R. L., Tenth Intersociety Energy Conversion Eng. Conf., August, 1975; Paper 759017.
2. Biggs, F., Sandia Laboratories Report SAND 74-0113, November, 1974.
3. Dugger, G. L., et al, Johns Hopkins University Applied Physics Laboratory Report PB-213035, March 1972.
4. Rabenhorst, D. W., 1971 Intersociety Energy Conversion Eng. Conf., Paper 719148.
5. Gilbert, R. R., et al, Lockheed Report LMSC-D007915, April 1971.

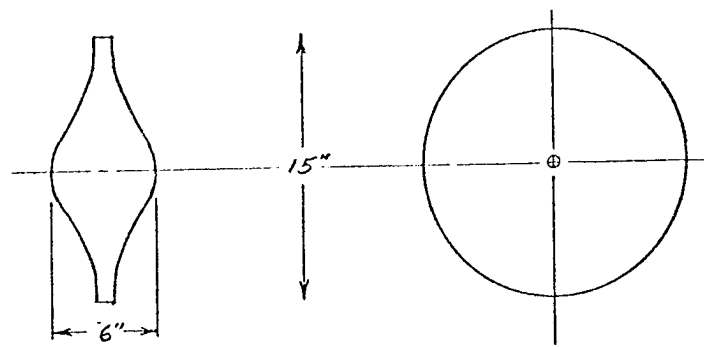


Figure 1. Optimized Disk

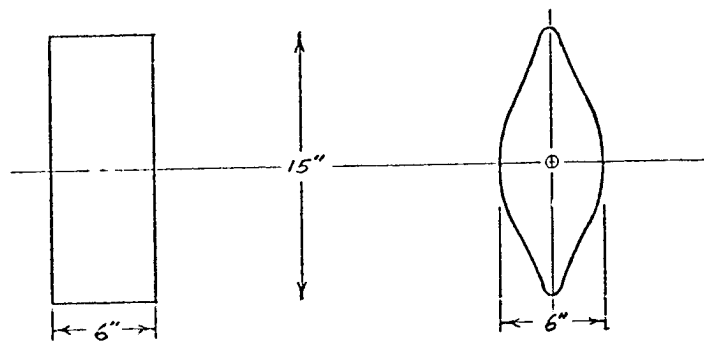


Figure 2. Optimized Bar

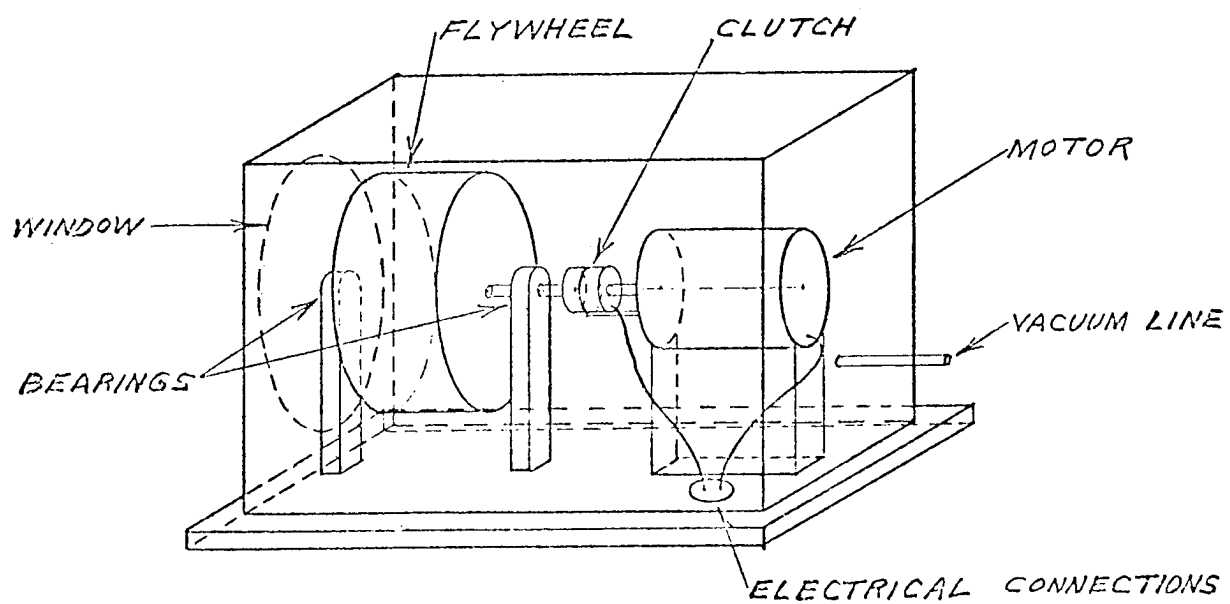


Figure 3. Flywheel Test Chamber

KEVLAR/EPOXY FLYWHEELS: AN EXPERIMENTAL STUDY*

M. Moss and F. P. Gerstle, Jr.
Composite Materials Development Division 5844
Sandia Laboratories
Albuquerque, New Mexico 87115

ABSTRACT

Regardless of configuration, the energy density of a flywheel is some fraction of the specific strength of the material of which it is made. Because those engineering materials that have the highest specific strengths (filament-reinforced resins) are highly anisotropic, there is no single optimum configuration for all such materials if their mechanical properties are to be fully exploited. Based upon our analytical and experimental studies, we have found that a highly efficient flywheel geometry for anisotropic materials is a circumferentially-wound solid disk. Using flat disks 21 cm in diameter and 3 cm thick, made from Kevlar 49 yarns that were wet-wound circumferentially with epoxy resin, speeds of 21,000 rpm were achieved (the maximum in our present facility) without visible damage to the disks. At this speed the energy density was 1.7 watt-hour/lb.

*This work was supported by the U. S. Energy Research & Development Administration.

Fabricated Kevlar 49-Epoxy Flywheels

Flywheel	ID (cm)	OD (cm)	t (cm)	m (kg)	V _f	E _θ [*] (Msi)	E _r [*] (Msi)	Epoxy	Cure
A	1.0	20	3.0	1.22	0.44	8.6	1.0	a	2 days 70°F + 16 h 165°F
B	1.0	21	3.1	1.31	0.63	12.3	1.0	a	2 days 70°F + 16 h 165°F
C	2.0	41	6.0	10.5	0.61	12.2	1.1	a	70°F
D	2.0	22	6.0	2.91	0.70	12.0	1.2	b	16 h 70°F + 2 h 130°F (step cured)

* Measured ultrasonically.

^a DER 332/Jeffamine T-403:100/36

^b DER 332/DER 732/Jeffamine T-403:80/20/36

TEST RESULTS

Flywheel	Max. Speed (10 ³ rpm)	Energy Density (Wh/lb)	Failure Mode	Maximum Strain (%)			
				Calculated Radial	Calculated Hoop	Measured Radial	Measured Hoop
A	21	1.7	None	0.078	0.057	--	--
B	21	1.7	None	0.067	0.041	--	--
C	16.2	3.9	Circumferential crack	0.16	0.11	0.20	0.11
D	19	1.5	Flywheel damaged as result of shaft failure	0.072	0.045	--	--

CONCLUSIONS TO DATE

1. Steady-state analysis supported.
2. Failure controlled by radial tensile strain.
3. Fabrication and curing stresses must be controlled.



GARRETT'S OUTLOOK ON VEHICLE FLYWHEELS

J. A. Friedericy and A. E. Raynard
Garrett Airesearch
2525 West 190th Street
Torrance, California 90509

ABSTRACT

The following viewgraph presentation has been given by Garrett at the Flywheel Technology Symposium hosted by the Lawrence Livermore Laboratories, November 10, 11, 12, 1975:

1. ENERGY STORAGE CAR (R32)

This viewgraph presents a picture of the MTA32 subway car running in New York and the introduction of a schematic of the flywheel-flywheel motor system.

2. PROPULSION SYSTEM SCHEMATIC

This chart describes the schematic of the propulsion and energy storage electrical networks.

3. ESC FEATURES

The goodness of the energy storage principles are summarized in this chart.

4. ENERGY SAVINGS

Typical percent energy savings are plotted against station dwell time. The savings in terms of the energy storage car with the flywheel and without the flywheel are shown in graphic form.

5. DESIGN CONSIDERATIONS

This chart summarizes the four major areas that need to be considered on the design of an energy storage car. The four areas are:

Material selection for the flywheel rotor

Specific energy capabilities of the flywheel rotor

Design for safety, and

Flywheel system efficiencies (losses)

6. MATERIALS FOR FLYWHEEL APPLICATIONS

This chart shows candidate materials, steel as well as composite, in terms of their working stresses, specific strengths and raw material cost per pound.

7. ROTOR SPECIFIC ENERGY

This chart presents in graphic form watt-hrs/lb that can be expected from steel and composite material flywheels. Its purpose is to illustrate the superiority of the composite material flywheel over the steel flywheel in terms of specific energy.

8. DESIGN FOR SAFETY

In this chart the pros and cons of safe life vs fail safe design are summarized. Typically, safe life design is required for steel flywheels since fail safe design (containment) for these flywheels is expensive and very heavy. Composite material flywheels are much easier to contain and require much less material (steel) to do this. Further, safe life design is expensive because it requires inspections at regular intervals. This is not required in fail safe design since the containment ring is not expected to deteriorate during service life.

9. CONTAINMENT COMPARISON

A comparison is given between containment requirements for steel flywheels and containment requirements for composite material flywheels. The reasons why this is so are also given.

10. ENERGY SAVINGS DUE TO FLYWHEEL
STORAGE

The dependency of the effectiveness of the flywheel energy storage approach is demonstrated here in terms of station distance.

11. TYPICAL ENERGY STORAGE FLYWHEEL--
ROUND TRIP LOSSES

Percent losses are given for the various components in the flywheel and shows percent losses in bearings, seals, pumps, and windage losses. Also given are the percent losses in the electrical systems, such as the flywheel motor and traction motor, as well as mechanical losses in the gearboxes.

12. GEARBOX LOSSES VS LOAD/SPEED

The changes in gearbox losses in terms of operating speed levels and mechanical torque load levels are plotted.

13. BEARING LOSSES/SEAL LOSSES VERSUS
LOAD/SPEED

This chart demonstrates the importance of minimizing bearing/seal losses.

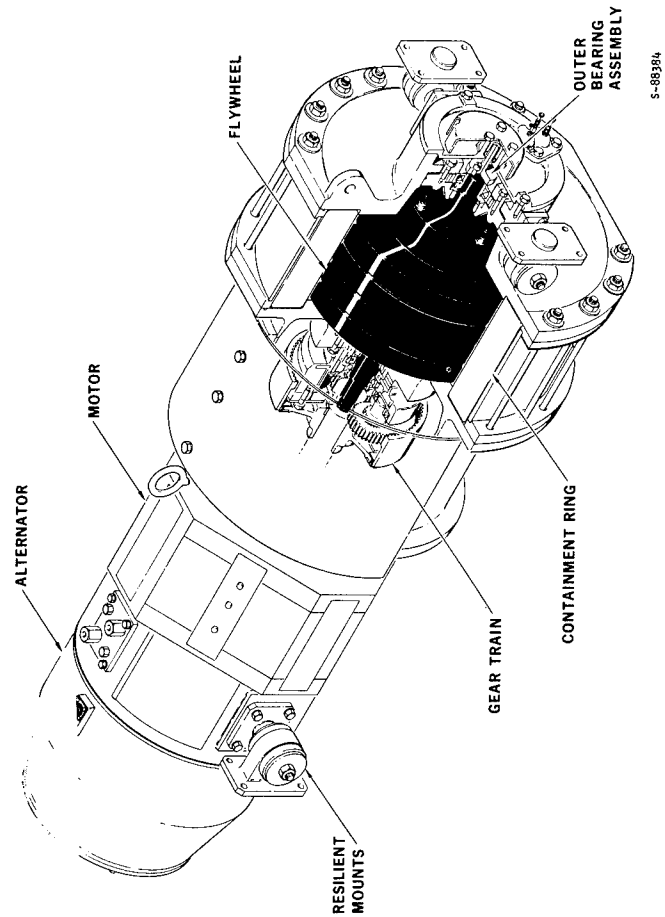
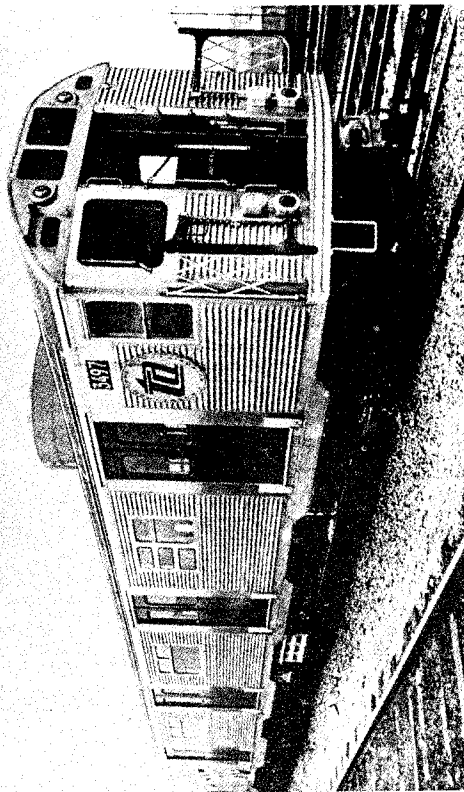
14. WINDAGE LOSSES VS SPEED/HOUSING
PRESSURE

The windage losses of the rotor are shown in terms of the vacuum levels in the housing. It shows the amount of vacuum pressure required such that windage losses are not significant.

15. COMPOSITE FLYWHEEL VIEW

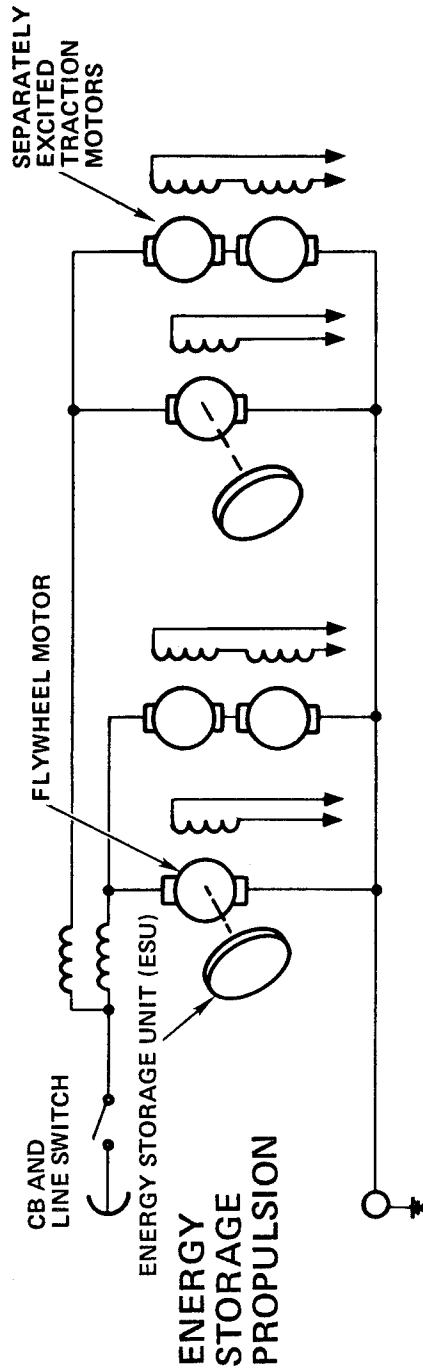
The purpose of this chart is to make the audience aware that AiResearch is involved in studying a composite material flywheel under a MERDC contract.

NYCTA R-32 CARS WITH ENERGY STORAGE SYSTEM

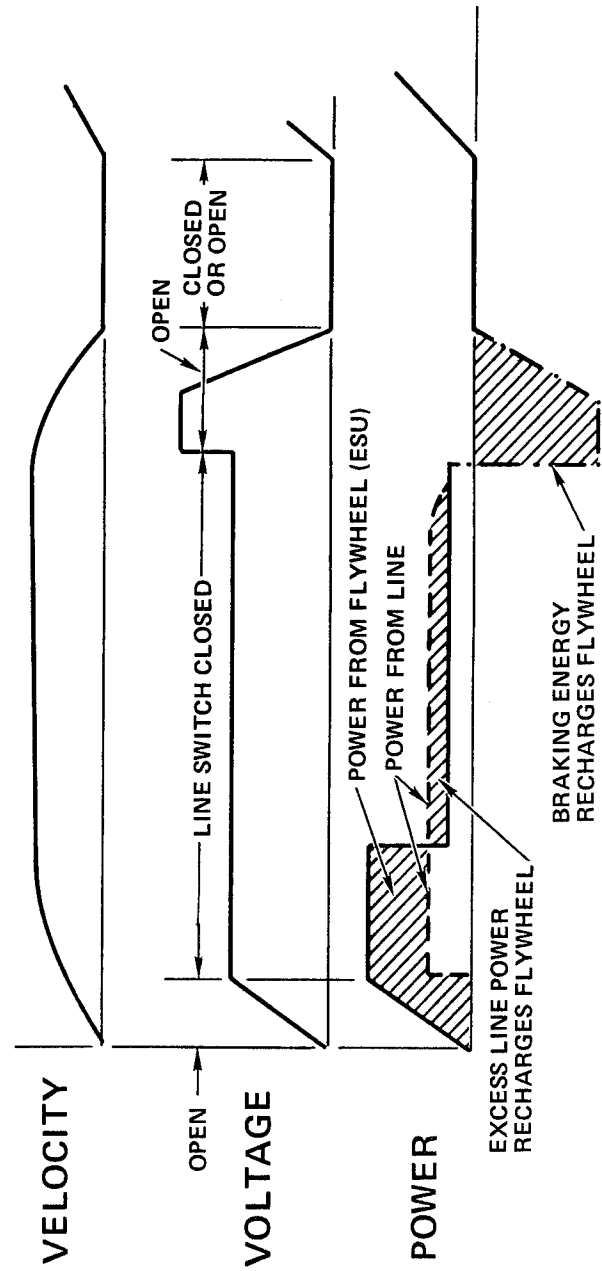


ENERGY STORAGE PROPULSION SYSTEM

ESU SCHEMATIC



ESU TYPICAL CYCLE

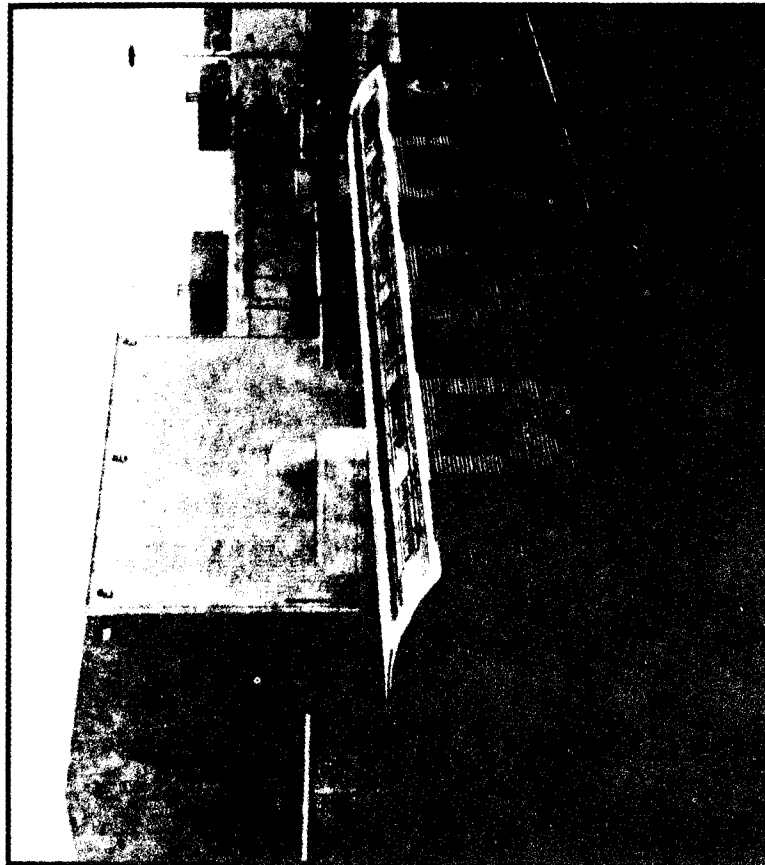
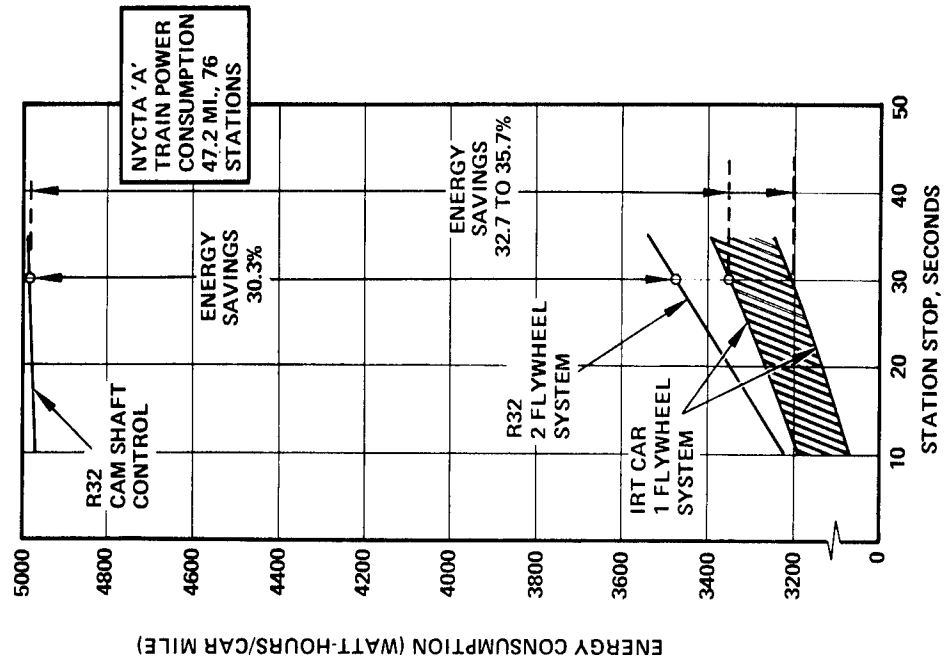


ENERGY STORAGE ADVANTAGES

- **REDUCTION IN POWER CONSUMPTION**
- **REDUCTION IN TUNNEL HEATING**
- **SAFETY FEATURES DURING POWER LOSS**
- **INCREASES CAPACITY OF EXISTING SYSTEM**



ENERGY SAVINGS



DESIGN CONSIDERATIONS

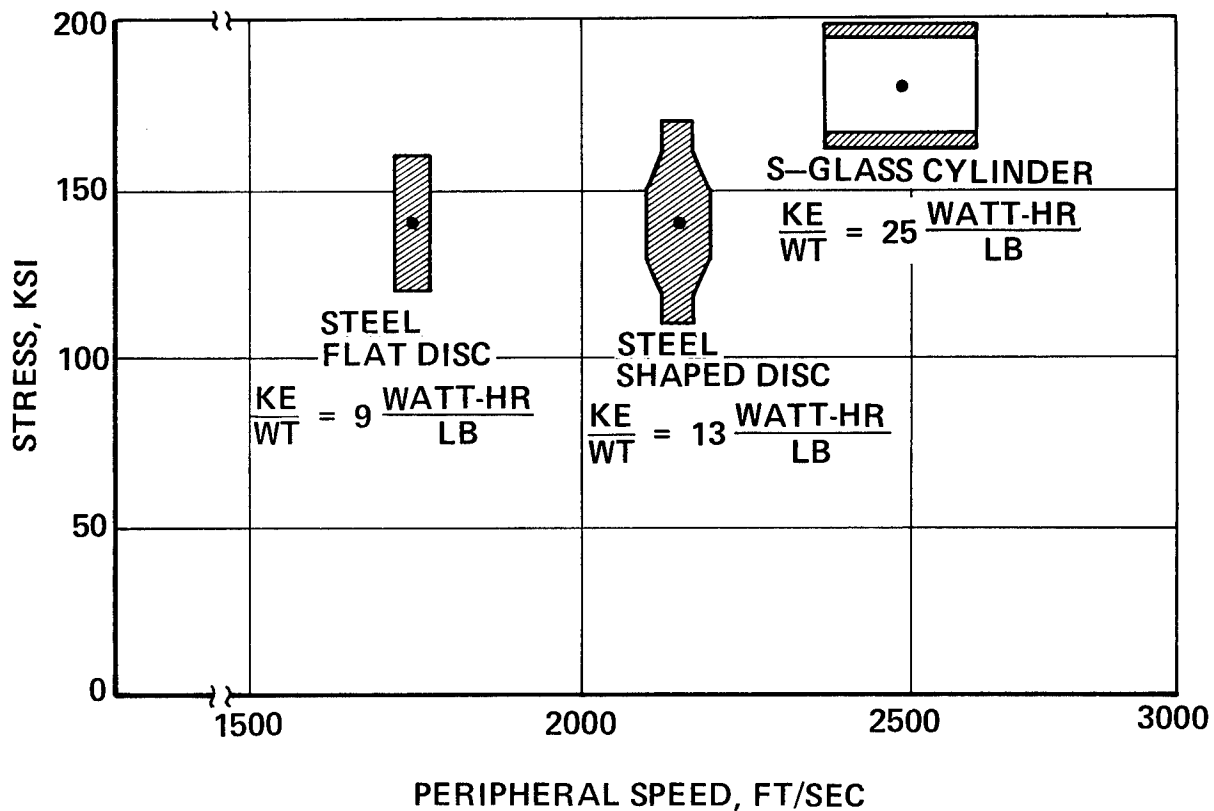
- MATERIALS FOR FLYWHEEL APPLICATION
- ROTOR SPECIFIC ENERGY
- DESIGN FOR SAFETY
- FLYWHEEL SYSTEM EFFICIENCIES



MATERIALS FOR FLYWHEEL APPLICATIONS

MATERIAL	ULTIMATE TENSILE STRENGTH, KSI	"USABLE" TENSILE STRENGTH, KSI		DENSITY LB/IN.	STRENGTH/DENSITY IN.-LB/LB x 10 ⁶		RAW MATERIAL COST \$/LB	RELATIVE RATING STRESS
		LONG TERM	SHORT TERM		LONG TERM	SHORT TERM		DENSITY / COST IN.-LB/\$ LONG TERM
STEELS								
4340 STEEL	220	140	160	0.283	0.49	0.56	0.90	0.54
HP 9-4-20	200	140	160	0.284	0.49	0.56	2.90	0.17
18 Ni (300)	300	150	200	0.289	0.52	0.69	6.00	0.09
COMPOSITES								
E-GLASS EPOXY	200	120	150	0.080	1.50	1.87	1.20	1.25
S-GLASS EPOXY	300	180	225	0.079	2.28	2.84	1.90	1.20
KEVLAR-EPOXY	280	170	210	0.052	3.27	4.04	4.80	0.68
GRAPHITE-EPOXY	230	140	170	0.058	2.41	2.93	44.00	0.06

ROTOR SPECIFIC ENERGY



DESIGN FOR SAFETY

SAFE LIFE

FRACTURE MECHANICS
INSPECTION INTERVAL

INSPECTION
ACOUSTIC HOLOGRAPHY
FLUORESCENT PENETRANT

MAINTENANCE
ACOUSTIC HOLOGRAPHY
FLUORESCENT PENETRANT

- MORE APPLICABLE FOR METAL FLYWHEELS

- COSTLY

FAIL-SAFE

CONTAINMENT DESIGN

ATTACHMENTS DESIGN

- LIGHTER WEIGHT DESIGN WITH COMPOSITE FLYWHEELS



CONTAINMENT COMPARISON

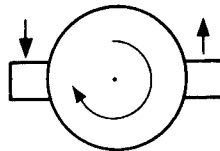
METAL FLYWHEELS

DESIGN FOR PIERCING

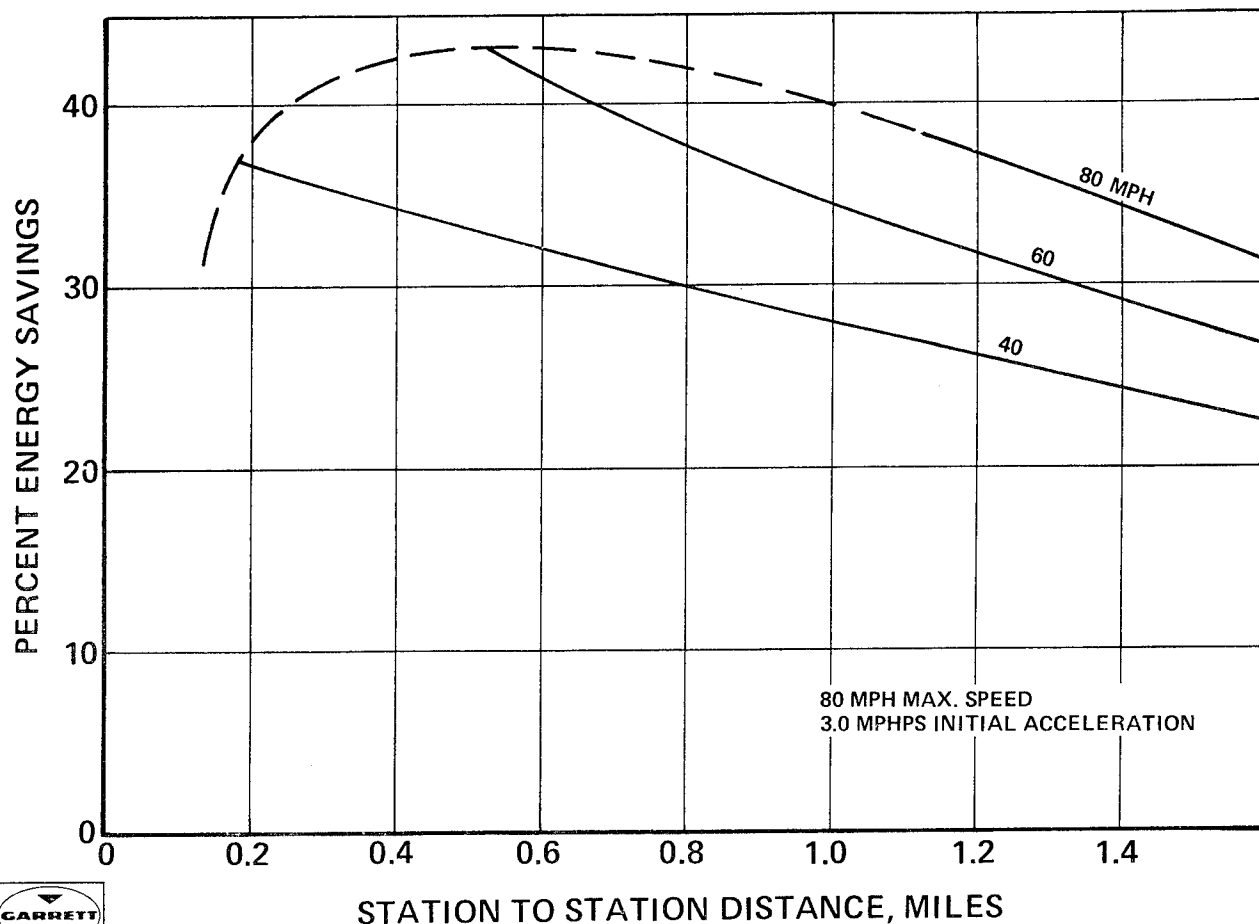
COMPOSITE MATERIAL FLYWHEELS

DESIGN FOR HYDRODYNAMIC BURST

FORCES TO GROUND FROM BURST OF A COMPOSITE MATERIAL FLYWHEEL ARE ESTIMATED TO BE 20 PERCENT OF THOSE EXPERIENCED BY A METAL FLYWHEEL



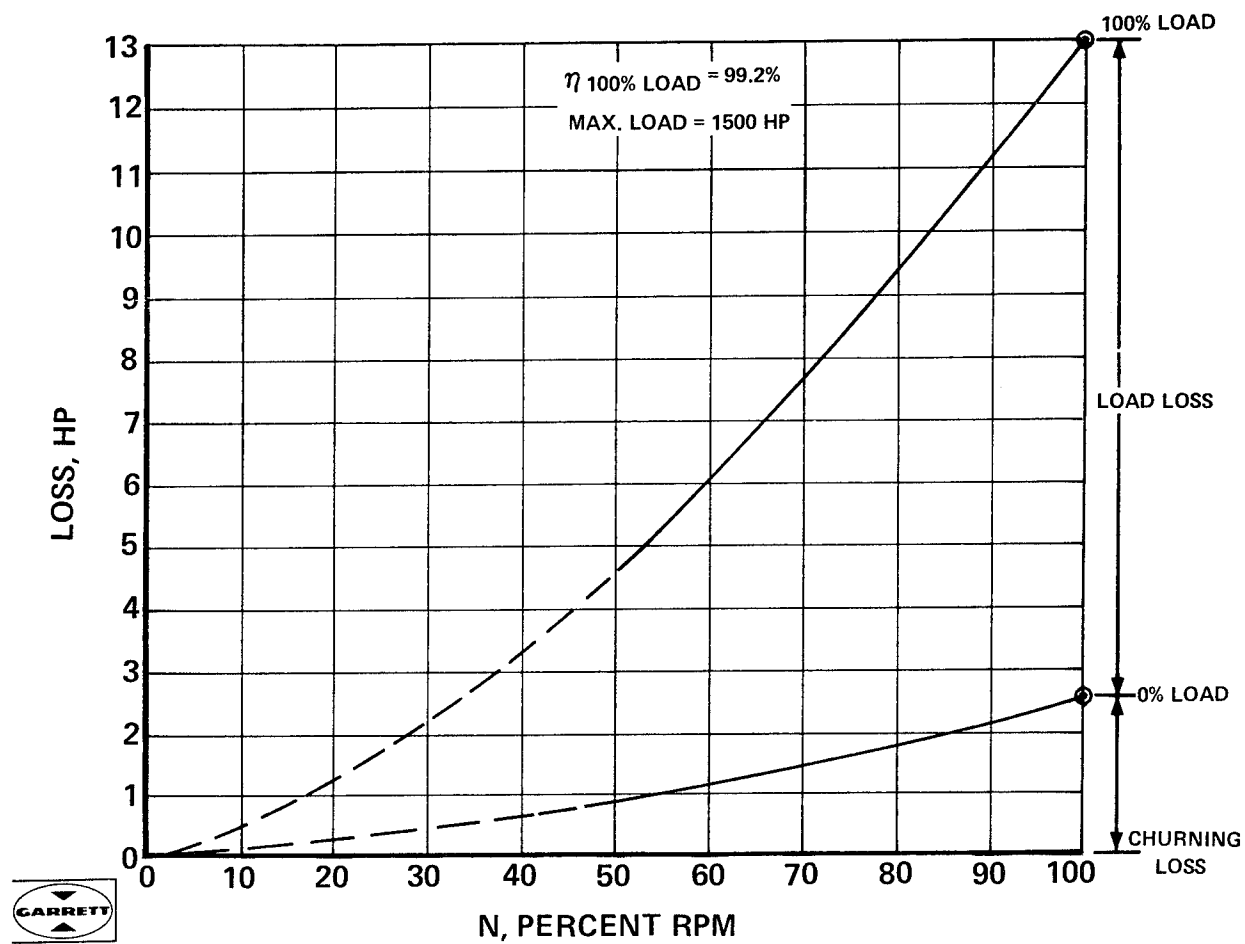
ENERGY SAVINGS DUE TO FLYWHEEL STORAGE



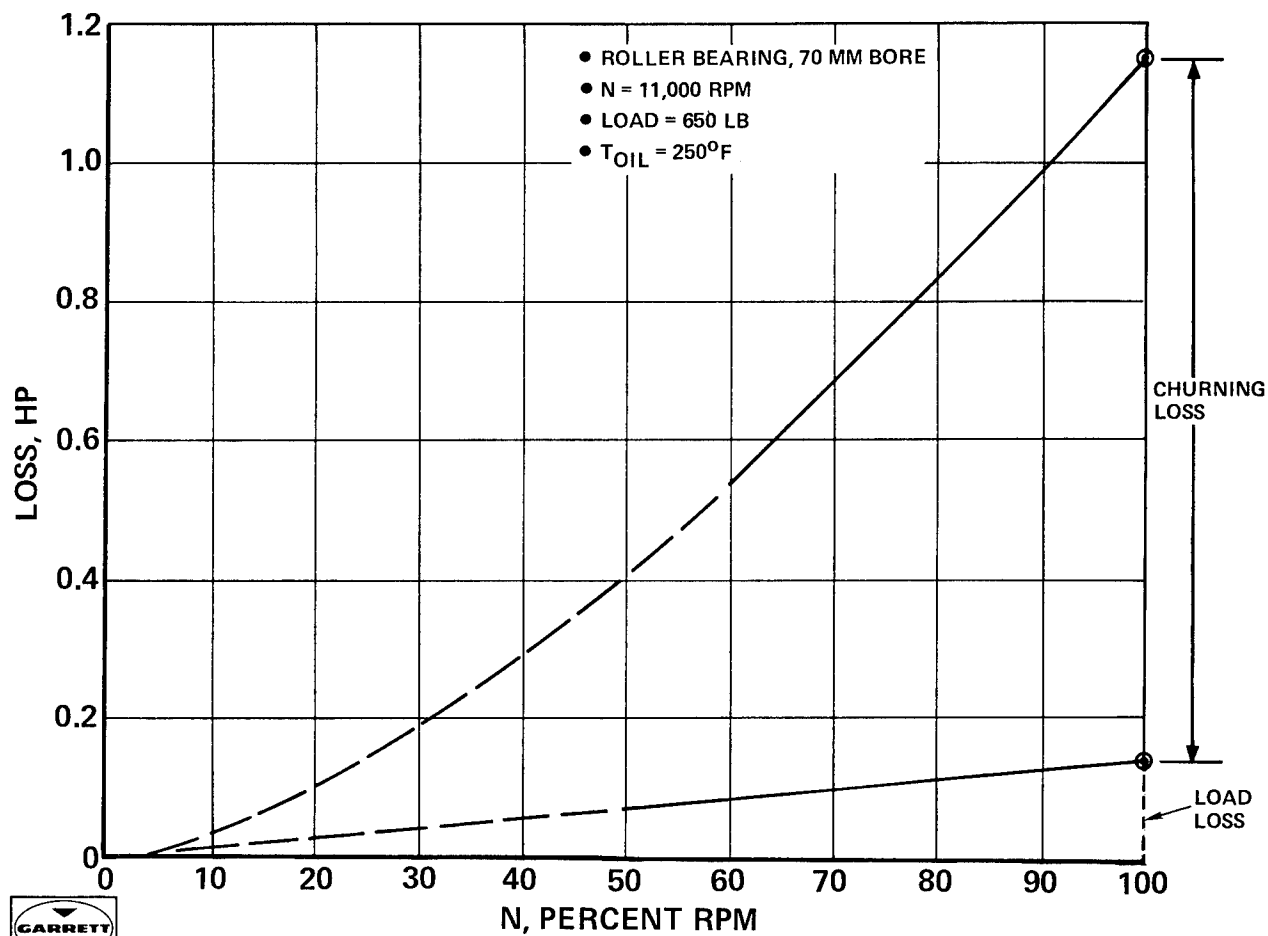
TYPICAL ENERGY STORAGE FLYWHEEL ROUNDTrip LOSSES

● STANDBY LOSSES AT 100 PERCENT RPM		PERCENT LOSS
● WINDAGE, FLYWHEEL	15	} 0.5% OF RATED LOAD
● ROTOR BEARINGS (2)	30	
● ROTOR SEALS (2)	5	
● PLANETARY GEARS (NO LOAD)	25	
● PLANETARY BEARINGS (6)	10	
● LUBRICATION PUMP	8	
● VACUUM PUMP	7	
● INPUT/OUTPUT EFFICIENCY AT RATED LOAD		67% ROUND TRIP
● ELECTRICAL – FLYWHEEL	93%	
● ELECTRICAL – TRACTION MOTOR	93%	
● GEARBOX – FLYWHEEL	99%	
● GEARBOX – TRACTION MOTOR	95%	

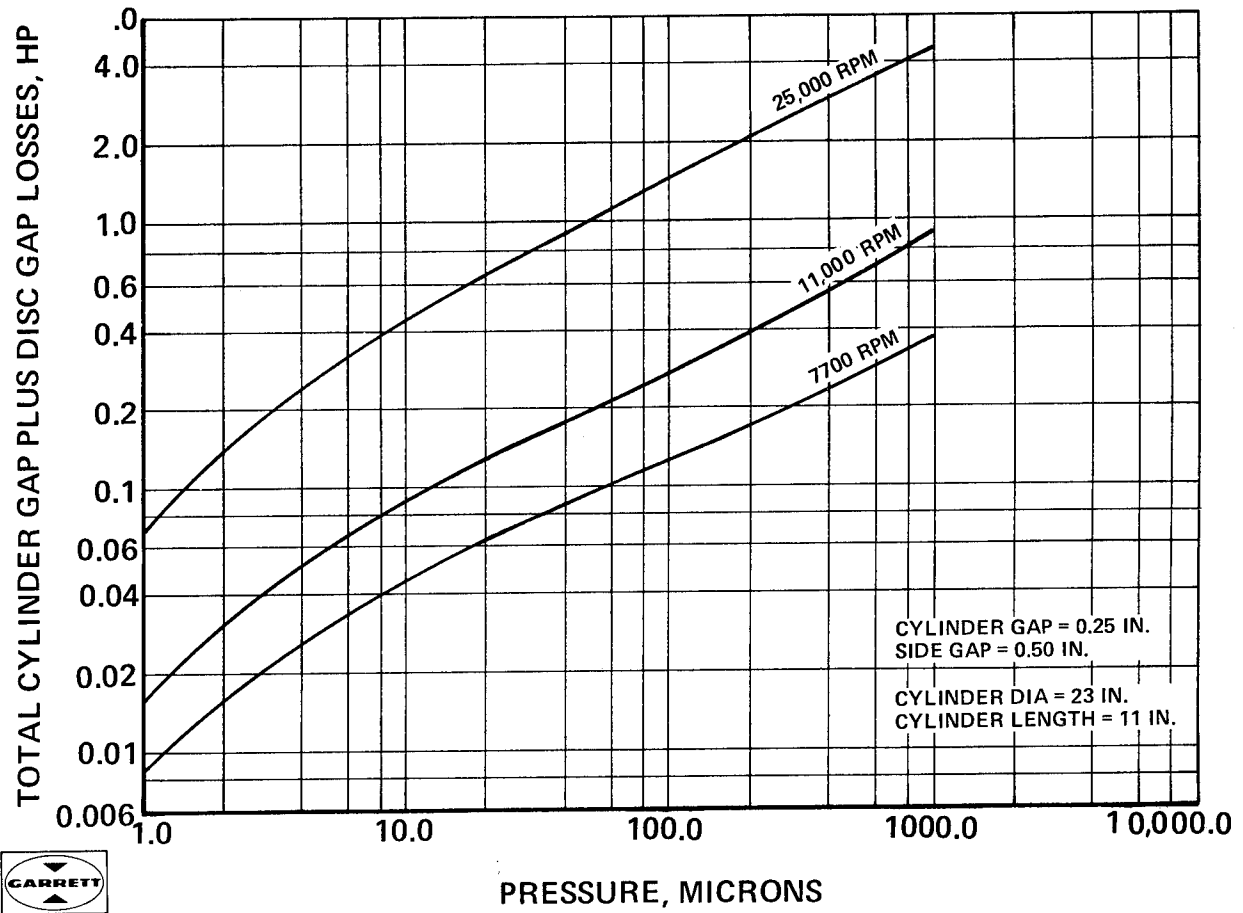
TYPICAL GEARBOX LOSSES VS LOAD/SPEED



TYPICAL BEARING LOSS VS LOAD/SPEED

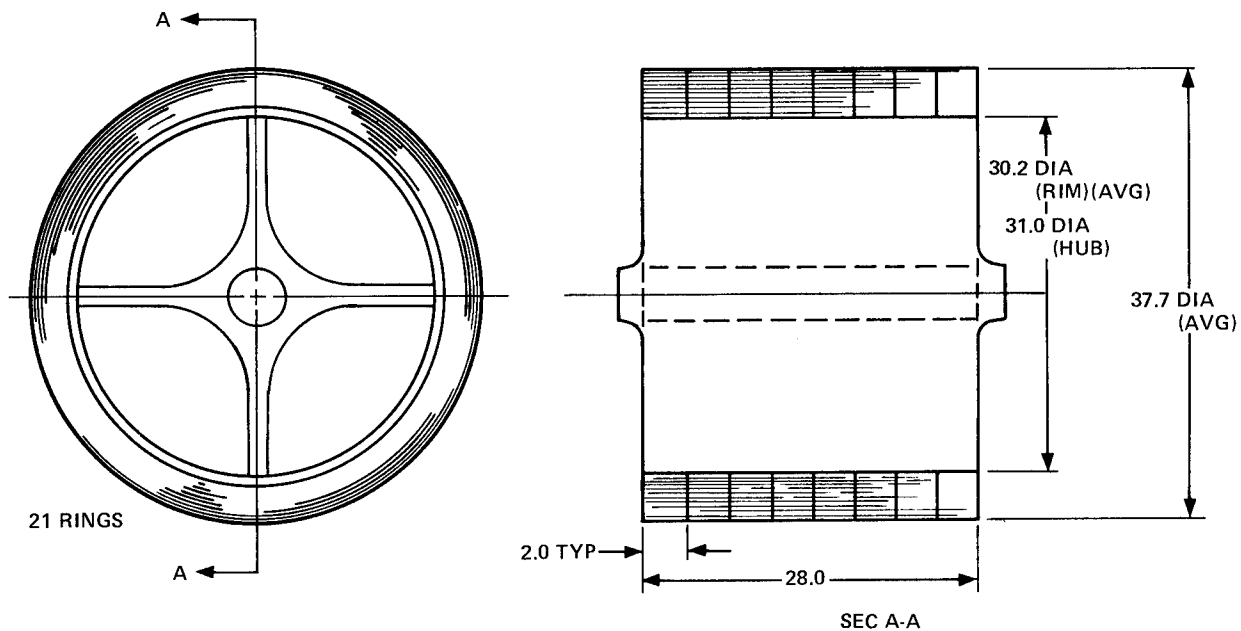


ROTOR WINDAGE LOSS



TYPICAL COMPOSITE FLYWHEEL-ROTOR CONFIGURATION

SELECTED CONCEPT FOR 20,000 RPM ROTOR SPEED – TYPICAL



WEIGHT

RIM – 580 LB KEVLAR/EPOXY
HUB – 170 LB ALUMINUM



FEATURES

RIM STRESS, UNIAXIAL – SIMPLIFIED FABRICATION
INTERFERENCE FIT, 4 SPOKES TO RIM – ROTOR
DYNAMIC STABILITY
STATUS – PROVEN CONCEPT

IMPROVED FUEL ECONOMY IN AUTOMOBILES BY USE OF A FLYWHEEL ENERGY MANAGEMENT SYSTEM

A. A. Frank and N. Beachley
Associate Professors
Department of Electrical and Computer Engineering
University of Wisconsin
Madison, Wisconsin 53706

ABSTRACT

A high-performance, low fuel consumption automobile is being built that will contain a flywheel package powered intermittently by a standard internal combustion engine and connected to the road through two transmissions arranged in series. The design of the 23-inch diameter, steel alloy flywheel is based on current technology. The flywheel will run in a vacuum and will have useable energy storage of $2/3$ hp-hr, maximum windage of 1 hp at maximum speed, a maximum torque transmission capability of 250 foot pounds, overspeed protection and protection against locked bearings. Special controls and instrumentation peculiar to this design will be necessary, since the torque-converter transmission will be used for both propulsion and regenerative braking. Computer simulation of operating aspects shows that a standard 1976 car modified to the new design should have 58% better gasoline mileage. If certain other design improvements can be realized, ultimate gasoline mileage could be 117% better.

INTRODUCTION

A standard automobile engine driving a modern, contemporary automobile cannot operate at its best thermal efficiency at all times. The engine must perform over a wide torque-speed range, yet in standard city driving it must operate in a so-called idle-mode much of the time. In today's society fuel economy is becoming increasingly important, and non-productive modes, such as idle, and inefficient modes such as low-torque, high-speed operation, should be eliminated.

Also, safe acceptable performance in city driving requires that the brakes of an automobile be used to slow it down. This kind of braking is inefficient because it turns kinetic energy into heat. If one were not interested in performance, it would be possible to drive a vehicle without brakes, using only aerodynamic and rolling friction to slow down the car. But traffic as we know it today will not tolerate such a pattern of driving. Regenerative braking that re-uses this energy will be required if maximum fuel efficiency is to be achieved.

A flywheel power plant system is being built at the University of Wisconsin that we believe will retain the desirable features of present-day automobiles, but

will improve fuel economy considerably and will minimize pollutant emission. The system will be installed in a 3,000-pound vehicle to be completed in the summer of 1976.

SYSTEM DESCRIPTION

The configuration of the proposed flywheel engine vehicular system is shown in Figure 1. This particular configuration has been chosen because of practical considerations and efficiency.

The design features of this automobile are that it must have equal or better performance than the standard unmodified vehicle in all respects. The performance criteria are: acceleration from 0 to 60 mph, top speed, gradability and braking performance. These constraints dictate that the engine in this vehicle be approximately the same size as the engine in the standard vehicle.

The system configuration consists of two transmissions in series: a standard four-speed manual shift transmission and a continuously-variable transmission unit. The continuously-variable transmission is designed to be integral with the standard rear axle assembly, necessitating four-wheel independent suspension. The reason for using two transmissions is to provide

a system which can operate at its best efficiency with off-the-shelf components.

The flywheel package is based on current, proved technology. An installation sketch of the flywheel system is shown in Figure 2 and Figure 3 shows the flywheel configuration and the vacuum housing plus the steel protective system. The flywheel runs in a vacuum at 11,000 rpm. Wheel disc diameter is approximately 23 inches. Full safety protection is provided.

The basic flywheel system specifications are: useable energy storage: 2/3 hp-hour, maximum windage: 1 hp at maximum speed, over speed protection, and locked bearing protection.

The flywheel design is based on currently sponsored government research. Material is steel alloy, and the maximum torque transmission capability is 250 ft-lbs. The basic continuously-variable transmission (CVT) features are: ratio range - 3.5:1, power split principle for good efficiency, and torque control (that is, the driver's foot commands torque and the ratio is adjusted to provide the demanded torque). An internal spur gear differential is used for power splitting. Torque capability of the CVT is \pm 400 ft-lbs. Top speed is designed for 80 mph vehicle speed. The CVT configuration is shown in Figure 4.

Figure 5 shows the vehicular controls, that is, the acceleration and braking controls of the CVT. The control system uses pressure feedback torque control for both acceleration and braking. This is accomplished by feedback of hydrostatic system pressures to a control valve which controls the continuously-variable ratio pistons. The particular design uses a single valve to accomplish both acceleration and braking. Maximum control torque is plus or minus 400 ft-lbs. This kind of control is necessary to minimize problems with stability.

In addition to the CVT controls there are other special controls and instrumentation required for driving this particular vehicle. These are shown in Figure 6. In addition to the standard operating equipment in a vehicle (i.e., the clutch, brake, shift lever, accelerator pedal, steering wheel and speedometer) there is an engine start clutch lever, a gear shift meter, gear shift indicators, a gear shift warning light, a flywheel speed meter,

a vehicle velocity function meter, a minimum charge warning light, a maximum charge speed warning light, and an engine start light. It should be pointed out that all these controls are easily automated, thus a production vehicle would only have accelerator and brake pedals and perhaps a flywheel charge meter.

The system has been designed using both an all-digital program and a real-time hybrid computer version of the program to test driver reaction to all the additional instrumentation and controls. All component losses have been calculated on a continuous basis in the simulation program. They have been modeled from test data obtained from component manufacturers.

The results of the simulations show that the standard 1976 vehicle can be modified to provide a 58% improvement in gas mileage with an ultimate developed potential of 117% improvement. An energy comparison table is shown in Table 1. Here we see three columns: the first column indicating the standard 1976 2.3 liter vehicle and its various energy consumptions and mileage on the bottom line. The second column (middle column) is the proposed vehicle discussed here and its various energy losses and utilization.

It is important to note that the flywheel and continuously-variable transmission use up about as much energy as was used up in the standard vehicle for deceleration and braking over the EPA-CVS cycle. It is further important to note that the idle and coast conditions use up as much fuel as is required to supply energy for the flywheel gears, the charge pump, excess brakes, engine clutch, engine inertia, and engine start. Thus, there is very little difference between the total amount of work done by the vehicles. The gain, however, is in the fact that the brake specific fuel consumption can be reduced from an average of .808 lbs. of fuel per hp-hour to .50 lbs. of fuel per hp-hour.

It should be pointed out that both vehicles are assumed to be of the same inertial weight. This is possible in a production vehicle because of system integration and component development.

The third column is important to concentrate on because it shows what the potential of the concept is. Note:

1. The four-speed transmission can be eliminated and its function included in a specially-designed continuously-variable transmission.
2. The flywheel system parasitic losses can be reduced by half by advanced design bearings and use of lighter weight wheels.
3. The losses in the continuously-variable transmission can possibly be reduced by half by application of new hydrostatic design concepts.
4. The charge pump can be designed, by use of a variable delivery system, to have approximately 1/6 of the loss now presently experienced.

These four improvements would allow one to obtain approximately 52 mpg for a 3,000-lb. car over the EPA-CVS city cycle as compared to the standard vehicle's 24 mpg for a 117% improvement.

We must look at the possible expected loss of fuel economy as a result of future new emissions standards. As the standards become more restrictive, the estimates for a standard vehicle and the hybrid flywheel vehicle are as shown in Table 2. It should be noted that a degradation in mileage occurs in both vehicles. These estimates are made by the automobile manufacturer involved in this particular project.

A continuous time simulation of the flywheel vehicle over the driving cycle is shown in Figure 7. The top trace shows the driveshaft torque. The 2nd trace shows the flywheel speed and the 3rd trace shows the engine speed. It should be noted that the engine is on at the beginning to give the flywheel its initial charge, and then comes on four more times during the cycle. The 4th trace is the vehicle speed over the EPA-CVS city driving cycle. The last trace shows the engine torque.

Note that the engine torque is not constant, but rather follows the wide-open throttle engine torque-speed characteristics. Note also that there is considerable energy left in the flywheel at the end of the cycle. A number of possible alternatives have been suggested to use this energy. One way may be to have a homing mode in which the last flywheel charge from the engine brings the flywheel to a speed corresponding to the distance

required to travel which will be much less than the maximum. Another possible alternative is to use the flywheel energy at the end of the cycle to charge the battery of the vehicle. If we keep the battery only partially charged while driving, this technique seems entirely practical.

The second trace shows the effect of regenerative braking, in which the flywheel speed increases as the vehicle is braked. Regenerative braking continues until the transmission is no longer able to provide the proper ratio, which occurs at approximately 5 mph. Below this speed the regular vehicle brakes must be used.

There are four current program objectives:

1. To perform component tests to obtain verification of component data and to obtain new data where data are not currently available.
2. To investigate control techniques, stability of operation, ease of operation and computer control aspects of the vehicle control system.
3. To evaluate engine operation impacts on emissions, on temperature and heat control and on insulation requirements.
4. To compare theoretical and actual performance with respect to mileage and emissions.

After initial assessment, transmission and engine modifications may be required. The computer program will be used to assess the necessary modifications.

After the demonstration vehicle is constructed and tested, future programs will include continued investigation of advanced hydrostatic transmission concepts such as the use of balanced force systems to minimize bearing load and reduce parasitic losses, and of techniques to reduce pumping and flow losses. The objective will be to achieve maximum efficiency with a wide ratio range. The flywheel vehicle requires a ratio range determined by the maximum vehicle speed and minimum flywheel speed. Typically a ratio range of 20:1 is required. By use of some special techniques this can be reduced to about 10:1 as in the vehicle being constructed.

Other transmissions will also be investigated, such as an electric transmission, a multi-gear torque converter transmission, traction drive transmissions, and possibly other drive systems.

All of these continuously-variable transmission systems will be studied by simulation and designed for maximum fuel economy, mechanical simplicity and reliability. The objective will be a fully automatic transmission system. Vehicle size effects will be investigated with respect to 1500 lb., 3000 lb., and 10,000 lb. vehicles. System weight, of course, will be a primary parameter and must be considered in any design evaluation. Reliability must also be given a high priority.

The design and construction of an advanced continuously-variable transmission will then be undertaken. This will be based on a computer-optimized design using realistically measured dynamometer data for all components. The purpose of the construction exercise is to assess the control aspects, shifting criteria, clutch losses, ease of control, reliability and the feasibility of a fully automatic system.

Flywheel subsystems will continue to be investigated with respect to such vehicles. Of course advanced flywheels, that is composites, will be evaluated with respect to overall system impact. Other flywheel configurations will be considered. For example, a variable inertia flywheel whose use would eliminate the need for a continuously-variable transmission appears to be an interesting idea. However, the complexity of such a wheel and the weight impact may offset entirely the elimination of the CVT, thus the overall system must be studied for feasibility. It is anticipated that a flywheel subsystem will be incorporated into the continuously-variable transmission to give a single mechanical package. The flywheel subsystem, however, would be subcontracted.

Finally, the system will be installed in a vehicle and evaluated. Driveability of this automobile system will be assessed, measured fuel consumption and emissions data taken, and vehicular weight and cost impact will be evaluated.

CONCLUSIONS

It has been demonstrated by computer techniques that a vehicle containing an integral high-speed flywheel can have greatly enhanced fuel economy within emission constraints. Further, current vehicle performance levels can be completely retained.

The program described will evaluate practical consideration of flywheel systems in automobiles. It will concentrate on the most important aspect of the flywheel system, which is the transmission that connects the flywheel to the road. The main objective of the program is system overall efficiency. Thus, parasitic losses in all components are being minimized by careful system design. It should be noted that if the system is put together without extreme care to control the parasitic losses, it is very easy to obtain a vehicle with worse mileage performance than the standard unmodified vehicle. Finally, a carefully designed flywheel-engine system provides a real alternative for future transportation.

Acknowledgements

The following members of the University of Wisconsin research team have contributed to the results described in this paper.

Richard R. Radtke
Peter Ting
Tom Hausenbauer
Douglas Brooks

This project is sponsored by the United States Department of Transportation, Office of University Research, Contract No. DOT-OS-30112.

EPA-CVS CYCLE ENERGY COMPARISON

ITEMS	STANDARD 1976 2.3 LITER VEHICLE (HP-SEC)	1976 FLYWHEEL 2.3 LITER VEHICLE (HP-SEC)	POTENTIAL FROM CONTINUED R & D (HP-SEC)
Road Load	3700	3702	3702
Rear Axle	470	536	536
Transmission	648	648	200**
Deceleration and Brakes	<u>2555</u>	855	400
	CVT	1809	900**
Total (+) Work	7373	172	172
	FW Gears	172	172
	Charge Pump	634	100
	Excess Brakes	50	50
Idle & Coast Fuel 0.25 lb	1111*	99	99
	Engine Clutch	99	99
	Engine Inertia	93	93
	<u>Engine Start</u>	<u>66</u>	<u>66</u>
Total Work	8484	8664	6318
Fuel for (+) Work	1.655 lb	1.202 lb	0.876 lb
Fuel Total	1.905 lb	1.202 lb	0.876 lb
(+) BSFC	0.808 lb/HP-HR	0.50 lb/HP-HR	0.50 lb/HP-HR
Mileage	24.0 MPG	38.0 MPG	52.0 MPG
Improvement		58%	117%

*Equivalent Work Computed at 0.808 lb/HP-HR

**A Single CVT Package Will Replace Both Units

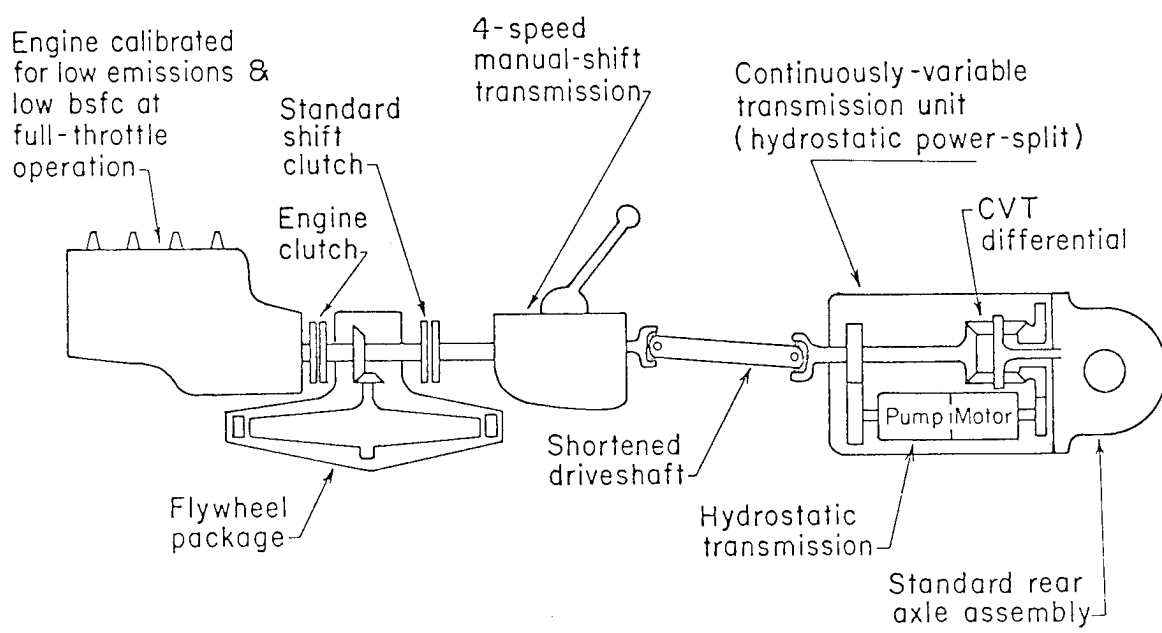
ENERGY COMPARISON TABLE

Table 1.

EXPECTED LOSS IN FUEL ECONOMY AS A FUNCTION OF EMISSION STANDARDS

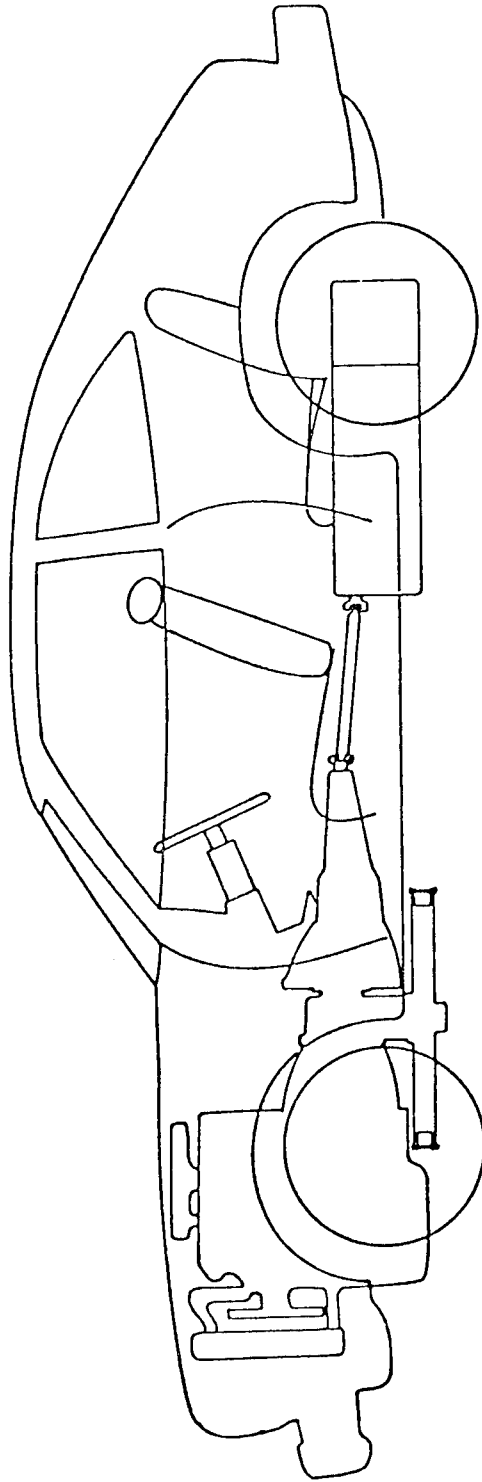
	Emission Standards, gms/mi	2.3 Liter Standard Manual 24.0 mpg, percent loss	2.3 Liter Hybrid Vehicle 38.0 mpg, percent loss
1976 49 states	HC 1.5 CO 1.5 NO 3.1	---	---
1977 49 states	HC 1.5 CO 15 NO 2.0	4 - 5%	5 - 10%
1976 California	HC .9 CO 9.0 NO 2.0	11 - 12%	5 - 10%
1977 California	HC .4 CO 9.0 NO 1.5	24 - 33%	10 - 15%
1978	HC .41 CO 3.4 NO 0.4	Unknown	Unknown

Table 2.



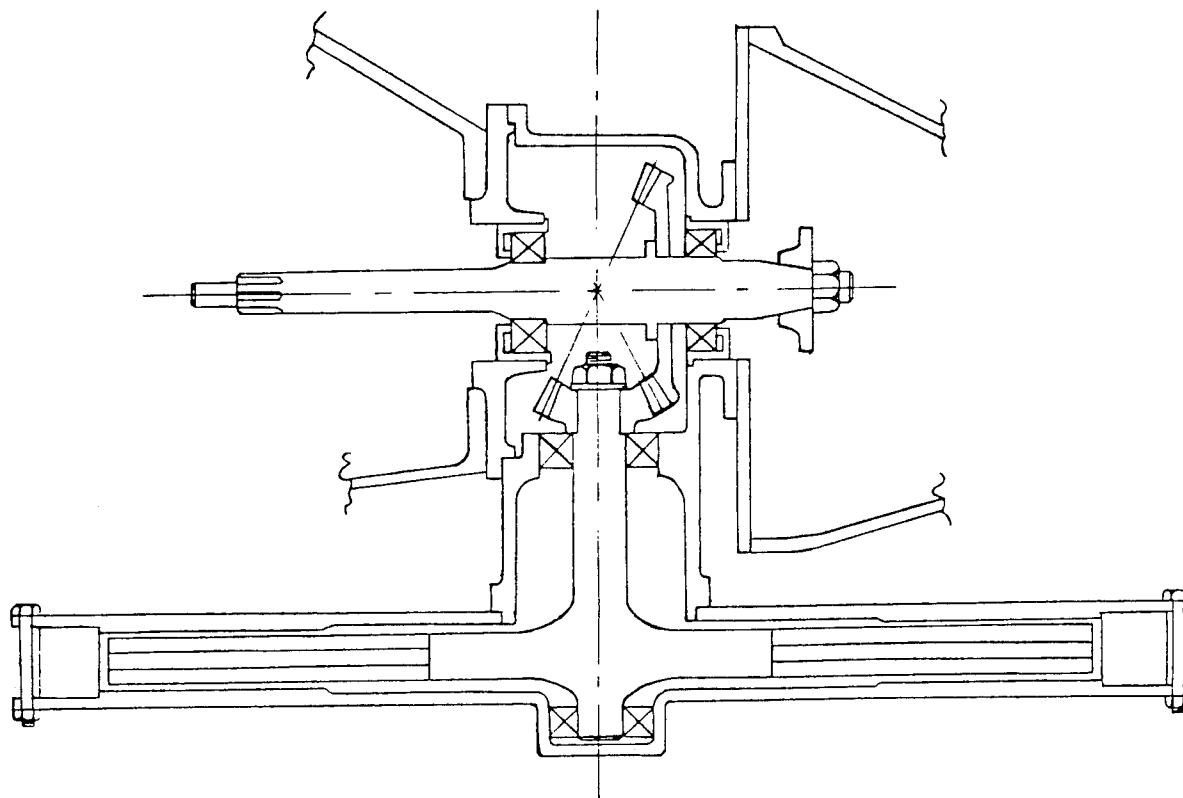
SYSTEM CONFIGURATION

Fig. 1.



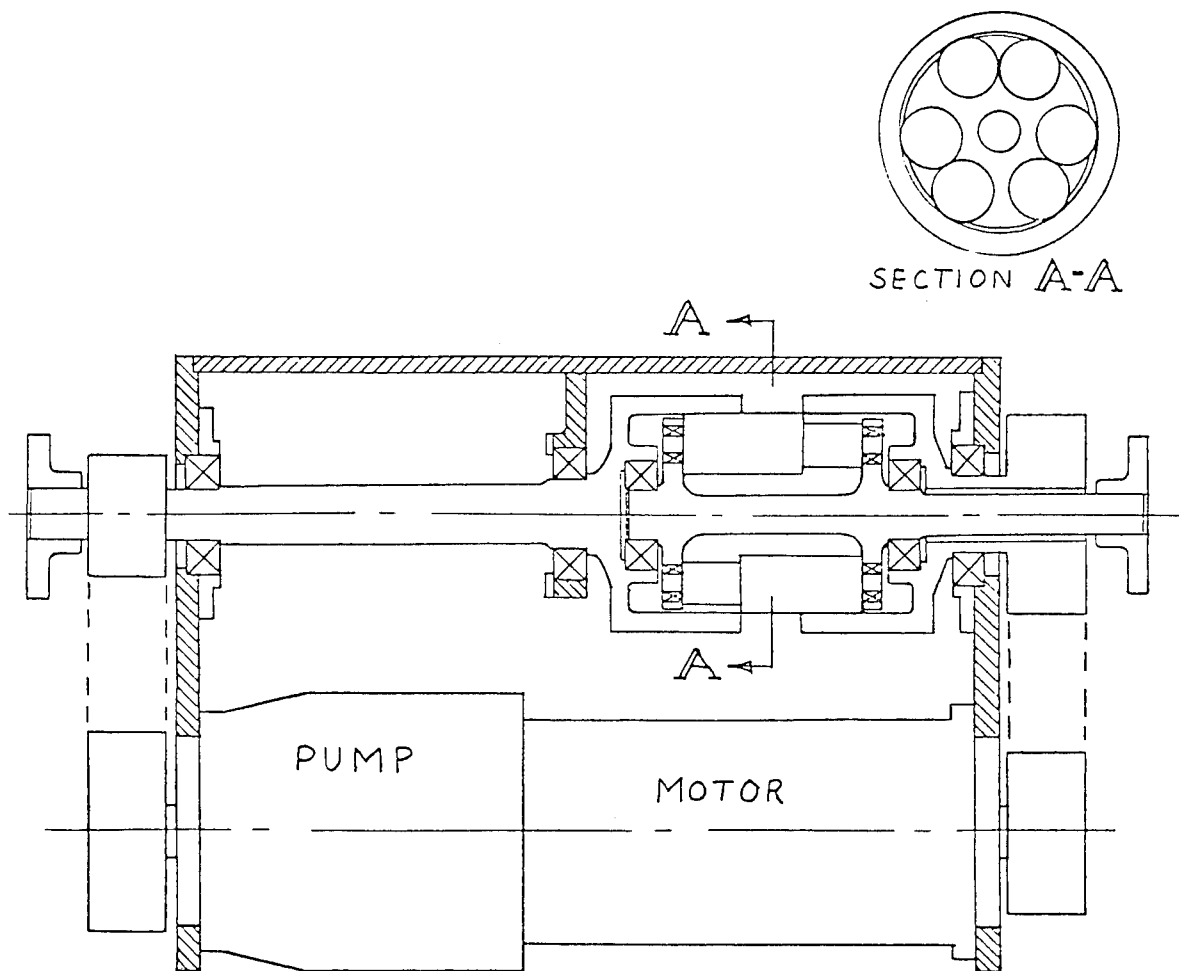
INSTALLATION SKETCH

Fig. 2.



FLYWHEEL CONFIGURATION

Fig. 3.



CONTINUOUSLY VARIABLE TRANSMISSION CONFIGURATION (CVT)

Fig. 4.

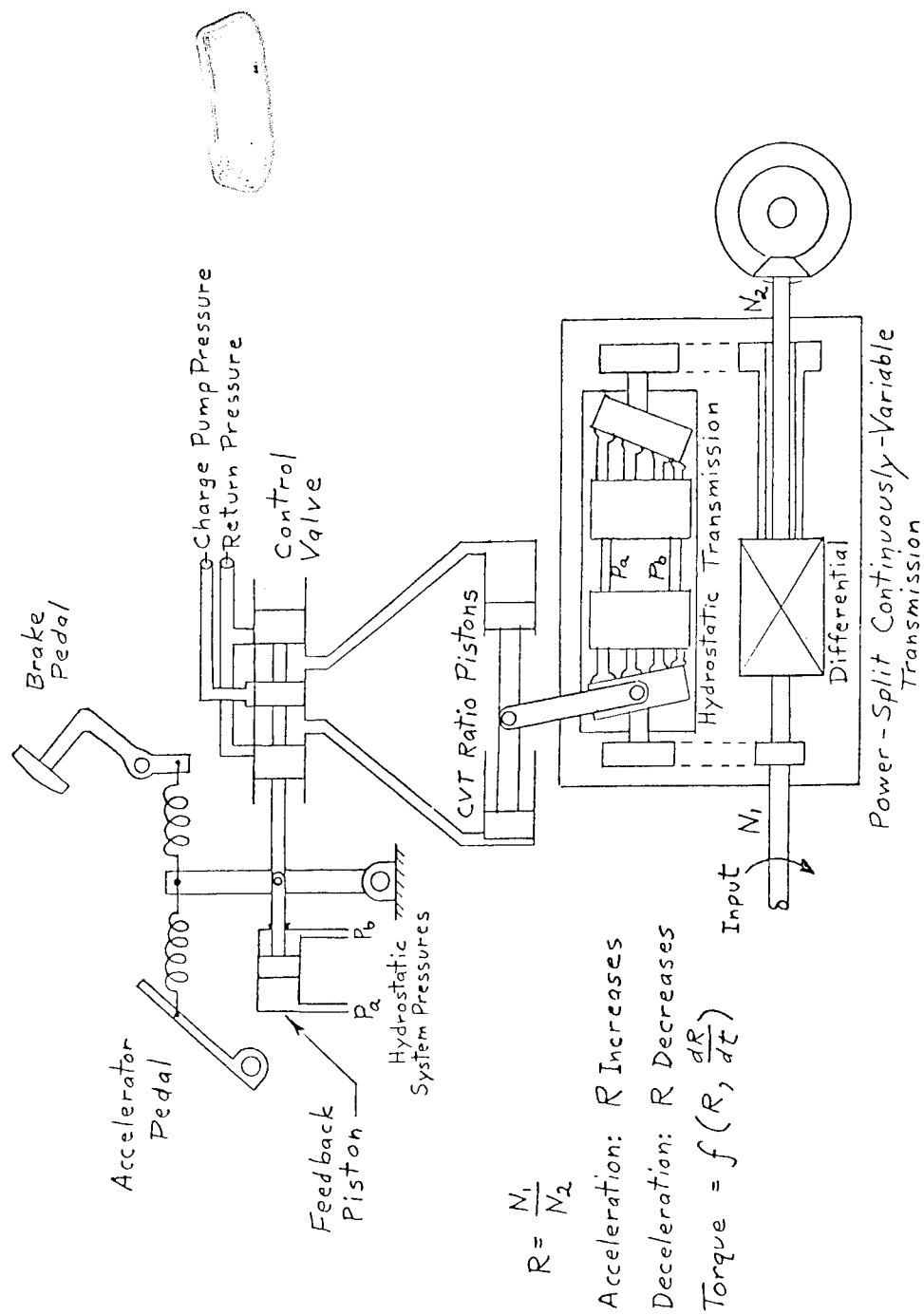
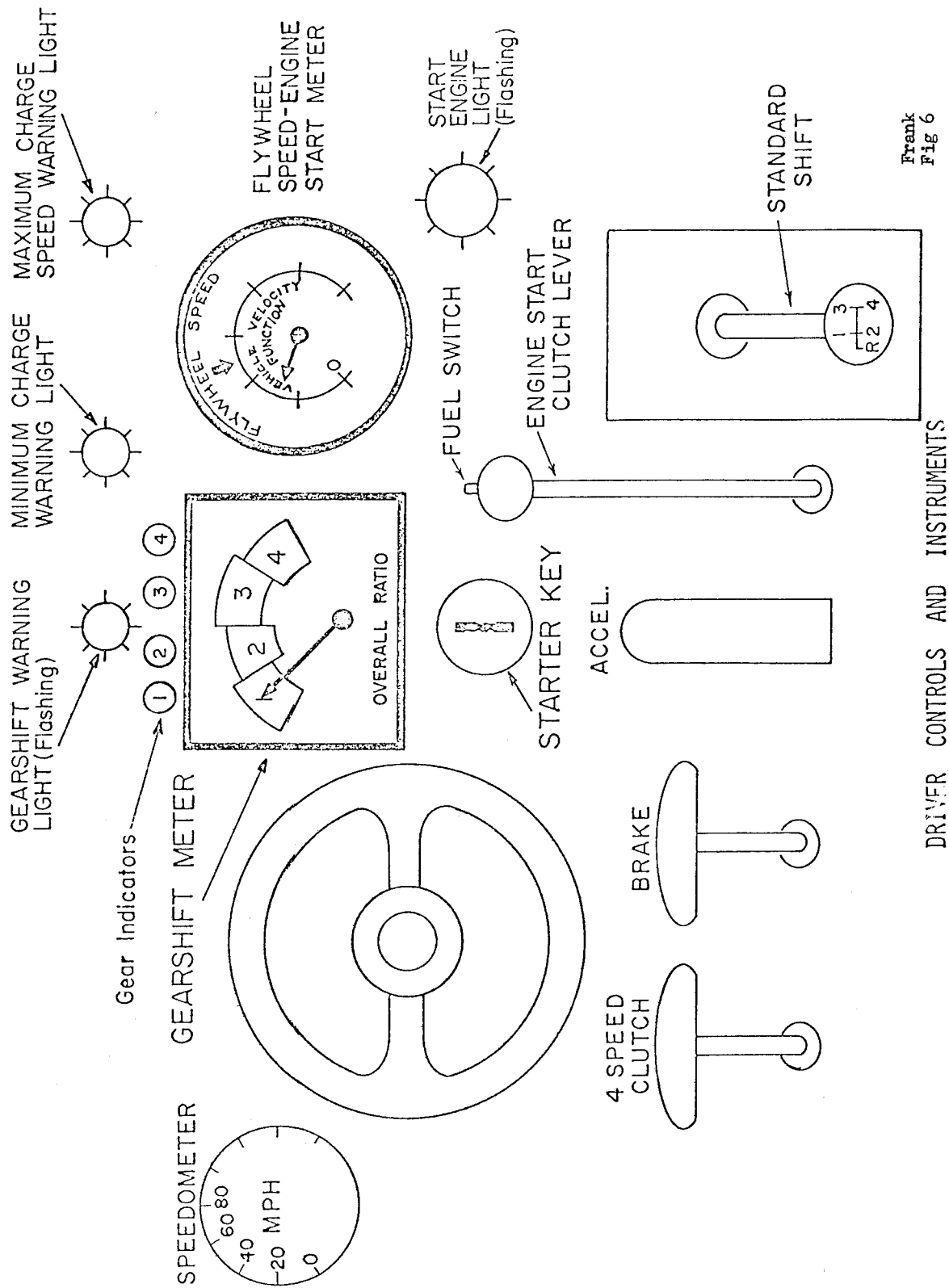


Fig. 5.

VEHICLE ACCELERATION AND BRAKING CONTROLS



Frank
Fig 6

DRIVER CONTROLS AND INSTRUMENTS

Fig. 6.

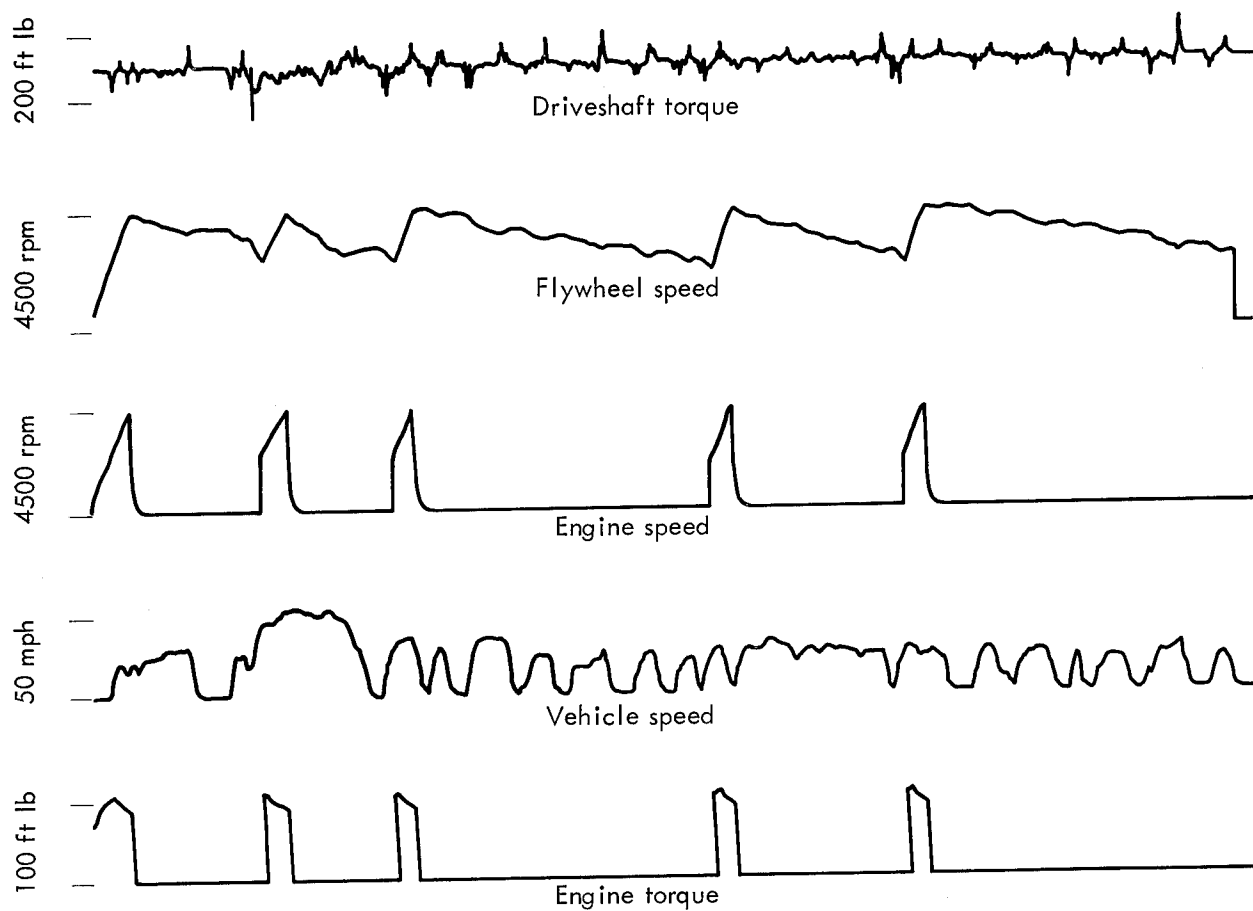


Fig. 7. Recorder traces of a flywheel vehicle simulation over the EPA-CVS city driving cycle

POLAR WEAVE COMPOSITE FLYWHEELS

A. M. Garber
Re-Entry and Environmental Systems Division
General Electric Company
P. O. Box 8555
Philadelphia, Pennsylvania 19101

NOTE: This paper arrived too late to include the figures in this proceedings.

INTRODUCTION

Since the maximum specific energy that can be stored in a flywheel is proportional to the strength/density ratio of the material from which it is made, there has been considerable interest in the utilization of advanced composite materials. Attempts to utilize the high strength of unidirectional composites have resulted in concepts that are not efficient, are too flimsy, and in the case of filament wound wheels rely on the load carrying capability of the unreinforced matrix materials to carry radial tensile loads. To date performance has been disappointing in that theoretical estimates of performance have not agreed with test results.

GE-RESD has developed a three-dimensional reinforced composite material Polar Weave. Polar Weave, a G.E. proprietary process, was developed several years ago to meet the severe mechanical and thermal environments experienced by re-entry vehicle nose-tips. Its potential application to high energy flywheels was identified just recently, and preliminary evaluations to date are most encouraging.

BACKGROUND

Polar Weave is a derivative of a general class of three-dimensional orthogonal composites developed by General Electric's Re-Entry and Environmental Systems Division (GE-RESD) to provide characteristics not attainable in typical reinforced composites or two-dimensional reinforced plastics, such as filament wound composites. These are high strength and improved shear capability in all directions. Polar Weave was found to be particularly effective in those geometries and loading conditions in which the principal stress directions are coincident with

a cylindrical coordinate system which is just what a spinning disc is. Both cylindrical and conical bodies have been produced. While the bulk of our activities with Polar Weave has centered around carbon-carbon materials, there has been sufficient work done with most plastic matrix materials (epoxy, phenolic, etc.) and advanced fibers (graphite, boron, glass, etc.) to provide a high degree of confidence that a strong tough epoxy base system can be woven and processed successfully.

In order to perform reliable design calculations, GE-RESD has developed a sophisticated analytical methodology utilizing three-dimensional finite element techniques on a macroscopic and micro-mechanical level. These two approaches, coupled together and reinforced with experimental data, provide a powerful tool which is in place at GE-RESD and can be applied effectively to the flywheel problem. Since Polar Weave consists of unidirectional high strength filaments aligned in the radial, circumferential, and axial directions, it is possible by varying the number and kind of filaments in each of the three directions, to provide a broad spectrum of stiffness and strength levels in each direction. Since the weave variation can be changed as a function of radius, it is possible for the designer to specify a Polar Weave design where density, stiffness, and strength can be tailored to provide a near uniform stress distribution in the disc within a parallel-sided composite disc. Thus, Polar Weave has the potential of providing a constant stress situation in a parallel-sided disc with the high strength to density ratio of composites. The controllable and variable anisotropy provided through the Polar Weave process will produce higher values of weight and volume efficiency factors than those concepts

based upon essentially one-dimensional composite materials.

FLYWHEEL APPLICATION

Preliminary calculations using realistic estimates for strength and stiffness values indicate that energy densities of 40 watt-hrs/lb can be obtained with an Epoxy-Kevlar 49 Polar Weave design. A typical solution would be a wheel, 36 inches in diameter, 12 inches thick, operating at slightly in excess of 20,000 RPM. This configuration would weigh approximately 625 lbs and store 25 KW hrs. Doubling the length would provide 50 KW hrs. Power would be transmitted to and extracted from the wheel by means of a metallic shaft approximately three inches in diameter. Another unique aspect of the Polar Weave concept is the fact that the shaft is initially part of the weave fixturing. Axial and circumferential grooves are machined in the shaft and the disc fibers are woven directly into the hub resulting in an integral disc-shaft interface. Thus the load transfer mechanism between the two does not depend entirely upon adhesion between the matrix and the metal surface of the shaft, but is substantially aided by fiber reinforcement action. The shaft is an integral part of the flywheel and remains with the wheel throughout the entire fabrication cycle.

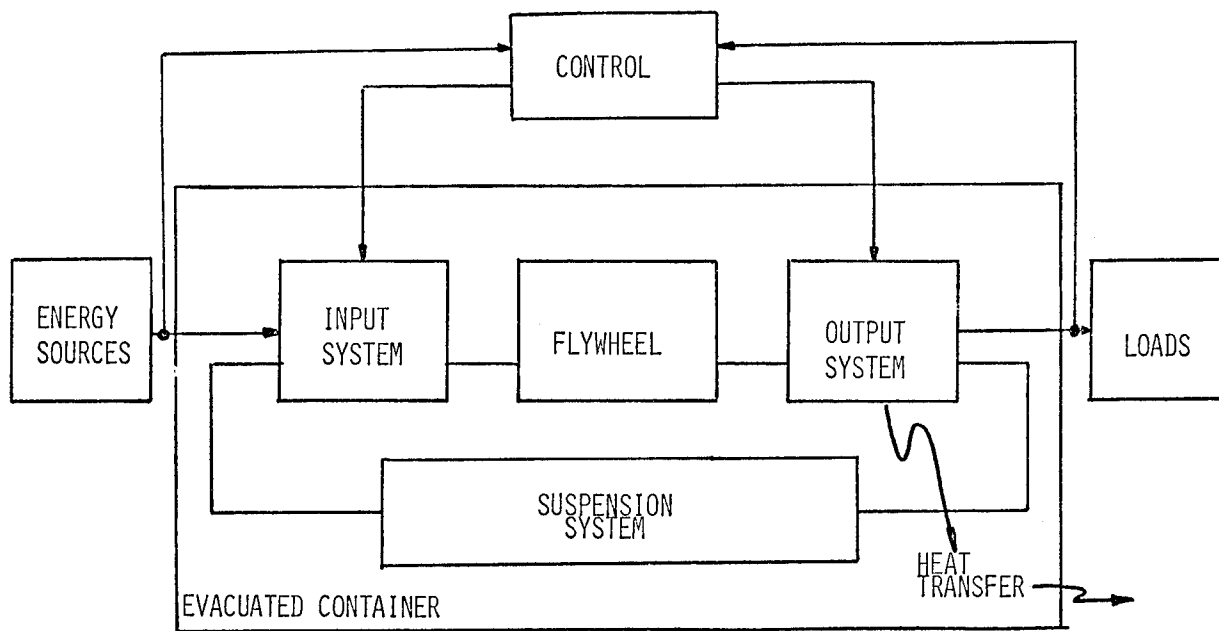
The simple geometries attainable with Polar Weave result in efficient packaging and eliminates many of the dynamic problems found in other concepts, which are quite flimsy from a vibrational viewpoint. The Polar Weave wheel can be treated as a rigid body over the operating range of frequencies. Our preliminary analyses indicate there are no natural modes of vibration in the flywheel close to any of the possible speed ranges.

BEARING AND ELECTRICAL INPUT-OUTPUT FOR FLYWHEEL ENERGY STORAGE SYSTEMS

A. F. Veneruso
Division 5715
Sandia Laboratories
P. O. Box 5800
Albuquerque, New Mexico 87115

ABSTRACT

As an ERDA laboratory, Sandia's interest in flywheel energy storage stems from our capabilities in systems integration and advanced composite materials and considerations for storage in our solar and wind energy conversion projects. In other talks, Frank Gerstle and Bob Reuter, both of Sandia, cover various theoretical and experimental aspects of the flywheel itself. In this talk I present a tutorial review of magnetic bearings and electrical input-output for flywheel systems. This presentation is the result of discussions between Sandia Laboratories and the industries shown on the third viewgraph. In our flywheel/hybrid systems project for vehicles, Sandia Laboratories is basically a catalyst for the development of these systems by private industry. Hence the industry list given is in no sense restrictive. This presentation begins with basic principles, gives application examples and suggests avenues for future research and prototype development.



FLYWHEEL ENERGY STORAGE SYSTEM

FLYWHEEL SYSTEM

COMPONENTS

- FLYWHEEL { ISOTROPIC
COMPOSITE
 - BEARINGS { CONVENTIONAL
MAGNETIC
 - INPUT/OUTPUT
 - MOTOR/GENERATOR { SEPARATE { SYNCHRONOUS
COMBINED { INDUCTION
DC BRUSHLESS
 - VARIABLE SPEED FLYWHEEL DRIVE
 - VARIABLE SPEED TRACTION MOTOR DRIVE
 - REGENERATION
- CONTAINMENT
 - VACUUM
 - SAFETY
 - HEAT

INDUSTRY CAPABILITIES FOR FLYWHEELS

<u>ORGANIZATION</u>	<u>EXPERTISE</u>
AIRESEARCH	INPUT/OUTPUT, CONTAINMENT REGENERATIVE SYSTEMS
BATTELLE	STRUCTURES, COMPOSITES, OVERALL DESIGN
BELL AEROSPACE	MATERIALS
BORG WARNER	INPUT/OUTPUT, CONTROLS
BRUNSWICK	WHEEL DEVELOPMENT
GENERAL ELECTRONIC	INPUT/OUTPUT, WHEEL FABRICATION
HITTMAN ASSOCIATES	SYSTEMS
ROCKWELL INTERNATIONAL	SYSTEMS
SPERRY FLIGHT SYSTEMS	MAGNETIC SUSPENSIONS AND BEARINGS
STANFORD RESEARCH INSTITUTE	WHEEL DEVELOPMENT
UNION CARBIDE	CONVENTIONAL BEARINGS, WHEEL DEVELOPMENT, TESTING
UNIVERSITY OF WISCONSIN	CONVENTIONAL/FLYWHEEL CAR SIMULATION, STUDIES
WESTINGHOUSE ELECTRIC	SYSTEMS, WHEEL DEVELOPMENT

MAGNETIC BEARING CHARACTERISTICS

- ADVANTAGES

- HIGH RELIABILITY
 - NO WEAR
 - NO LUBRICATION
 - NO FATIGUE
- LOW STARTING AND TORQUE DRAG
- HIGH SPEED CAPABILITY
- LOW NOISE AND VIBRATION
- NO SINGLE POINT FAILURES (WITH REDUNDANT ELECTRONICS)
- COMPATIBLE WITH VACUUM ENVIRONMENT
- INSENSITIVE TO THERMAL CONDITIONS

- LIMITATIONS

- LOWER CAPACITY THAN CONVENTIONAL BEARINGS
- LOWER STIFFNESS THAN CONVENTIONAL BEARINGS
- CONTROL ELECTRONICS REQUIRED
- ADDITIONAL MECHANICAL TOUCHDOWN BEARING REQUIRED

CLASSIFICATION OF MAGNETIC BEARINGS

- DC MAGNETIC BEARINGS
 - RADIAL PASSIVE - AXIAL ACTIVE
 - RADIAL ACTIVE - AXIAL PASSIVE
 - ALL AXES ACTIVE
- AC MAGNETIC BEARINGS
 - EDDY-CURRENT REPULSION
 - AC RESONANT
- ALL-PASSIVE BEARINGS
 - DIAMAGNETIC
 - SUPERCONDUCTING

STABILITY IN STATIC FIELDS

- EARNSHAW'S THEOREM (1842)

3-DIMENSIONAL STABILITY IMPOSSIBLE FOR
FERROMAGNETIC SYSTEMS.

- PERMANENT MAGNETS

STIFFNESS RELATION:

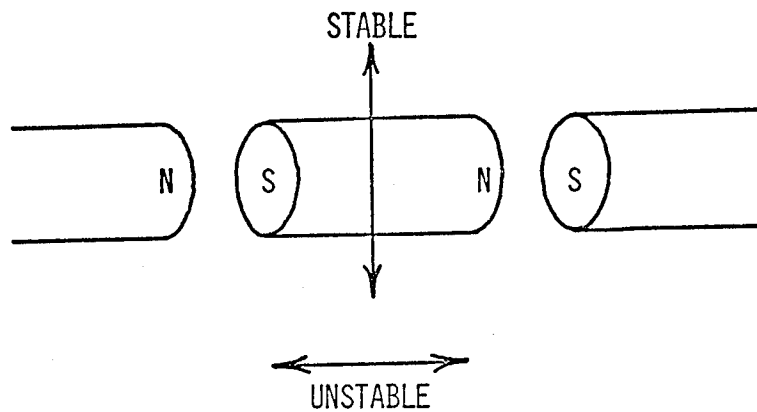
$$K_X + K_Y + K_Z = 0$$

FOR EXAMPLE, WITH
RADIAL SYMMETRY,

$$K_X = K_Y = K_R$$

HENCE

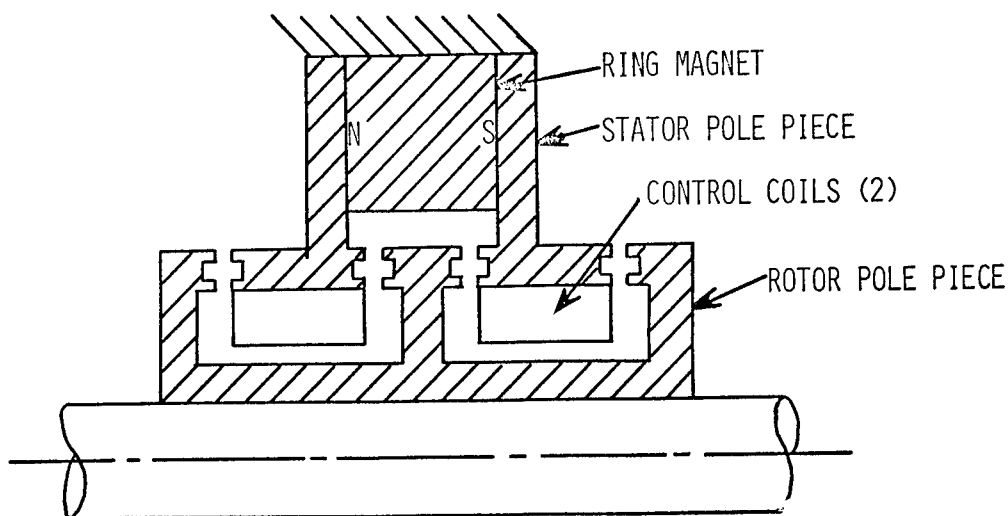
$$K_Z = -2K_R$$



COMPARISON OF D.C. MAGNETIC
BEARING SYSTEMS

CHARACTERISTIC	RADIAL PASSIVE AXIAL ACTIVE	RADIAL ACTIVE AXIAL PASSIVE	ALL-ACTIVE
STIFFNESS RADIAL AXIAL	LOW ADJUSTABLE	ADJUSTABLE LOW	ADJUSTABLE ADJUSTABLE
CONTROL SYSTEM	1-AXIS (1 DEGREE OF FREEDOM)	2-AXES (4 DEGREES OF FREEDOM)	ALL-AXES (5 DEGREES OF FREEDOM)
RELIABILITY	HIGHEST	LOWER	LOWEST
TORQUE	LOW	HIGHER	LOW
POWER LOSS	LOW	HIGHER	HIGHER
DESIGNERS	AEROSPATIALE (FR) SPERRY HUGHES BACKERS (UK) NASA GODDARD HONEYWELL		COMSAT/ TELDIX NASA GODDARD/ GE
DEMONSTRATED CAPACITY	30 KG (SPERRY)		18 KG (NASA)
DEMONSTRATED SPEED	10,000 RPM (NASA)		12,000 RPM (NASA)

RADIAL RELUCTANCE AXIALLY ACTIVE 3-LOOP BEARING



- LOW RELUCTANCE CONTROL PATH
- NO DEMAGNETIZATION OF MAGNET
- BOTH MAGNET AND COILS NON-ROTATING
- RADIAL STIFFNESS CAN BE AUGMENTED

FROM: SABNIS, A. V. "MAGNETICALLY SUSPENDED LARGE MOMENTUM WHEELS"
AIAA, MECH & CONTROL OF FLIGHT CONF., AUGUST 5-9, 1974.

MAGNETIC BEARING SUMMARY

- MODEL BEARINGS HAVE DEMONSTRATED
FEASIBILITY FOR USE IN FLYWHEEL
ENERGY STORAGE SYSTEM
- DESIGN TECHNOLOGY EXISTS FOR
HIGHER SPEEDS AND LOADS

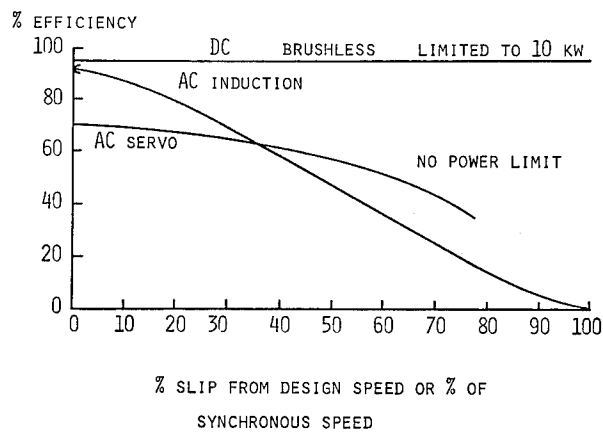
ENERGY INPUT/OUTPUT REQUIREMENTS

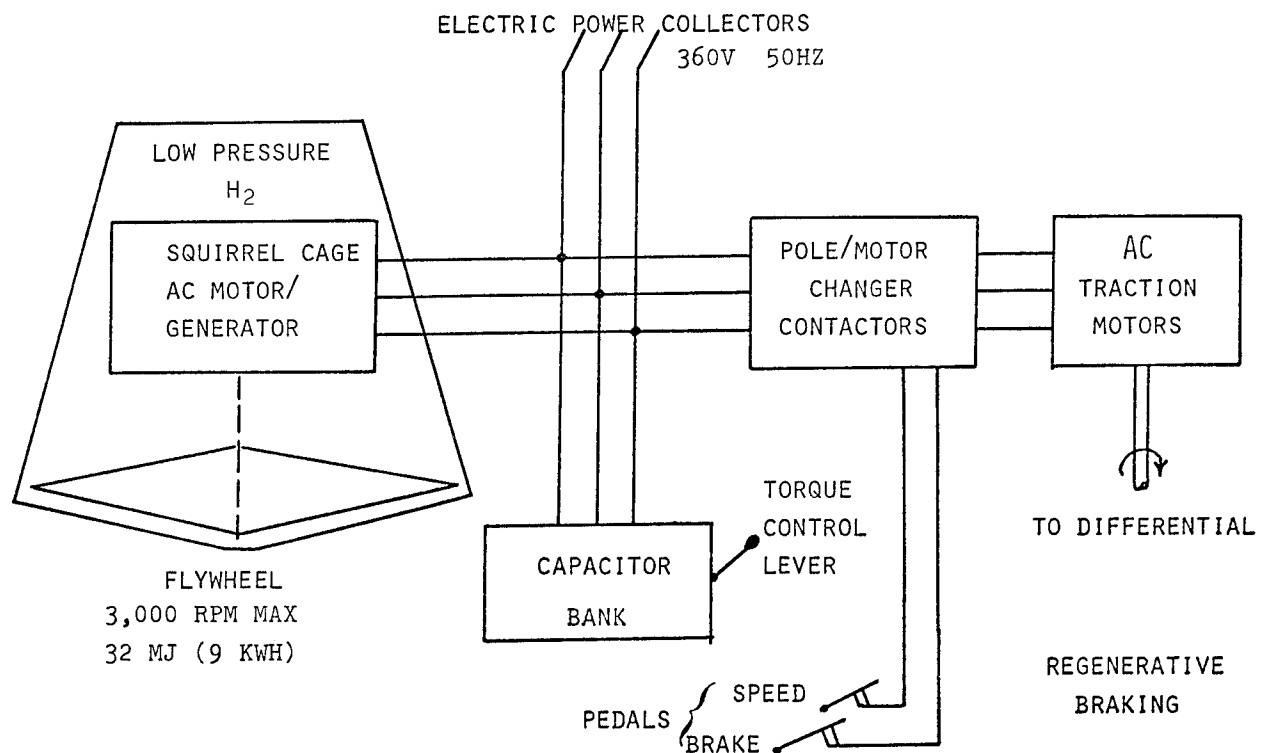
HIGH EFFICIENCY IN OVERALL SYSTEM

EXTENSION TO USEFULLY HIGH VALUES OF POWER
LEVELS AND SPEEDS

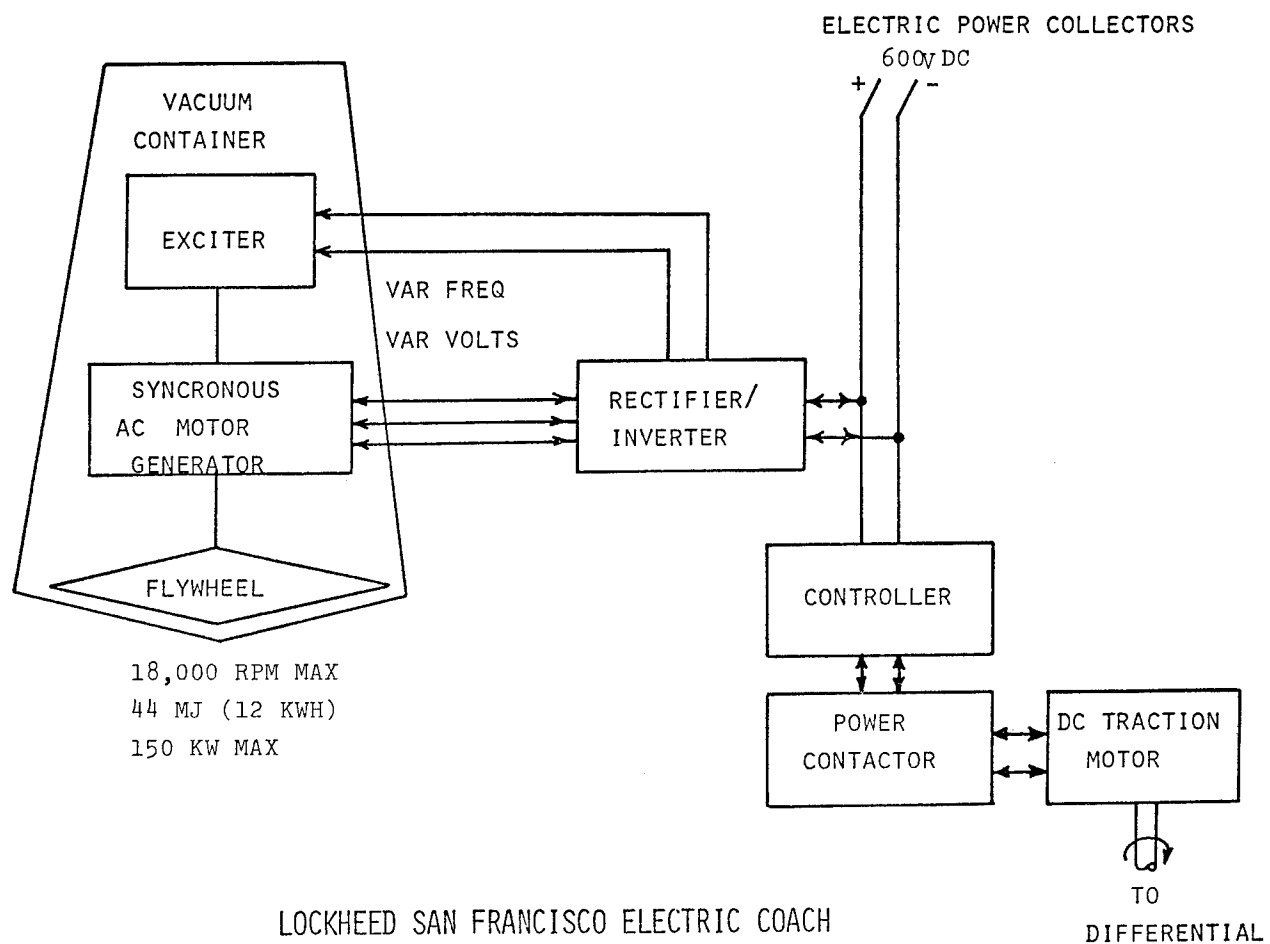
COMPATIBILITY WITH INTERFACES

MOTOR EFFICIENCY VERSUS SLIP

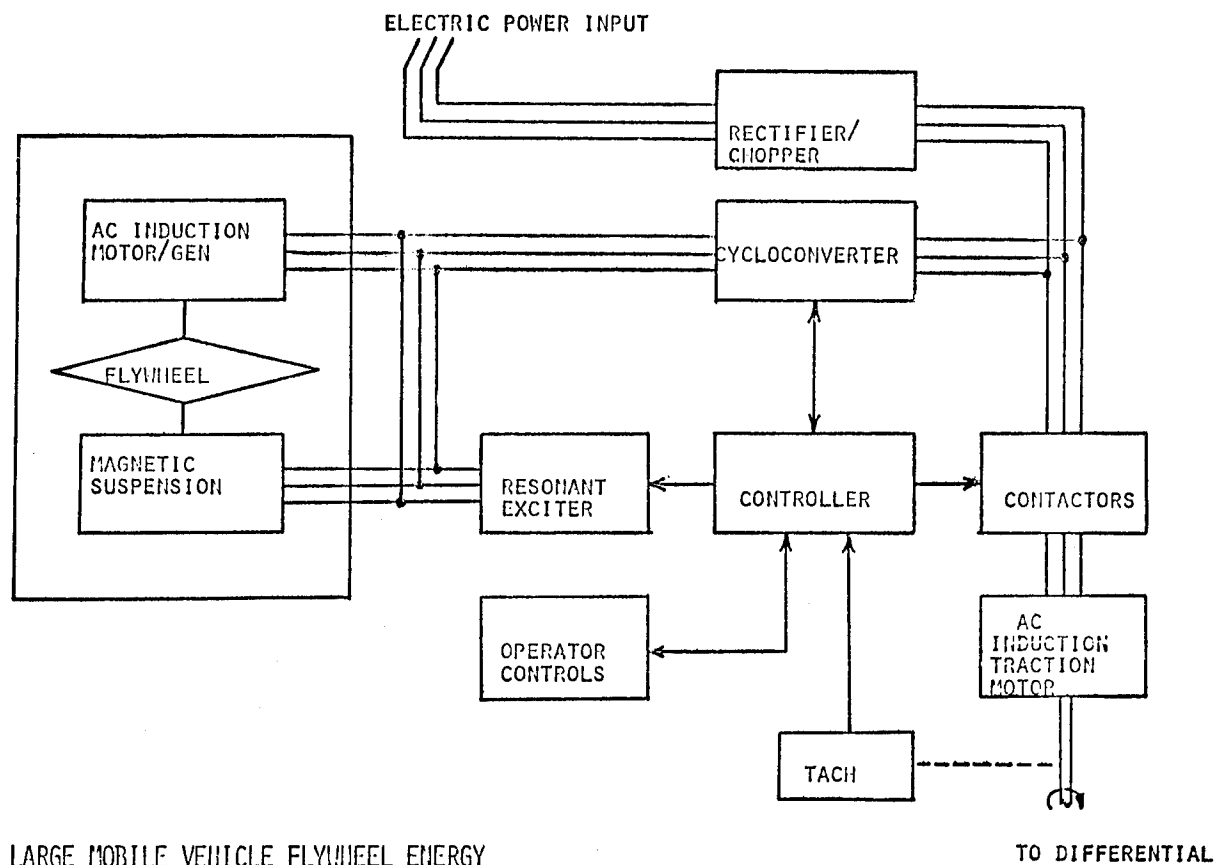




OERLIKON ELECTROGYRO BUS 1950-1969 SWITZERLAND



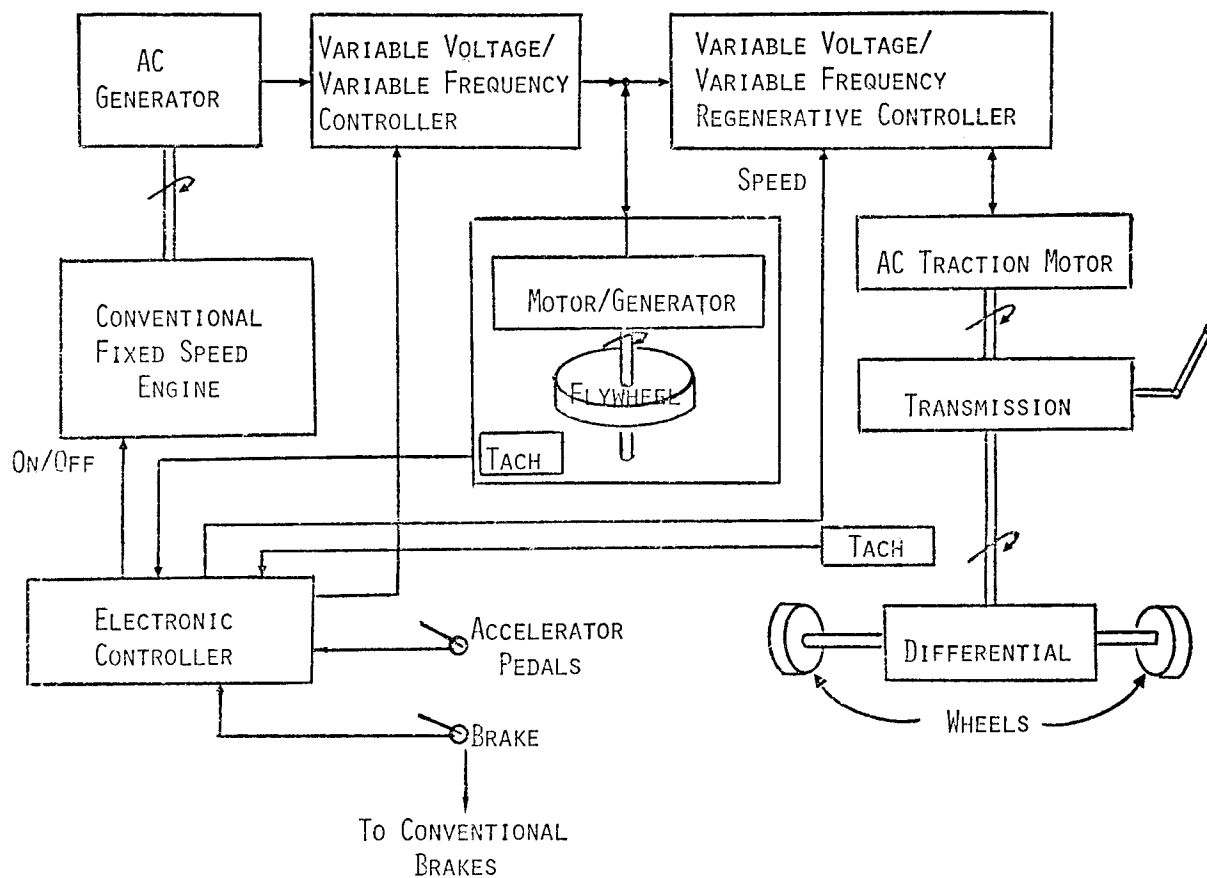
LOCKHEED SAN FRANCISCO ELECTRIC COACH



LARGE MOBILE VEHICLE FLYWHEEL ENERGY STORAGE SYSTEM

PROTOTYPE SYSTEM OPTIONS

1. CONVENTIONAL ENGINE/FLYWHEEL MECHANICAL
(FORD AND UNIVERSITY OF WISCONSIN INDICATE 38 MPG)
2. CONVENTIONAL ENGINE/FLYWHEEL ELECTRICAL
(MORE VERSATILE THAN MECHANICAL)
3. BATTERY/FLYWHEEL ELECTRICAL
(EXTENDS BATTERY LIFE, IMPROVES PERFORMANCE)
4. EXTERNAL BURNING ENGINE/FLYWHEEL ELECTRICAL
(SHIFT TO CHEAPER FUELS, LOWER EMISSIONS)
5. CONVENTIONAL ENGINE/BATTERY/FLYWHEEL
(COMBINES ADVANTAGES OF EACH)



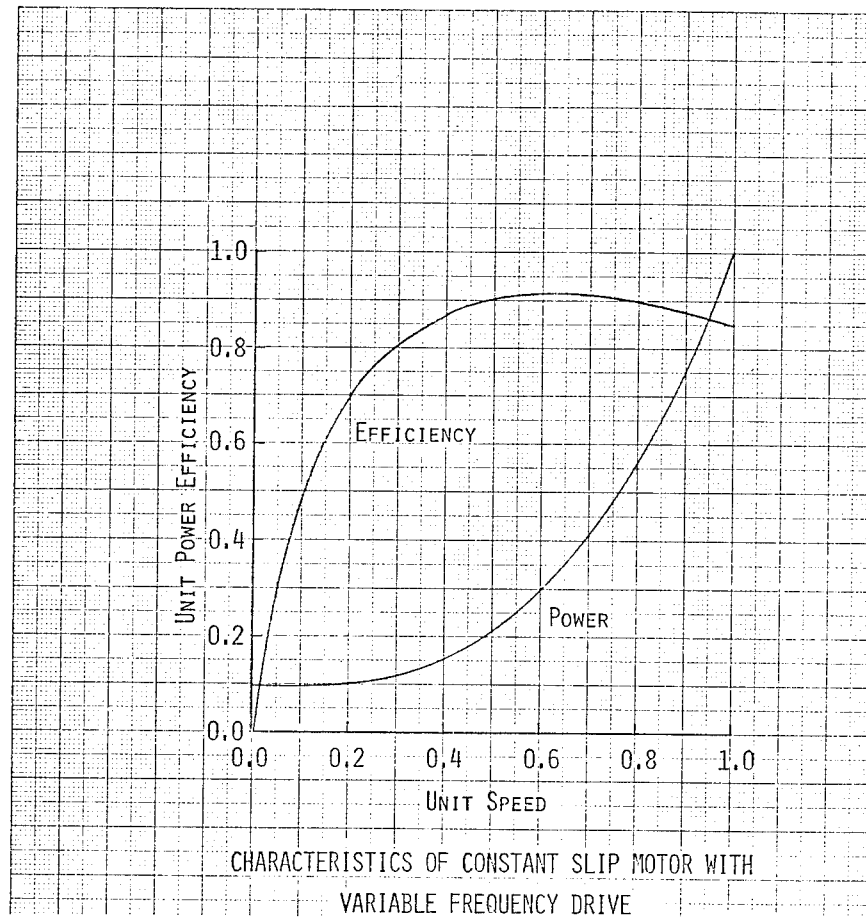
AC ELECTRIC DRIVE FOR VEHICLES WITH FLYWHEELS

ADVANTAGES

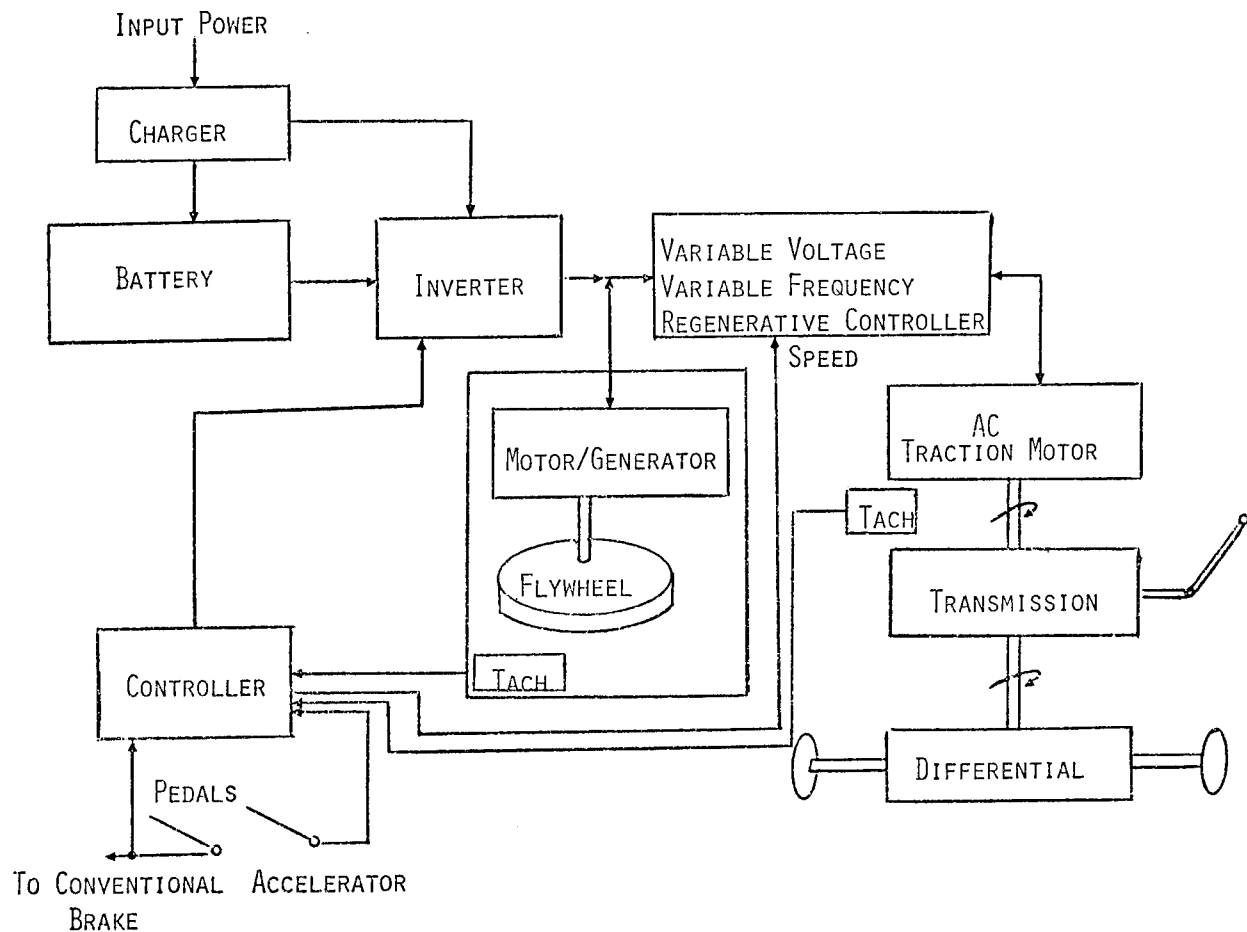
- VERSATILITY
- HIGH EFFICIENCY
- MAXIMUM POWER TRANSFER
- COST EFFECTIVE MOTORS & GENERATORS
- SIGNIFICANT REGENERATIVE BRAKING AT ALL SPEEDS
- CONTROLS TO OPTIMIZE PERFORMANCE & DRIVEABILITY
- TECHNOLOGY AND COMPONENTS AVAILABLE

DISADVANTAGES

- MORE COMPLICATED THAN DC SYSTEM
- MORE EXPENSIVE CONTROLS THAN DC SYSTEM
- INTERFACES REQUIRE POWER CONDITIONING
(AC → DC, DC → AC, AC → AC)
- MAY HAVE HIGHER VOLTAGES THAN DC SYSTEM



EXAMPLE BATTERY/FLYWHEEL ELECTRIC HYBRID



BATTERY/FLYWHEEL ELECTRIC HYBRID

ADVANTAGES

- USES FLYWHEEL FOR TRANSIENT POWER
- USES BATTERY FOR LONG-TERM DISCHARGE AND CHARGE
- MINIMIZES RAPID BATTERY CHARGING AND DISCHARGING
- EXTENDS BATTERY LIFE
- FULL USE OF REGENERATIVE BRAKING
- CONTROLS TO OPTIMIZE ENERGY CONVERSION
- CONTROLS TO SIMPLIFY AND TAILOR DRIVEABILITY

DISADVANTAGES

- MORE EXPENSIVE THAN BATTERY-ALONE SYSTEM
- MORE COMPLICATED THAN BATTERY-ALONE SYSTEM

CONCLUSIONS

- THE TECHNOLOGY EXISTS FOR EACH OF THE SEPARATE COMPONENTS REQUIRED FOR THE ENERGY STORAGE FLYWHEEL.
- SPECIALIZED SYSTEMS HAVE BEEN BUILT AND TESTED WHICH DEMONSTRATE THE NECESSARY PIECEPARTS OF AN EFFICIENT ENERGY STORAGE SYSTEM.
- SYSTEM INTEGRATION NEEDS TO BE APPLIED TO THE SEPARATE COMPONENT TECHNOLOGIES.

DESIGN AND TEST OF A SPACECRAFT ENERGY MOMENTUM FLYWHEEL

J. E. Notti, Jr.
Rockwell International Corporation
Downey, California 90241

ABSTRACT

This paper summarizes the design of a prototype flywheel energy storage assembly developed to evaluate the spacecraft Integrated Power and Attitude Control System (IPACS) concept. In the IPACS application, the flywheel assembly is used for kinetic electrical energy storage as well as conventional angular momentum control. The kinetic storage function dictates high rotational speeds which require new approaches to the design of the major components: rotors, motor-generators, bearing systems, and electronics. The paper includes a general description of a NASA contracted prototype assembly, a discussion of major component design characteristics and the presentation of selected test results. The energy flywheel has demonstrated a power capability of 2.5 KW with a maximum stored energy of 1480 watt-hours. The operating speed range is from 17,500 to 35,000 rpm. The unit has completed performance verification tests and is being delivered to the NASA.

FLYWHEEL-POWERED AUTOMOBILES

Peter M. Newgard
Stanford Research Institute
Menlo Park, California 94025

ABSTRACT

A hypothetical, dual-mode automobile is described that would be powered by both a conventional heat engine and by 10 kWh of stored flywheel energy coupled to an electric drive. Analysis of the system suggests that, compared to a battery powered car, the dual-mode flywheel car would have higher specific power, better potential for early development and a broader potential market.

INTRODUCTION

Over the past several years, SRI has been engaged in a wide variety of energy-related research, including studies of alternative fuels for automotive use. Recently we completed a study for the NSF comparing alternative ways to use coal to power automobiles, i.e., should we make syncrude and gasoline for ICE cars or would it be better to use our coal to make electricity for electric cars? The NSF study indicated an overall energy advantage for the electric car, and, of more immediate importance, a significant advantage in petroleum conservation. In addition, depending on how well we actually control ICE emission, electric propulsion could have a beneficial effect on air quality. Thus, it has become evident to us at SRI that converting to electric vehicles powered by utility-produced electricity would be desirable.

While electric cars are desirable from a societal viewpoint, they are not especially desirable from the viewpoint of a potential owner. The most advanced electric cars, using high-temperature batteries that reputedly will result from a decade of research, will still fall far short of the versatility of liquid-fueled heat engine machines. Electric vehicles can only have a significant impact on our present situation if they can be sold to the auto-buying public. They won't sell unless they can compete with alternatives in traditional terms to provide:

- Instant mobility
- Infinite range
- Good acceleration
- Low cost (first cost and operating cost)

Above all, there must be a rational transition path to the deployment of any new vehicle. It must be evolutionary, and not demanding the simultaneous development of new industries or major facilities.

HYBRID ELECTRIC CARS

It appears to us that the all-electric personal automobile cannot survive in a free-market competition against advanced heat engine machines, even with major improvements in electric energy storage. This has led us to consider various hybrid schemes using heat engines for sustained travel and stored utility electricity for short-range driving. Because this type of machine requires energy storage characterized by high specific power (rather than high specific energy), flywheel energy storage becomes a potential contender.

We have identified two families of hybrids distinguished by market goals. The concept most generally studied has been one of using the energy-storage system for load leveling, with the objective of improving fuel economy and reducing heat engine emissions. Extensive study* of this concept shows that only minor improvements are realized for a major increase in complexity and cost. The improvements in operating cost may be worthwhile in fleet operation with high daily mileage but probably not to a private owner who typically uses the car about one hour per day.

*The EPA Program on Hybrid Vehicles 1969-72 with subsequent reviews by Aerospace Corporation continuing through 1975.

SRI has evolved an alternative concept termed a dual-mode hybrid. The basic design strategy is to use the heat engine as little as possible--only to augment the range of an electric drive. We envision a high-performance, short-range, electric vehicle. A heat engine and generator (sized to provide average power) is added to provide the benefits of:

- Instant mobility--independent of battery charge condition
- Infinite range

These are identically the two features that have and will limit the market for all-electrics. Therefore, the resulting hybrid design has the potential for competing in the first-car market.

Figure 1 shows one physical embodiment of the dual-mode hybrid. The power train can operate in the following ways:

- All electric--clutch open--ICE on (for urban commute driving).
- Series hybrid--clutch open--ICE off (for extended urban driving).
- Parallel hybrid--clutch engaged--ICE on (for extended high-speed driving).

The vehicle is normally charged, overnight, with about 10 kWh of utility power. During the following day's travel, the flywheel-stored energy is used first. When the stored energy is nearly depleted, the ICE/generator begins to provide average motive power and maintains a low energy-charge state. In this engine-powered mode, the electrical system provides load leveling and regeneration advantages. For low-speed urban driving the machine operates as a series hybrid; above a set speed (about 35 to 40 mph) the clutch couples to provide a more efficient mechanical link from heat engine to rear wheels.

The energy-storage device needed for the dual-mode hybrid is distinctly different from that proposed for all-electric propulsion. An energy/power diagram (Figure 2) illustrates this difference and indicates the status of contending devices. The high-energy batteries under development with federal money are aimed at a five-hour nominal discharge. The batteries required for the dual-mode hybrid would discharge in about one hour, with brief excursions to the ten-minute rate. The four nickel-based batteries shown in this area of the figure are relatively near term. They are under active development--mostly with commercial

money, and could be available in two to five years. Although the application of these batteries to automotive propulsion are all limited by the availability of nickel, our resources could easily sustain the initial development and market deployment of vehicles. The flywheel can be viewed as a low-cost, efficient replacement for the nickel battery required to sustain market penetrations beyond about 10 percent.

The hybrid power system described here was derived for the purpose of using utility electricity to power personal automobiles. Let us examine how effective it would be in achieving that goal. In practice, most of our driving consists of a series of short-range trips accumulating to average about 30 miles per day. The proposed hybrid takes advantage of this fact by allowing the first portion of each day's driving to be entirely electric powered. Using data available from two major U.S. cities,^{1,2} we have derived the relationship plotted in Figure 3. This illustrates that the goal of converting urban driving to electric power can be substantially achieved with a modest electric energy store. These data are based on average driving habits. There would, of course, be some natural market selection so that buyers with short-range commutes would favor the hybrid. Thus, actual conversion per car should be much greater than indicated by this chart. In fact, we believe that, on a car-for-car basis, the dual-mode hybrid would achieve much greater conversion to utility power than a limited-range all-electric car. When this is coupled with the potential for early development and a broader potential market, the result is a much greater and earlier potential impact. If R & D effort is to be devoted to electrifying the personal automobile, then the dual-mode hybrid and its high-power storage device should receive the highest funding priority.

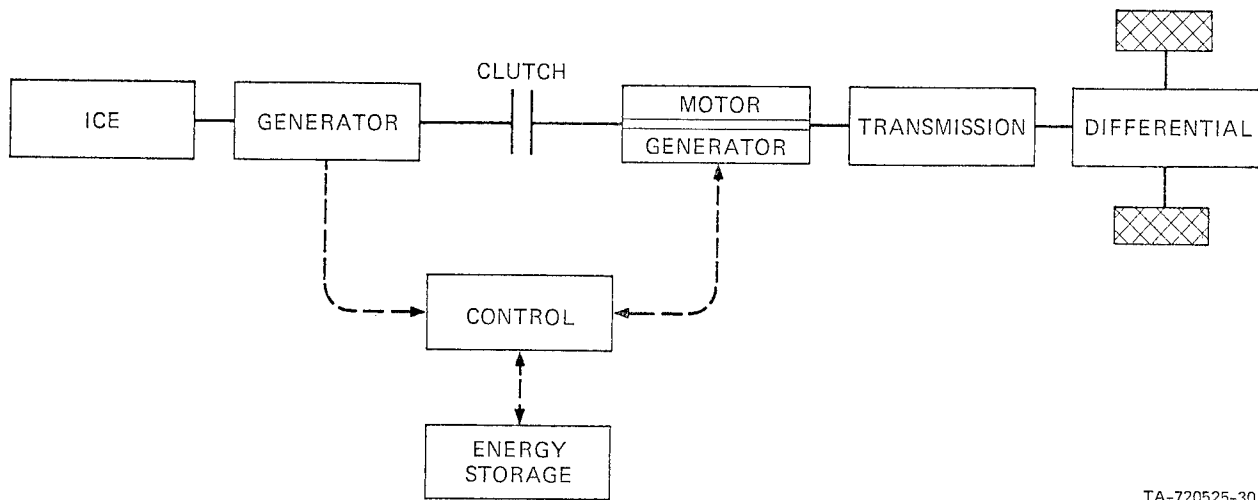
Prepared for: The 1975 Flywheel Technology Symposium, University of California, Berkeley, California, 10-12 November 1975.

References

1. "Chicago Area Transportation Study," Final Report, Survey Findings, Chicago Department of Commerce (December 1959).
2. G. Hagey and W. F. Hamilton, "Impact of Electric Cars for the Los Angeles Intrastate Air Quality Control Region,"

paper 7470, Third International Electric
Vehicle Symposium and Exposition, Washing-
ton, D. C. (19-21 February 1974).

SRI HYBRID CONFIGURATION PARALLEL/SERIES



TA-720525-30

FIGURE 1.

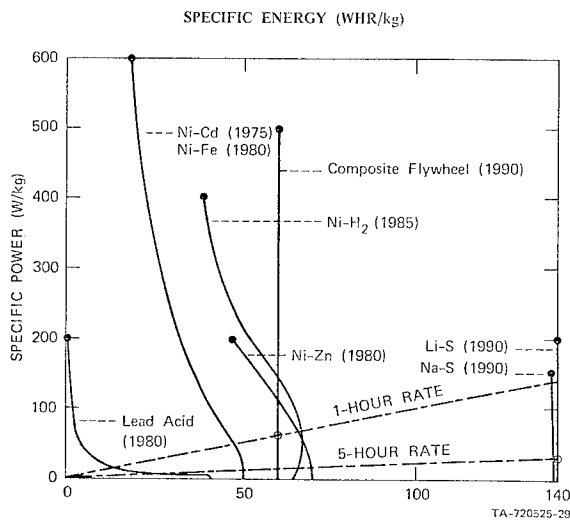


FIGURE 2.

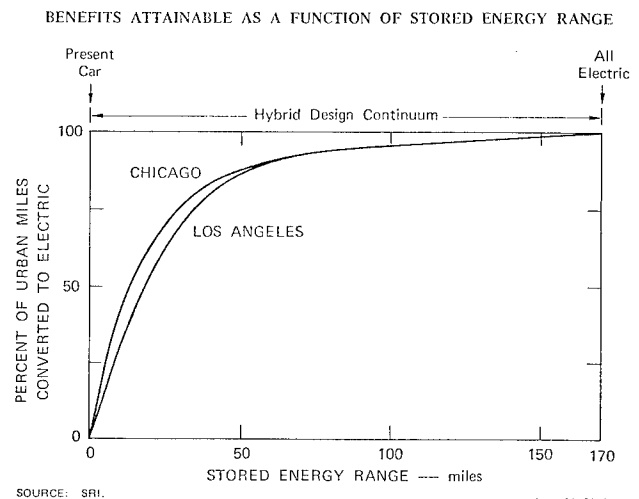


FIGURE 3.

RIM-SPOKE COMPOSITE FLYWHEELS: DETAILED STRESS AND VIBRATION ANALYSIS

C. C. Chamis and L. J. Kiraly
NASA-Lewis Research Center
2100 Brookpark Road
Cleveland, Ohio 44135

ABSTRACT

NASTRAN is used to perform a detailed stress and vibration analysis of thin-wall, cylindrical-shell, rim-spoke, single-rim and multi-rim composite flywheels. The results obtained indicate in a preliminary way that such flywheels have potential for the power storage requirements of the ERDA-NASA 100 KW wind turbine generator.

INTRODUCTION

The use of fiber composite materials in flywheels offers several advantages over metal flywheels. The major advantages result primarily from the high longitudinal specific strength (strength/density) and high longitudinal specific stiffness (modulus/density) of composites compared to conventional metals. Additional advantages of composites are: (1) the large number of composites available with a wide range of mechanical properties (Illustration 1) from which selections can be made to meet diverse design requirements, (2) various flywheel configurations can be readily fabricated using the extensively-developed filament winding capability that already exists, and (3) less material is required for containing flywheel bursts.

Elementary strength-of-materials relationships show that, of the various composite flywheel configurations possible, the thin-wall, cylindrical-shell, rim-spoke configuration utilizes composites most efficiently. The distinct advantages of this configuration are:

1. The rim is stressed primarily in the hoop direction in the centrifugal force field.
2. The rim can be fabricated using hoop windings only.
3. The thickness of the rim can be selected to minimize radial stresses resulting from the fabrication process (winding, thermal, phase-change shrinkage) and the centrifugal forces.

4. The spokes can be sized to undergo radial deformation equivalent to that of the rim. For example, one can make the spokes from the same composite but with a pseudo-isotropic laminate configuration. This will yield a spoke modulus of one-third that of the hoop, a relationship which can be shown to be the required condition for equivalent radial deformation. Equal radial spoke-rim deformation eliminates stress concentrations at the spoke-rim juncture and the resulting induced bending in the rim. It also avoids the designing of a radially sliding joint between spoke and rim in order to minimize bending and stress concentrations.

5. The concept is easily adaptable to multi-rim composite flywheels with specified clearance between rims.

Because the rims already described are thin-wall cylindrical shells, they can vibrate readily in one or several of their many natural frequencies within the wide range of flywheel operational rotation speeds (excitation frequencies). In order to assess the suitability of the composite thin-wall, cylindrical-shell configuration in a flywheel environment, the vibration resistance of these configurations in the presence of a centrifugal force field needs to be determined.

The objective of the investigation summarized herein was to perform detailed stress and vibration analyses of the thin-wall, cylindrical-shell, rim-spoke composite flywheel using NASTRAN in order to demonstrate:

1. The adequacy of this configuration for a specific flywheel application.

2. That available structural analysis tools can be used to assess the potential vibration problem that might arise in such flywheels.

DESIGN STUDIES

The specific flywheel application investigated was for energy storage during calm or low wind velocity conditions for the ERDA-NASA 100 KW wind-turbine generator (WTG) now being made operational at the NASA-Lewis Research Center, Plum Brook facility. Based on available data the assumed design requirements for the flywheel are:

- | | |
|-------------------------------------|------------|
| 1. Required energy supply | 4 days |
| 2. Minimum reserve energy | 25 percent |
| 3. Charging rate, maximum | 100 KW |
| 4. Excess overspeed charging rate | 5 percent |
| 5. Power delivered during down-time | 10 KW |

The resulting total energy storage requirement is 1410 KW-hr (4.5×10^{10} in-lb).

The above design requirements and mechanical properties of candidate unidirectional composites (Illustration 2) were input to a computer-programmed algorithm. This algorithm is designed to size single-rim and multi-rim flywheel configurations based on a highest specific strength basis.

The following two configurations were selected by the algorithm (Illustration 3):

1. Single-rim

- | | |
|--------------------------|---|
| single-rim energy stored | 1410 KW-hr |
| composite | T300/epoxy at 0.7 fiber-volume ratio (FVR) |
| configuration | 9 ft mean dia,
15.5 ft high,
6.5 in thick |
| angular velocity | 6740 RPM
3180 ft/sec tip speed |
| rim weight | 23,550 lb |

- | | |
|-------------------------|------------|
| power density | 60 W-hr/lb |
| maximum charging torque | 1250 in-lb |

2. Multi-rim, with five composite rings and metal core (rings selected to store 75 percent of the energy)

- | | |
|-------------------------------------|--|
| five-rim energy stored | 1065 KW-hr |
| composite | T300/epoxy (0.7 FVR)
S-G/epoxy (0.7 FVR)
boron/6061 Al (0.5 FVR) |
| configuration | 6 ft outer dia,
10 ft high |
| angular velocity | 10,105 RPM
3180 ft/sec tip speed |
| five-rim weight | 25,930 |
| five-rim power density | 41 W-hr/lb |
| maximum charging torque (outer rim) | 230 in-lb |

The above results show that the single-rim composite flywheel has about one and one-half times greater power density than the five-rim wheel. This means that a penalty is paid when an attempt is made to make greater use of the space occupied by the flywheel as compared with a thin single-rim flywheel.

It should be noted that a flywheel made from T300/epoxy will not be cost effective at today's graphite prices. However, a flywheel made from an equal or greater strength E-glass/epoxy will be about 15 percent heavier but will be about 100 times less expensive than the single-rim T300/epoxy flywheel evolved in the present study.

Stress and vibration characteristics of both the single-rim and the five-rim flywheel configurations were analyzed using NASTRAN. The rim was assumed to be made from hoop-wound composite and the spokes to be made from a pseudo-isotropic layup of the same composite. The finite element representation consisted of 72 homogeneous, anisotropic, quadrilateral plate elements, 84 nodes, and 504 degrees of freedom (DOF) for the single-rim

(Illustration 4). For the five-rim wheel 300 elements, 360 nodes, and 2160 DOF were used. The spokes were represented using frame elements. Both gravity and centrifugal forces were considered. Both the static and vibration analyses were carried out using NASTRAN L 15.5 rigid format 13, which determines vibration frequencies in the presence of force fields.

Stress data from the static analysis showed that the rim was stressed to its maximum design allowable and that both the rim and the spokes sustained equal radial displacements as desired. Both of these results may also be determined using elementary strength of materials relationships. The results also showed that the desired clearances between rims in the five-rim configuration were preserved.

The NASTRAN vibration analysis results showed that the lowest frequency of both the single-rim and five-rim hoops could be within the operating frequency of the flywheels. However, the higher harmonics should be well beyond the operating frequency of the flywheels. Though a parametric study was not performed during this investigation, it is possible to vary the flywheel configuration (geometry) variables (radius, height, and thickness) so that the lowest natural frequency of the flywheel is greater than its highest operating frequency.

Also, NASTRAN results were obtained for an additional mass (weight and location) for possible dynamic balancing. These results showed that the lowest frequency of the single-rim wheel can be increased by about 11 percent using only a one-half ounce mass. This mass, however, increased the local hoop stress by about 30 percent.

CONCLUSIONS

NASTRAN can be used for the detailed stress and vibration analysis of both single-rim and multi-rim, thin-wall, cylindrical-shell, rim-spoke composite flywheels. It was also demonstrated on a preliminary design basis that these types of flywheels would be adequate to supplement the power of the ERDA-NASA 100 KW wind turbine generator during periods of low wind velocity.

LONGITUDINAL COMPOSITE STRENGTH AND STIFFNESS TO DENSITY RATIOS COMPARED WITH METALS

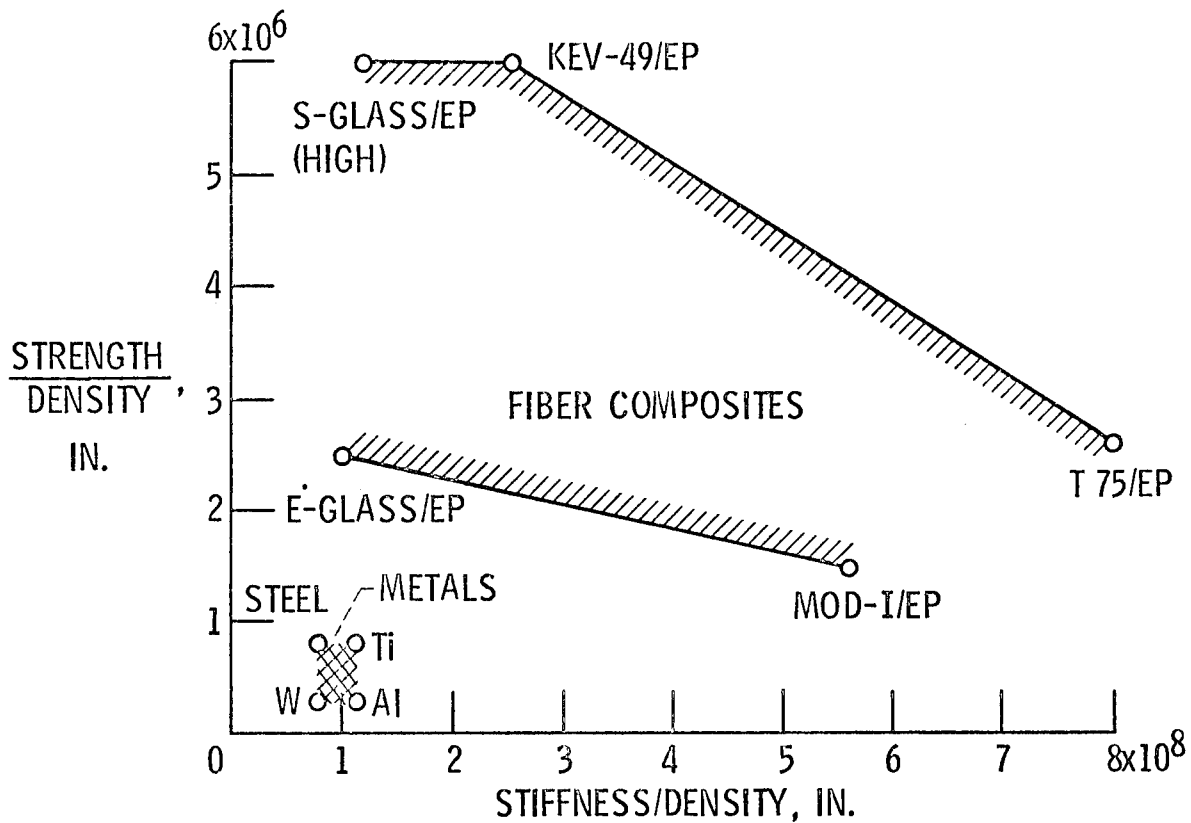
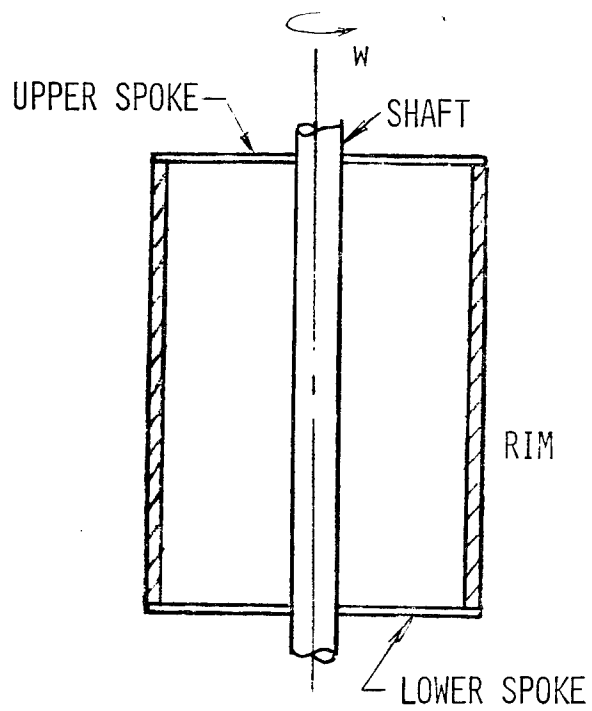


Illustration 1

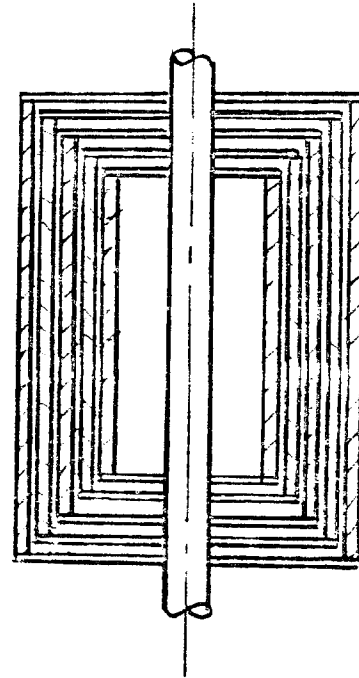
TYPICAL PROPERTIES OF UNIDIRECTIONAL FIBER COMPOSITES AT ROOM TEMPERATURE

PROPERTIES	UNITS	BORON/ EPOXY AVC05505	BORON/ POLYIMIDE WRD9371	SCOTCHPLY EPOXY 1009-26-5901	MODMOR I/ EPOXY ERLA4617	MODMOR I/ POLYIMIDE WRD 9371	THORNEL 300/ EPOXY NARMCO 5208	KEVLAR 49/ EPOXY CE-3305	BORON/ ALUM. 6061-T6
1. FIBER VOLUME RATIO	--	0.50	0.49	0.72	0.45	0.45	0.70	0.54	0.50
2. DENSITY	lb/in ³	0.073	0.072	0.077	0.056	0.056	0.058	0.049	0.095
3. LONGITUDINAL THERMAL COEFFICIENT	10 ⁻⁶ in/ in/of	3.4	2.7	2.1	--	0.0	0.01	-1.60	2.20
4. TRANSVERSE THERMAL COEFFICIENT	10 ⁻⁶ in/ in/of	16.9	15.8	9.3	18.5	14.1	12.5	31.3	9.00
5. LONGITUDINAL MODULUS	10 ⁶ psi	29.2	32.1	8.8	27.5	31.3	26.3	12.2	31.5
6. TRANSVERSE MODULUS	10 ⁶ psi	3.15	2.1	3.6	1.03	0.72	1.5	0.70	20.0
7. SHEAR MODULUS	10 ⁶ psi	0.78	1.11	1.74	0.9	0.65	1.0	0.41	6.0
8. MAJOR POISSON'S RATIO	--	0.17	0.16	0.23	0.10	0.25	0.28	0.32	0.23
9. MINOR POISSON'S RATIO	--	0.02	0.02	0.09	--	0.02	0.01	0.02	0.13
10. LONGITUDINAL TENSILE STRENGTH	psi	199,000	151,000	187,000	122,000	117,000	218,000	172,000	216,000
11. LONGITUDINAL COM- PRESSIVE STRENGTH	psi	232,000	158,000	119,000	128,000	94,500	247,000	42,000	250,000
12. TRANSVERSE TENSILE STRENGTH	psi	8,100	1,600	6,670	6,070	2,150	5,850	1,600	20,000
13. TRANSVERSE COM- PRESSIVE STRENGTH	psi	17,900	9,100	25,300	28,500	10,200	35,700	9,400	30,000
14. INTRALAMINAR SHEAR STRENGTH	psi	9,100	3,750	6,500	8,900	3,150	9,800	4,000	20,000

ILLUSTRATION 2



SINGLE THIN-WALL RIM

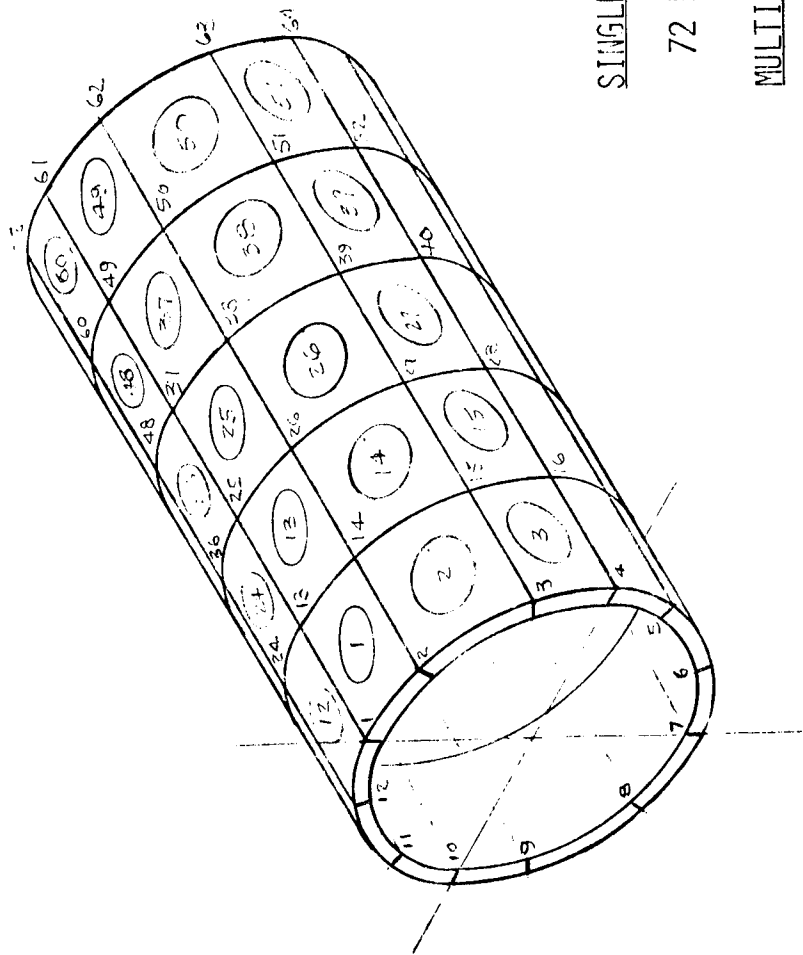


FIVE THIN-WALL RIMS

SCHEMATICS OF FLYWHEEL CONFIGURATIONS INVESTIGATED

Illustration 3

FINITE ELEMENT REPRESENTATION



SINGLE RING FLYWHEEL

72 ELEMENTS 84 NODES

MULTI RING FLYWHEEL

60 ELEMENTS 72 NODES PER RING

300 ELEMENTS 360 NODES TOTAL

Illustration 4

THE USA-MERDC HIGH ENERGY STORAGE HOMOGENOUS FLYWHEEL MODULE

Donald E. Davis
Dynamic Energy Systems
Rocketdyne Division
Rockwell International
6633 Canoga Avenue
Canoga Park, California 91304

ABSTRACT

A 30 kWh flywheel energy storage module is being designed by Rockwell International, Rocketdyne Division, for the U. S. Army Mobile Equipment Research and Development Center (USA-MERDC). This module represents a major milestone toward high energy density, high energy storage flywheel systems.

INTRODUCTION

A flywheel has an inherent capability to store large amounts of energy in a fairly small design envelope and an ability to accept or supply energy at rates much higher than batteries and other storage systems can. These two characteristics are important to many military applications.

Flywheel systems have generally been low energy density, heavy, low-speed systems. The introduction of the modified constant stress flywheel configuration has dramatically modified the scope of flywheel systems in general. The conception and experimental evaluation of composite flywheel systems has further enhanced the creditability of flywheel systems. Until the modified constant stress flywheel was demonstrated in the early 1970's, flywheel energy densities of 1 to 3 watt-hrs /pound was the generally accepted design mode. The recent Rockwell International flywheel systems, which include the B-1 Landing Gear Retraction System, the Integrated Power and Attitude Control System and the USA-MERDC module have been designed on the basis of flywheel energy storage densities in excess of 10 watt-hrs /pound.

DESIGN CRITERIA

The USA-MERDC flywheel module (Figure 1) represents a state-of-the-art configuration which incorporates 12 watt-hrs./pound flywheels with theoretical safety factors (stress) in excess of 1.60. Table 1 represents the basic design criteria used for the flywheel module.

TABLE 1

DESIGN CRITERIA FOR FLYWHEEL MODULE

1. TOTAL ENERGY STORAGE OF 30 kWh
2. COUNTER ROTATING SHAFTS
3. TOTAL ENERGY STORAGE MAXIMUM RELEASE RATE OF 3215 KW
4. TOTAL MAXIMUM ENERGY TRANSMITTAL THROUGH MODULE OF 6430 KW
5. TOTAL ENERGY TRANSMITTAL DUTY CYCLE \approx 38%
6. CYCLE LIFE = 5000 CYCLES
LIFE SPAN = 5000 HOURS

The flywheel module illustrated in Figure 1 provides power at a rate greater than 8,000 horsepower and a duty cycle of approximately 38%. The remaining 62% of the time frame is necessary for recharging and parasitic loss recovery.

Because of the many possible, severe, module operational motions, significant consideration was given to gyroscopic loads and the anticipated overload conditions to be experienced by the bearings. These considerations and other high reliability constraints dictate a conservative bearing and seal approach, which by necessity causes fairly high parasitic losses. Table 2 shows the possible bearing configurations and the anticipated losses associated with each.

TABLE 2

BEARING LOSS SOLUTIONS

JET LUBRICATED DUPLEX BALL/ ROLLER	27.6 HP	CONVENTIONAL CONSERVATIVE
MIST LUBRICATED DUPLEX BALL/ ROLLER	10 HP	NOMINAL R & D NEEDED TO ESTABLISH PRACTICALITY
MAGNETIC BEARINGS	1-5 HP	IN-DEPTH R & D NEEDED TO DEVELOP PRACTICAL BEARING SYSTEM

The relative trade-offs between seal configurations and losses is shown in Figure 2. The anticipated upper and lower limits of parasitic losses to be experienced by the module and the trade-offs based on components selection are shown in Figure 3.

FLYWHEEL CONFIGURATIONS

A full spectrum of flywheel sizes, operational speeds and modified constant-stress configurations have been considered. In the design approach chosen, a flywheel with a "weak-link", outer rim ring will be utilized in the module. The "weak-link" rim ring provides several advantages over the thin-rim, modified, constant stress configuration shown in Figure 4 as #0. The outer rim ring (configurations 7, 10 and 17) provides the added advantages of (a) improved moment of inertia distribution, (b) a failure mode which can be safely contained, and (c) the possibility of flywheel self-braking during over-speed conditions. Configuration #17 is the prime candidate being considered for flywheel incorporation into the module. This dual-nested wheel configuration provides a theoretical factor of safety of 1.37 (based on ultimate stress) at the design overspeed limit (110% of rated).

CONCLUSIONS

The USA-MERDC flywheel module will be a more sophisticated, high-energy storage flywheel module than has been constructed to date. The parasitic losses are going to be higher than those originally conceived, although under the proposed operational modes the parasitic losses are not critical.

As a result of the study phase of this program, it is apparent that high-speed, low-loss bearings with long life spans are basically non-existent. Also, low-loss, high-speed vacuum seals are not available as state-of-the-art items. Both of these flywheel subcomponents must be significantly improved before flywheel systems with long run down times (> 24 hours) can be designed.

It is also apparent that operational energy density values greater than 15 watt-hrs /pound will be obtainable only in anisotropic composite flywheels.

USA-MERDC HYBRID GAS TURBINE/FLYWHEEL HIGH ENERGY STORAGE MODULE

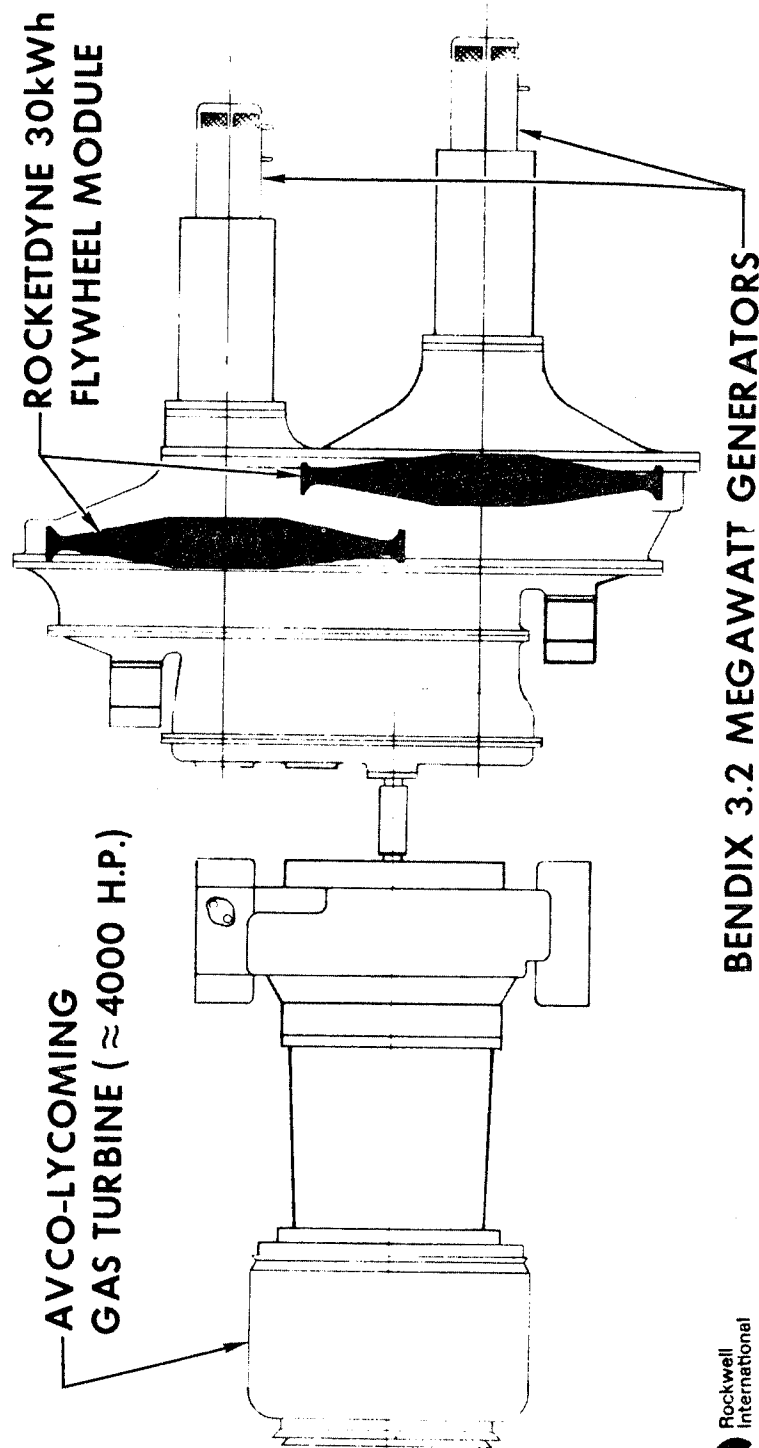


Figure 1

SC375-529



Rockwell
International
Rocketdyne Division

SEAL AND VACUUM REQUIREMENTS

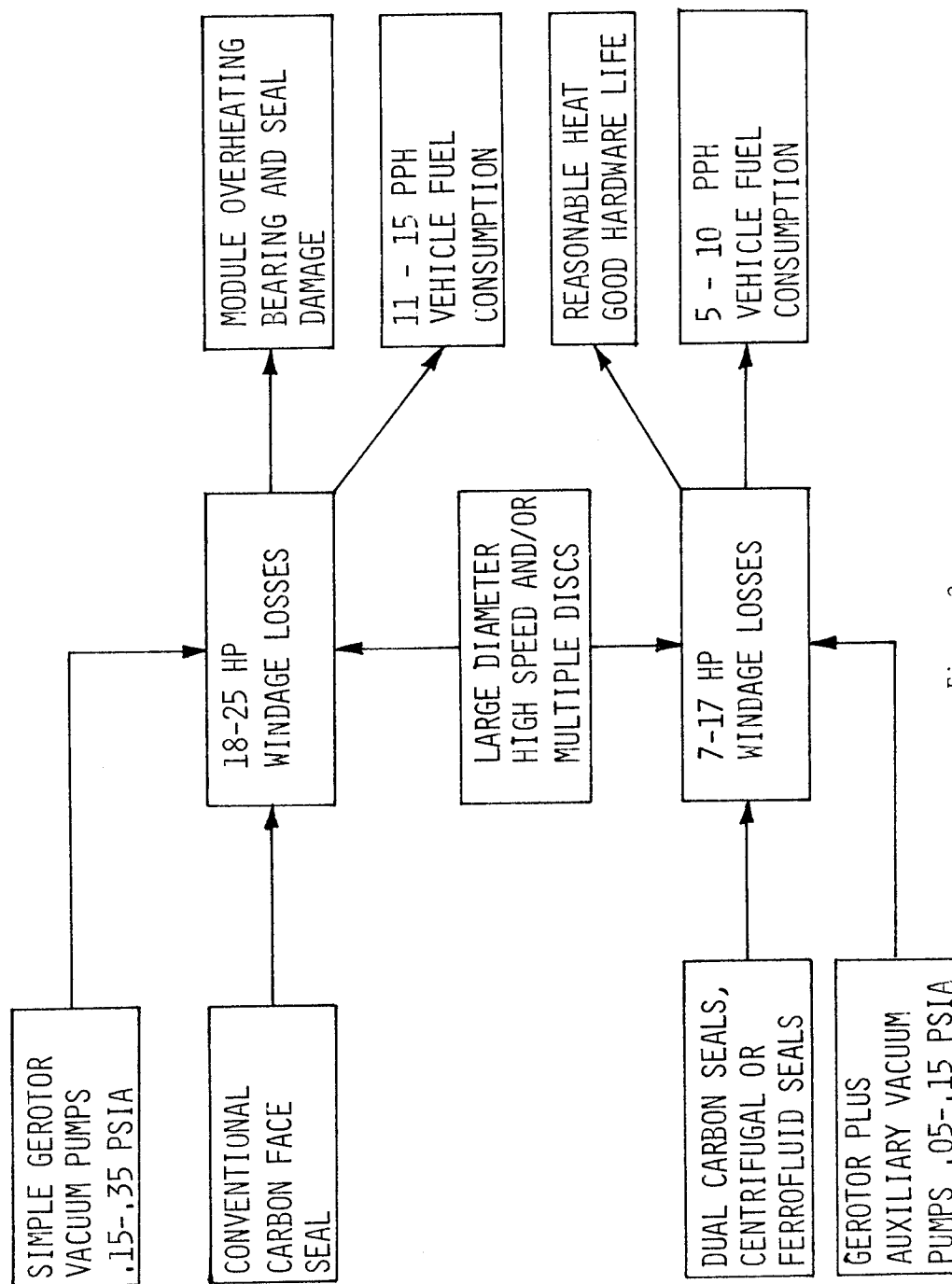


Figure 2

TOTAL PARASITIC LOSS COMPARISON

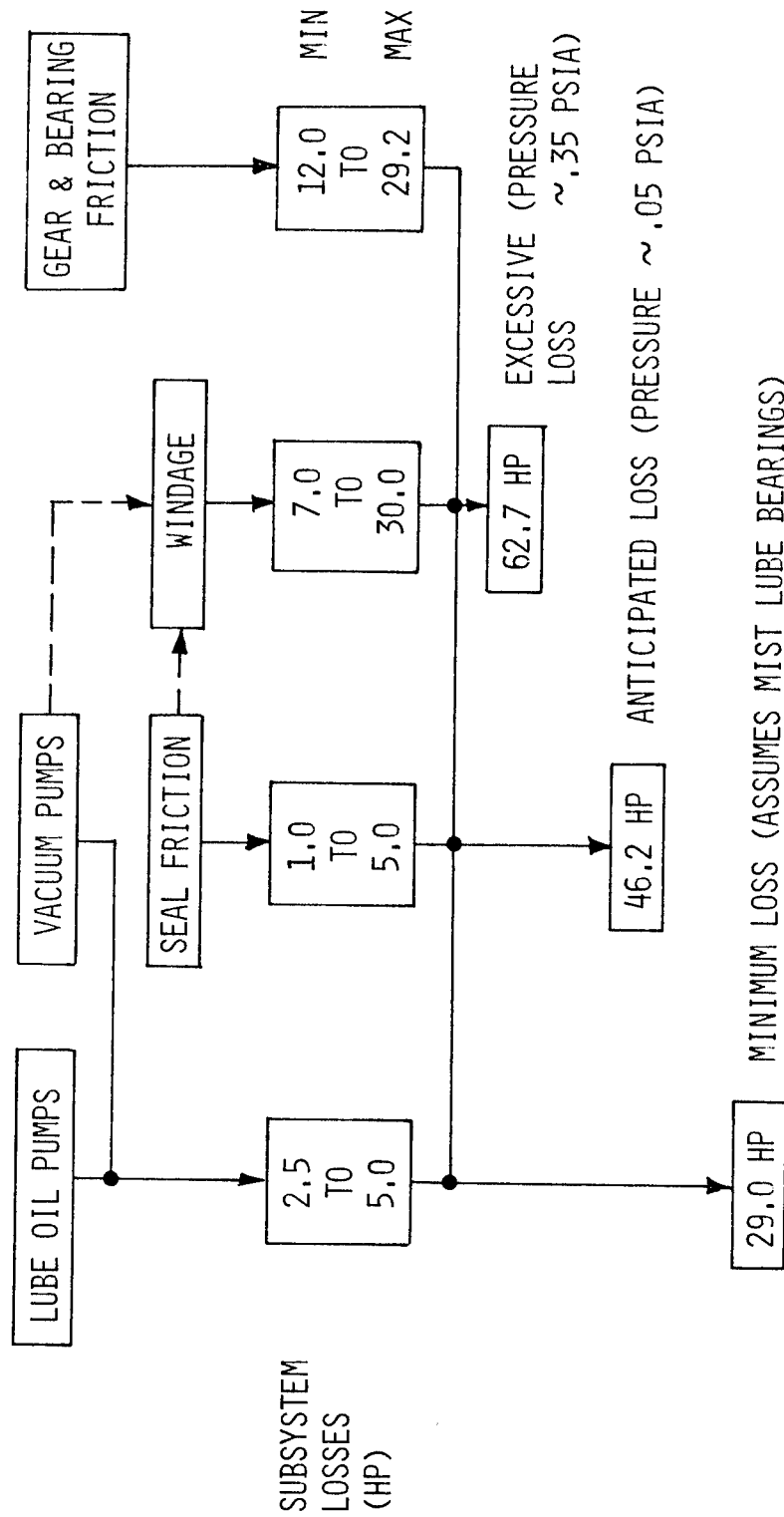


Figure 3

FLYWHEEL CONFIGURATIONS

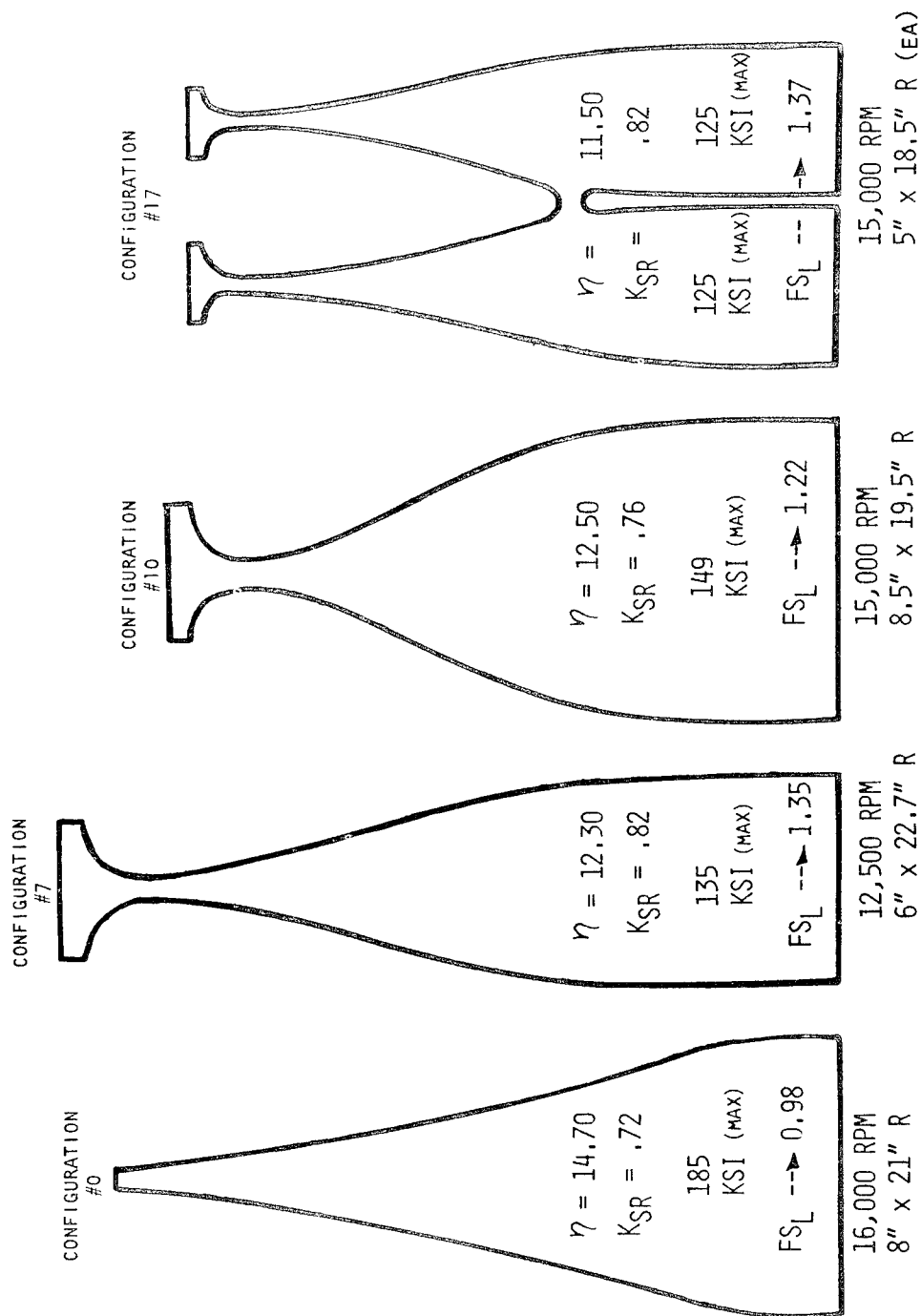


Figure 4

IDEAS AND EXPERIMENTS IN MAGNETIC INTERFACING*

Kristian Aaland and Joe.E. Lane
Lawrence Livermore Laboratory, University of California
Livermore, California 94550

ABSTRACT

Simulated experiments on a small scale have begun as a result of developing magnetomechanical devices. Rim-only suspension and driving wheels for automobiles are envisioned, with energy coming from two counter-revolving rim-only flywheels. The taboo that magnetic bearings can only be stable by active feedback is denied.

INTRODUCTION

To operate a town at night on solar power requires an energy storage system in the 10^{12} -J range. If high strength fibers are used in a rim-only flywheel, the 10^{12} J of energy is contained within a 100-m circumference. This should be easy to bury beneath any utility load center. The ring would spin at a velocity of 1000 m/s in near vacuum and weigh 2000 t, clearly indicating the need for no-contact and no-wear magnetic bearings. Magnetics for power input/output interfacing is also understood.

To coordinate these magnetic circuit requirements, we have started to do simulated experiments on a small scale. We have also reported very encouraging results leading to new ideas of small-scale uses. The next goal should be the building of working models to aid in the testing of composite fibers. A sample ring accelerated to failure would give unique data on modules and one-dimensional tensile stresses. The model would operate at the same peripheral velocity as a large-scale product.

A visual presentation of this report is shown in the Appendix.

MODELING

The hoop stresses in the rim of a flywheel is Dv^2 , where D is density and v is peripheral velocity. We are considering fiber composites with $D = 2000 \text{ kg/m}^3$ and tensile strength around 2 GPa (300,000 psi); regardless of flywheel size, velocity thus becomes

$$\sqrt{\frac{2 \times 10^9}{2000}} = 1000 \text{ m/s.}$$

We are aiming at a 60-Hz power line interfacing on a large scale. This means a distance ($1000/60 \approx 17 \text{ m}$) is transversed for each power cycle. This becomes the physical distance between pole pairs at no slip (synchronous) operation. In a 1% scale model this becomes a reasonable 17-cm dimension, but the powering has to be at $100 \times 60 = 6000 \text{ Hz}$. This frequency can be handled by the largest of thyristors in the single-cycle ferroresonant circuit.¹ For a flywheel, we will be operating on a demand schedule of power pulses. Each cycle is 6000 Hz, putting special requirements on the magnetic materials. Permanent magnets composed of insulating materials like ferrite work well, except for their poor coercivity (easily demagnetized). Ferrite magnets are available in a rubber matrix. These "rubber magnets" are very convenient to shape for experimental work.

Working models require stronger magnets like samarium cobalt (SmCo_5). Because SmCo_5 is metallic and electrically conducting, eddycurrents are induced that detract from their strength. If the SmCo_5 is broken into 30- μm -size particles that are insulated from each other, the eddy-current concern is eliminated. The high density packing and magnetic alignment of these particles do, however, require special technology.

Kamerbeek² indicates that large-scale magnetics is most economically done by superconductors. This implies, of course,

*This work was performed under the auspices of the U.S. Energy Research & Development Administration, under contract No. W-7405-Eng-48.

that the flywheel ring is operated at a very low temperature. If a cryogenic temperature is going to be used for the fiber composites, testing of the composites should be done at that temperature too.

This exploratory work was done most expediently with rubber magnets. Moreover, the physical motion of magnetics at $v = 1000$ m/s was simulated by electromagnetic waves of sufficient strength physically to observe and to measure lift and drag components of force. It must also be noted that the magnetic materials have not been exposed to the extreme pressures that would exist in a rotor rim of a small model.

MAGNETIC LEVITATION OF A SPINNING STORAGE RING

Magnetic journal bearings have been at work for decades. These are all of a design involving "active feedback positioning control."³ Dr. J. Lyman of Cambridge Thermionic Corporation* stationed only three lifting and centering magnets around the rim of a large momentum ring for NASA, Langley, Virginia.⁴

We have chosen to consider only fail-safe ideas; thus excluding active feedback. Taking notice of magnetic levitation and guidance work in transportation,⁵ we set out to model an "endless train on a circular track." Just like the train, the magnets were to be contained in the moving part, in this case the ring. Eddycurrent-generated heat in the stationary groundplane becomes easy to remove, or the electrical losses can be controlled down toward zero by superconductivity (cryogenics). (In practice, certain losses are required for damping and stability.)

Our experiments revealed lift but no sideways or centering stability. (See Fig. 1.) It was afterwards found that a radial cut in the groundplane was all that was required for stability. (See Fig. 2.)

An improved demonstration was made one after another by different cuts and bends of the groundplane. (See Fig. 3.)

*Reference to a company or product name does not imply approval or recommendation of the product by the University of California or the U.S. Energy Research and Development Administration to the exclusion of others that may be suitable.

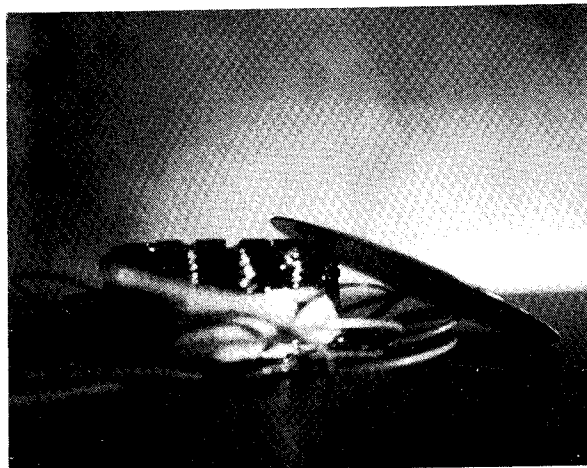


Fig. 1. Experiments revealed lift but no sideways or centering stability.

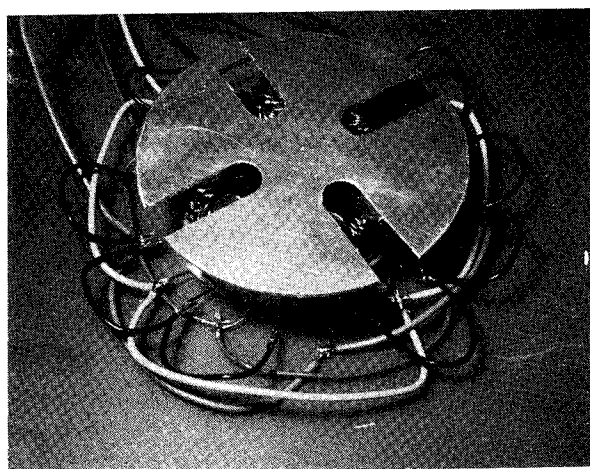


Fig. 2. A radial cut in the groundplane was all that was required for stability.

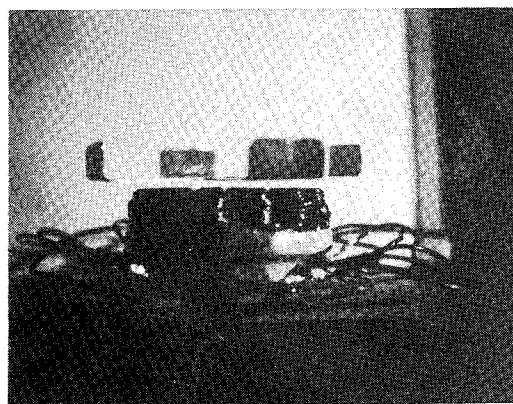


Fig. 3. Different cuts and bends of the groundplane.

In considering the real fiber flywheel with high-density concentrations of magnets on the sides, these geometrics seem unrealistic. We can only conceive of

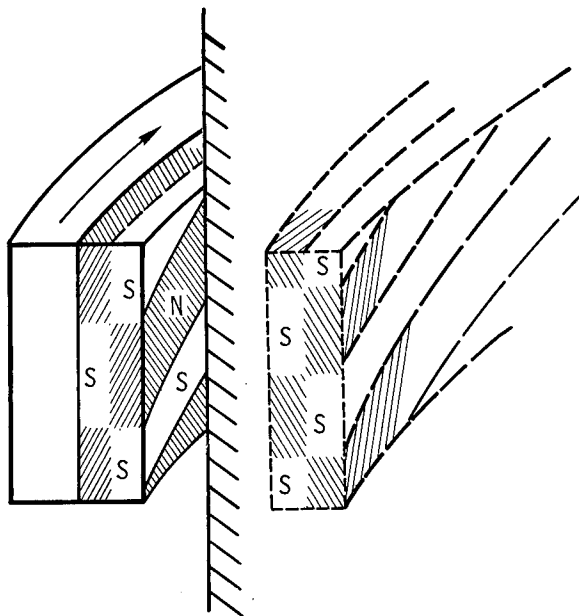


Fig. 4. Magnetic shear forces by induction.

magnets being contained on the inside periphery of the fiber ring. Now, how do you produce magnetic shear forces by induction? Figure 4 depicts an idea that should work. The spiral pattern of magnetic poles will have both vertical (lift) and circumferential (drag) components of velocity. As reflected from a stationary cylindrical-conducting surface, the repulsive force will provide centering stability. This force increases with velocity.⁵ The drag-force is highest at a certain low velocity, resulting in a quick lift at startup. A simulated experiment was performed. Experiments with shapes of poles as well as conduction surfaces are pending. This must be done finely with actual motion. Now it is time to think about motor concepts. Could it possibly be combined with this magnetics levitation?

A NEW PULSED MOTOR-GENERATOR

Today's commercially produced ac motor depends upon magnetic materials for economy. By minimizing the airgap between rotor and stator, less reactance and, consequently, more horsepower is obtained for a given amount of copper investment. On the other hand, the narrow gap puts very high forces on the bearings. This local radial force may be an order of magnitude higher than the tangential driving force.

New permanent magnets are changing the picture of dc motors. Samarium cobalt

magnets are capable of 1-T induction with an airgap that is 10 times longer than the length of the magnet. We have a new world in magnetics of available flux in free space with no or little concern for the return flux path.

New designs of permanent magnetic dc motors have taken forms of rotating, open-frame armature coils (no iron). We will pursue the concept of rotating magnets around a stationary armature. The pole strength of our magnets will allow us to use a greater spacing, thus reducing radial pull. Also, we will program the stationary coil to be excited before and then reversed after the passage of a magnet. If these two forces are equal, there will be no net radial force during each powering cycle. The powering cycle is quite fast (a fraction of a millisecond) so the mass of the magnet integrates the radial pull-push action. The same pulse-width powering cycle will perform well over a 1 to 2 speed range. In principle, the horsepower will be constant for a given repetition rate of pulsing. Because the repetition rate is completely programmable down to zero, so is horsepower input. Interestingly, this motor may have a much higher revolution per second than input pulse rate per second.

Needless to say, this system may also function as a generator. Selected cycles are triggered at the opposite pole passage; energy is returned to the single-cycle circuit and to the line. We have attempted to make a model of this motor for the 500- to 1000-m/s speed range. The

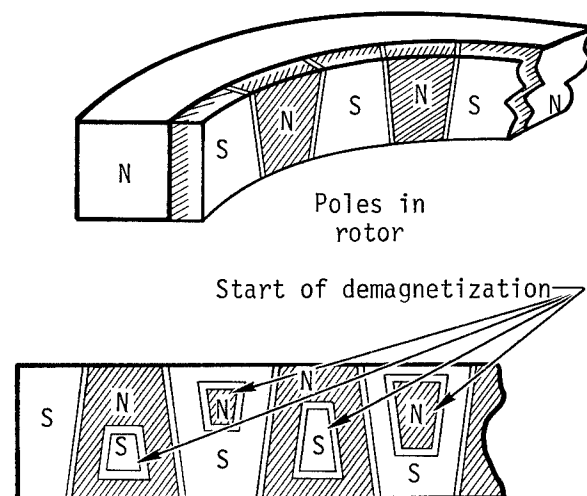


Fig. 5. Demagnetization started in the low coercivity rubber magnets.

ferroresonant circuit,¹ triggered from an optical mark on the rim, pulse powered the armature well. However, at a few percent only of the available current, demagnetization started in the low coercivity rubber magnets as shown in Fig. 5. This made it impossible to bring the rotor up to a high enough speed for adequate efficiency to accelerate. However, the predicted torque was observed. Polepieces composed of solid SmCo₅ magnets did not work at all because of eddycurrent repulsion at kiloHertz frequency.

Samarium cobalt was obtained in 30- μ m, individually oriented, particles. These were cast in an epoxy. The field strength from these compound magnets were even less than rubber magnets. The problem relates to the alignment needs of the particles.

EXPERIMENTAL APPROACHES IN MAGNETICS

Modeling was done by maintaining the velocity as a constant. Thus, any physical size hoop puts the fibers under the same tensile stress. The ballpark figure of 1000 m/s was handled by simulation for the magnetics part. By merely creating traveling magnetic fields simulating the shapes and velocities of permanent magnets attached to a flywheel, a rapid succession of experiments were done. There was no need for

going in and out through vacuum. Magnetic forces were created strong enough to produce actual levitation and were measured without the confusion of physical friction.

The succession of discrete electromagnets along the trajectory is not exactly equivalent to a smoothly moving magnet. For gross effect there were no noticeable differences with experiments with the smooth Gramme-Ring. This ferrite ring is a continuously wound, square, cross-section toroid. Excited with three-phase current, field lines emerge perpendicular to the ring surface at each pole. With field lines available on each of the four sides of the ring, planar as well as cylindrical experiments can be performed. The penalty is that for a given input power, the magnetic fields are spread out and, consequently, are diluted.

As in any of the simulations, the traveling field velocity is the product of pole-pair distance (pitch) and powering frequency. In this case, 0.1 m times 10 kHz equals 1000 m/s pole-moving velocity.

The 10-kHz, three-phase power came from a multikilowatt transistor amplifier. The maintenance of sinusoidal wave shapes with proper 120° phasing for varying

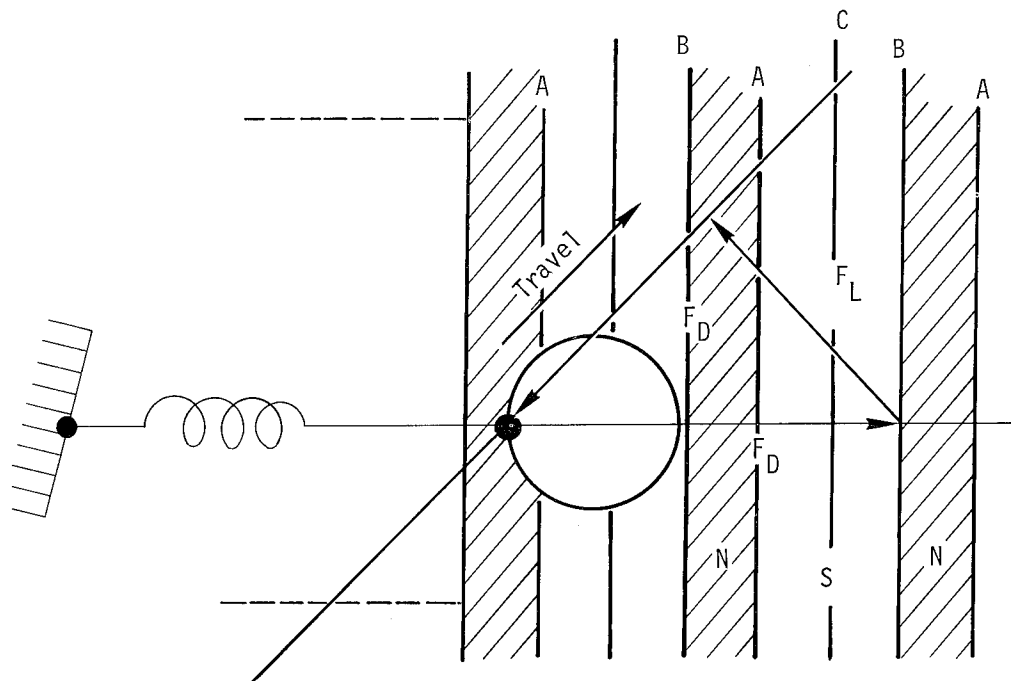


Fig. 6. The spiral-shaped moving poles were simulated by means of a plane of parallel

inductive loading (experiments) are troublesome. For expediency and quality of wave shape, which also translates to a smooth motion of poles, we resorted to the use of an 800-Hz alternator.

With the power and stiffness of an alternator, we could easily drive air coils. This becomes important in the simulations of bands of moving poles. We simulated the spiral-shaped moving poles (Fig. 6) at first by means of a plane of parallel wires. The object was to observe the effect of groundplane shape. News! We found none. There is no apparent difference in the drag-force between a circular, rectangular, or strip conductor shape. In the plane, the drag-force is orthogonal to polestrips. No torque was observed.

SUMMARY

In the process of picking up a century old subject of developing magnetomechanical devices (motors), fresh ideas are stimulated as well as verified through experimental simulation.

We hope to have wiped out the taboo that magnetic bearings can only be stable by active feedback.

We envision new designs in motors without physical bearings. One day there

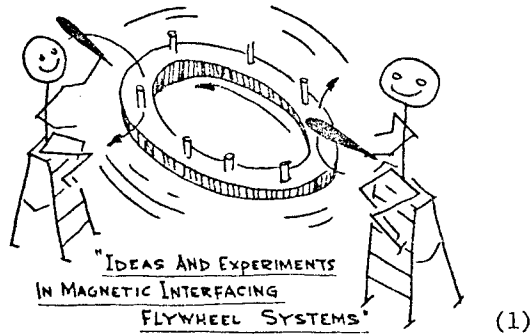
will be a rim-only wheel for automobiles. The magnetic fields generated on board will provide suspension, guidance, and drive to the "tire." Maybe the energy will come from two counter-revolving rim-only flywheels. The passengers might occupy the center of these storage rings. The success of the floating wheel ideas depends upon small, mobile, superconductive technology as well as magnetic circuit configurations.

A first use of rim-only flywheel is likely to be in stationary installations of up to 10^{12} -J storage units.

REFERENCES

1. K. Aaland "The Ferroresonant Circuit," to be presented at the IEEE Power Electronics Conference, June 8-10, 1976, Lewis Research Center, Ohio.
2. E. M. H. Kamerbeek, Phillips Techn. Rev., 35 (4), 116 (1975).
3. F. T. Backers, Phillips Techn. Rev., 22 (7), 232 (1960).
4. Analysis report available from W. W. Anderson and N. J. Groom, contract No. NAS-1-12529, NASA, Langley, Virginia 23665.
5. R. D. Thornton, IEEE Trans. Magn., 11, 981 (1975).

KRISTIAN AALAND AND JOE E. LANE
LAWRENCE LIVERMORE LAB

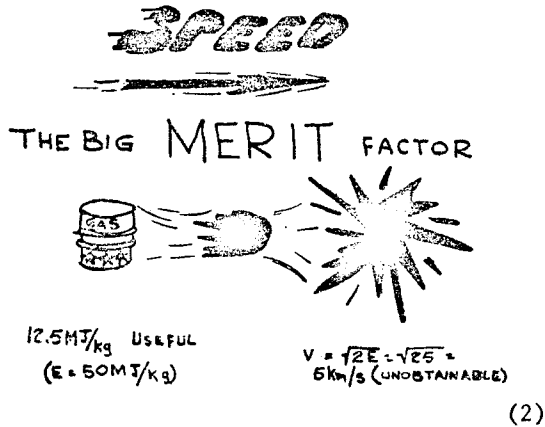


(1)

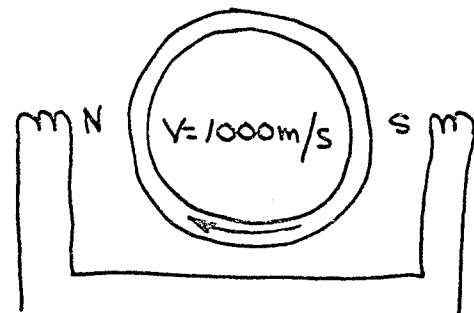
NEW FACTORS:

POLE PITCH
($\frac{1}{2}f = 8 \text{ METERS (!) FOR } v=1000$
AND
BEARINGS

(4)

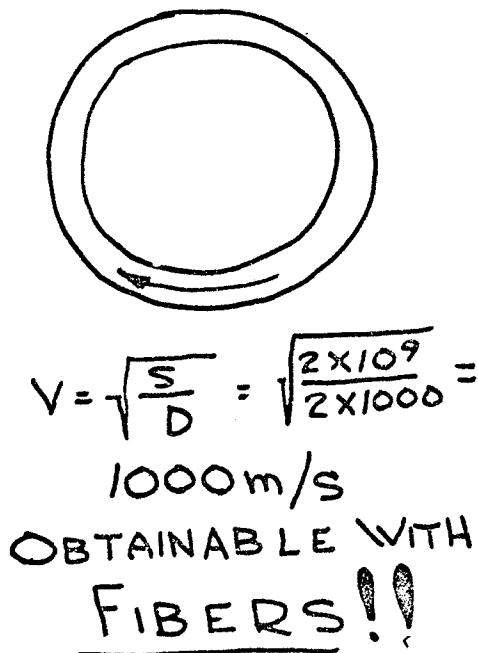


(2)

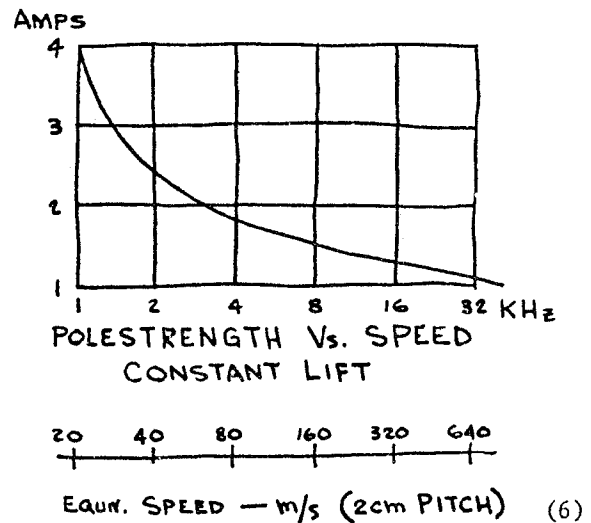


REDUCES
MACHINERY SIZE
10 X FROM TODAY'S
100 m/s

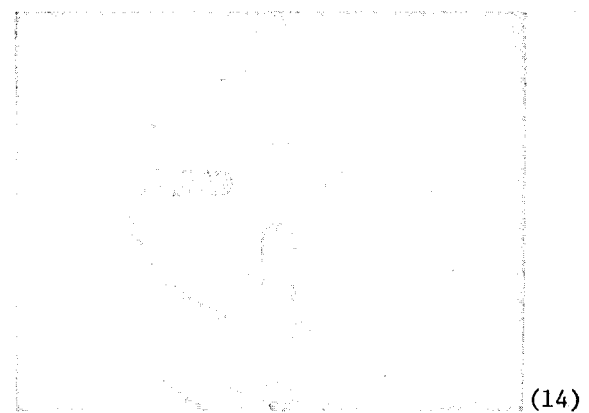
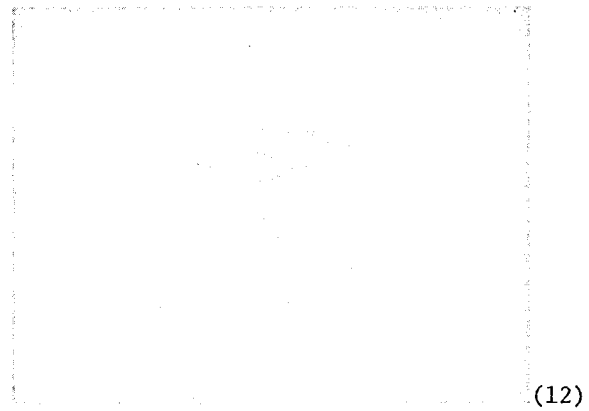
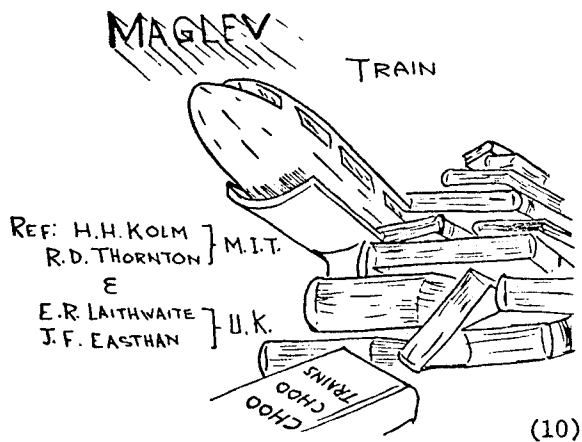
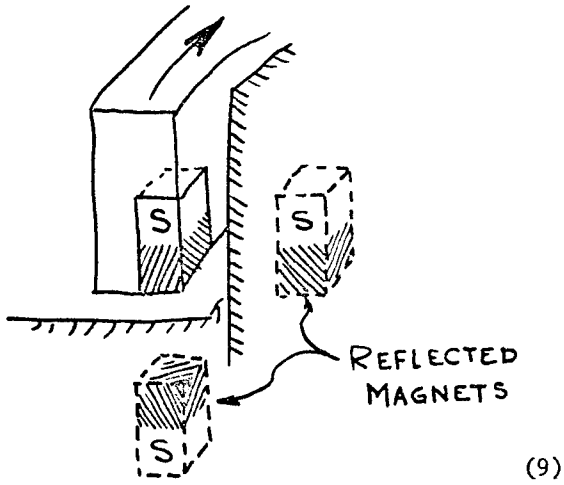
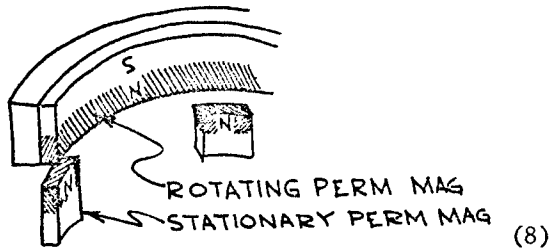
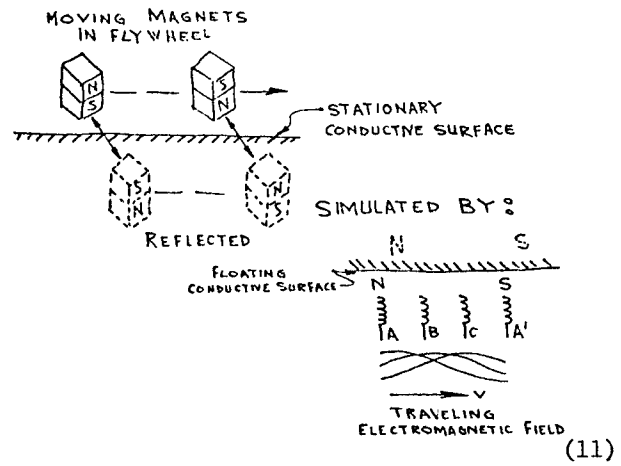
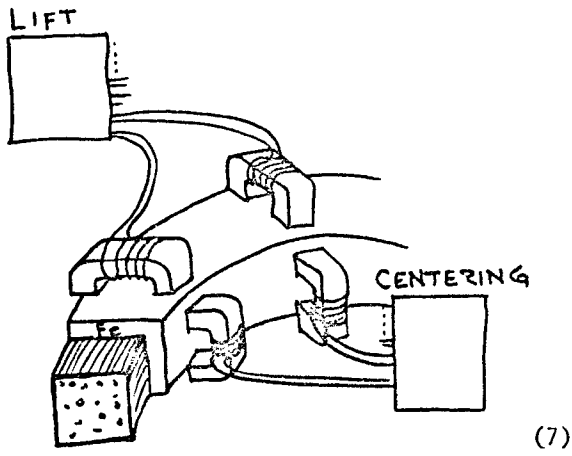
(5)

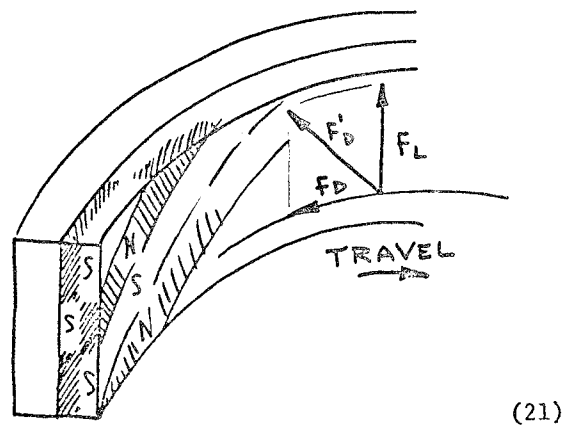
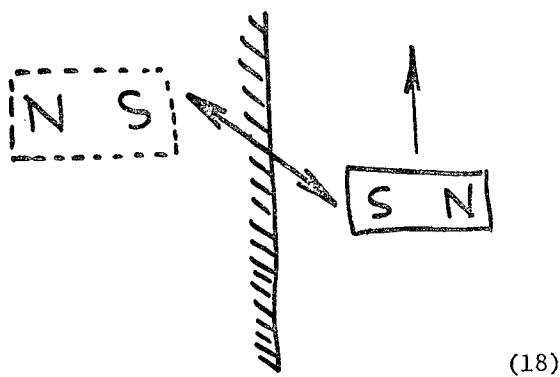
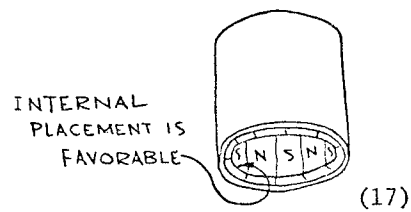
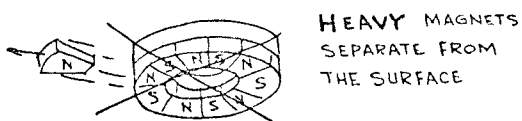
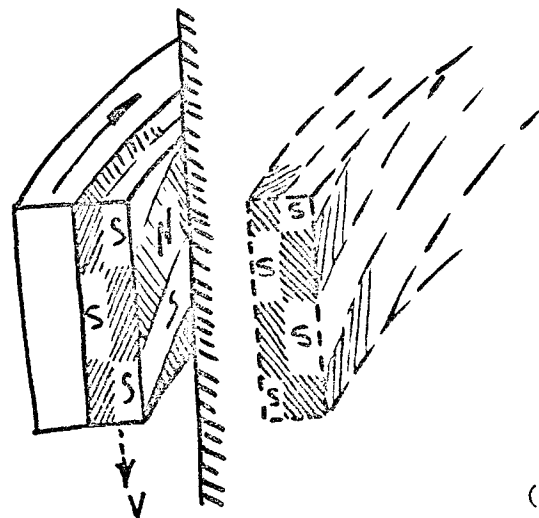
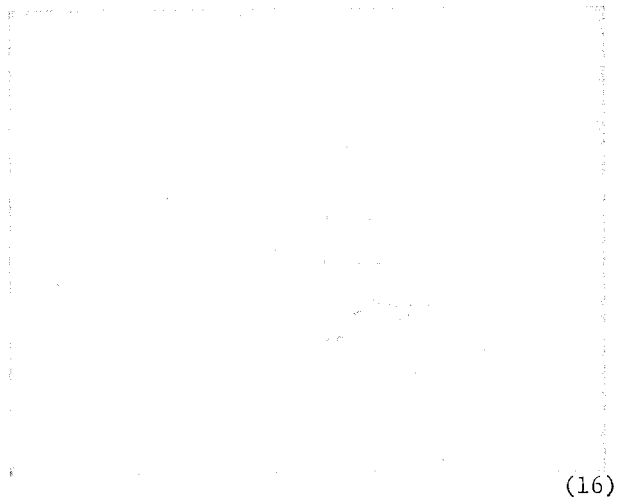
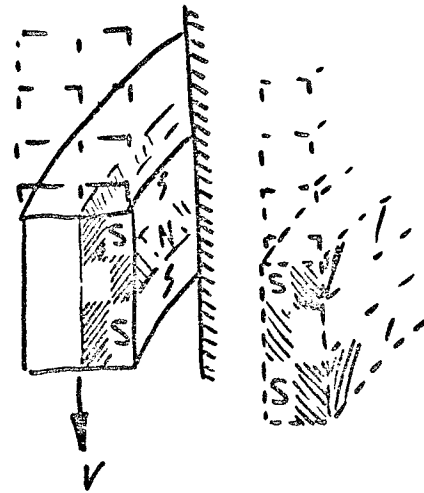
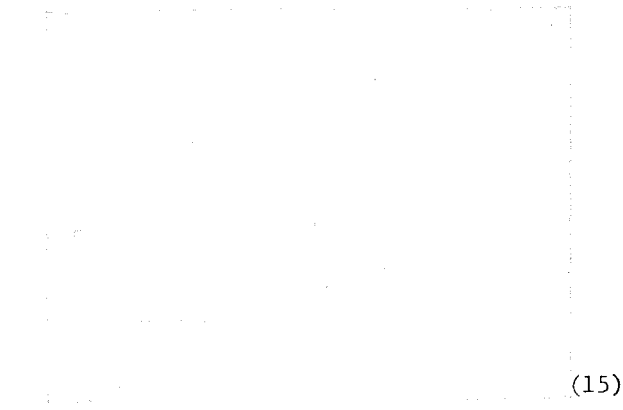


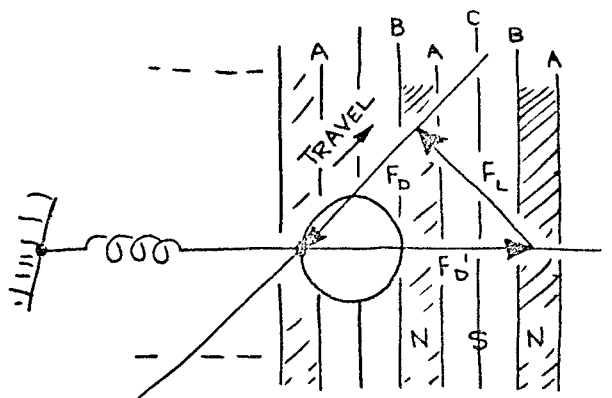
(3)



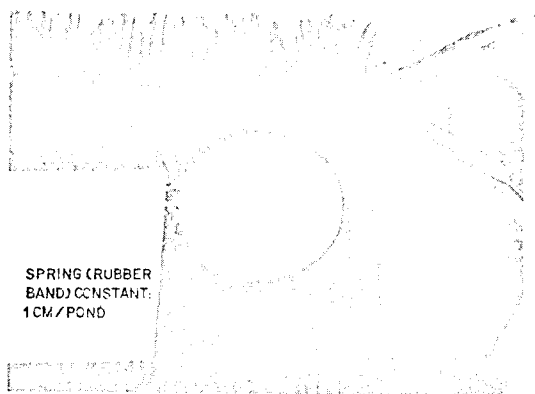
(6)







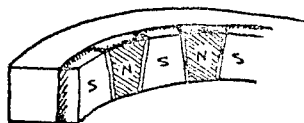
H OVERING DISC
ON PLANAR MODEL (22)



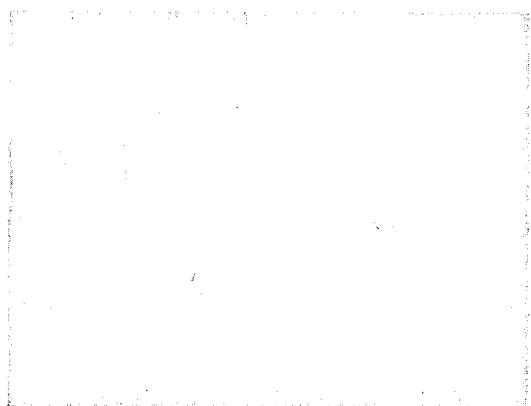
LINEAR MODEL

(23)

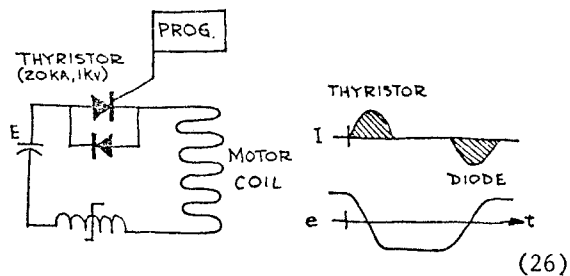
MOTOR/GENERATOR REQUIREMENT — VARIABLE SPEED AND SYNCHRONOUS (PERMANENT MAGNET ROTOR)



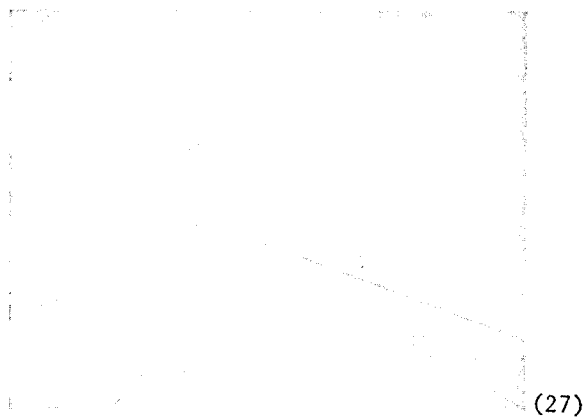
(24)



(25)

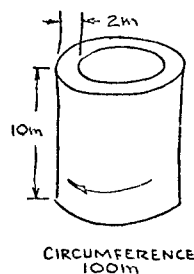


(26)



(27)

10¹² JOULE MAGNETICS



INSIDE SURFACE AREA $\approx 10000\text{m}^2$

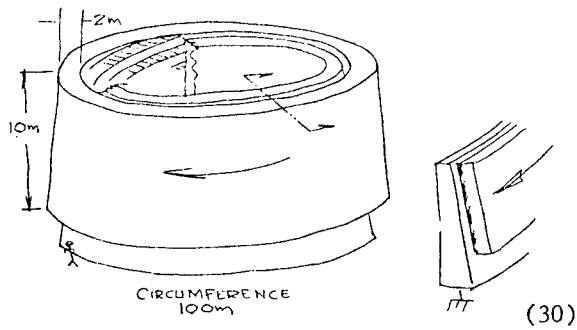
AVERAGE SHEAR - FIELD (B_s)
REQUIRED FOR LEVITATION OF

MASS = $2 \times 10^6 \text{ kg}$ ($F = mg$)

$$B_s = \sqrt{\frac{F \cdot 2m_0}{A}} \approx 0.2 \text{ TESLA}$$

IF THE (WEAK) 0.2 TESLA FIELD ALSO
IS USED FOR MOTOR/GEN, ONE
VERTICAL WIRE INDUCES $B_{lv} =$
2000 VOLTS (PEAK). $\rightarrow 1\text{KV RMS}$
AT 1GW POWER LEVEL, THEN
1000 WIRES (1KARMS EACH) WILL DO. (29)

10^{12} JOULE-MAGNETICS



SUMMARY

WE HAVE SHOWN — LEVITATION WITH CENTERING
WITHOUT ACTIVE FEEDBACK

— A PULSED SYNCHRONOUS
MOTOR/GEN. OF UTMOST
SIMPLICITY

THAT WILL DIRECTLY INTERFACE
TO D.C.

OR FOR LARGER THAN 8m RINGS
WILL ADAPT TO 60Hz

(31)

APPROACH TO FLYWHEEL DEVELOPMENT

Gerry B. Andeen
Stanford Research Institute
Menlo Park, California 94035

ABSTRACT

At Stanford Research Institute we designed, built and tested a 26"-diameter, high-speed composite-type flywheel that had a 1/2-inch square cross-section Kevlar^R/epoxy rim and two S-glass/epoxy spokes. Instabilities created by whirling in a vacuum test chamber at supercritical speeds were controlled with a Coulomb-type frictional damping device. This paper discusses rotor dynamics, stresses, balancing and some supercritical speed considerations that arise in flywheel design. A list of references is appended. Though clever design may solve short-run problems, we believe that successful composite flywheels will require new technology that will 1) extend the theory of balancing flexible rotors, 2) characterize and measure mass and stiffness uniformity, and 3) assure stability from self-excited motions without excessive loss of energy from the wheel.

INTRODUCTION

We are all aware of the need for energy storage mechanisms on many different scales. At one extreme we need a replacement for gasoline for our cars because of the gloomy oil situation. At the other size extreme, we need load-leveling devices for our utility power supply grids to reduce capital costs.

We all recognize the potential of the flywheel as an energy storage device that can serve across the size spectrum. Considerable recent effort has also made us aware of the special advantages of flywheels, i.e., long life and high power. In particular, we must give credit to those workers, such as Lawson,¹ who have been active in optimizing conventional flywheels and in promoting their advantages. We take special note of the pioneering efforts of Rabenhorst² and Post³ in calling our attention to the new materials of exceptional specific strength, such as Kevlar^R, and their potential impact on energy storage. These workers have also done a great deal to bring flywheels to the attention of the public in general.

We would like to note, and this is a perception not shared by all, especially the public, that we are dealing with a new technology. Most flywheels with which we are familiar are what can be called momentum flywheels rather than energy flywheels. Whereas the momentum and energy storage aspects are inseparable, the purpose of the

usual flywheel is to smooth a cycle by means of providing a large moment of momentum. The design of this kind of a flywheel is covered in the textbooks that tell you to put a large mass at a large moment arm. Since the wheel is usually not subjected to significant self-loading forces, the texts fail to discuss the strength to mass, specific strength parameter that we know is important in the energy storage function. In a certain sense, the familiarity with the conventional flywheel, its appearance in the pottery shop, in the sewing machine, in the automobile, and the like, is an impediment to development, since the fact that we are dealing with a new technology is obscured and implicitly ignored.

That we are dealing with a new technology is especially evident when we begin to consider the nonisotropic materials, as in most of the super-strength materials where the greatest performance appears to lie. These fiber materials, and the composite structures formed from them, have seldom been used in self-loading situations; situations in which the loads are caused by the dynamic body forces of the components themselves rather than by external forces. The continuum approximation usually used in stress analysis comes into question at a much larger scale when composites are used under self-loading conditions than when much more nearly uniform isotropic materials are considered. The continuum approximation is under attack not only because the stress is not

smooth but also because the loading is irregular.

The experimental results to date further indicate that we are dealing with a topic beyond our comprehension. No successes and many failures of composite-material rotating devices are on record. Most notable perhaps is Pratte and Whitney's well documented government project.⁴ Also there is Lockheed's demonstration with the "bullet composite" flywheel to show that they should indeed concentrate on the steel wheel.⁵ Rabenhorst⁶ also indicated difficulty in getting his early bar superflywheel operating. In addition to these well known difficulties are many unreported failures not supported by public money. We are privately aware, for example, of the failure of the ultracentrifuge people to be able to exploit the apparent advantages of the super-strength materials.

The basic question that we want to address in dealing with a new technical area is how close one can realistically approach theoretical limitations and how to identify limiting factors. A most interesting aspect of this conference will be to hear how well other people have done in approaching theoretical limits for composite flywheels, to hear what they think are the limiting factors, and how they have approached their solutions.

SRI APPROACH

The purpose of this presentation is to explain what we have done up to the present and why, to discuss what we see as the significant limiting factors, and to elucidate our plan for the future.

The best way to identify the limiting factors is to build a composite wheel, run it, and identify the problems as they appear. We have designed flywheels and chambers in which to run them, and we have run wheels, and come to problems. One by one we have overcome these problems; we are gradually moving up in speed. At present we have succeeded in running a composite wheel at half the speed calculated to be required for self-rupture. This is not that good because it amounts to only a quarter of the energy stored at the breaking speed. It should be noted that titanium and other isotropic material centrifuges are run at speeds well over 90 percent of that of self-destruction. We have identified several of the problems

that limit our progress and that we feel will limit the ultimate usefulness of composite energy flywheels. We have also laid out what we feel is a rational flywheel development program for this time.

We wish to lay out the problems and what is known about the problems in a logical fashion in order to focus on them. Even more important is to strip the mystery away from many of the problems so that clever designers can begin grappling with the interrelated concerns. Perhaps by identifying the problem and by calling upon clever designers we may be able to get a flywheel operational before all of the principles are analyzed mathematically.

CONCENTRATION ON ROTOR DYNAMICS

There are many places to begin scrutinizing an area that could become a new technology:

1. One must have or be able to develop a market.
2. One must solve a set of technical problems; for energy storage flywheels these problems are:
 - a. How to provide the power input and output compatible with the rest of that system whether it be for an automobile or a power grid;
 - b. How to provide low-friction bearings with acceptably long life for the high speeds and/or large loads; and
 - c. How to solve the rotor dynamics problems that are inevitably associated with rotating equipment.
3. One must assure the safety and the social acceptability of the product. In a way, the development of safe flywheels is a great deal like the development of nuclear power. The safety must be assured and must be accepted by the public.

All of the problems are interlocked. They must be solved simultaneously to have a valid new technology. However, if we are considering whether we can have a new technology, we want to focus on the portion of the problem that appears to be the most critical.

Many people, including ourselves, are looking at potential uses. As the fly-

wheels with their housings approach the energy densities of batteries, one market estimate can be based upon the size of the battery market. Furthermore, it appears likely that the development of a good energy storage flywheel applicable over a broad size range would have advantages over batteries and create new markets for itself. A great many of the early flywheel projects have been aimed at identifying potential markets or uses. We are satisfied that there is enough of a market to look more closely at the other concerns.

The safety problem already has also attracted considerable attention. A prestigious National Research Council subcommittee has favorably reviewed the safety considerations of kinetic energy storage systems applied to buses.⁷

As has already been intimated, we believe that new technology is involved and is the crucial question. We believe that technical feasibility as regards the non-isotropic material flywheels has not been satisfactorily addressed. It is time to get into the laboratory and take a good hard look at the technical difficulties involved.

When we turn to the technical problems we are again faced with determining which technical problem is most critical. If we do go into the laboratory, we have to work with all the problems, but we do not have to solve them with the same rigor. In a test facility, for example, it is not necessary to extract power but only to spin the flywheel to test its rotor dynamics. It is acceptable for the bearings to have a relatively short life. The converse is not true. One cannot develop the bearings without knowing the life, the loads, and the other environmental conditions they must endure. There is hardly any point in designing a power train or the bearings if the rotor dynamics problems cannot be solved. Therefore, there seems to be a natural ordering of the technical problems; the design of the rotor and its suspension stands at the head of the list.

The approach that I have outlined is the approach of an engineering researcher. It is possible that a funding agency might want to approach the problem in an entirely different way. For example, a plausible strategy might be to ignore the composite flywheel concepts entirely, putting emphasis on development of the conventional steel flywheels. The market would be

developed using these steel wheels and presumably some entrepreneurial organization would come along and find the way to get greater performance by using the high-promise, high-specific-strength materials. We are looking at what the entrepreneurial organization would have to do.

STRESSES

Stresses may be associated with the mounting or may be purely internal to the rotor itself. A perfect flywheel has only internal stresses, symmetrical about the rotational axis. It is these stresses that are dealt with in discussions of shape factors; these stresses were primarily responsible for delamination in early experiments. Analysis of the symmetrical stresses, based on continuum assumptions, are well in hand⁸ and have led to the thin shell concepts. The symmetrical stresses are clearly important, but the limits that they identify are only limits to be approached depending upon the stresses introduced by the second set of sources, imbalance and lack of symmetry. These sources contribute both to mounting-associated stresses and internal stresses.

The ideal shape for an isotropic material flywheel is one that gives constant stress throughout. This shape is very thick near the hub and thin near the periphery and is a good one for relatively minimizing the effect of the imbalance and lack of symmetry stresses. Mounting forces act upon the thickest part of the wheel, producing minimum stresses. Imbalance in remote parts of the wheel distribute their imbalance to thicker sections thus reducing their effect. These isotropic flywheels are also made of high modulus materials that are inherently uniform on a small scale. There is no lumpy loading and there is minimum distortion because of the stiffness of the material.

On the other hand, the optimum shape for a composite flywheel is the thin ring. There is clearly not much material available near the hub to distribute mounting forces because this material detracts from the energy density efficiency of the rotor. In addition, most of the fibers have a much lower modulus than steel. At the same stress a Kevlar^R wheel would have 1.5 times the strain of a steel wheel and a glass wheel would have 3 times the strain. Because the composites are made up of fiber, with some matrix material,

such as an epoxy, the scale of nonuniformity is on the order of the size of the fiber. Therefore we expect the forces due to nonuniformity to be larger, we expect the wheel to distort more in response to those nonuniform forces that may further amplify the stresses.

These kinds of effects are difficult to analyze and have generally been handled by computer programs based upon finite element analysis. This kind of analysis, although able to account for the gross effects described, is even more inadequate to the basic nature of the composite material. The grid size chosen for any such analysis is inevitably larger than the scale of the nonuniformity involved. This nonuniformity, however, cannot be ignored; breakdown of a composite material will inevitably commence at the boundaries described by the nonuniformity.

The basic question being addressed in a consideration of the symmetrical versus imperfection-originated stresses is whether to run the rotor with a subcritical or a supercritical mounting. With a subcritical rotor, where rotation rate is below the first resonant frequency, the mounting stresses are proportional to the speed and the imbalance. With the supercritical rotor the mounting stresses are determined by the stiffness of the mounting and the extent of the imbalance. If the mounting is made soft enough, the mounting forces can be made arbitrarily small leaving only internal stresses in the rotor.

It is natural to decide to run the steel wheel subcritically. The steel wheel is naturally thicker at the axis, which makes it very stiff so that the resonant frequency is easily made high, it is easy to design to run below resonance.

The opposite choice seems to be a natural for the composite flywheel. The thin ring is subject to much greater natural imbalance and is not likely to have a very rigid configuration at the center for its support. Decision to go to a supercritical design seems altogether rational in the light of anticipated stretching and inherent nonuniformity. Instead of these contributing to greater and greater mounting stresses with increasing speed, these forces can be limited to those provided by a flimsy shaft or soft mounting springs. Hardly any design choice, however, is without disadvantages and, as might have

been anticipated, there are many difficulties associated with supercritical operation.

BALANCE

When rotors are out of balance our experience with car tires tells us we should get them balanced. Certainly there are very fine and sophisticated balancing machines available. In fact, at one time we at SRI had a rotor balanced on a device used for balancing jet engine rotors, but for a variety of reasons this rotor did not perform any better than a rotor that was very carefully statically balanced.

The problem is that nearly all experience with balancing is with rigid rotor balancing. At most, two weights are required to completely balance a rigid rotor at any speeds. If the rotor is not rigid the weights add stresses that create strains and pull the rotor out of balance at a different speed. In addition, the mass creates a stress riser and becomes a point where the rotor may first fail. A general statement for a flexible rotor is the following: Addition of mass can balance a flexible body for only a single speed. Balancing for more than one speed requires at least springs in addition to masses. A general method that deals with this question of balancing flexible rotors does not exist.

It should be noted that there is a subject called "flexible rotor balancing."⁹ This subject deals with the balancing of specific kinds of flexibility in rotors. Essentially, the kind of flexibility dealt with is a flexibility in the shaft where it is considered that relatively rigid objects are mounted on this shaft. Flexible rotor balancing is appropos to gas turbines and deals with the question of minimizing body-to-body resonances along the shaft.

It seems that any time engineers are brainstorming on the dynamics of balancing, someone brings up the mechanism that balances the automatic washing machine.¹⁰ Such a mechanism, of course, is not directly applicable to energy storage flywheels because the balancing mechanism would introduce rotor stresses that would become probable points of failure. The automatic washing machine mechanism, however, does raise the question of whether or not there is a way of winding a composite flywheel that will in some analogous way cause the

masses to shift so as to correct for imbalance. This is a question for creative dynamics designers to examine.

Quite closely associated with the question of balancing, of course, is the description of the imbalance involved. Just exactly how should we specify characteristics of imbalance that we find in certain kinds of composite materials. Manufacturers literature on Kevlar^R shows that this material is more uniform than glass or carbon fibers. What the manufacturer shows is the deterioration and strength with the increase in length of the sample: The ultimate strength drops off more slowly with increased sample length than with other materials. However, we should note that we are dealing with rovings and not with single fibers and that additional nonuniformities are involved in such rovings. Furthermore, we are interested in the mass distribution as well as the strength distribution and ultimately in the uniformity of the composite produced as well as in the basic components.

It is clear to us that there is a great deal more to be done in the subject of balancing techniques and in characterizing the materials to be used in nonisotropic flywheels. Our approach thus far has been simplistic. We have merely balanced statically using small dabs of epoxy.

SUPERCritical CONSIDERATIONS

Running above the first critical opens the Pandora's Box of self-excited instabilities^{11,12,13,14} known by a variety of names usually including "whirl." Unlike the first critical, the vibration on whirl frequency does not match the rotating frequency and thus the stresses oscillate at the difference. The stresses may not be high but because of the oscillation of stresses, fatigue becomes a major consideration. Furthermore, it should be noted that in materials with damping, oscillations in stress will generate heat. Since composite materials generally have greater damping than isotropic materials, especially those used in flywheels, heat generation could be a problem. It is especially serious when we consider that the flywheel will be operating in a vacuum environment in which heat transfer through fluid medium is eliminated. We also note that the manufacturer of Kevlar^R advertises that there is con-

siderably more damping in Kevlar^R composites than in glass fiber composites.

Although there is probably no all-inclusive cause of rotating instabilities, a great many of the excitations have been analyzed to arise from the forces associated with hysteresis in the rotor. Historically there have been cases of friction in joints between the shaft and disks as well as material hysteresis. Although it is not true that all parts of a rotor need avoid hysteresis--and, in fact, certain portions subject to excitations, such as the blades of a turbine, use hysteresis to advantage--one needs to be careful in using composite materials in rotors above the critical speed. Hysteresis in rotor components subjected to mounting stresses should be avoided.

A classical solution to supercritical instabilities is to balance as well as possible and then find, verify, and always run at a speed that does not cause trouble. This solution is used in turbines, including jet aircraft engines. Unfortunately this simple solution is not available to the energy storage flywheel since it must traverse large speed ranges so as to exchange energy. Ideally, the energy storage flywheel is capable of idling at any speed for extended periods of time.

A conventional mechanism to control supercritical instabilities is to use external damping.^{15,16,17} This is energy that is removed due to the motion of the rotor bearings and is to be distinguished from damping from hysteresis or other mechanisms within the rotor itself. A sufficient amount of external damping can usually overcome the instabilities excited by internal damping. Damping also makes it easier to accelerate through the critical speed of the rotor.

Damping to eliminate instabilities creates two problems that have not been considered here. This damping is a heat source similar to that of the internal rotor dissipation. One must be sure to provide a heat path from the damping to the external environment. The second problem is that the damping saps energy from the wheel where one is trying to preserve energy. Although the rate of this energy loss may be small compared to input and output rates, the accumulated energy loss could be appreciable over the extended periods that one might expect to

store energy in a flywheel for some applications. In fact, we anticipate that damping deliberately induced will be a critical factor in the self-discharge time constant; it will be easy to provide bearings that sap less power.

DESIGN

We decided to go the composite flywheel route and to see whether we could run a thin ring at high speed. What we had in mind was to mount this rim on flexible spokes designed to accommodate the radial strain with speed.

We designed a simple spoke system made of a lower specific modulus material from the hub material so that self-loading would keep the joint between the spoke and the rim at zero tension. Our intention was to make a very soft suspension and to make the hub very small and light. We realized that the ring created different principle stiffnesses in the plane of the ring and was equivalent to the elliptical shafts that can cause problems. We made some aluminum models (Figure 1) with spokes of various stiffnesses and ran them up through calculated natural frequencies with a high speed grinder motor. Success of these smaller models gave us the confidence to proceed. Although we do not recommend the simple diametral spoke model, it did simplify the construction of the wheel.

We ordered the ring, 26 in. overall diameter, 1/2 in. square cross-section, and the spokes (Figure 2) from a winding house so as to take advantage of their good commercial practices. The rim was made up of Kevlar^R/epoxy and the spokes of S-glass/epoxy. The spokes were more difficult to manufacture as the packing fraction was hard to maintain in the long straight sections. The 26-inch diameter was selected to be the largest that would fit into an available vacuum test chamber. The largest possible size was desired to minimize the speed and thus the bearing problem.

We measured the properties of the rim and of the spokes by sonic vibration tests and by deflection tests. The tests did not give similar results nor did the results correspond to those expected on the basis of the raw material properties and the manufactured specifications. We suspect, on the basis of this single data point, that there is room for improvement

in measuring of the properties of these finished composite structures.

Since the center of the crossbar was to be subjected to high stresses, and in our design we decided to put the shaft of the drive arrangement through that point, we determined to examine the kind of failure that might occur. The tests we were able to achieve easily were to bend the beam and therefore load the side elements in high tension. Figure 3 shows the kind of failure at the edges of the hole through the shaft made for the spoke we designed to avoid this tested failure.

As a result of this disparity between measured and expected properties we modified our procedure. We set the spoke in position with an initial compression, that is, we distorted the rim somewhat toward an elliptical shape hence there was a change in shape with speed in addition to a mere change in size. As we ran up in speed the rim became more and more circular. For drive power we used a three-phase squirrel cage induction motor. This unit was rated for continuous duty at 12,000 rpm on 400-Hz power. We applied the results of a previous motor control project to build a transistorized controller that can drive the motor to 30,000 rpm with smooth control of torque and speed. The test facility is partly shown in Figure 4.

We found very quickly that it was desirable to run with a mounting system that is symmetric so as to separate the wobble from the back-and-forth modes of vibration. We also rediscovered that one has to be careful with motion-limiting devices that touch the rotor else they excite, rather than limit oscillations.

Once we got through the preliminaries, we actually began to do some runs above the critical speed, which, incidentally, we could drive through easily. We began to encounter the supercritical instabilities. The solution we have used is the one described of providing external damping. We used a rotating brake, consisting of a coil and faceplate that draws a rotating plate up against it and uses friction to stop the rotation. One of these was mounted above and one below, in close proximity, to the level of the ring on the outside of the bearings. When we observed the shaft beginning to wobble we could simply apply current to the brakes, which extracted energy when

the shaft wobbled back and forth (did not slow rotation). The solution appeared to work well except that it applied tremendous stresses to the hub section. The failures that we have experienced have been failures of this hub section apparently due to the stresses and/or fatigue or heating experienced there. Note that we did not provide springs external to the rotor but merely put additional bearings on the shaft very close to the ring elevation and added damping at those bearings. The shaft going to the end bearings, one in the motor and one away from the motor, still provided the basic flexibility that determined the lowest frequency of the rotor.

The damping we have introduced is a very crude Coulomb type friction. We would like to improve upon this, since it is a critical element. We plan to implement the more sophisticated mounting system shown in Figure 5. It consists of a pair of sensors and drivers to replace the friction devices on the shaft bearings immediately above and below the level of the ring. The sensors pick up the motion of the rotor and through external amplifiers and drivers apply whatever force programmed to correct for the disturbance sensed. This would of course increase the complexity of the device, going from passive to active damping. However, the active damping may only be desirable in the experimental device to determine what passive damping is required.

Now that we have been through the process in a rather disorganized and haphazard fashion, I would like to present the design procedure in a pattern where the decisions follow sequentially in an ordered way. Shown in Figure 6 is a design tree. The first choice is whether or not to have an evacuated housing. The answer is that the evacuated housing is a necessity if you want to have energy storage for any period of time. Then you move on to the next choice, should we have a composite flywheel or should we go the conventional flywheel route. Our choice has been made on the basis of our interest in exploring a new area that appears to be the more promising. In the next step we choose the ring shape for reasons of efficient use of material. The subcritical/supercritical choice seems to follow on naturally from the shape selection. It is important to note, however, that it is a significant choice, since many problems are implied. We choose a light suspension

with external damping, again largely as a consequence of the previous choice. Finally, we seek a spoke system, preferably with greater symmetry than the two-spoke model we have chosen. We desire to accommodate radial expansion of the hoop, while retaining lateral (and torsional) stiffness.

In the future, we will have to deal with the transition from rings to shells and the additional modes that are involved. We shall also have to make efficient use of space, which seems to imply a nesting of the shells. Figure 7 shows many of the features that we believe will eventually be incorporated in operational flywheels. Each shell has its own, independent suspension although torque is transmitted from shell to shell.

CONCLUSIONS

The composite flywheel represents the greater possibilities, involves new technology, and is not merely an extension of the art. Basic considerations involve rotor dynamics: (1) extension of the theory of balancing to flexible rotors; (2) characterization and measurement of properties, especially mass and stiffness uniformity; and (3) the assurance of stability from self-excited motions without an excessive loss of energy from the wheel and without creating local hot spots.

Ultimately, new theory will be required to solve some of these problems and will show how close we can approach the performance limits dictated by material properties and ideal behavior. However, the composite flywheel seems to be an area where clever design may be applied to solve problems in the short run.

There are certainly technical difficulties that need to be overcome before flywheels will become practical hardware and we have tried to identify some of these. The greatest difficulty of all, however, appears to be the posture or belief that there are no problems.

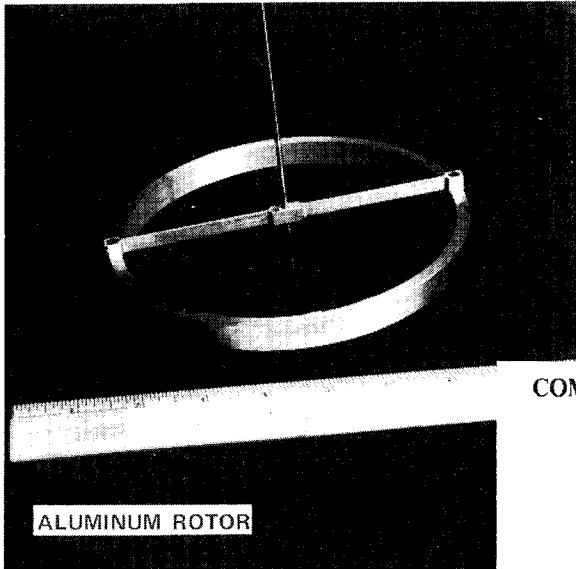
Prepared for: The 1975 Flywheel Technology Symposium, University of California, Berkeley, California, 10-12 November 1975.

References

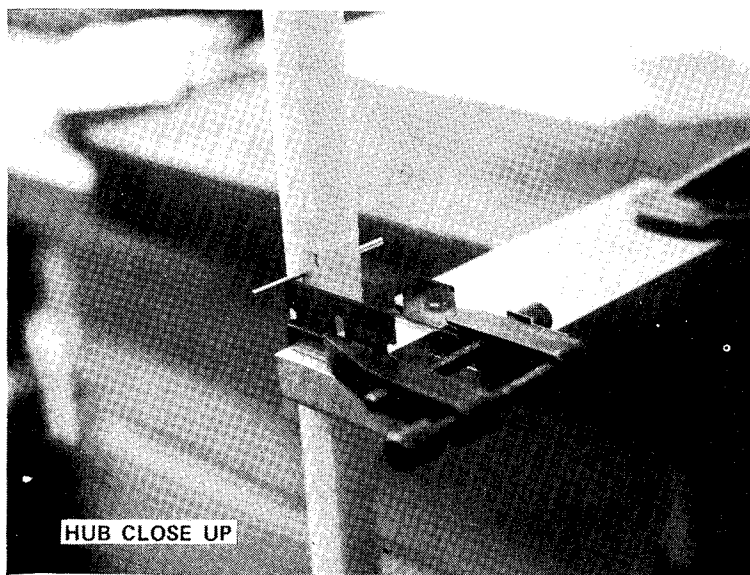
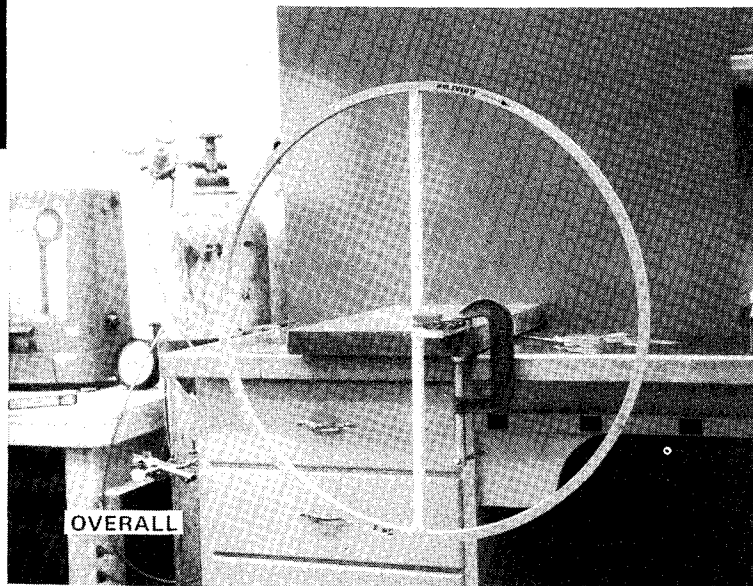
1. "Kinetic Energy Storage for Mass Transportation," L. J. Lawson, Mechanical Engineering, pp. 36-42 (September 1974).

2. D. W. Rabenhorst, "The Multirim Super-flywheel," Technical Memorandum TG 1240, Johns Hopkins University, Applied Physics Laboratory, Silver Spring, Maryland (August 1974).
3. R. F. Post and S. F. Post, "Flywheels," Scientific American, Vol. 229, No. 6 (December 1973).
4. A. Svensson, Jr. and A. E. Wetherbee, Jr., "Final Report, Feasibility of Flywheel High-Energy Storage," AD 851 (15 April 1969).
5. R. R. Gilbert, et al, "Flywheel Feasibility Study and Demonstration," PB 200 143, Lockheed Missiles & Space Company (30 April 1971).
6. G. L. Dugger, A. Brandt, J. F. George, L. L. Perini, D. W. Rabenhorst, T. R. Small, and R. O. Weiss, "Heat-Engine/Mechanical-Energy-Storage Hybrid Propulsion Systems for Vehicles," APTD-1344, Johns Hopkins University (March 1972).
7. "Safety Review of the Kinetic Energy Wheel System for Bus Application," Committee on Transportation, Assembly of Engineering, National Research Council, Washington, D.C. (1974).
8. W. Ettmering and W. B. Soetebeer, "Calculations and Measurements on the Stress Behavior in Rotating Shells," Technical Report AFML-TR-70-64, Air Force Materials Laboratory, Air Force Systems Command, Wright-Patterson Air Force Base, Ohio (March 1970).
9. N. F. Rieger, "Balancing High Speed Rotors to Reduce Vibration Levels," ASME Design Conference Chicago (May 8, 1972).
10. J. P. Den Hartog, Mechanical Vibrations, 4th edition, McGraw Hill (1956).
11. E. J. Gunter, Jr., "Dynamic Stability of Rotor-Bearing Systems," NASA SP-113, Washington, D.C. (1966).
12. F. F. Ehrich, "Identification and Avoidance of Instabilities and Self-Excited Vibrations in Rotating Machinery," ASME paper 72-DE-21.
13. C. D. Mote, Jr. and S. Holroyd, "Confirmation of the Critical Speed Stability Theory for Symmetrical Circular Saws," ASME Paper 74-WA/Prod-17, also published in J. Engineering for Industry.
14. D. R. Chivers and H. D. Nelson, "The Natural Frequencies and Critical Speeds of a Rotating, Flexible Shaft-Disc System," ASME Paper 74-WA/DE-14, also published in J. Engineering for Industry.
15. J. Genin and J. S. Maybee, "External and Material Damped Three-Dimensional Rotor Systems," Int. J. Non-Linear Mechanics, Vol. 5, pp. 287-297 (1970).
16. J. M. Vance and J. Lee, "Stability of High-Speed Rotors with Internal Friction," ASME paper 73-DET-127, also published in J. Engineering for Industry.
17. N. Magge, "Philosophy, Design and Evaluation of Soft-Mounted Engine Rotor Systems," J. Aircraft, Vol. 12, No. 4 (April 1975).

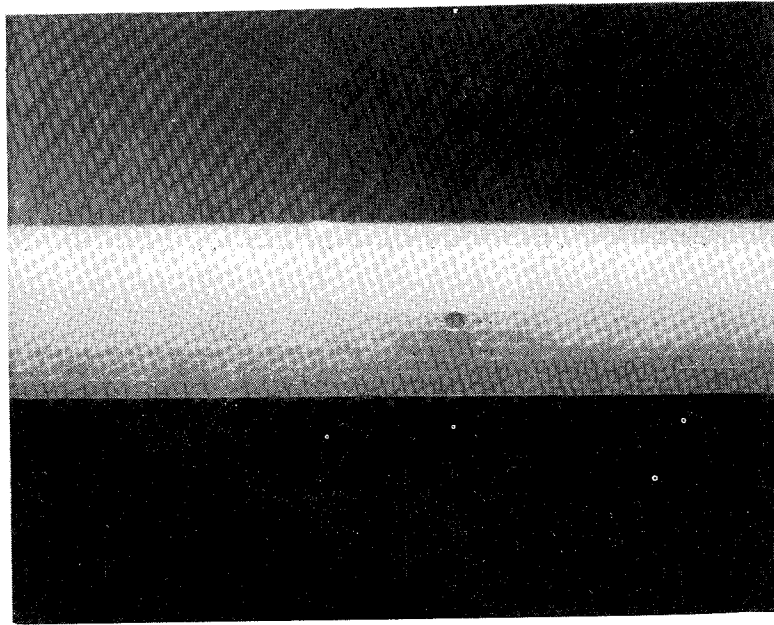
MODEL ROTORS



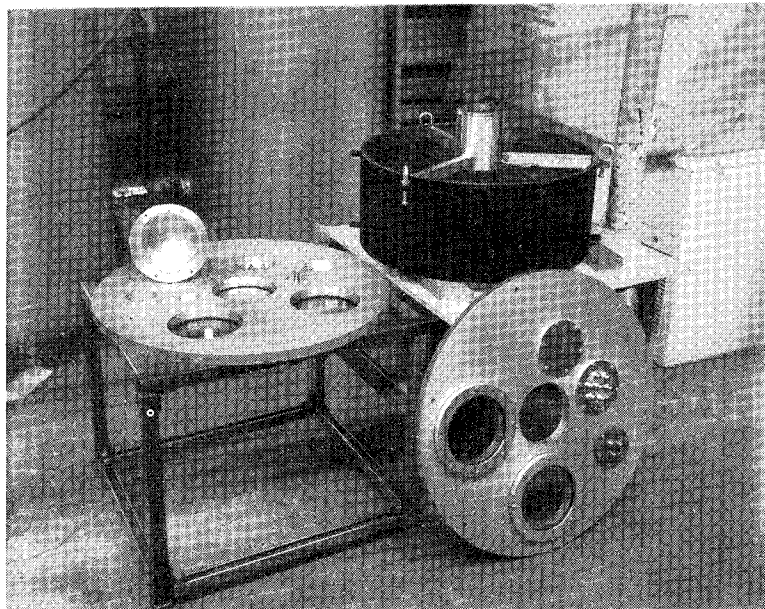
COMPOSITE ROTOR BEING STATICALLY BALANCED

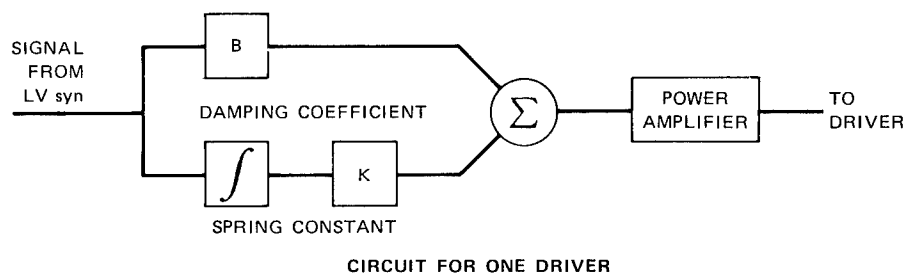
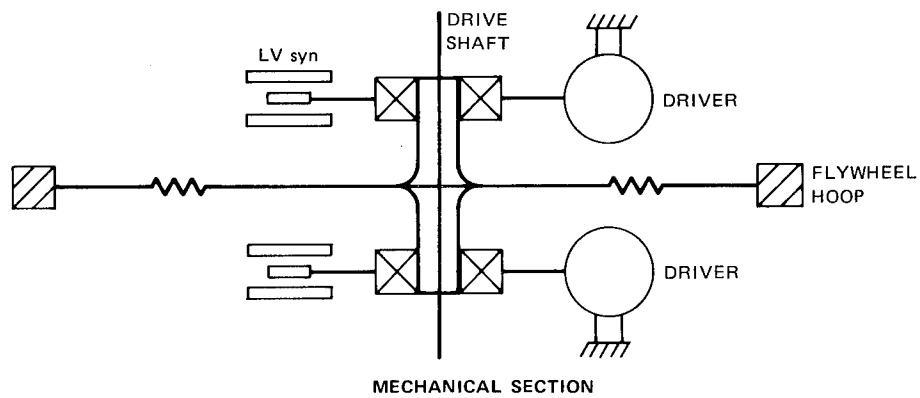


DELAMINATION DUE TO SHEAR STRESS CONCENTRATION

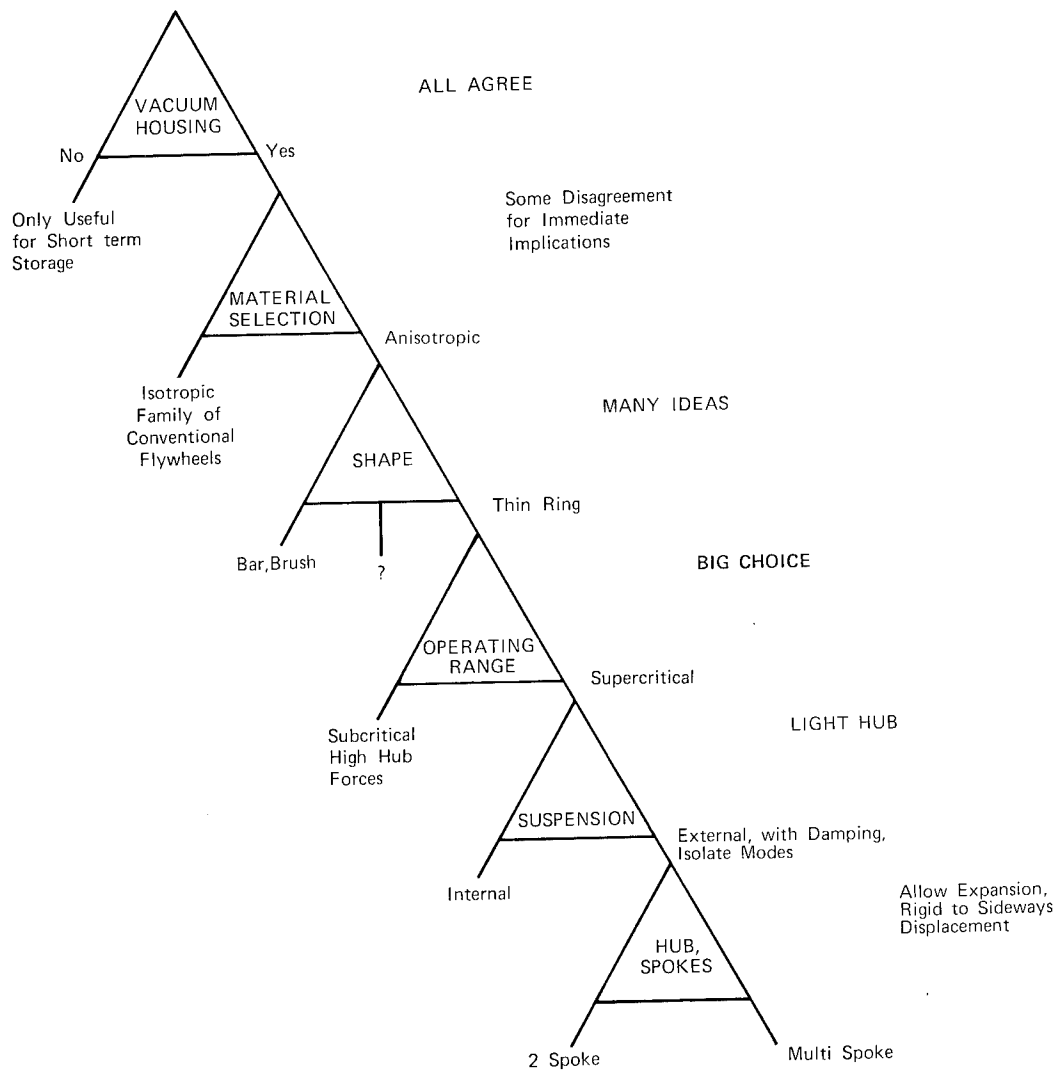


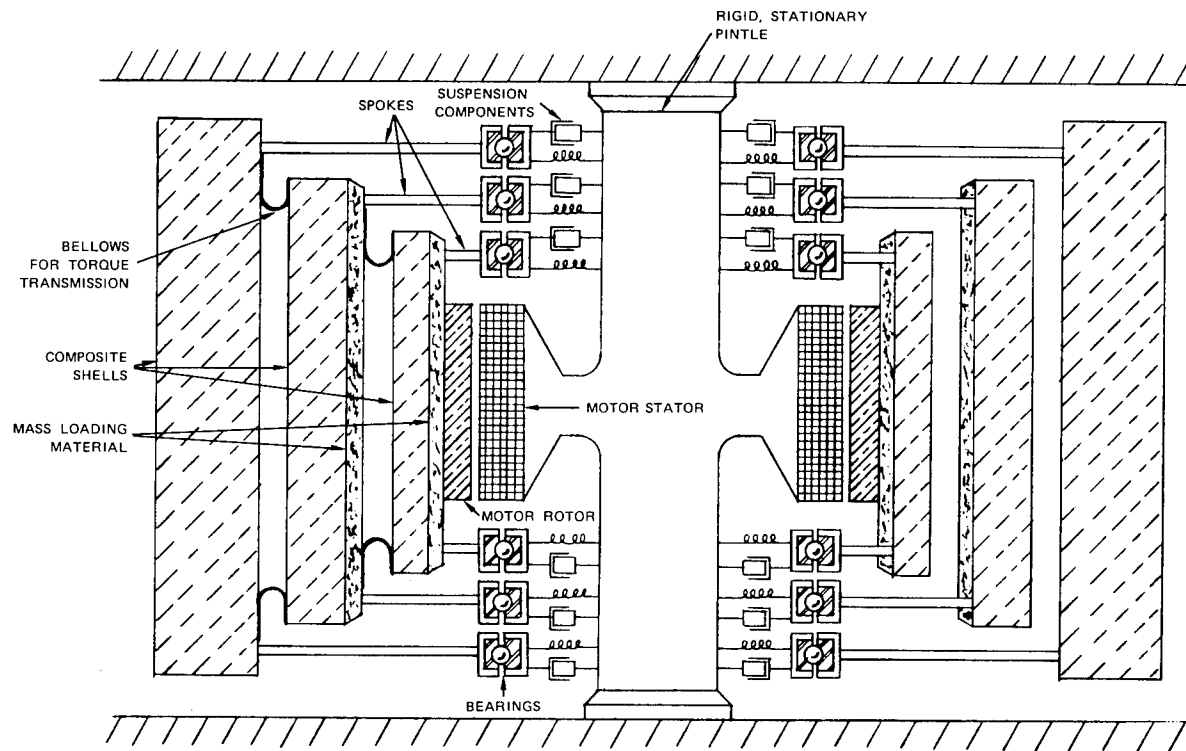
TEST FACILITY





DESIGN TREE





MULTISHELL ROTOR WITH SHELL-TO-HUB SUPPORT

ON EFFECTIVE USE OF FILAMENTARY COMPOSITES IN FLYWHEELS*

F. P. Gerstle, Jr. and F. Biggs
Composite Materials Development Division 5844
Sandia Laboratories
Albuquerque, New Mexico 87115

ABSTRACT

The characteristics of a class of efficient flywheel shapes suitable for high strength filamentary composites were explored mathematically. The basic rotor shape selected for optimization was a circumferentially-wound solid disk of varying axial thickness. An efficient shape is described that may be simple to manufacture.

INTRODUCTION

The anisotropic character of high-strength filamentary composites dictates a different approach to flywheel design than that employed for isotropic structural materials. The energy stored per unit mass (E/m) in a flywheel is proportional to, and limited by, the specific strength or strengths of the rotor material. For an isotropic material with yield strength Y and density ρ ,

$$E/m = C(Y/\rho), \quad C \leq 1$$

The proportionality constant C is a shape factor; it approaches unity for the equi-stress tapered disk of Stodola.^{1,2} For an anisotropic material with significant strength in only one direction, the maximum value of C is 0.5, achieved in either the thin-rim or tapered-rod designs. However, both of these shapes suffer from poor volumetric efficiency (energy stored per unit swept volume).

CIRCUMFERENTIALLY-WOUND DISK FLYWHEELS

In this paper a class of flywheel shapes is explored, shapes which are efficient from both a mass and volume standpoint. The basic rotor shape is that of a circumferentially-wound disk of varying axial thickness. This configuration results in a cylindrically anisotropic structure with high circumferential stiffness and strength but compliant in the radial and axial directions. This structure was first analyzed under the assumptions of plane stress with axial thickness

h expressible as

$$h = h_0 \left(\frac{r}{a}\right)^q \quad a \leq r \leq b$$

where h_0 is the thickness at the hub ($r = a$) and b is the outer radius of the disk. The solution is similar to that of Sen Gupta;³ typical stress fields for a flat ($q = 0$), thick ($\alpha \equiv b/a = 21$) disk are given in Figure 1. The low radial stiffness of the anisotropic rotors ($E_\theta/E_r = 16,64$) eliminates the high hoop stress at $r = a$ seen in the isotropic disk: the maximum of σ_θ moves towards $r = b$. Also, the magnitude of $(\sigma_r)_{\max}$ decreases as the ratio E_θ/E_r increases. Some interesting results have been identified: the radii at which the maximum stresses occur are proportional to α , and the magnitude of these maxima are proportional to α^2 .⁴

These shapes were investigated for energy storage with respect to the thickness parameter q . For anisotropic disks, the highest energy density resulted from flaring, rather than tapering, of the disk.⁴ Typical results are plotted in Figure 2, where K_θ is the maximum hoop strain of the disk. The case $q = 0$ results in a value of $C = 0.33$, while $q = 1$ gives $C = 0.4$.

To approach an optimum shape, the function h was divided into k piecewise linear segments of the form

$$h = h_i + v_i r \quad i = 1, 2, \dots, k$$

*This work was supported by the U. S. Energy Research & Development Administration.

The equilibrium equation with this substitution may be solved by a Greens function containing hypergeometric functions. However, it was simpler to use a numerical solution to the equation than to deal with the Greens function. This direct numerical approach is also applicable to more general forms of the thickness function $h(r)$, and permits the use of numerical optimization techniques. Details of the numerical solution and optimization routine are given in Ref. 4.

The optimization routine was used to select shapes having large C values and high ratios of $(\epsilon_\theta)_{\max}$ to $(\epsilon_r)_{\max}$. The latter constraint was imposed to produce a design in which hoop failure would be the more probable. One attractive shape is shown in Figure 3, along with its radial and hoop strain distributions. This configuration should be relatively simple to manufacture and makes efficient use of the composite material. Its predicted C value is 0.47 on either a mass or a volume basis.

References

1. Stodola, A., Steam and Gas Turbines, McGraw Hill, New York (1927).
2. Lawson, L. J., "Design and Testing of High Energy Density Flywheels for Application to Flywheel/Heat Engine Hybrid Vehicle Drives," 1971 IECEC Proceedings, Boston, Mass.
3. Sen Gupta, A. M., "Stresses in Some Aeolotropic and Isotropic Disks of Varying Thickness Rotating about the Central Axis," Bulletin of the Calcutta Mathematical Society, Vol. 41, No. 3, pp. 129-139, Sept. 1949.
4. Gerstle, F. P. Jr. and F. Biggs, "On Optimal Shapes for Anisotropic Rotating Disks," Proceedings of the 12th Annual Meeting of the Society of Engineering Science, Inc., Austin, Texas, Oct. 20-22, 1975 (Invited Paper).

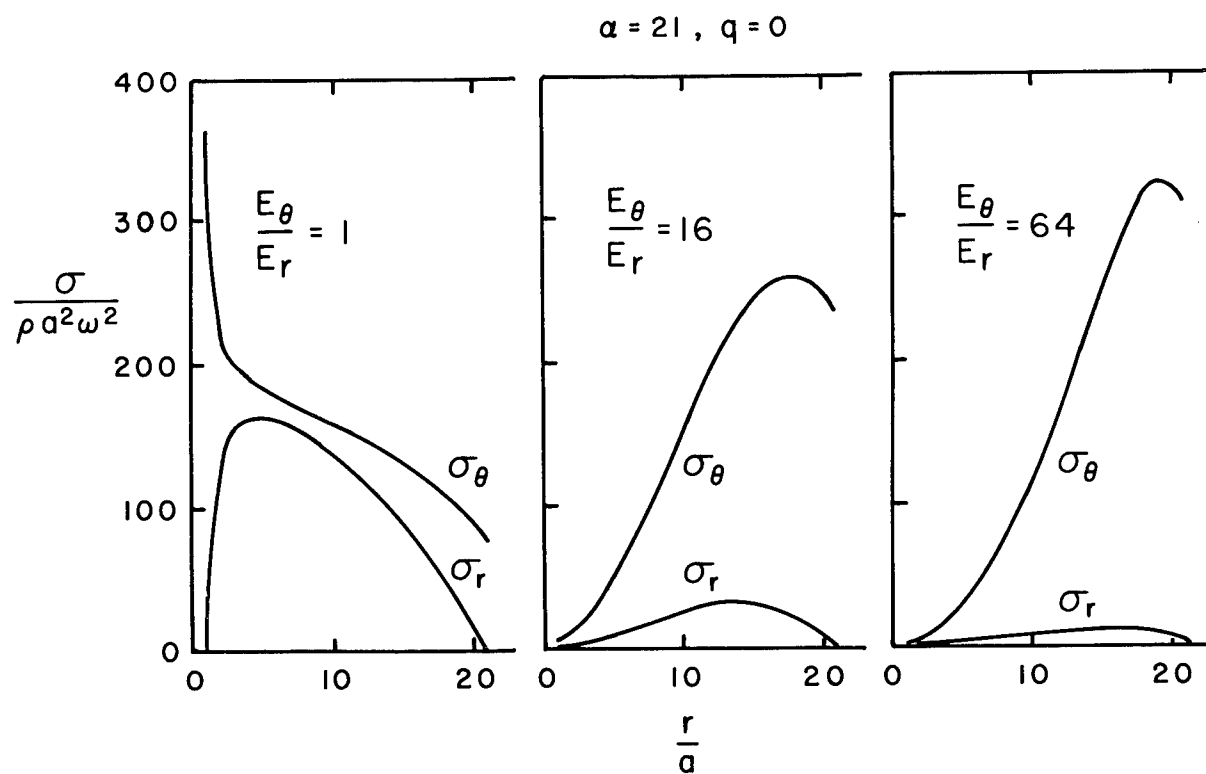


Figure 1. Hoop and radial stress distributions in flat rotating disks; $\nu = 0.3$.

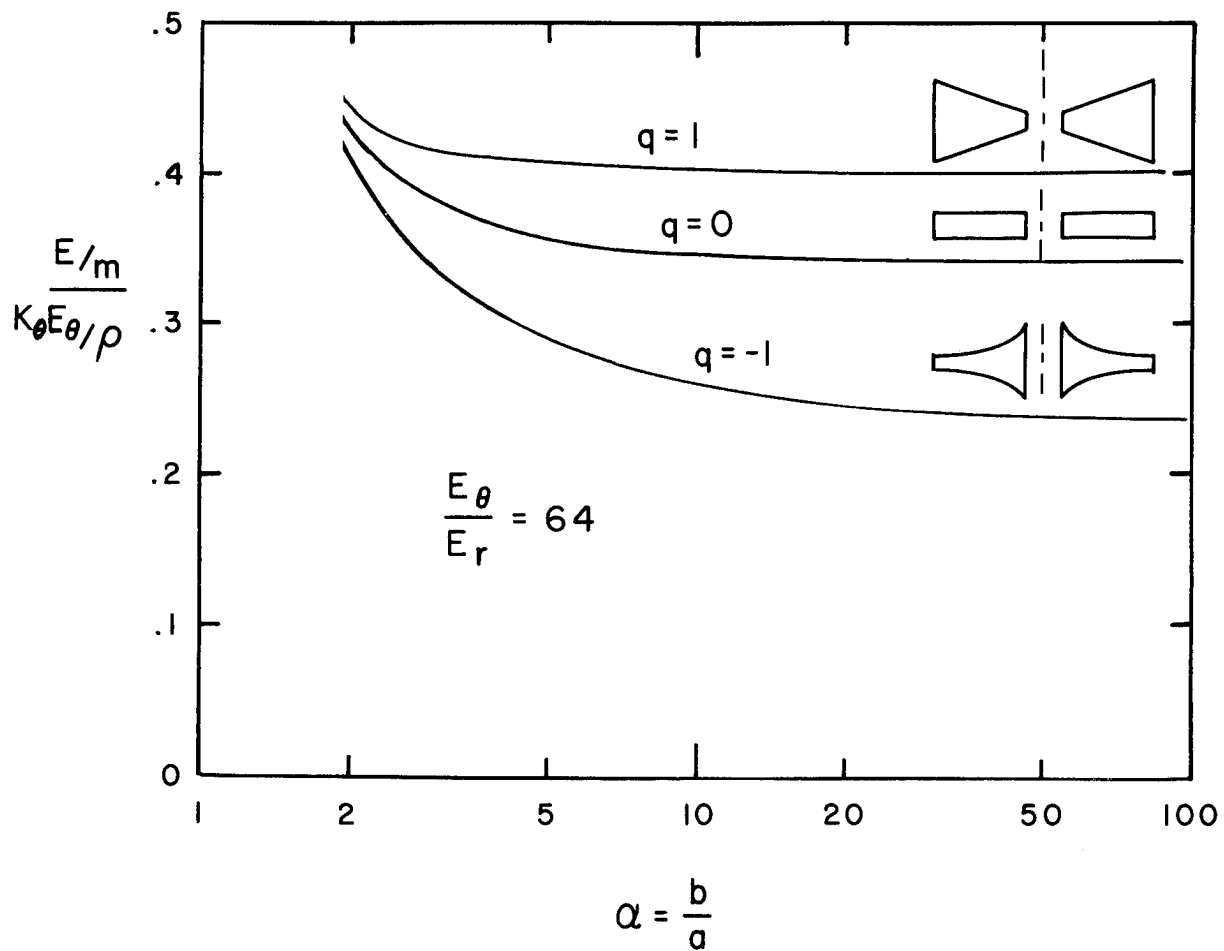


Figure 2. Normalized energy density for tapered, flat and flared anisotropic rotating disks; $\nu = 0.3$.

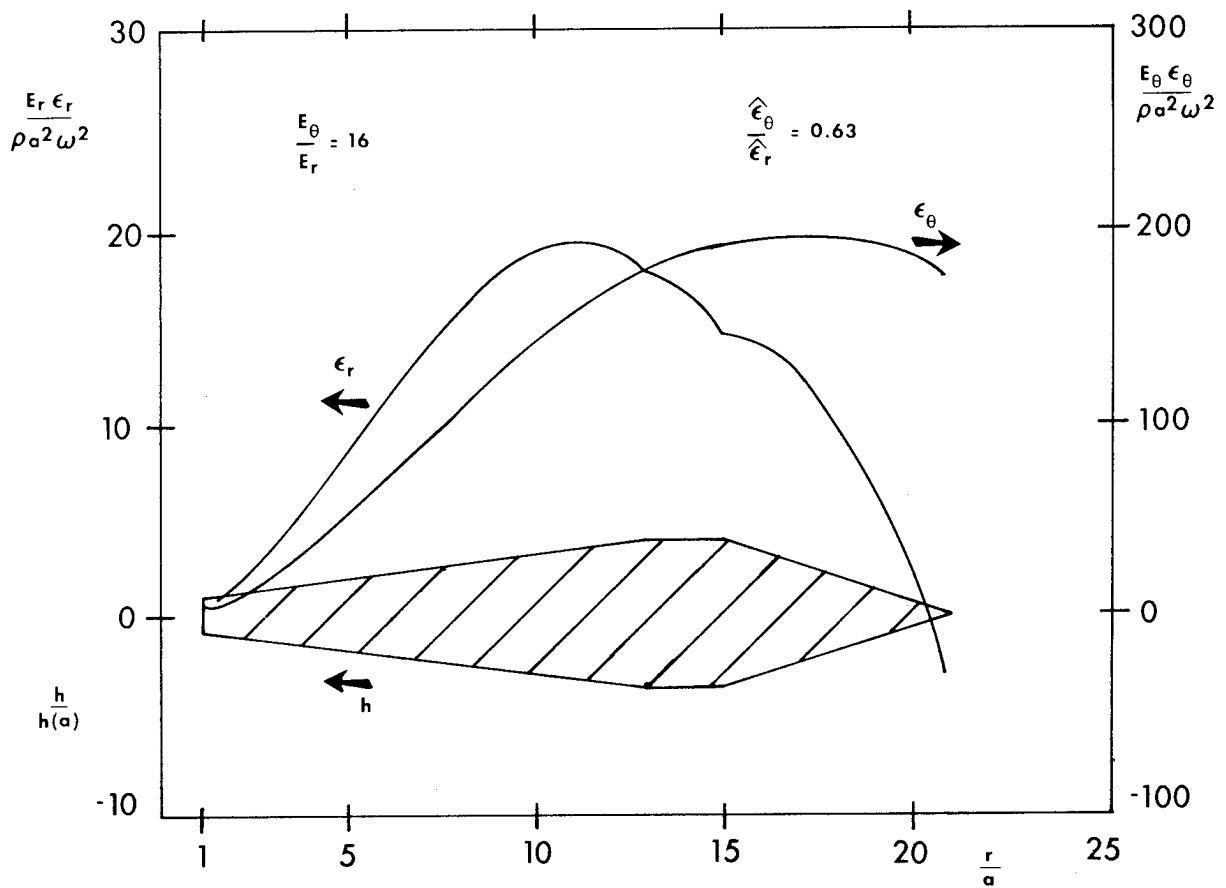


Figure 3. Strain distributions for an efficiently shaped flywheel; $\nu = 0.3$.

FIBER EVALUATION FOR FLYWHEEL APPLICATIONS*

Lynn Penn and T. T. Chiao
Lawrence Livermore Laboratory, University of California
Livermore, California 94550

ABSTRACT

This paper reports initial results of tensile tests of two kinds of epoxy-coated glass fibers and an epoxy-coated Kevlar 29 aromatic polyamide fiber. Data show that fiber strengths depend directly on resin content.

INTRODUCTION

A good data base of fiber information for use in flywheel applications depends on reliable testing of meaningful specimens under realistic conditions. Much of the data in the literature is valueless because it was derived from tests made under questionable conditions or from unrealistic specimens. As a result, valid comparisons of the properties of fibers and fiber systems are often not possible.

The LLL materials study of fibers for flywheel applications has two goals: (1) to develop fiber property and performance data that will permit valid comparison of candidate materials, and (2) to use these data for guidance of subsequent detailed investigations for flywheel design.

A further goal is to evaluate and improve processing and fabrication techniques while producing specimens for testing. Void content in composites is a typical problem, as is uneven tension in strands coming off the manufacturer's spool and uneven resin distribution within the thick fiber bundle. These and other problems are under study.

SPECIMENS AND TESTS PERFORMED

Four fibers are being compared: E glass, S-2 glass, Kevlar 29** and Kevlar 49. The E glass is a single-end roving with more than 2000 filaments per strand, and was coated by the manufacturer with a sizing that was compatible with epoxy resins. The roving unwound from the

manufacturer's spool with even tension. The S-2 glass is a twenty-end roving also coated by the manufacturer with an epoxy-compatible sizing. Kevlar 29 and Kevlar 49 are 1500 and 1420 denier single-end rovings without sizing.

All fibers were coated with 25% to 35% by volume (65% to 75% fiber volume) of DER/Jeffamine T 403 epoxy resin by running them over resin-saturated, felt-covered rollers. The coated fibers were wet-wound on mandrels and cured at 60°C for 16 hours.

Simple coated fiber strands were tested in tension. NOL rings, which are relevant in shape to flywheel geometry, were stressed to failure in hydroburst apparatus.

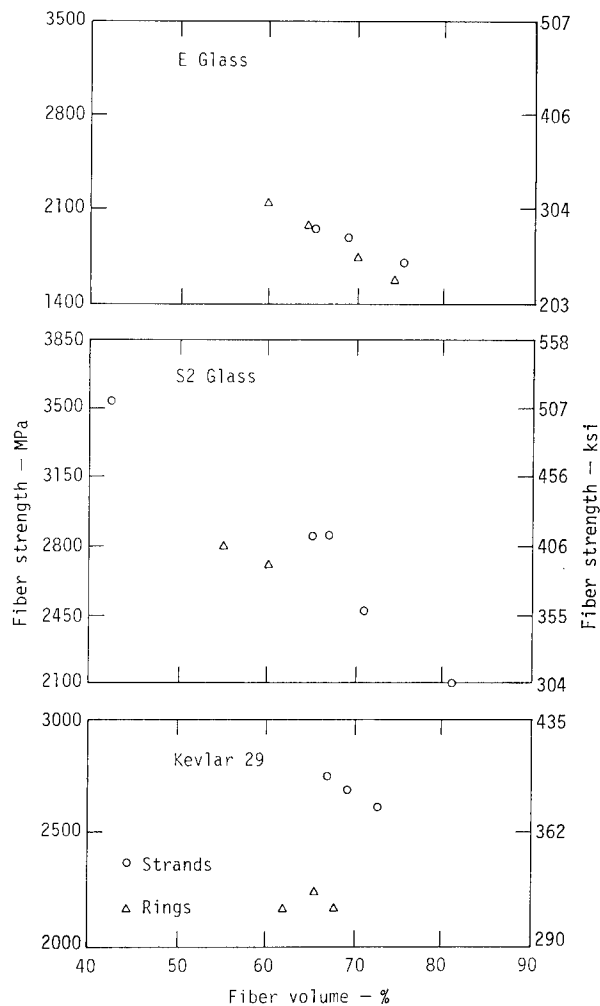
RESULTS

Figure 1 summarizes the fiber strength data obtained so far on three of the four epoxy-coated fibers. Each data point in this figure is an average of the results from testing 20 to 30 strands or 4 to 8 NOL ring specimens.

It is evident from the data that coated fiber strength of all three fibers increased as the epoxy resin content of the fiber bundle increased. At 70% fiber volume there was little difference between the fiber strengths of coated S-2 glass and coated Kevlar 29 specimens, but

*This work was performed under the auspices of the U. S. Energy Research & Development Administration under contract No. W-7405-Eng-48.

**Reference to a company or product name does not imply approval or recommendation of the product by the University of California or the U. S. Energy Research & Development Administration to the exclusion of others that may be suitable.



E glass epoxy fibers had much lower tensile strength.

Since the strength to density ratio of Kevlar 29 is higher than in the other two fibers, Kevlar is more attractive from a weight standpoint.

These studies are being continued to build up a catalogue of data that will allow us to compare fibers and fibers systems that were tested under the same or equivalent conditions.

Fig. 1. Tensile strengths of epoxy-coated E glass, S-2 glass and Kevlar 29 fibers.

EPOXY RESINS FOR FLYWHEEL APPLICATIONS*

J. A. Rinde

Lawrence Livermore Laboratory, University of California
Livermore, California 94550

ABSTRACT

Key properties of three epoxy resin systems of different characteristics were found to be suitable for filament winding and useful for flywheel applications.

The properties of composite materials are being studied, both separately and as composite structures, at Lawrence Livermore Laboratory. For optimum performance of any flywheel design, both the matrix material and the fiber properties must be fully utilized. This paper reports the formulation and selected properties of three epoxy resin systems of different characteristics.

Because the criteria for selecting the matrix material are not established, we chose to study epoxy resins instead of polyesters because of their lower shrinkage, higher elongation, better adhesion to fibers, and higher strength. However, in general, polyesters are less expensive than epoxies. We are studying several types of epoxy resin systems because it is expected that no single resin system will be optimum for all flywheel applications.

We studied three epoxy resins with the following characteristics:

1. Room or moderate temperature cure,
2. High fracture toughness,
3. High shear strength.

All of these resins were intended for filament-winding applications and were required to meet the following processing requirements:

- Viscosity at 25°C of 0.7 – 0.9 Pa·s
- Gel time for 30 g at 25°C greater than 30 h.

The formulations of the three resins studied are given in Table 1.

For formulation No. 1, the properties of the cured resin vary with curing conditions. At room temperature, the cure progresses to about 70% after 56 days, but a higher degree of cure (85%) can be obtained if curing is carried out at 50–90°C. The tensile stress-strain properties are improved by the elevated temperature cure as shown by the curves in Fig. 1. By increasing the cure temperature we have increased the tensile strength about 10% and the strain at maximum stress by about 50%. The other two curves show the tensile stress-strain results for formulation Nos. 2 and 3. Both of these formulations show higher strengths and strains than the low temperature curing resin emphasizing the reduction in properties that result from the requirement for room temperature curing.

Fracture toughness data were not obtained on our formulation No. 2; however, some information has appeared in the literature¹ on a similar system. Figure 2 illustrates this data. In this figure, the fracture energy is shown for both the neat resin and a carbon fiber composite with and without 6% Carboxy Terminated Polybutadiene rubber. It is clear that the presence of the rubber greatly increases the fracture toughness of the neat resin, but only slightly increases the fracture toughness of the composite.

Shear properties of resin formulation No. 3 were obtained on Kevlar composites. Table 2 presents this shear data compared with ERL2256/Tonox 60-40, a resin with normal shear strength properties.

*This work was performed under the auspices of the U.S. Energy Research & Development Administration, under contract No. W-7405-Eng-48.

These results demonstrate that high shear strengths can be obtained in high tensile-strength epoxy resins (see Fig. 1).

We have shown key properties of

three epoxy resin systems suitable for filament winding that are useful for flywheel applications. Other properties of these resins can be found in Refs. 2-5.

REFERENCES

1. D. C. Phillips and J. M. Scott, Matrix Toughening and its Effect on the Behavior Properties of CFRP, AERE Harwell, Oxfordshire, UK, Rept. AERE-R779 (August 1975). Also presented at the 1975 International Conference on Composite Materials, Geneva and Boston.
2. T. T. Chiao, E. S. Jessop, and L. Penn, "Screening of Epoxy Systems for High Performance Filament Winding Applications," in Proc. 7th National SAMPE Technical Conference (Albuquerque, New Mexico, 1975).
3. T. T. Chiao and R. L. Moore, "A Room-Temperature-Curable Epoxy for Advanced Fiber Composites," in Proc. SPI Reinforced Plastics/Composites Institute 29th Annual Technical and Management Conference (Washington, DC, 1974).
4. T. T. Chiao, E. S. Jessop, and H. A. Newey, "An Epoxy System for Filament Winding," SAMPE Quart. 6, 1 (October 1974).
5. T. T. Chiao, E. S. Jessop, and H. A. Newey, "A Moderate-Temperature-Curable Epoxy for Advanced Composites," SAMPE Quart. 6, 3 (April 1975).

Table 1. Formulations of epoxy resin systems.

Mixture	Parts	Cure
1. Room temperature cure resin		
Dow ^a DER 332	100	R.T. or
Jeffamine T-403	36	60°C for 16 h
2. High fracture toughness resin		
Dow XD7818	50	4.5 h at 60°C
Dow XD7575.02	50	+3 h at 120°C
Dow XD7114	45	
UniRoyal Tonox 60-40	33.7	
3. High shear strength resin		
Dow XD7818	50	5 h at 80°C
Dow XD7575.02	50	+3 h at 120°C
Dow XD7114	45	
UniRoyal Tonox 60-40	14.1	
2, 6-Diaminopyridene	14.1	

^aReference to a company or product name does not imply approval or recommendation of the product by the University of California or the U.S. Energy Research and Development Administration to the exclusion of others that may be suitable.

Table 2. Shear properties of the epoxy resin formulated for high shear strength compared with ERL2256/Tonox 60-40.

Shear property, MPa ^a	2256	Resin 3
Shear, $\pm 45^\circ$ laminate	21	41
Modulus	1690	1890
Interlaminar shear	29	46

^aFor conversion, 6.89 MPa = 1 ksi.

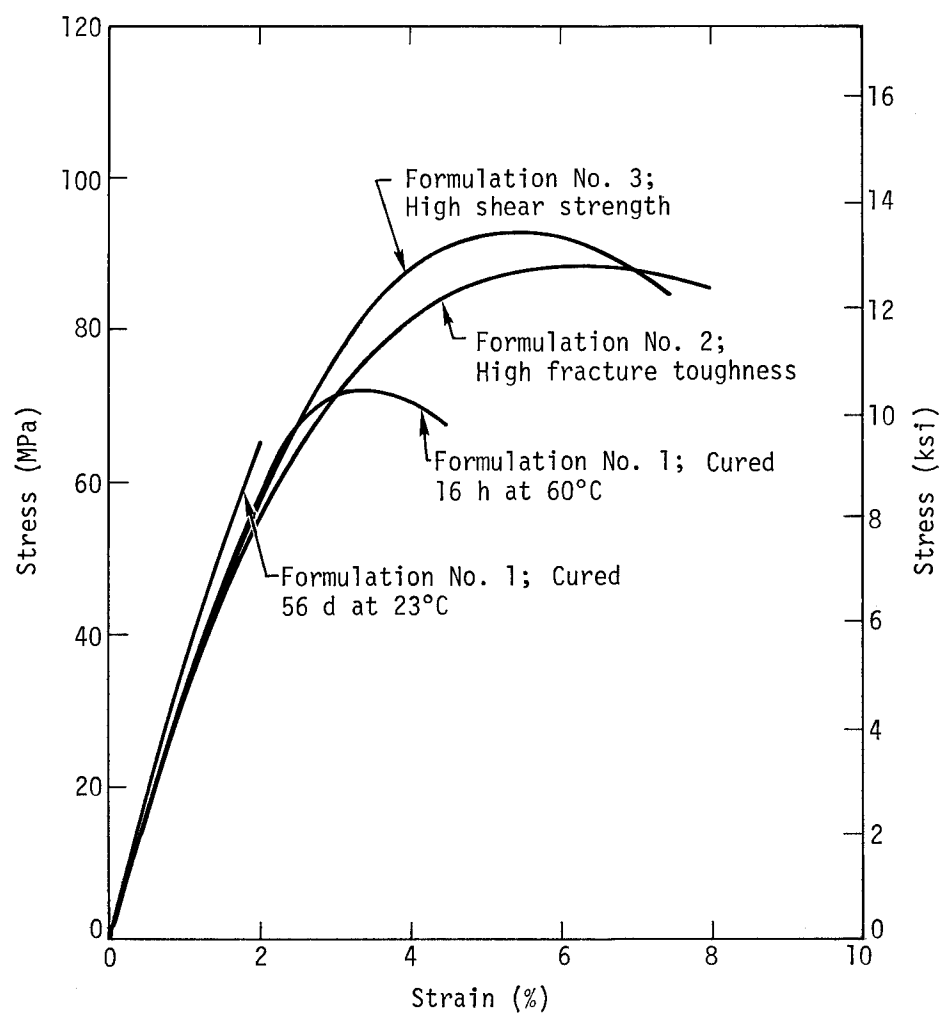


Fig. 1. Tensile stress-strain curves showing relative strength of resin systems.

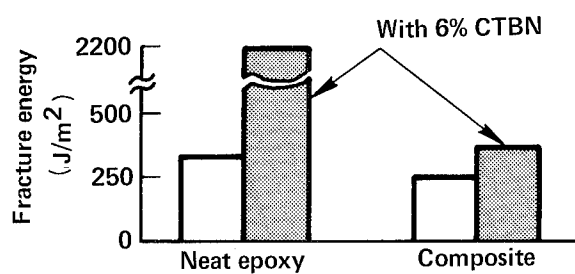


Fig. 2. Epoxy resins containing CTBN copolymers have increased fracture toughness in the resin and composite.

STRESS REDISTRIBUTION DUE TO RADIAL DISPLACEMENTS AND ITS EFFECTS ON ENERGY STORAGE CAPABILITY

E. J. Brunelle
Department of Mechanics
Troy Building, Room 304
Rensselaer Polytechnic Institute
Troy, New York 12181

ABSTRACT

Two very simple models are used to determine qualitatively the effects of radial displacement on the maximum attainable rotational speed of a mass, the stress redistribution that occurs and the maximum kinetic energy that can be stored. Since the text below is abbreviated, the actual nonlinear model will not be discussed, nor will the imperfection sensitivity analysis. Some pertinent references are listed.*

THE BASIC MODEL

We consider a mass M rotating with an angular velocity Ω and restrained by a spring whose spring constant is k and whose unstretched length is ℓ . We denote the radial displacement of the mass by u , define a quantity $\Omega_D^2 = k/M$ and freely use the strength of materials result $k = AE/\ell$ where A is the area and E is Young's Modulus of an "equivalent rod" represented by the spring constant k . A free body diagram of the mass shows the restoring force $-ku$ and the centrifugal force $M\Omega^2(\ell + u)$. Solving for u we find that,

$$u/\ell = \left[(\Omega_D/\Omega)^2 - 1 \right]^{-1}.$$

We note that as $\Omega \rightarrow \Omega_D$, $u/\ell \rightarrow \infty$, which is a static nonconservative instability classified as divergence. This value of $\Omega = \Omega_D$ is an upper bound to the attainable angular velocity; in a ductile nonlinear softening material we may reach divergence before tensile fracture occurs. This would certainly be an unusual case. Usually the spring breaks (tensile fracture) first and we will use that assumption in the sequel.[†] Assuming a finite

spring constant k yields the spring stress σ and the system kinetic energy T to be,

$$\sigma = E \left[(\Omega_D/\Omega)^2 - 1 \right]^{-1}$$

and

$$T = 1/2 M \Omega^2 \ell^2 \left[1 - (\Omega/\Omega_D)^2 \right]^{-2}$$

If we let $k \rightarrow \infty$ we obtain the corresponding classical results,

$$\sigma_{c1} = M \Omega^2 \ell / A \quad \text{and} \quad T_{c1} = 1/2 M \Omega^2 \ell.$$

Furthermore, we record the ratios of the above quantities for their possible interest to the reader.

$$\sigma/\sigma_{c1} = \left[1 - (\Omega/\Omega_D)^2 \right]^{-1}$$

and

$$T/T_{c1} = \left[1 - (\Omega/\Omega_D)^2 \right]^{-2}$$

*The author will be happy to supply Xerox copies of the transparencies used during the presentation of this paper at the symposium.

[†]In reference (1) Bisshopp uses a first order correction for area decrease due to Poisson contraction effects and finds the refined estimate of Ω_D to be 30% lower than the result given by the crude model used in this presentation.

We now turn our attention to the value of $\sigma = \sigma^*$ at which the spring breaks. The rotational speed Ω^* at which this occurs will be different for classical ($k \rightarrow \infty$) and nonclassical (k finite) results. Also, the kinetic energy stored at $\sigma = \sigma^*$ will be different for classical and nonclassical results. After some manipulation we find the desired ratios,

$$\frac{\Omega^*}{\Omega_{*c1}} = [1 + (\sigma^*/E)]^{-1/2}$$

$$\text{and} \quad \frac{T^*}{T_{*c1}} = 1 + (\sigma^*/E).$$

If we let $\sigma^*/E = 0.2$ (for a "future-day super material") we find that

$$\frac{\Omega^*}{\Omega_{*c1}} \approx 0.91 \quad \text{and} \quad \frac{T^*}{T_{*c1}} = 1.2.$$

Therefore Ω^* must be $\approx 91\%$ of Ω_{*c1} to prevent breaking (tensile fracture); but even at this reduced angular velocity, 20% more kinetic energy is stored!

REDUCTION IN Ω^* AND INCREASE IN STRESS ATTRIBUTABLE TO RADIAL ACCELERATION

If the mass M is vibrating radially as well as rotating at an angular velocity Ω , our previous free body for the basic model has a D'Alembert force $-M\ddot{u}$ added to it. This results in the equation of motion

$$\ddot{u} + \omega^2 u = \Omega^2 \ell \quad \text{where} \quad \omega^2 = \Omega_D^2 - \Omega^2.$$

For $\Omega < \Omega_D$ the motion is bounded (it is unstable for $\Omega \geq \Omega_D$), and if we impose unit impulse boundary conditions ($u(0) = 0$ and $\dot{u}(0) = 1/M$) the solution for the stress $\left(\frac{\sigma}{E} = \frac{ku}{\ell}\right)$ is given by

$$\frac{\sigma}{E} = \frac{1}{M\omega\ell} \sin \omega t + \left(\frac{\Omega}{\omega}\right)^2 (1 - \cos \omega t).$$

If we assume $\frac{\sigma^*}{E} = 0.2$ and let $\omega t = \pi$ we can easily calculate the reduced allowable angular velocity $\Omega_{*DYN.}$ at which the system will break under the additional dynamic stresses caused by the unit impulse. Calculation shows that

$$\frac{(\Omega^*)_{DYN.}}{\Omega^*} = 0.7386.$$

If only a unit impulse is applied to the rotating mass, the safe angular velocity is less than 74% of its steady state Ω^* value. Note also that a very likely manner to obtain a radial impulse (probably much larger than unity) is to lose a fragment of the flywheel.

At this point we have talked about the maximum kinetic energy storage for a given σ^*/E at a constant Ω^* , and the reduction in Ω^* caused by impulsive radial loads. A more careful discussion would have to include (i) vibratory stresses (and hence further decreases in Ω^*) arising from imperfections and rotational shaft flexibility and (ii) transient stresses caused by changes in Ω during "charging" and "discharging" kinetic energy (once again the operating value of Ω would have to be less than Ω^* calculated for steady state conditions). For brevity we delete these topics and proceed to a more realistic model which can yield qualitative results about rim-spoke flywheels and other similar hybrids.

THE ROTATING ROD WITH A TIP MASS M

Referring to (2)*, where we also find the plane stress solution for the rotating constant thickness disk, the relevant differential equation and boundary conditions in terms of a nondimensional distance $\zeta = x/\ell$ and a nondimensional frequency squared $k^2 = m\ell^2 \Omega^2/EA$, where m is the mass per unit length of the rod, are given by

$$\frac{d^2 u}{d\zeta^2} + k^2 \ell \zeta$$

$$u(0) = 0$$

$$\frac{du(1)}{d\zeta} = \frac{M}{m\ell} k^2 [\ell + u(1)\epsilon],$$

$$\epsilon = \begin{cases} 0 & \text{; classical equations} \\ 1 & \text{; exact equations} \end{cases}$$

*There are misprints in the classical results, equations (4) and (5), in (2).

These equations can readily be solved for u and $(u)_{c1}$ and since $\frac{\sigma}{E} \approx \frac{\partial u}{\partial x}$ we obtain

the desired σ/E solutions easily. They are,

$$\frac{\sigma}{E} = \frac{\cos k\zeta}{\cos k \left[1 - \frac{M}{m\ell} k \tan k \right]} - 1$$

$$\left(\frac{\sigma}{E}\right)_{c1} = \frac{k^2 c1}{2} \left[1 - \zeta^2 + 2\left(\frac{M}{m\ell}\right) \right]$$

Letting $\frac{M}{m\ell} = 4$, to be representative of a rim-spoke flywheel model, and letting $\frac{\sigma(0)}{E} \equiv \frac{\sigma^*}{E} = 0.2$ we find that

$$k = 0.1930, \quad k_{c1} = 0.2108$$

and hence $\Omega^* = 0.916\Omega_{c1}$, that is to say that the actual rod-tip mass configuration can be spun at only 91.6% of the classical solution for Ω_{c1} . Further calculation will show approximately a 20% increase in maximum stored kinetic energy. Other results may be seen in (3), where the SUPER FLYWHEEL configuration was studied in some detail.

References

1. Bisshopp, K. E., "Discussion of The Super Flywheel: A Second Look," Jour. Eng. Mat'ls. and Technology, Trans. ASME, Series H, No. 3, July 1973, p. 195 (also see Author's Closure on p. 196).
2. Brunelle, E. J., "Stress Redistribution and Instability of Rotating Beams and Disks," AIAA Jour., Vol. 9, No. 4, April 1971, p. 758.
3. Brunelle, E. J., "The Super Flywheel: A Second Look," Jour. Eng. Mat'ls. and Technology, Trans. ASME, Series H, No. 1, Jan. 1973, p. 63.

LONG-TERM PERFORMANCE OF FIBER COMPOSITES*

Cherry C. Chiao
Lawrence Livermore Laboratory, University of California
Livermore, California 94550

ABSTRACT

Lawrence Livermore Laboratory has been evaluating the long-term performance of fiber composites for over 6 years. Several years of stress-rupture data for S-glass/epoxy and Kevlar/epoxy composites have been obtained. Other composites are now being studied for the flywheel program. An accelerated test to predict life of composites is also being developed.

Fiber composites have been used in many important applications. Recently they are also being considered as the key materials for flywheels to store energy. Because an operating flywheel is under sustained load, data on the life of composites are very important. The life or long-term performance of composites is usually evaluated by the stress-rupture test. Figure 1 shows a schematic representation of the test.

Lawrence Livermore Laboratory began its stress-rupture test program in 1969. One of our facilities (Fig. 2), which houses 400 test apparatuses, has been in operation for several years. At present, we have 5 years of life data for S-glass/epoxy** (Fig. 3), and 4 years of data for Kevlar 49/epoxy† composites (Fig. 4). Apparently, there is an exponential dependency of time-to-failure on the applied stress.

Currently, we are concentrating our work on E-glass/epoxy composites for flywheel applications. The large fiber bundle of E-glass created some problems for specimen impregnation and testing. We have modified our filament winding process to achieve uniform penetration of epoxy

on E-glass. We have designed and built high-load stress-rupture apparatus (Fig. 5) specifically for testing flywheel materials. For this application, the long-term performance of S-2 glass/epoxy and Kevlar 29/epoxy composites will also be evaluated.

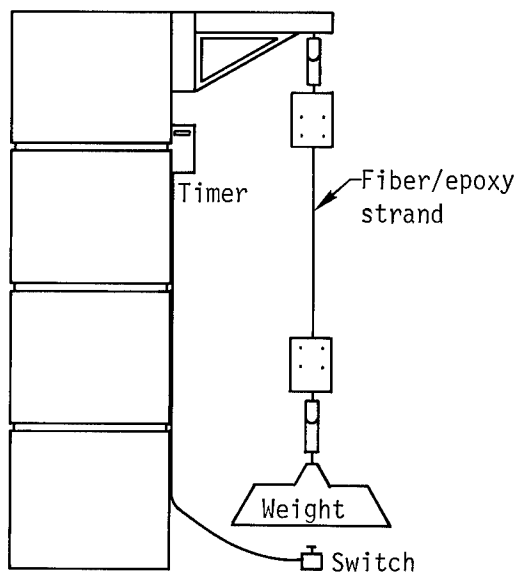


Fig. 1. The stress-rupture test.

*This work was performed under the auspices of the U.S. Energy Research & Development Administration, under contract No. W-7405-Eng-48.

**Two epoxies were studied: (1) Dow DER 332/Union Carbide ERL-4206/Celanese Epi-Cure 855 (70/30/40) in 40% acetone solution. These specimens were gelled at 60°C for 16 h, again at 76.7°C for 24 h, and cured at 176.7°C for 45 min. (2) Dow DER 332/Jefferson Chemical Jeffamine T-403 (100/36). Specimens gelled at room temperature for 16 h and cured at 76.7°C for 24 h.

†Union Carbide ERL 2258/ZZL 0820 (100/30). The specimens were gelled 3 h at 93°C, then cured 2 h at 163°C. Reference to a company or product name does not imply approval or recommendation of the product by the University of California or the U.S. Energy Research and Development Administration to the exclusion of others that may be suitable.

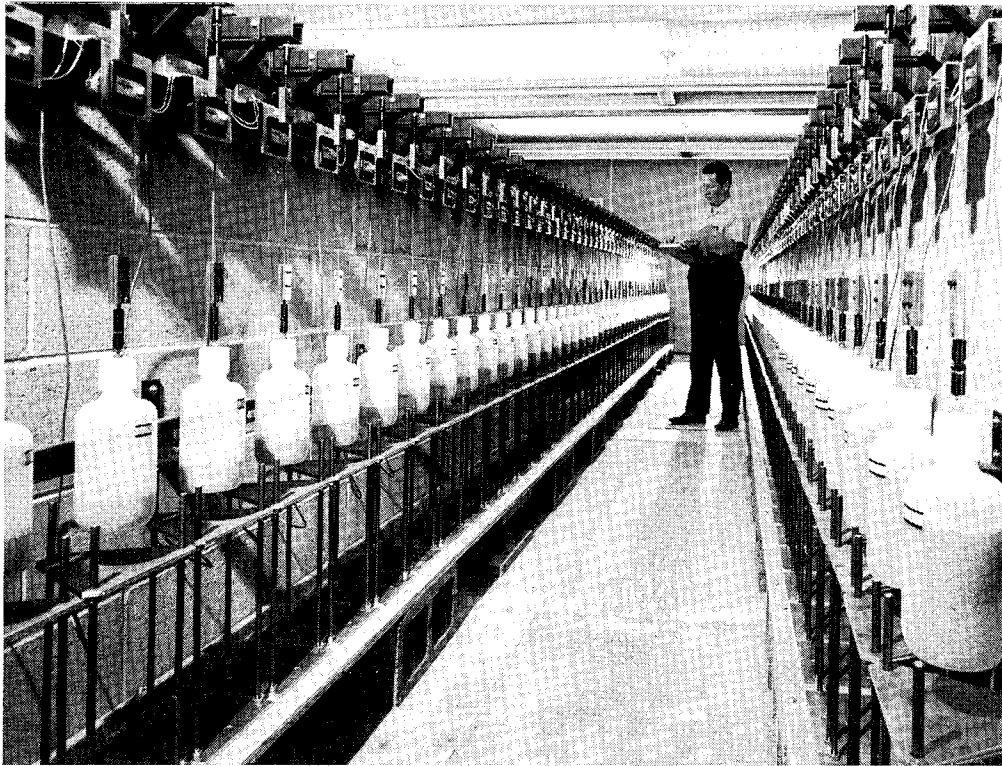


Fig. 2. One of the stress-rupture test facilities in the Lawrence Livermore Laboratory.

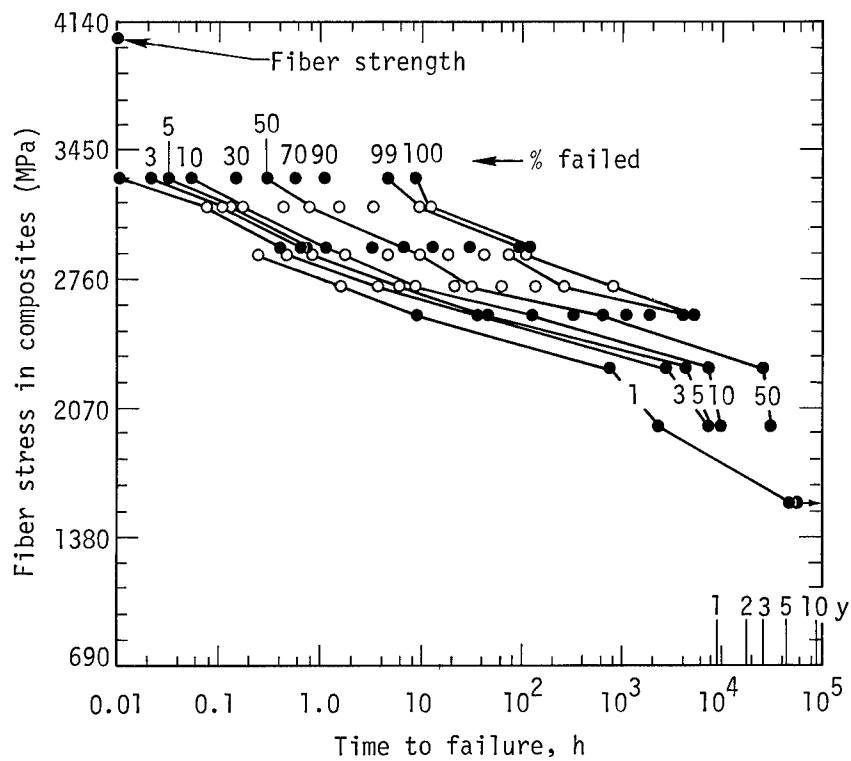


Fig. 3. Stress-rupture failure contour lines of S-glass/epoxy strands.

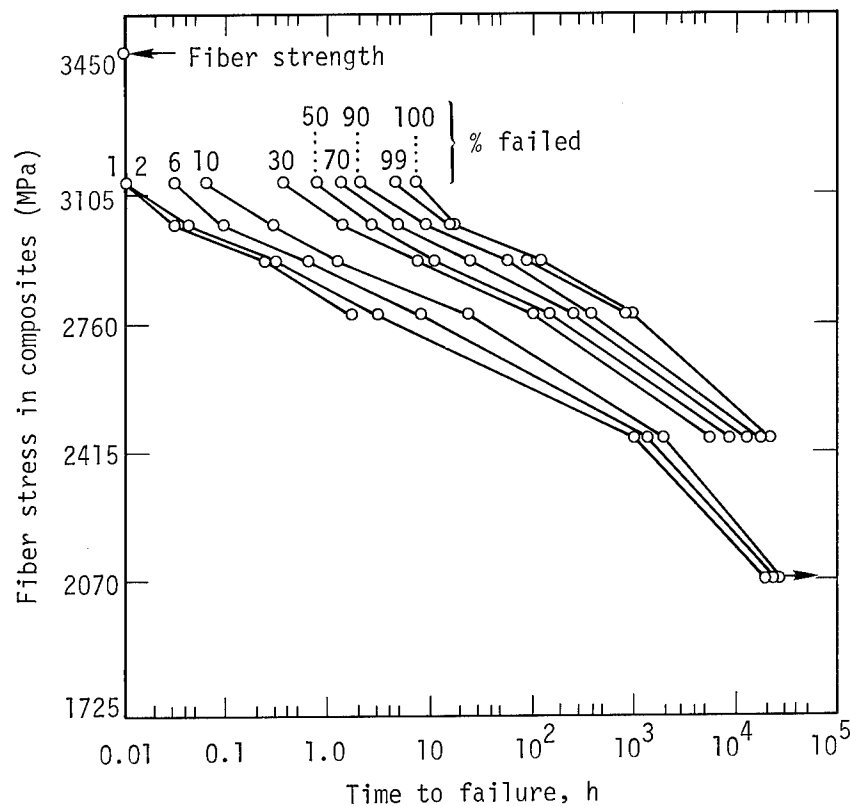


Fig. 4. Stress-rupture failure contour lines of Kevlar/epoxy strands.

The general problem of the conventional stress-rupture test is that it is impractically long and expensive. We are presently developing an accelerated test to predict life of composites. The acceleration involves both temperature and stress. The relationship among life-time, t , applied stress, σ , and absolute temperature, T , can be represented by Zhurkov's modified Arrhenius equation:

$$t = t_0 \exp [(U_0 - \alpha\sigma)/kT],$$

where k is Boltzmann's constant; t_0 , U_0 , and α are material constants that can be obtained experimentally.

We are equipping close to a thousand stress-rupture apparatuses in a new test building that will provide:

1. High-load stress-rupture testing for flywheel applications,
2. Temperature control for accelerated testing, and
3. Additional room temperature testing equipment.

In summary, we already have several years of stress-rupture data for S-glass/

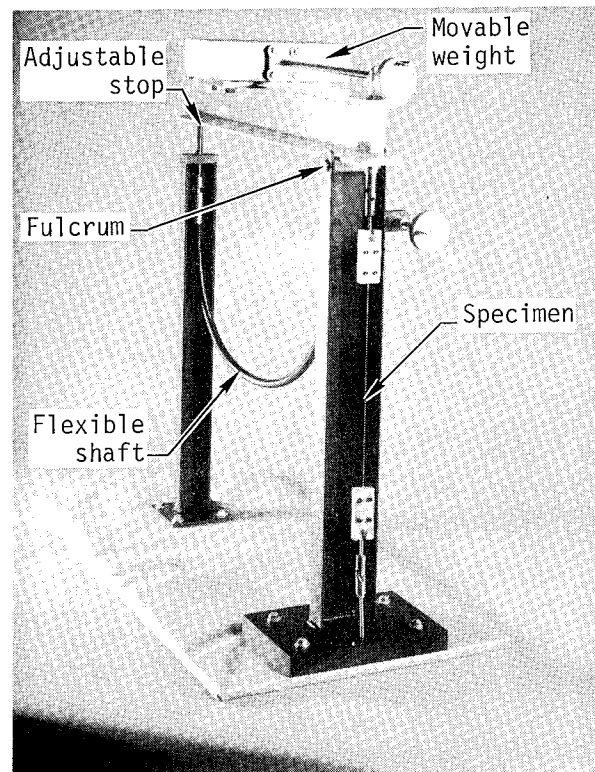


Fig. 5. High-load stress-rupture apparatus for flywheel program.

epoxy and Kevlar/epoxy composites, and we have begun to collect data on other composites for the flywheel program. We

also have started an accelerated testing program for predicting the long-term performance of fiber composites.

POTENTIAL MERITS OF THERMOPLASTIC COMPOSITE MATERIALS FOR MODULAR RIM FLYWHEELS

J. H. Laakso
Boeing Aerospace Company
P. O. Box 3999
Seattle, Washington 98124

ABSTRACT

This paper discusses the unique properties of certain thermoplastic composite materials and their application to the fabrication of low-cost flywheels. Experience in laboratory filament winding of thermoplastic vessels is described. Cost related aspects in making large thermoplastic flywheels are discussed.

INTRODUCTION

Flywheel concepts currently being studied for energy storage involve a variety of filamentary composite materials. Small prototype flywheels have already been fabricated by several companies using Kevlar 49, E-glass, and S-glass as fibers and thermosetting epoxy resins as matrix materials.

Thermosetting composites may not be suitable for large flywheels because of problems such as residual thermal strain after curing, resin shrinkage, and short shelf (pot) life. Though new understanding of these problems is coming out of current flywheel research programs, practical fabrication processes have not been developed yet.

The purpose of this paper is to present thermoplastic composites as alternate candidate materials for composite flywheels. While thermoplastic flywheels have not been actually fabricated, there is sufficient evidence from other thermoplastic research and applications to suggest that thermoplastics should be seriously considered for flywheels.

This paper presents briefly (1) some ideas and related background for filament winding flywheels with thermoplastics, (2) properties of selected materials, and (3) cost considerations.

THERMOPLASTIC COMPOSITE DESIGN CONCEPT

For purposes of discussion, the thermoplastic, rim-type, flywheel design concept selected is illustrated in Figure 1. The construction would be essentially

the same as an S-glass/epoxy flywheel, except that the resin material would be thermoplastic. Though a wide variety of engineering thermoplastics are candidates, phenoxy and polysulfone resins (both Union Carbide products) are of main interest because of our previous experience with them (References 1 and 2).

MANUFACTURING ASPECTS

Because thermoplastic resins need only heat to soften them, the flywheel fabrication process can be simplified, as indicated in Figure 2. Figure 3 shows a winding setup in which dry pre-impregnated thermoplastic composite material (strands, tow or tape obtained from vendors) is heated to the softening point of the resin and fed to a rotating rim unit. A significant aspect of this process is that each winding rapidly becomes a structural (self-supporting) part of the rim as soon as the resin cools.

This process introduces interesting possibilities for lightweight mandrels and programmed winding to produce residual radial tension. The strength degradation caused by resin migration and fiber buckling that is seen in some thermosetting composites should be eliminated with this process (such problems have occurred previously with large filament-wound epoxy rocket motor cases).

MATERIAL PROPERTIES

Figure 4 shows typical properties for phenoxy and polysulfone resins. Also, the resins have high ductility, good strength, and they do not burn. Since phenoxy resin has a lower heat distortion

temperature and lower melt temperature (about 500°F) than polysulfone resin does, it would be a first choice for filament-wound flywheels. Furthermore, phenoxy resin is low cost. However, because of its high heat distortion temperature, polysulfone is the preferred resin if an elevated temperature environment exists.

Figures 5 and 6 depict the tensile properties of glass fabric laminates made from the selected thermoplastics using epoxy resins as the matrix (Reference 1). The properties are comparable over a wide range of temperatures.

The stress-strain curves in Figure 7 illustrate the ductility of thermoplastics. The higher impact strengths (Figure 8, Reference 1) and fatigue resistance (Figure 9, Reference 1) of thermoplastic composites may be attributable to the ductile nature of the thermoplastic resins. The beneficial effects of resin ductility also appear in short-beam interlaminar and in transverse laminate bending tests, in which brittle fracture typically does not occur.

Polysulfone resin is remarkably creep resistant (Figure 10). This property translates into creep-resistant laminates, as indicated in Figure 11 (Reference 2). Creep resistance is obviously an important material property requirement in flywheel applications.

PREVIOUS FILAMENT WINDING EXPERIENCE

The Boeing Aerospace Company conducted research on filament-wound thermoplastics in the period 1966 to 1970. The work established a laboratory process for winding pressure vessels that can be scaled up to make large flywheels. Figure 12 shows a tested vessel having an S-glass/phenoxy hoop overwrap on a 2219 aluminum liner. The liner was relatively thin, compared to the overwrap, and served as the "mandrel" during winding. Figures 13 and 14 illustrate the laboratory winding setup used. In principle, this setup is similar to the schematic shown in Figure 3. Other pressure vessels, such as the one shown in Figure 15, were successfully wound using both S-glass and Kevlar 49 filaments in phenoxy resin.

COST CONSIDERATIONS

In 1968, a limited study was made of large-scale, thermoplastic, filament

winding applications. Conclusions from that study, summarized in Figure 16, are pertinent to the low-cost flywheel fabrication problem. In particular, the elimination of wet resin processing and oven curing of epoxies by replacing them with thermoplastics should result in fabrication cost savings. Also, because of the thermoplastic process simplicity, flywheels could be fabricated by a number of manufacturers.

As part of the previous study, a cost analysis was conducted on the large scale vessel shown in Figure 17a. In several respects this vessel would have design features similar to flywheels. The cost analysis assumptions used in the study are also listed in Figure 17a.

Figure 18 shows the resulting vessel fabrication costs as a function of number of vessels. Of main interest is the rapid amortization of non-recurring costs, which were initially high. With volume production, the unit costs would approach the basic material costs.

Another cost-related aspect of thermoplastics is their recycling possibilities. Figure 19 suggests that used flywheel rims can be either resized or recovered by grinding into pellets for other commercial injection molded products. Furthermore, while this may be only an interesting speculation, flywheel rims, like all thermoplastics, would have value to the scrap market.

SUMMARY

The potential merits of the thermoplastic composite flywheels highlighted in the preceding discussion are summarized in Figure 20. The potential aspect is emphasized because much research and development will be required before the feasibility of large thermoplastic composite flywheels can be established. This is also the case with composite flywheels in general.

Recommended research tasks appear in Figure 21. We believe that future research and development efforts should be directed at large, thick prototype thermoplastic composite flywheels in the areas of (1) design synthesis, (2) radial (transverse) property characterization, (3) prototype fabrication and (4) spin testing.

References

1. Boeing Report D180-17531-1, "Investigation of Reinforced Thermoplastics for Naval Aircraft Structural Applications - Final Report," J. T. Hoggatt, May 1973, prepared under Naval Air Systems Command Contract N00019-72-C-0526.
2. Boeing Report D180-18034-1, "Study of Graphite Fiber Reinforced Thermoplastic Composites - Final Report," J. T. Hoggatt, February 1974, prepared under Naval Air Systems Command Contract N00019-73-C-0414.

PT-19656

PT-21052

FIGURE 1

Modular Rim Flywheel Concept

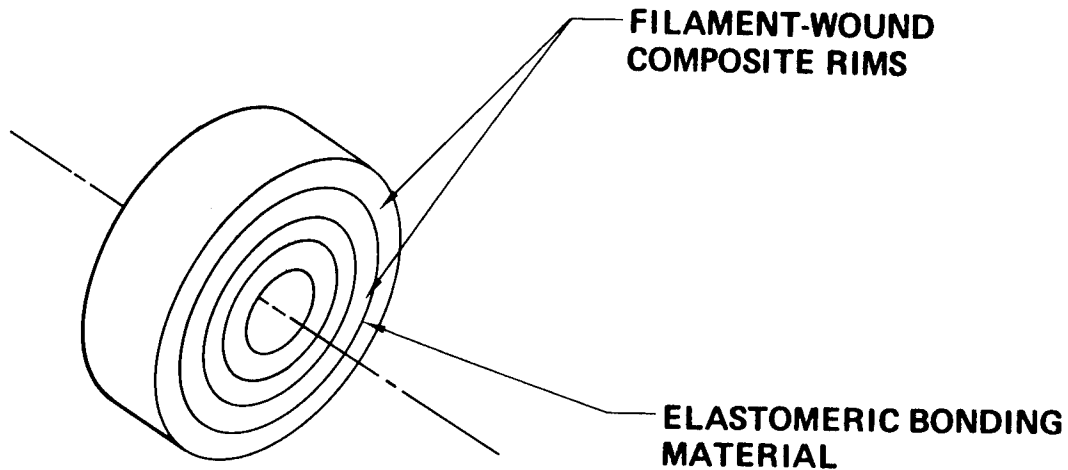


FIGURE 2 THERMOPLASTICS PROVIDE MANUFACTURING SIMPLICITY

- O EXISTING FILAMENT-WINDING FACILITIES CAN BE EASILY MODIFIED FOR THERMOPLASTICS
- O THERMOPLASTIC COMPOSITES REQUIRE LESS FABRICATION EFFORT THAN THERMOSETS
 - RAW MATERIAL IS A DRY PREPREG
 - NO CURING (CHEMICAL REACTION) OPERATIONS REQUIRED
- O PROVISIONS REQUIRED FOR LOCAL HEATING/COOLING OF PREPREG
- O LIGHTWEIGHT WINDING MANDRELS CAN BE USED
- O QUALITY CONTROL IS SIMPLIFIED
 - NO SHELF-LIFE, CHEMISTRY PROBLEMS

FIGURE 3 Flywheel Rim Winding Set-Up

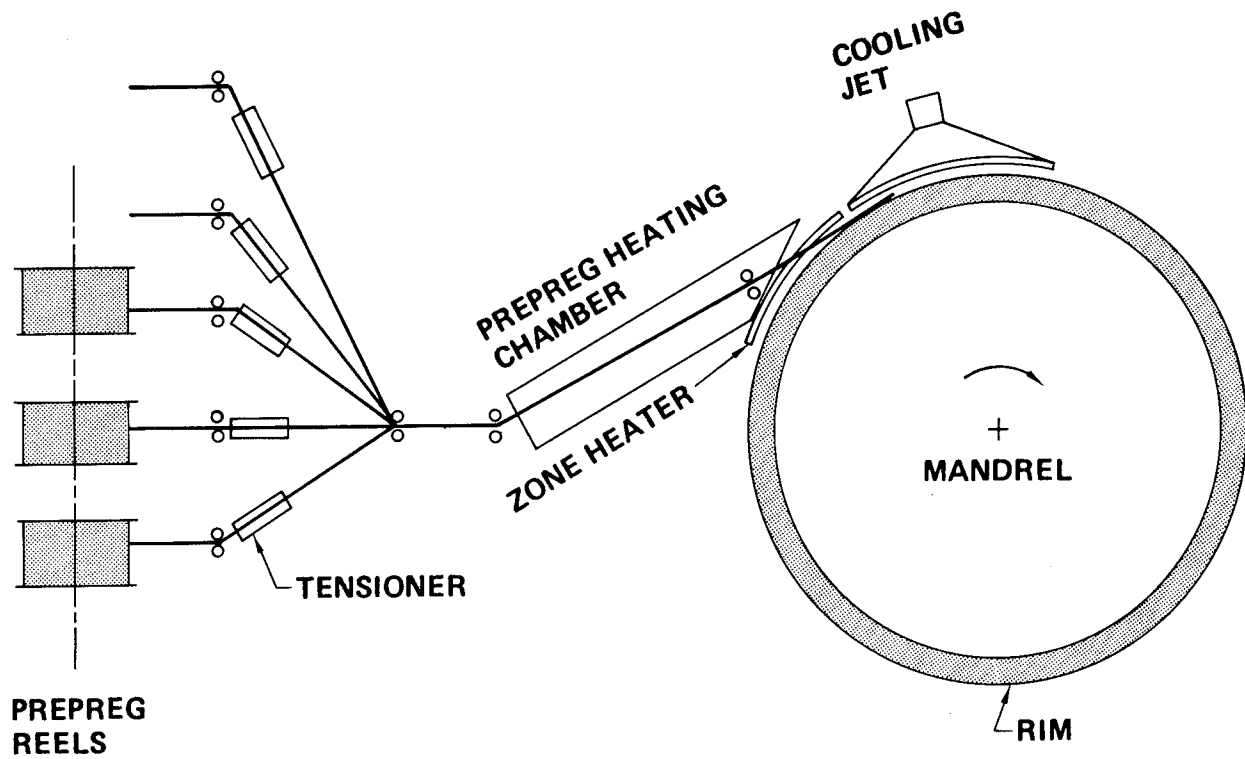


FIGURE 4 **Typical Properties of Polysulfone and Phenoxy Thermoplastic Polymers**

<u>Property</u>	<u>Polysulfone P-1700</u>	<u>Phenoxy PKHS-1</u>
General		
Density	1.24	1.32
Mechanical		
Tensile strength at yield, psi	10,200	9,000
Tensile modulus, psi	360,000	400,000
Tensile elongation at break, %	50-100	50-60
Flexural strength, psi	15,400	14,500
Flexural modulus, psi	390,000	400,000
Izod impact at 72°F, ft-lb/in. notch	1.3	2-5
Rockwell hardness	R120	R123
Thermal		
Heat distortion temperature at 264 psi, °F	345	175
Coefficient of linear thermal expansion, in./in./°F	3.1 x 10 ⁻⁵	3.0-3.5 x 10 ⁻⁵
Thermal conductivity, btu/hr/ft ² /°F/in.	1.8	—
Flammability	Non-burning	Self-extinguishing
Electrical		
Dielectric strength, v/mil	425	505
Volume resistivity, 72°F, ohm-cm	5 x 10 ¹⁶	2.75 x 10 ¹⁶
Dielectric constant, 72°F, 60 Hz-1 mHz	3.07-3.03	4.1
Dissipation factor, 72°F, 60 Hz-1mHz	.0008-.0034	.0009-.001

FIGURE 5

Comparison of Tensile Properties of 181 Glass Fabric Laminates

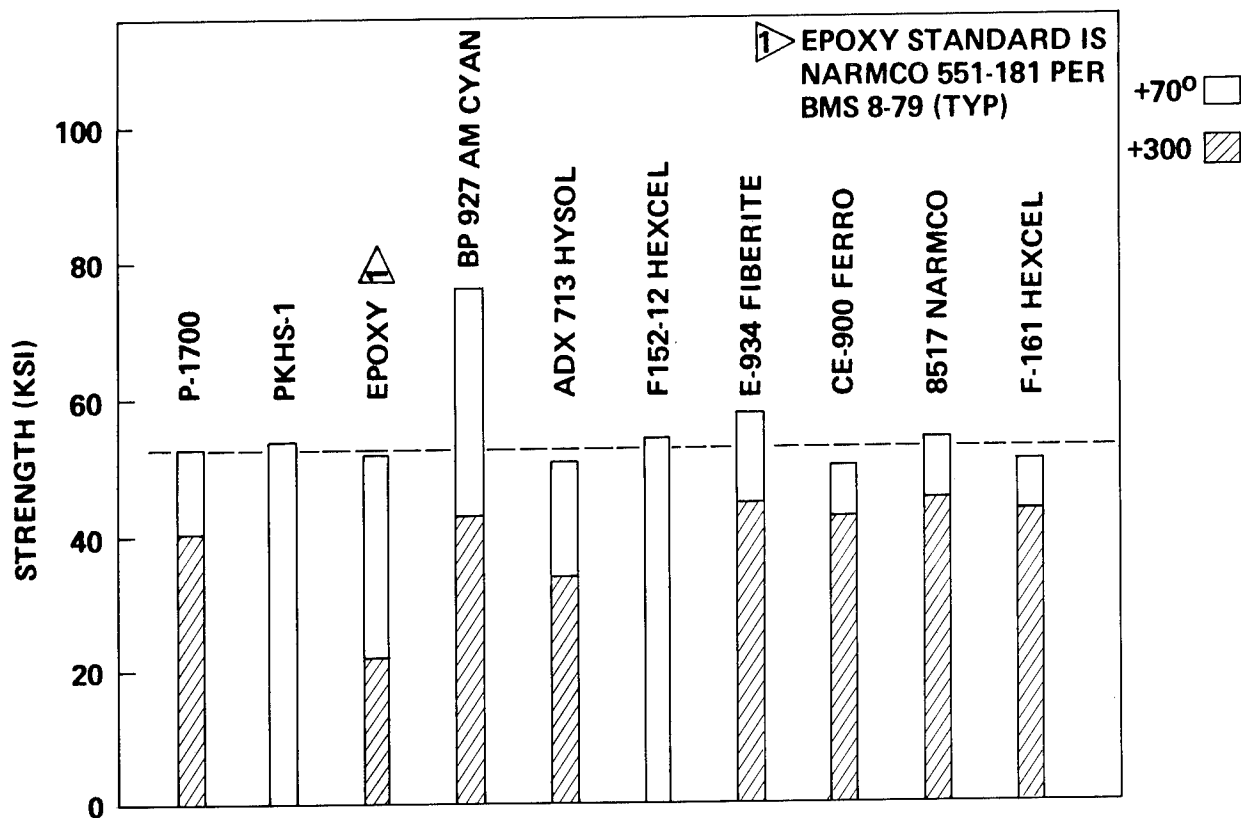


FIGURE 6 **Tensile Modulus vs Temperature of
181 Glass Fabric Laminates**

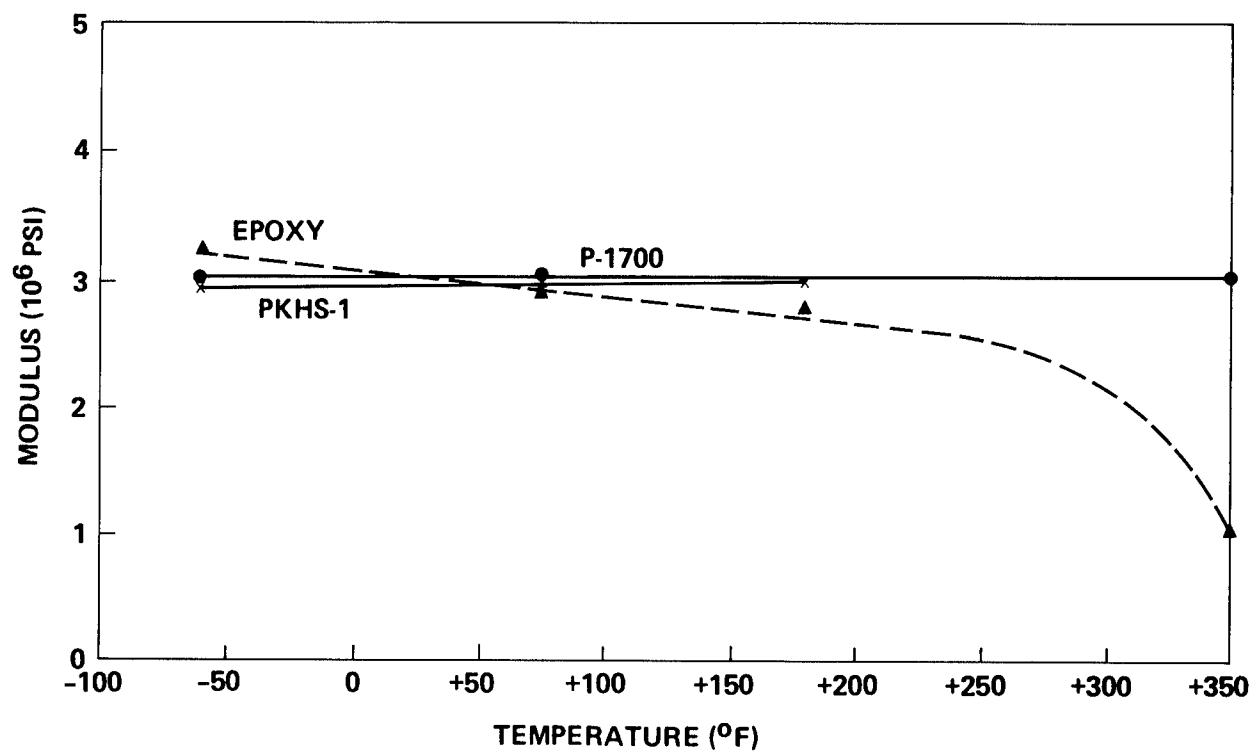


FIGURE 7 Tensile Stress-Strain Curves for Various Polymers

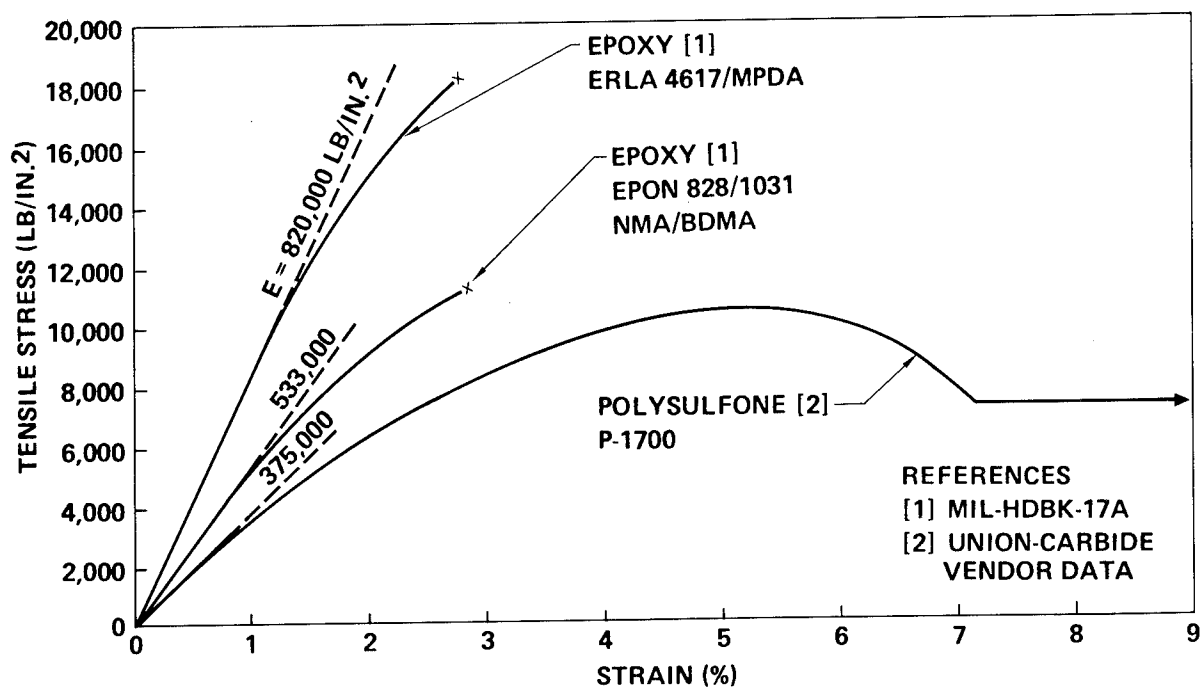
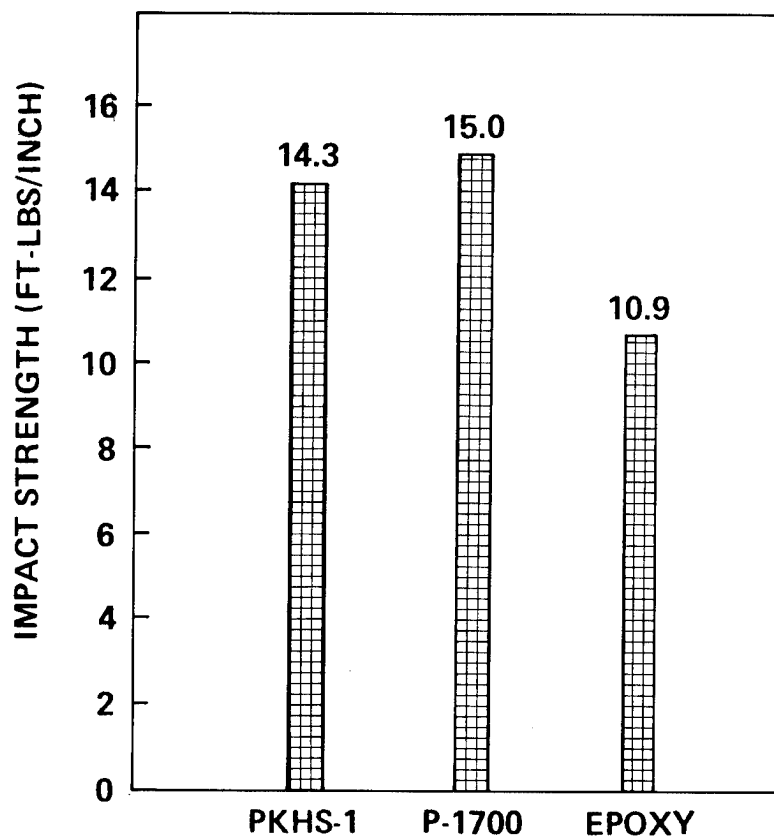


FIGURE 8 **IZOD Impact Strength* of 181
Glass Fabric Laminates**



***NOTCHED
(ASTM 256-56T)**

FIGURE 9 **Constant-Amplitude Fatigue Properties of Unidirectional Graphite Composites**

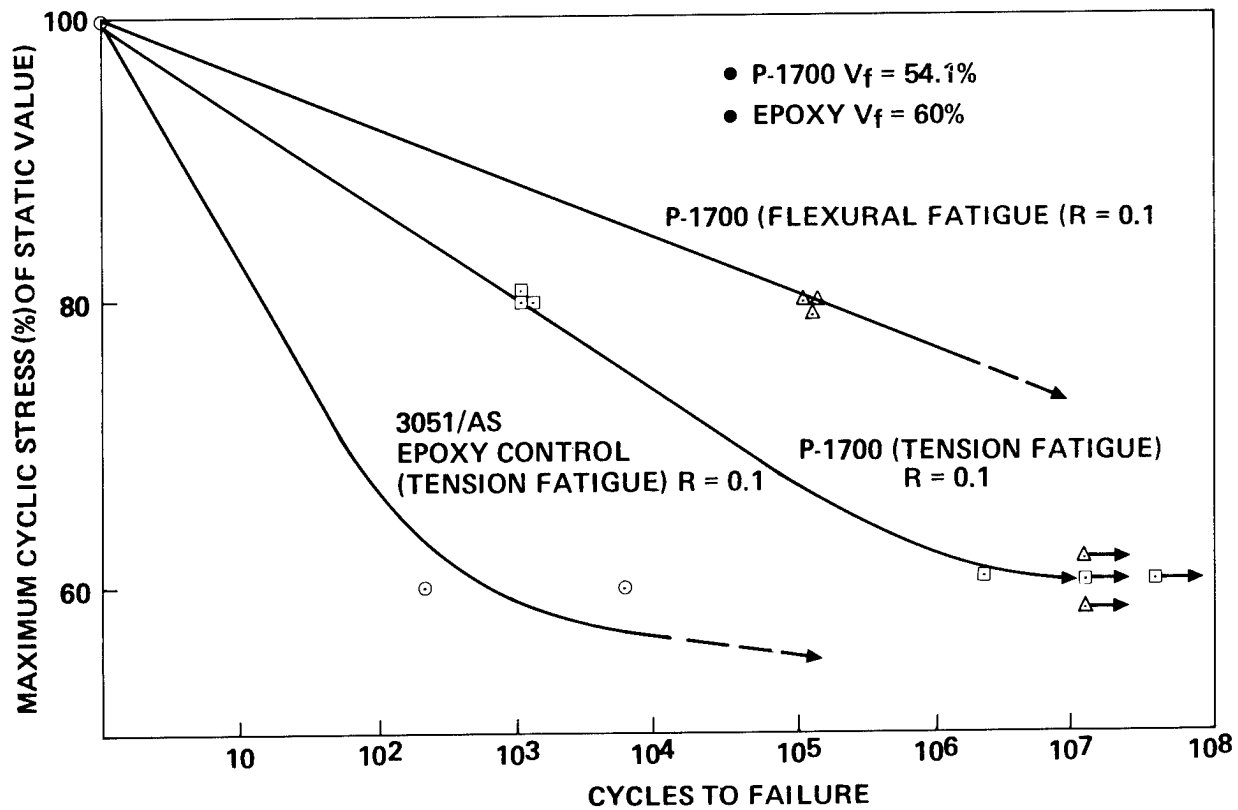
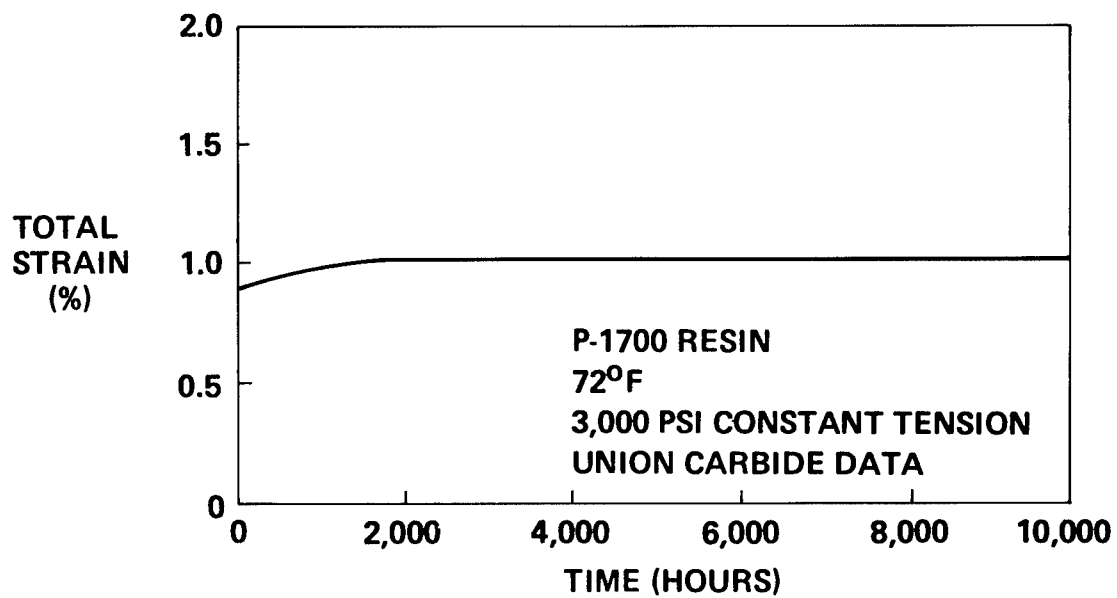
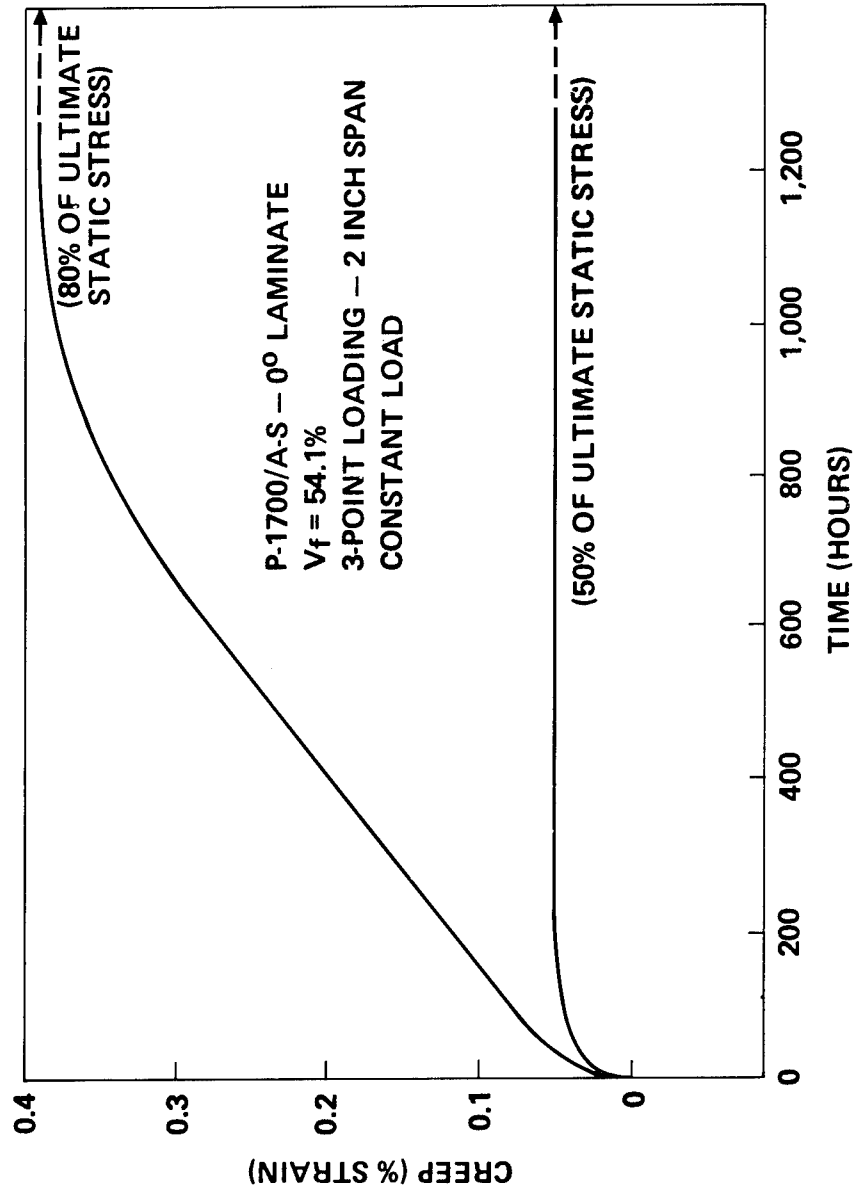


FIGURE 10 **Creep Behavior of Polysulfone Resin**



Flexural Creep Properties of Unidirectional Graphite Composites — +70°F

FIGURE 11



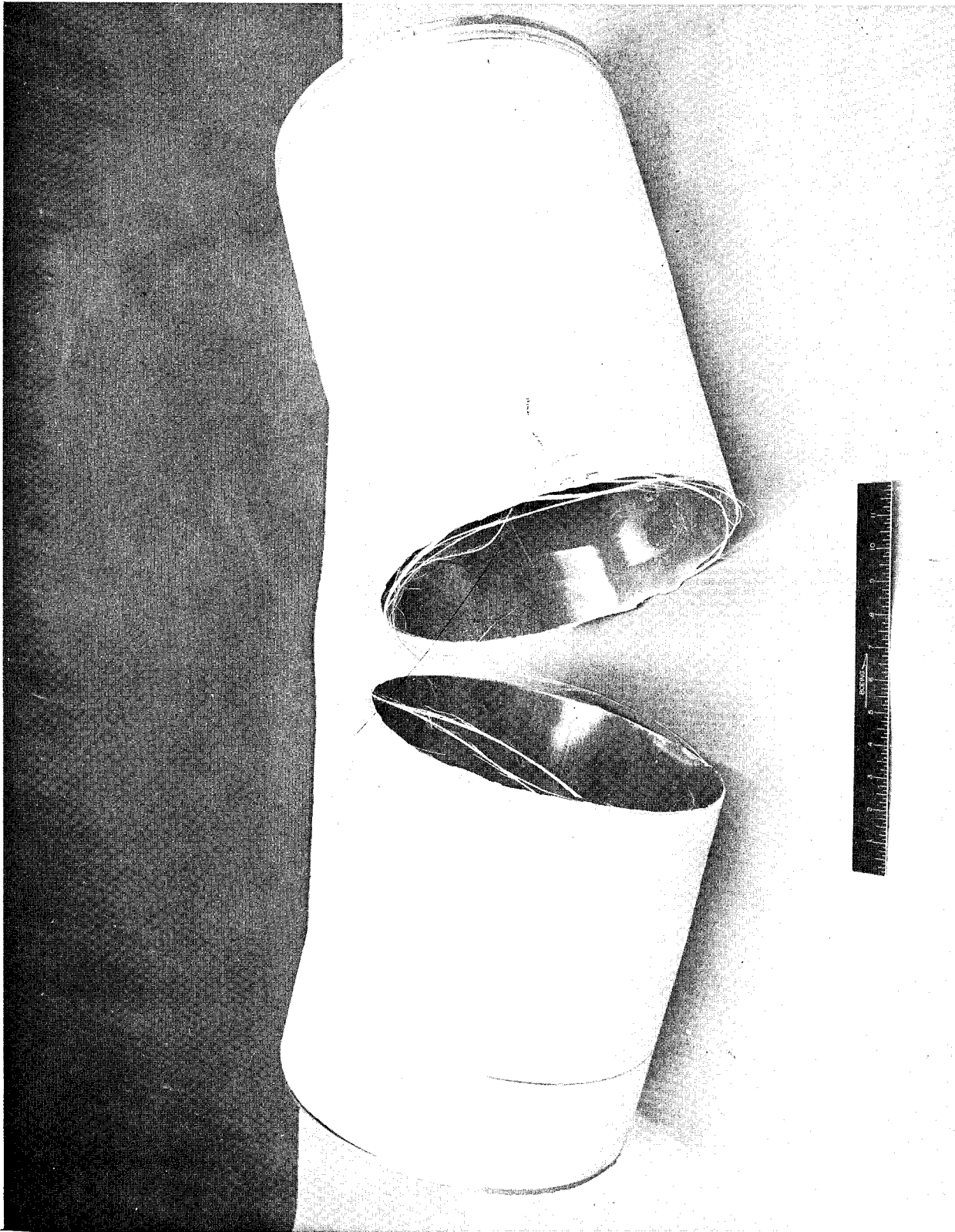


FIGURE 12 S-GLASS/PHENOXY OVERWRAPPED ALUMINUM PRESSURE TEST VESSEL
(BURST AT 1005 psi)

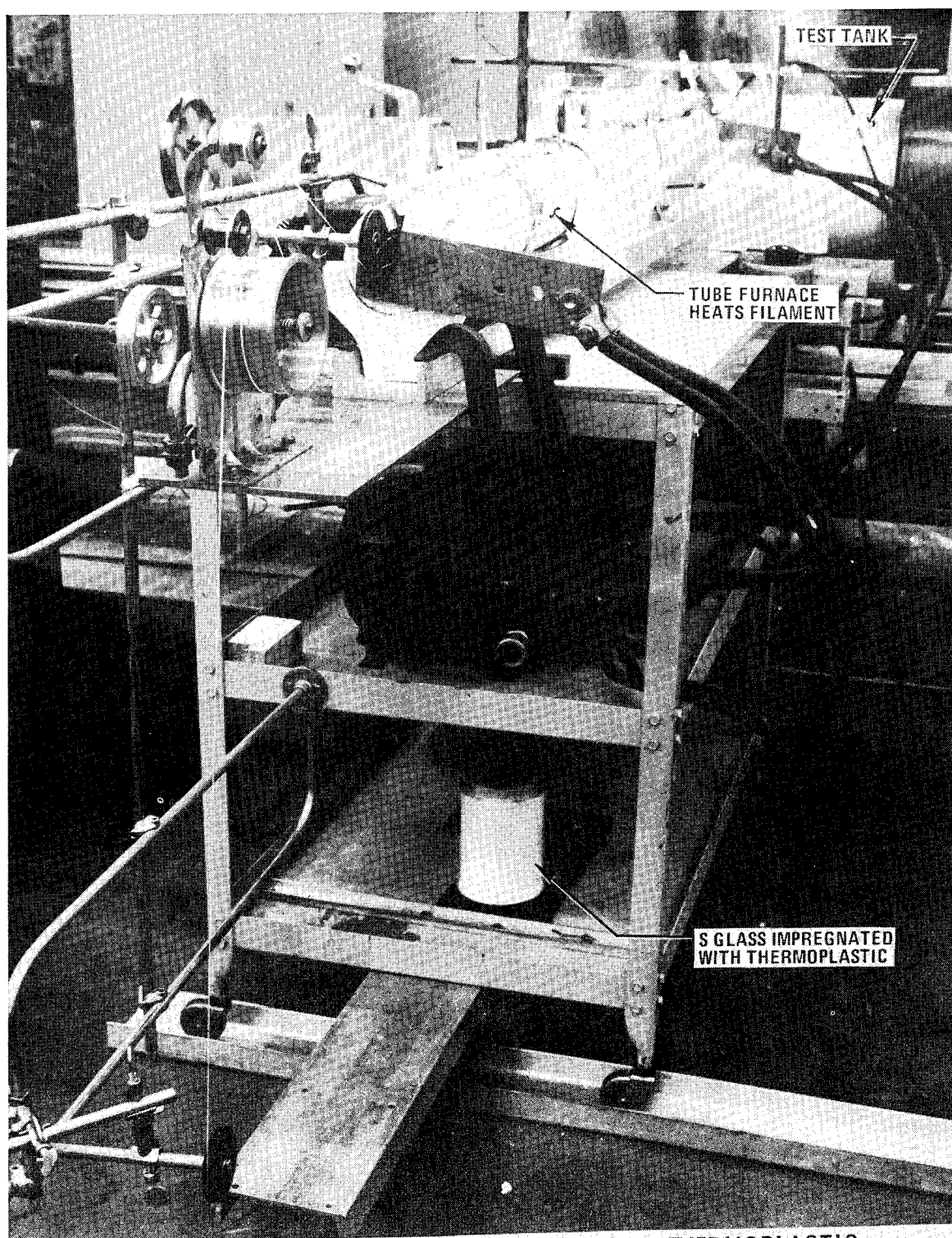


FIGURE 13 OVERWRAPPING TEST TANK WITH S GLASS AND THERMOPLASTIC RESIN SYSTEM

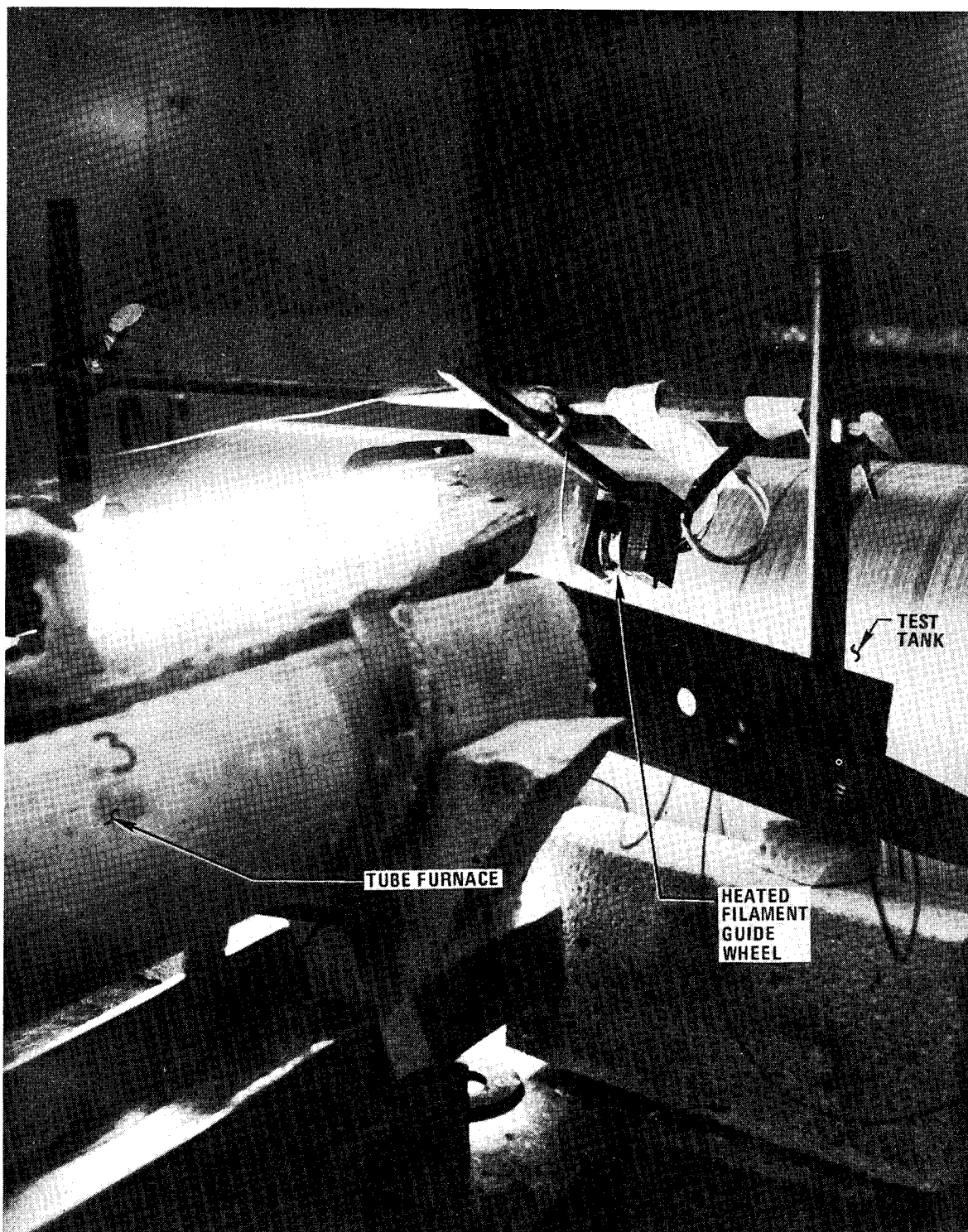


FIGURE 14 CLOSEUP OF OVERWRAPPING TEST TANK WITH THERMOPLASTIC RESIN SYSTEM AND S-GLASS

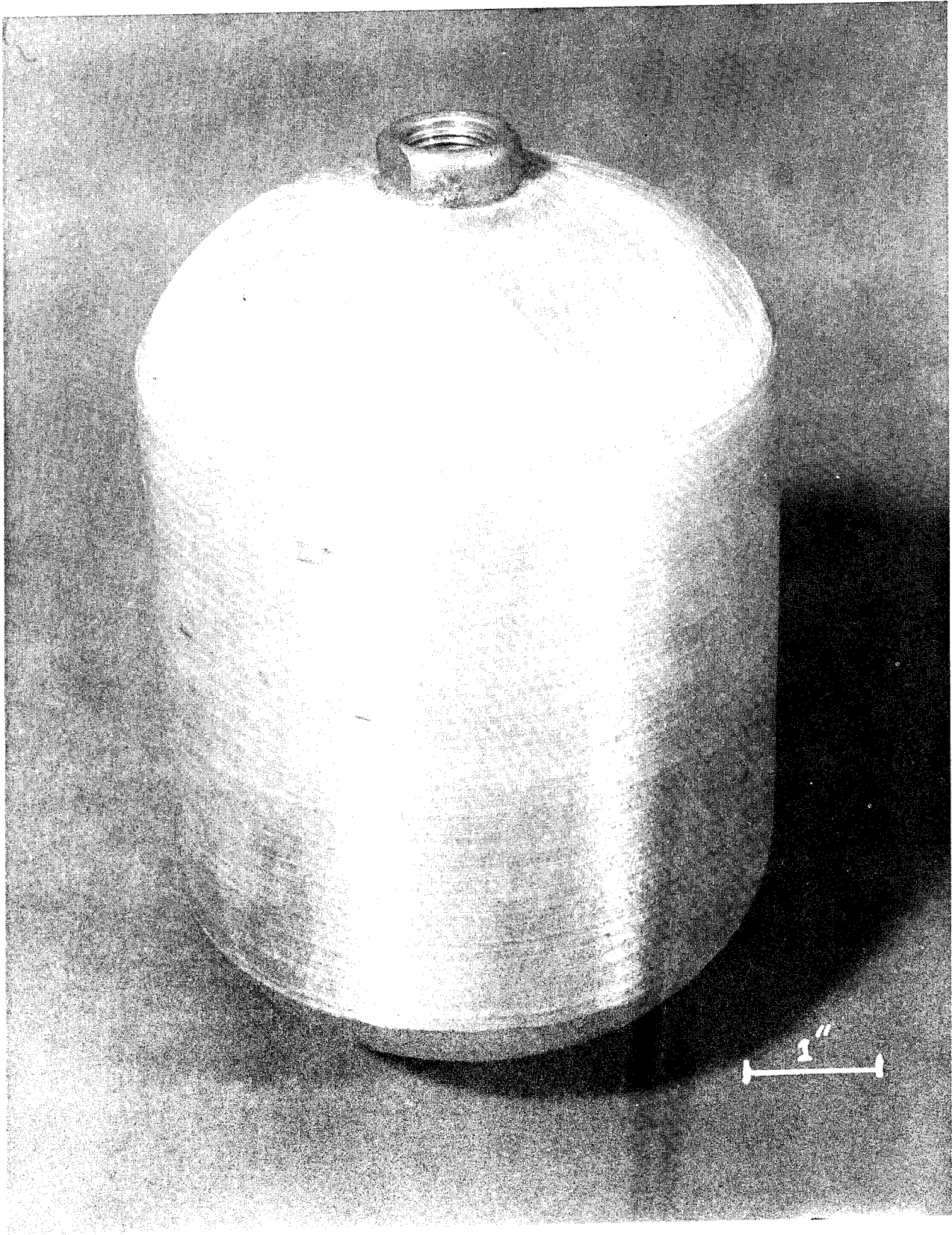


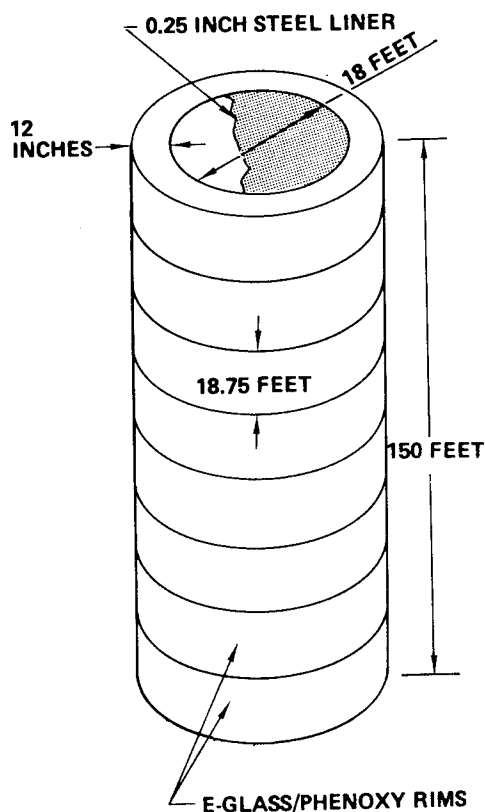
FIGURE 15 FILAMENT-WOUND KEVLAR-49/PHENOXY TEST BOTTLE

FIGURE 16 FABRICATION COST ADVANTAGES

0 THERMOPLASTICS COMPOSITES OFFER POTENTIAL FOR LOW FABRICATION COSTS

- HIGH WINDING SPEEDS
- REDUCED QUALITY CONTROL REQUIREMENTS
- NO CURING REQUIRED
- CONTINUOUS WINDING WITHOUT STAGING
- LOW RESIN COST
- REPARABLE
- SCRAP OF VALUE TO COMMERCIAL MOLDERS

FIGURE 17a **Filament-Wound Thermoplastic Vessel Cost Study**



● ASSUMPTIONS:

1968 COSTS

MATERIALS

E-GLASS ROVING—BEAMED, AT 31 CENTS PER LB (75% BY WEIGHT)

RESIN, AT 40 CENTS PER LB (25% BY WEIGHT)

STEEL LINER 1/4-INCH THICK, AT 50 CENTS PER LB — FABRICATED

LABOR COSTS AT \$15/HOUR

WINDING SPEED—25 FPM (100 FPM FEASIBLE)

COMPOSITE WEIGHT 1,056,000 LB PER VESSEL

● DEVELOPMENT COSTS

ENGINEERING: MATERIALS AND PROCESS DEVELOPMENT \$200K

AUTOMATED MACHINERY DEVELOPMENT: \$1,000K

MACHINERY MANUFACTURE: \$200K PER COPY

FIGURE 17b

0	RECURRING COSTS PER VESSEL	
-	SET-UP AT 30 MANHOURS PER SEGMENT	\$ 3,600
-	WINDING LABOR AT 185 MANHOURS PER SEGMENT (INCLUDES MACHINING END DOVETAIL JOINTS)	2,800
-	MATERIALS:	
.	LINER	4,500
.	RESIN (266,000 LBS.)	113,000
.	GLASS (790,000 LBS.)	<u>245,000</u>
-	TOTAL RECURRING COST PER VESSEL	\$368,900
0	CALENDAR TIME PER VESSEL (TWO-SHIFT OPERATION):	28 WORK DAYS
0	VESSELS PER YEAR:	10 PER MACHINE

FIGURE 18 **Filament-Wound Thermoplastic Vessel Costs**

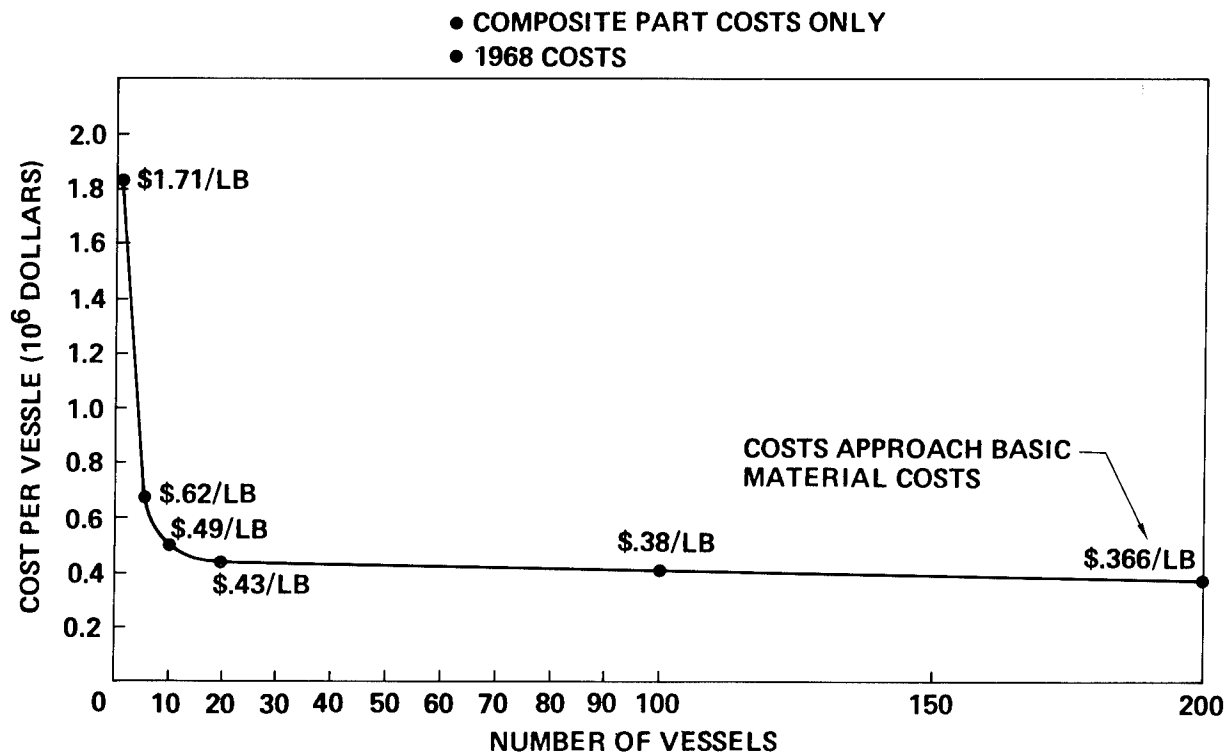


FIGURE 19

Recycling Possibilities

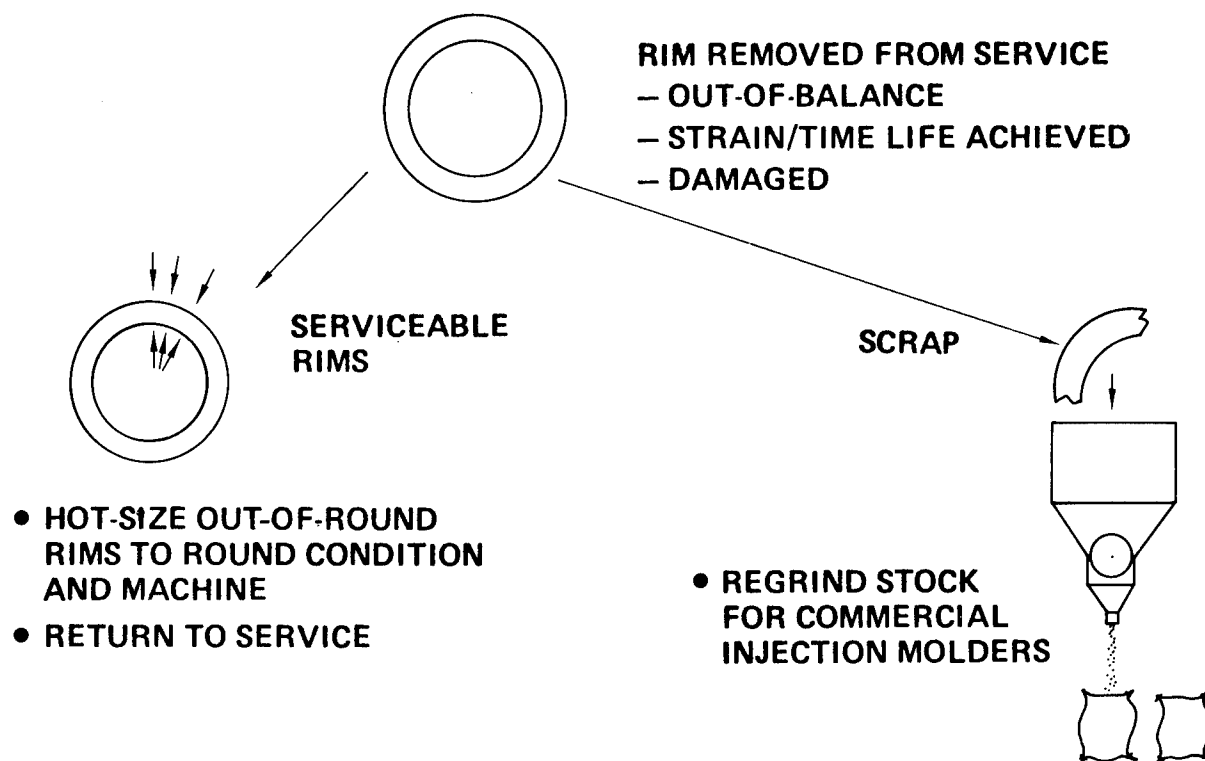


FIGURE 20 MERITS OF FILAMENT-WOUND THERMOPLASTIC COMPOSITES FOR FLYWHEELS

- O BENEFICIAL MATERIAL PROPERTIES
 - HIGH STRENGTH TO WEIGHT
 - GOOD CREEP RESISTANCE
- O CONVENIENT RAW MATERIAL FORM
 - DRY PREPREG HAVING LOW-COST RESIN
 - NO SHELF-LIFE PROBLEMS
- O SIMPLE FILAMENT-WINDING PROCESS
 - HIGH SPEED
 - PROCESS NOT TIME-DEPENDENT
 - RIGID RIM LAY-UP
 - NO CURING REQUIRED
- O MATERIALS ARE RECYCLABLE

FIGURE 21 FUTURE R & D REQUIRED

- O ADDITIONAL MATERIAL CHARACTERIZATION STUDIES
- O ESTABLISH PROCESS FOR FILAMENT-WINDING THICK THERMOPLASTIC COMPOSITE RIMS
 - S-GLASS/POLYSULFONE
 - KEVLAR-49/POLYSULFONE
- O FABRICATE PROTOTYPE FLYWHEELS
- O CONDUCT SPIN TESTING OF PROTOTYPE FLYWHEELS
- O INVESTIGATE CREEP AND STRESS RUPTURE RESPONSE LIMITS
- O ESTABLISH DESIGN ALLOWABLES
- O DEFINE IN-SERVICE MONITORING/TEST METHODS AND ACCEPTANCE CRITERIA

ENGINEERING PROPERTIES OF ELASTOMER/ADVANCED COMPOSITE LAMINAR STRUCTURES

A. F. Lewis and R. T. Natarajan
Lord Corporation
2100 West Grandview
Erie, Pennsylvania 16512

ABSTRACT

This paper reports studies of the adhesive joint strengths and the vibration damping properties of elastomer/composite laminates. The studies were made to develop data related to Post's design for a concentric composite ring/elastomer flywheel. Test specimens were made from carbon fiber/polysulfone and phenolic composites laminated to sulfur-cured natural rubber, SBR or nitrile rubber compounded in carbon black filled recipes. Conclusions were that elastomer/composite adhesive joint strengths and the vibration damping properties of composites depend on the orientation of the composite surface ply, but that the damping behavior of composite constrained layer laminates are independent of ply orientation.

INTRODUCTION

Advanced fiber-reinforced polymer composites and elastomeric materials each taken separately represent vast areas of materials engineering technology. Structures employing the combination of these two "divergent" material types are scarcely known. Among the various reported material structures employing this combination are bead wires in tire construction (1), gaskets for rocket nozzles (2), and energy storage flywheels (3). It is the intent of this paper to review, in broad detail, results of some studies conducted to determine the engineering properties of elastomer/advanced composite laminar structures. Such a configuration, shown in Figure 1, is known as a constrained (viscoelastic) layer laminate. Constrained layer laminates using sheet metal plies are well-known structures for vibration damping applications (4).

The reported concentric composite ring/elastomer superflywheel design proposed by Post (3) represents a constrained layer structure whose purpose is to minimize internal radial stresses in the various rings. The data presented in this paper may be useful in the context of such applications and structures. Of particular interest here is the need to know the adhesion strength properties of elastomer-to-composite bonds. It may also be helpful to know the vibration damping properties of composite materials and composite/elastomer laminar structures; this infor-

mation may be useful in estimating the long-term fatigue behavior of such structures.

EXPERIMENTAL

MATERIALS

The composites used in this study were fabricated from commercially-available, epoxy-based, unidirectional prepreg materials (Thorne^R 300/Epoxy Rigidite^R 5208, S-glass/Epoxy Rigidite^R 5208, Kevlar^R/Epoxy Rigidite^R 5208). For comparison purposes, the vibration damping properties of carbon fiber (Thorne^R 300)/polysulfone and phenolic composites were also measured (see Table 2). The composites were prepared by special order by Whittaker R & D, San Diego, CA. The elastomeric material used in this study was sulfur-cured natural, SBR or nitrile rubber. Standard carbon black filled rubber vulcanizate recipes were employed.

Thorne^R - registered tradename of Union Carbide Corporation for graphite fiber.

Rigidite^R - registered tradename of Narmco Division, Celanese Corporation for epoxy resin prepreg.

Kevlar^R - DuPont Co. tradename for polyaramid fiber.

The adhesive used in bonding the elastomer to the composite was the Chemlok^R 220 adhesive system; a product of the Hughson Chemicals Division of Lord Corporation.

METHODS

The adhesion tests performed in this study are described by the ASTM-D429-73 Method B. The so-called 45° peel test modification for rubber to metal bonding was employed. In order to prevent the bending of the composite during peel testing, the composite specimen was backed with 16 gauge steel (composite bonded to steel using Versilok^R 506, structural adhesive, Hughson Chemicals Division of Lord Corporation).

The loss factors of the composites and composite structures were measured using the forced vibration resonance method. A Brüel and Kjaer type complex modulus apparatus was used to determine the loss factors and storage moduli. These specimens were approximately 10" long and 1/2" wide and clamped at one end, under controlled pressure, in the apparatus. Details of these measurements have been published elsewhere (5).

RESULTS AND DISCUSSION

ELASTOMER/COMPOSITE ADHESION

A series of adhesion peel tests (ASTM-D429-73, Method B) were conducted on 1" wide unidirectional fiber/epoxy steel backed composite strips. The data obtained are presented in Table 1. In these experiments, the effect of composite surface ply orientation (against the rubber) on peel strength was determined. In the cases where cohesively-strong rubber types were used (Nitrile and SBR), peel strengths depended upon composite surface ply orientation relative to the direction of peeling. The peel strength was lowest when the samples were peeled 90° to the orientation of the composite surface ply; fiber-matrix (adherend) failure was observed. When the peel direction was parallel to the fiber ply direction, good "rubber tearing" bonds were observed. In the natural rubber studies, no effect of surface ply orientation was observed because cohesive failure in the rubber occurred before enough pulling stress could be imposed on the composite to disrupt and pull the fibers from the matrix.

It is of interest here to compare the peel strength behavior of the nitrile rubber against the carbon (graphite) fiber/epoxy composite and the aramid (Kevlar^R)/epoxy composite. In the case of aramid/epoxy composites, it is observed that some adherend (composite) failure was observed even for the peel tests conducted on the 0° orientation (see Figure 2). These data indicate that, under the imposed peeling stresses, the aramid/epoxy composite is cohesively weaker than the carbon (graphite) fiber/epoxy composite; the aramid fiber/matrix adhesion is poorer than the carbon (graphite)/matrix adhesion.

VIBRATION DAMPING PROPERTIES

Turning to the property of vibration damping of elastomer/advanced composite laminar structures, the vibration damping properties of several fiber/matrix composite systems were measured using the force of vibration resonance technique.

Data are presented in Table 2. The data were compared within the same frequency range (same decade). In these unidirectional composites, damping was 3 to 5 times greater when the beam was flexed across the fibers than when flexed parallel to the fiber direction. Cross-ply composites showed intermediate vibration damping properties. The loss factors for the composites flexed in a direction parallel to the fibers were generally low, and comparable to the loss factors of metals. The composite made using phenolic resin as a matrix had a higher loss than the other resin systems studied. It is believed that in the cured state, this matrix material, as a result of water liberated as a product in the cure reaction, exists in a more defect structure form. These defects most likely disrupt the fiber/matrix bonding thus increasing the potential for internal friction within the composite material.

In comparing the data in Table 2, an anisotropy in loss factor occurs depending upon the orientation of the fibers relative to the dynamic flexing direction. It may be said that the damping properties of a unidirectional composite that is flexed parallel to the fiber direction behaves as a "reinforced" composite (low damping), while a composite that is flexed perpendicular to the fiber direction behaves as a "filled" composite (high

damping, characteristic of the matrix polymer).

The vibration damping properties of constrained layer laminates made employing some of the unidirectional composites described in Table 2 are presented in Table 3. In these laminar structures, natural rubber was used as the viscoelastic interlayer media. As can be observed, the loss factors for these constrained layer laminates are much higher than the component composite plies. The loss factors approach the loss factors of the natural rubber interlayer. Furthermore, no strong anisotropy effects due to the fiber orientation were observed in these constrained layer laminates. The vibration damping results for the composites, constrained layer laminates and isotropic materials are summarized in Figure 3.

The dynamic elastic storage modulus, as determined from the resonance frequency of the vibrating beams, is also observed to be dependent upon ply orientation (see Tables 2 and 3). This is expected since such a property characterizes the planar mechanical stiffness of these composites. Planar mechanical anisotropy of fiber/polymer composite plates is well-known. How the storage modulus effects the vibration damping properties of composite systems is complex and goes beyond the scope of this paper (6).

CONCLUDING REMARKS

Several conclusions can be drawn from the experimental results presented:

1. Elastomer/composite adhesive joint strengths depend on the orientation of the composite surface ply.
2. Vibration damping properties of composites depend on the orientation of the composite surface ply.
3. Vibration damping behavior of composite constrained layer laminates are generally independent of ply orientation; higher than individual composite plies.

The adhesive peel strength and vibration damping data on the elastomer/advanced composite laminar structures presented in this paper are two of the important engineering properties of such materials; other engineering properties of this materials combination are presently under study. The application of this

unique materials structure to future flywheel technology is anticipated.

References

1. K. J. Niderost and A. J. Sherrin
Brit. Pat. 1,346,997, Dunlop Company, London, "Composites".
2. H. Sherard
AIAA Paper No. 73-1262
"Development of Advanced Flex Joint Technology", AIAA/SAE, 9th Propulsion Conference, Las Vegas, Nevada, November 1973.
3. R. F. Post and S. F. Post
Scientific American **229**, #6, 17, December 1973 "Flywheels".
4. A. F. Lewis
Inter-Noise 72 Proceedings, Washington, D. C., October 1972, pp. 31-36, "Laminated Metal Composites for Industrial Noise Control Applications".
5. R. T. Natarajan and A. F. Lewis
"Advanced Composite Constrained Layer Laminates" 31st Annual Reinforced Plastics Technical and Management Conference, Washington, D. C. February 1976 (Paper 12E).
6. T. F. Derby and J. E. Ruzicka
NASA, CR-1269, Washington, D. C., February 1969, "Loss Factor and Resonant Frequency of Viscoelastic Shear-Damped Structural Composites".

TABLE 1

ADHESIVE JOINING OF ELASTOMERS TO ORGANIC POLYMER ADVANCED
COMPOSITE MATERIALS

	Boundary Ply Orientation	Peel Strength* (PPI)
<u>Nitrile Rubber</u>	90°	79 M
<u>Carbon Fiber/Epoxy</u>	45°	104 M/R
	0°	140 R
<u>SBR</u>	90°	112 M/R
<u>Carbon Fiber/Epoxy</u>	45°	139 R/M
	0°	153 R
<u>Natural Rubber</u>	Any Orientation	46 R
<u>Carbon Fiber/Epoxy</u>		
<u>Nitrile Rubber</u>	90°	64 M
<u>Aramid Fiber/Epoxy</u>	45°	88 M/R
	0°	87 R/M

*R = Rubber Failure

M = Matrix Failure

TABLE 2
COMPARISON OF VIBRATION DAMPING PROPERTIES OF VARIOUS COMPOSITE
MATERIALS^(a)

<u>Material</u>	<u>Frequency (Hz) Mode Number</u>	<u>Loss Factor, η</u>	<u>Elastic Storage Modulus, 10^6 psi</u>
Carbon Fiber/Epoxy			
Longitudinal	111/#1	0.004	16.3
Cross-Ply (0,90) _s	186/#2	0.003	8.4
Transverse	178/#3	0.019	0.9
Glass Fiber/Epoxy			
Longitudinal	125/#2	0.003	6.9
Cross-Ply (0,90) _s	137/#2	0.004	4.4
Transverse	113/#2	0.011	2.4
Carbon Fiber/Polysulfone			
Quasi-Isotropic (90,45,0,-45,90) _s	232/#2	0.002	6.3
Carbon Fiber/Phenolic			
Quasi-Isotropic (90,45,0,-45,90) _s	192/#2	0.011	4.3
Steel	229/#2	0.002	24.7

(a) All composite thicknesses approximately 0.040"

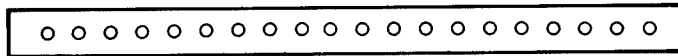
TABLE 3
VIBRATION DAMPING PROPERTIES OF ELASTOMER/COMPOSITE CONSTRAINED LAYER
LAMINATES

<u>Laminate</u>	Composite ^(a) <u>Ply Thickness</u>	<u>Frequency (H_z)</u> <u>Mode Number</u> ^(b)	<u>Loss</u> <u>Factor</u> <u>n</u>	Elastic ^(b) <u>Storage</u> <u>Modulus</u> <u>10⁶ psi</u>
Carbon Fiber/Epoxy				
Longitudinal	0.040"	309/#2	0.038	3.4
Transverse	0.040"	321/#3	0.055	0.5
Glass Fiber/Epoxy				
Longitudinal	0.045"	225/#2	0.039	-
Transverse	0.045"	199/#4	0.049	0.04
Natural Rubber	0.020"	246/#5	0.086	0.0012

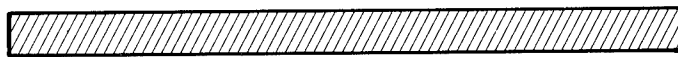
(a) All elastomer ply thicknesses 0.020"

(b) The elastic storage moduli of the constrained layer composite laminates could not be determined with any confidence; the mode numbers did not follow the prescribed mathematical relationships.

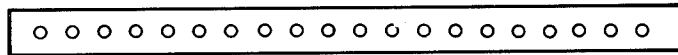
FIGURE 1
ELASTOMER/ADVANCED COMPOSITE
LAMINAR STRUCTURES



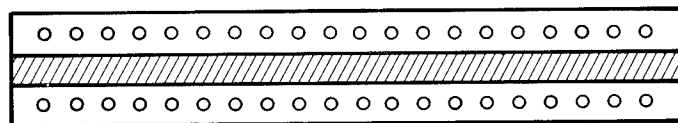
Composite Ply



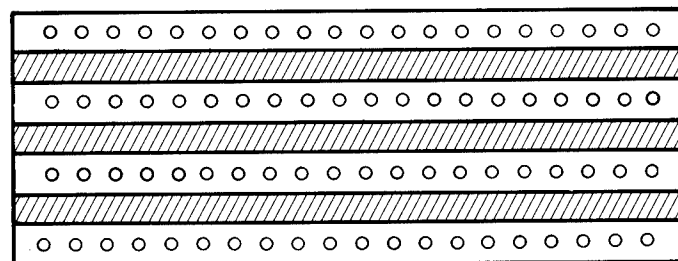
Elastomer



Composite Ply



**Bonded
Laminar
Structure**



**Multiple
Ply
Structure**

FIGURE 2
EFFECT OF COMPOSITE SURFACE PLY
ORIENTATION ON PEEL STRENGTH OF
ARAMID FIBER/EPOXY —
NITRILE RUBBER BONDED JOINT

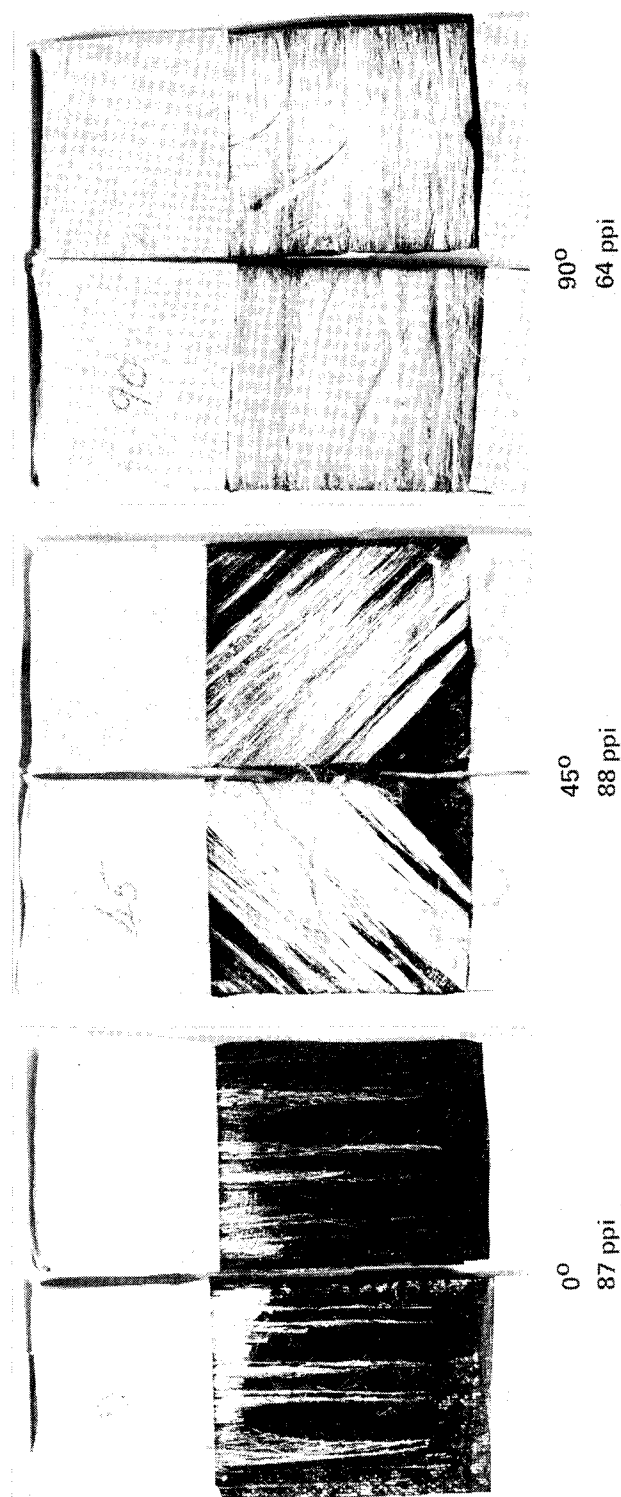
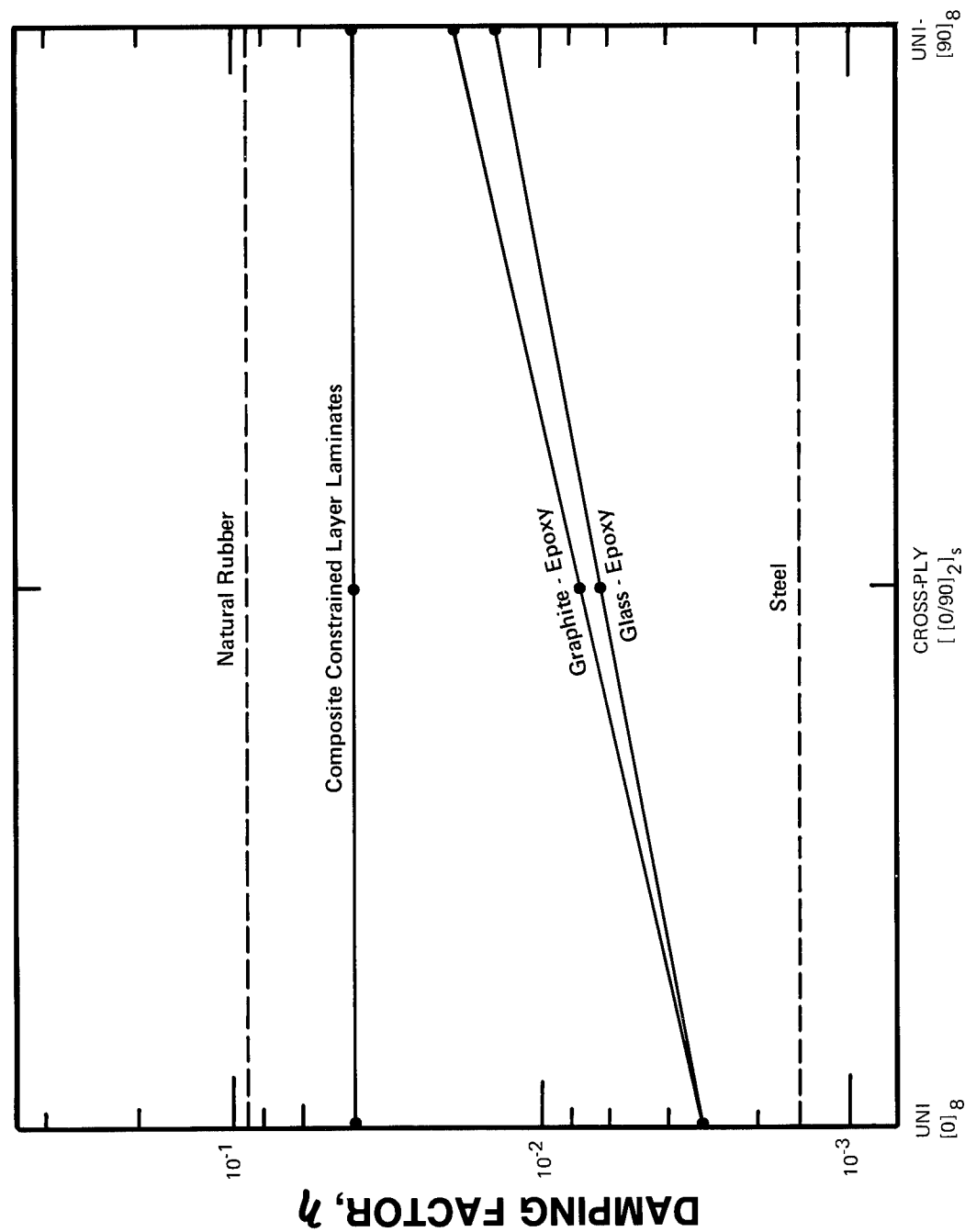


FIGURE 3
COMPARISON OF VIBRATION DAMPING
PROPERTIES OF LAMINAR COMPOSITES



MECHANICAL PROPERTIES OF COMPOSITES

T. J. Reinhart, Jr.
Air Force Materials Laboratory
Wright Patterson Air Force Base
Ohio 45419

No text or illustrations available at the publication deadline.

MOMENTUM WHEELS

Rene Torossian
Aerospatiale
78 Les Mureaux
France

ABSTRACT

The movie shown at the Symposium and the text below describe the Aerospatiale magnetically-suspended flywheels. In their design, five of the six degrees of freedom of the suspended rotor are controlled by permanent magnets and only one is controlled by electromagnets driven by electronic feedback loops. This ensures complete absence of physical contact between rotor and stator. Advantages are: reduced mass, improved performance and higher speeds. Operating at 8000 rpm, the present "breadboard" model develops a reaction torque of 0.1 Nm and a momentum of 50 Nms.

INTRODUCTION

Support bearings have traditionally been points of failure in flywheels running at high speeds. Bearings failed because lubricants failed at the high temperatures associated with excessive friction. Earlier magnetic flywheel suspension systems of the "fully-active" type used multiple electromagnets in comparatively complex systems.

MAGNETICALLY-SUSPENDED MOMENTUM WHEELS

GENERAL

Aerospatiale are currently developing magnetically suspended momentum wheels for both ESA and COMSAT.

The outstanding feature of these wheels is that their rotors are supported without any physical contact to their stators by almost entirely passive means (permanent magnets). Only one out of six degrees of freedom of the suspended part is controlled in an active way to ensure stability. Absence of contact between rotor and stator enhances the reliability of the most critical momentum wheel element, i.e., the bearing, and at the same time improves the functional performance of the wheel. Furthermore, the absence of contact permits high rotational speeds to be developed without incurring problems of bearing fatigue and wear. For the user, the implications of these advantages are:

Reduced Mass. The passive nature of the bearing allows this part to be disregarded

as a single point of failure. This makes it possible to replace two or more conventional wheels, e.g., those which have ball bearings, with one magnetically-suspended wheel, redundancy being implemented in the active parts only.

Improved Performance. The elimination of lubricants drastically reduces the effect of temperature variations on the friction of the bearing and hence ameliorates design and accuracy of the satellite pitch control loop. The elimination of mechanical contact (even at zero speeds) is a property of particular relevance to reaction wheels. Ball bearing reaction wheels are known to be particularly prone to failure as a result of bearing operation in the boundary lubrication regime.

Higher Speeds. The ability to operate at higher speeds without excessive power consumption and without bearing fatigue and wear improves the momentum/mass ratio of the wheel and is of great interest for simultaneous use of the wheel as an energy storage device and actuation element.

Up to now most magnetic suspension systems have been of the fully active type, i.e., those in which five degrees of freedom of a suspended shaft are controlled by electromagnets driven by electronic feedback loops. The electronic and mechanical complexity of such systems is comparatively high. In the Aerospatiale design, all but one of the five controlled degrees of freedom is constrained by permanent magnets. This results in a drastic reduction in the number of electronic and

electromechanical parts associated with the suspension system. The "passive" bearing concept developed by Aerospatiale has only recently become technically feasible, although inherently it is by far the simplest solution.

DESIGN AND CONSTRUCTION

The Aerospatiale magnetic bearing designs are based on radial suspension by high-energy, rare earth permanent magnet segments precision milled in the form of rings. With this arrangement, axial support can no longer be achieved in a purely passive way (Earnshaw's theorem). Control in the axial direction is provided by a servo-driven electromagnet that was specially designed to develop the high forces necessary during "start up" and normal suspended operation of the bearing with minimal power consumption.

A magnetic suspension system may be regarded as a nearly perfect loss-free spring; some means of damping the natural motions of the suspended part is therefore necessary. In the Aerospatiale wheels, radial damping is ensured by eddy current dampers free of moving parts and specially designed for low rotational drag at high spin speeds. Axial damping is achieved electronically.

Wheel drive is provided by a high efficiency, electronically-commutated d.c. motor with no iron in its armature circuit. This avoids the introduction of destabilizing forces which would detract from the performance of the bearing.

The design incorporates a set of "emergency mode" ball bearings which allow for temporary touchdowns and limited operation of the wheel in case of power or suspension system failures.

The whole is enclosed in a lightweight, aluminium housing (non-hermetically sealed). The electronics for the axial servo and motor commutation may be accommodated in the same housing as the wheel or in a separate package, as required.

CHARACTERISTICS

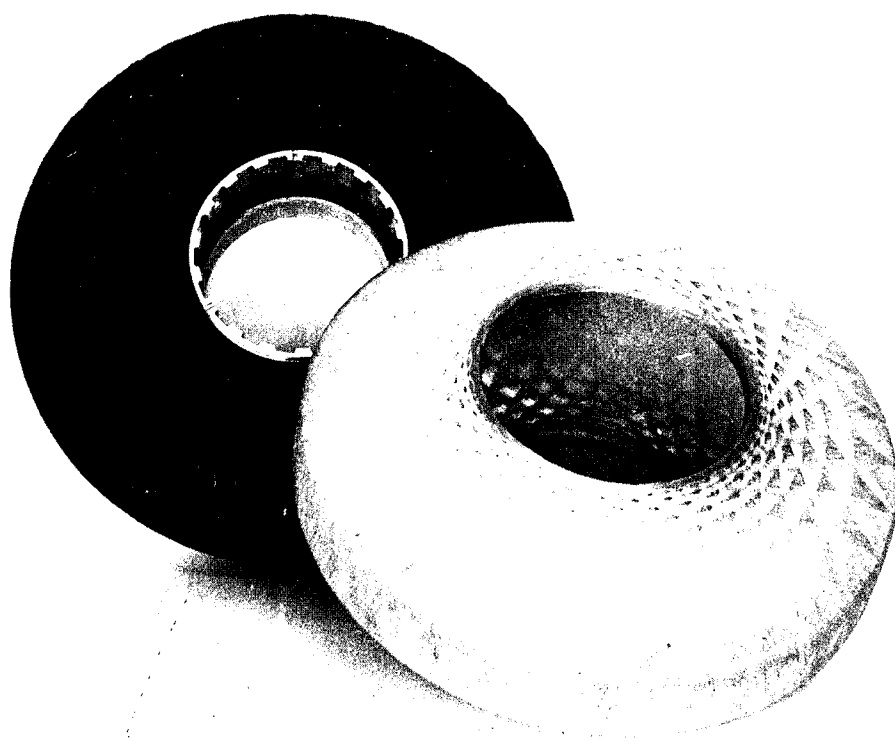
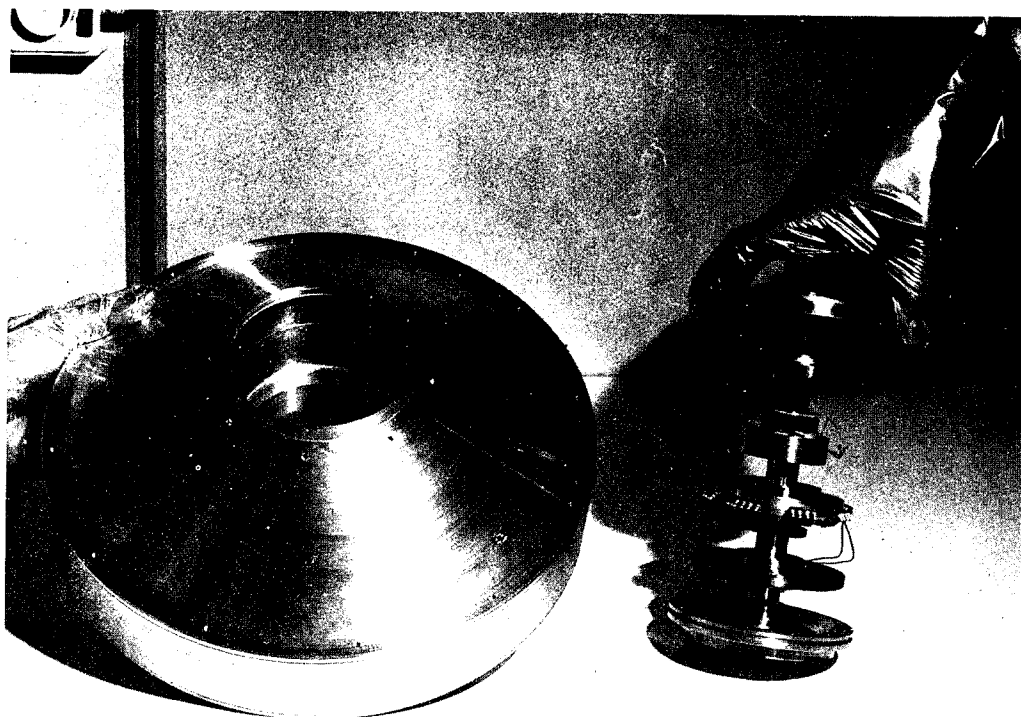
The magnetically-suspended wheel developed by Aerospatiale for ESA has the following characteristics.

Momentum	50 Nms
Speed	8000 rpm
Reaction torque	0.1 Nm
Mass	
- wheel	10.3 kg*
- electronics package	2.5 kg*
Power	
- suspension	4 W*
- rotation	4 W*
Max. slew rate	3.5 degrees/sec*
Dimensions	
- diameter	350 mm
- axial height	220 mm*
Reliability	0.996 for 7 years* (with redundant electronics)

The above parameters are applicable to a "breadboard" model--those marked with an asterisk would be further improved for flight hardware.

For further information:

Mr. P. Poubeau
Aerospatiales/Les Mureaux
P.B. 2
78130 Les Mureaux
France



FIBER GLASS FOR COMPOSITE FLYWHEELS

S. N. Loud
Manager - Office of Aerospace & Defense and
Manager - Electrical/Electronics Division
Owens-Corning Fiberglas Corporation
Fiberglass Tower - 7
Toledo, Ohio 43659

ABSTRACT

The potential performance of fiber glass reinforced plastics in flywheels is discussed in terms of 1) fiber glass characteristics and availability, 2) fiber glass economics and 3) the problem of projecting fiber glass properties to the performance of reinforced composites. Fiber glass properties emphasized are high tensile strength, especially under cryogenic conditions, and good fiber processing during composite fabrication. Problem properties for composites are fatigue resistance and the presence of moisture that may weaken the composite. For design calculations the strength of the composite, suitably derated for working stress and safety factors, appears to be a more reliable guide than virgin fiber strengths. Included are some thoughts about what information is needed in the industry to define a more suitable fiber composite for a flywheel.

INTRODUCTION

Composite materials offer the most cost-effective approach to inertial energy storage systems utilizing flywheels for electrical energy storage in utilities, military applications and transportation. Fiber glass reinforced plastics (FRP) should be considered as one of the most likely material system choices, because of their proved and projected performance capabilities and their low cost potential.

BENEFITS OF FRP

The performance of reinforced plastics is well known for over 30 years, in numerous commercial applications. In the area of inertial energy storage devices, however, there is extremely limited experience on materials performance, especially in flywheel configurations. Most information available is from laboratory materials screening tests.

To build high performance devices, we need more information on composite materials under flywheel operating conditions, specifically, the performance of various resins under dynamic stress, the value of hybrids of various fibers, characterization of the importance of tensile versus modulus versus shear, dynamic fatigue information in vacuum and cold conditions, the influence of manufacturing process,

reliable test methods for highly stressed composites. And, above all, we need regular dialogue among all interested parties to ensure that this information is accumulated in pursuit of this objective.

The following characteristics are the benefits known or believed to be important in the use of FRP composites for flywheels.

Glass fiber availability and historical experience contribute to the belief that FRP means high reliability and confidence in composites for flywheels. The glass fiber producers now sell an estimated 600 - 900 million pounds of fiber annually, and glass fiber has been commercialized since 1939. This kind of experience is worth a lot when you're considering the quantities of material involved in flywheel applications.

Versatility is excellent because of a broad choice of glass fibers ranging from E glass for lowest cost and good performance, to S-2 glass (an Owens-Corning Fiberglas Trademark) for medium-to-high performance at moderate cost, and to S901, the aerospace grade roving offering the highest performance capability in glass to date, but at a premium price.

All three types of glass fiber demonstrate good processability in wet resin filament winding, pultrusion and prepreg

systems. There is a broad manufacturing base of companies, each capable of producing fibers by one or more processes and with years of experience. These processes and fabricators are capable of producing the leading proposed forms of flywheels, the multi-rim and the brush. FRP rims can be produced as separate rings or stage-wound, and rods can be pultruded for the brush configuration.

Resin capabilities are also broad. Epoxy appears to be the leading contender due to its performance and well known processing characteristics for wet winding or prepreg laminating. However, polyester is also versatile and can be used in all processes. Using a chemical treatment, glass fibers are specifically sized for optimum compatibility with each resin specified, a list which might include vinyl ester, polyurethane, polyimide.

Glass fibers offer excellent tensile strength, their dominant benefit for this application area. In addition, shear strength in composites is high (10-13 ksi). Glass fiber modulus is lower than the graphite or aramid fibers being considered, but modulus appears to rate as a much less important benefit than tensile or shear in composite flywheel performance. Glass is the heaviest of the fibers at 2.49 - 2.60 specific gravity. However, specific tensile is still excellent.

Fatigue properties of glass fiber composites are well known in many commercial markets but are not readily available in products with stresses such as those in flywheels. Limited investigation indicates a potential loss in safety factor due to tensile fatigue. Results are few; however, no development has been applied to this unknown area yet to upgrade this performance. Flexural fatigue work has been more extensively pursued. Studies of automotive springs indicate 50% strength retention at 55% of ultimate loading, after more than 500,000 cycles (whether processed into finished springs or test specimens only).

FRP boats over the last 30 years have shown exceptional performance under cold conditions, and so have FRP nuclear reactor cable blocks in cryogenic conditions. FRP material systems become stronger as temperatures are lowered. Ultimate tensile and fatigue strengths of epoxy and polyester composites, whether E, S, or S-2 glass, improve with low temperatures. Plastec, the Plastics Technical Evaluation Center

at Picatinny Arsenal, concluded that "in general, most plastic materials are twice as strong at cryogenic temperatures as at room temperature" and "ultimate tensile strength of glass will increase approximately 40-100% when going from room temperature to -320°F", glass being a super-cooled liquid. This would tend to indicate a major advantage for glass fiber reinforced composites in flywheels operated under cold conditions. Glass has a low coefficient of elongation and high degree of recovery when stress is relieved. This should be good for its use under the cyclical stress of an operating flywheel system.

It is believed that most past derating of FRP composites under high stress at least in part were caused by the presence of moisture in a composite. If used at ambient conditions this may be a factor, requiring development work to improve upon this aspect. But, flywheels should be operated in low atmospheric or high vacuum conditions anyway, to prevent air drag problems and heat build-up, and this optimum condition for operation is also optimum to prevent moisture degradation of the composite.

Another benefit of composite flywheels and especially those made of glass fiber, is safety. Metal flywheels have a tendency to fragment into three large chunks at failure, releasing all their energy in a devastating manner. This necessitates strong and heavy containment vessels for any flywheel considered in metal. The containment vessels for composite flywheels can be much lighter in weight, an important feature in any consideration for transportation markets.

Lastly, a thing to keep in mind is that the materials, the processes to combine them, and the final product configuration must all work in harmony for the final performance to be achieved. Therefore, bench tests may be unreliable in proving current or projected performance, and the only true materials test (screening of long term performance/reliability) will be in a high speed rotating device of similar configuration to the final part objective, fabricated by the processes to be ultimately used.

PROJECTED PERFORMANCE CAPABILITIES

Too many people are touting and relying upon virgin fiber properties for their calculations and test objectives.

Ultimate properties of fibers are useful for comparative purposes on the percentage of ultimate retained for working stress. For practical reasons the composite strength values should be used instead, and these in turn derated for working stress or safety factor calculations. Otherwise composite values and flywheel performance capabilities are grossly overstated. (The same applies to metals - actual part experience should be used, rather than test bars reflecting ultimate properties). The following Table I indicates the well known virgin properties:

TABLE I

VIRGIN FILAMENT TENSILE STRENGTH

<u>FIBER</u>	<u>PSI</u>
E glass	550,000
S/S-2 glass	700,000
Graphite (Carbon)	400,000
Aramid	525,000

J. A. Rolston of the Owens-Corning Fiberglas Technical Center has made a start toward a summary of more practical performance numbers to use. We welcome all comment and any correction or adjustments seen needed, as our numbers (like most others) are based on some assumptions. However, the glass fiber composite numbers are based on a considerable amount of past FRP experience and numerous market sources.

The following Table II is based on a summary of unidirectional composite data available. We have assumed reasonably conservative values for composite strengths achievable with today's materials and processes. The ultimate virgin filament strengths have been derated, based on the "bundle theory" of Jim Hood (formerly with OCF), which showed that in E glass an achievable maximum breaking strength of approximately 360 - 400 ksi, where the average virgin fiber strength was 20% higher. These have then been further reduced to composite strengths as shown in the first column.

The achievable working stress will be somewhat less than these numbers, depending on actual test experience in the future and safety factors desired. We believe that 75 - 80% of these composite ultimates should be a feasible starting point.

From this point we must then determine the numbers which are achievable under dynamic stress and in a vacuum and cold conditions.

The most important conclusion outlined by Table II is that E glass and S-2 glass potentially offer the best watt-hour storage per pound capability of composites. The main point is that the Table II numbers should be a good reference point. Again, comment is welcomed. We would like to continually optimize this information.

ECONOMICS

Glass fiber should be most economical in the short and long term, as it is based mainly on plentifully available domestic materials, not petroleum derivatives. This, combined with the above performance, makes glass fiber potentially the most cost/effective choice of materials.

At the present time E glass roving is sold in the millions of pounds commercially at 45 - 49¢ per pound (as of October 1975) and E glass Type 30 (OCF trademark) is sold in quantity at 41¢ per pound. (Both products sell for less than 1962 prices.) These products are without doubt the most economical fibers to choose for stationary flywheel applications. If history is any indicator, then E glass can be expected to increase in price, with inflation, but at a lesser rate than inflation and the other basic materials.

S-2 glass roving (OCF trademark) is currently priced at \$2.04 - \$2.33 per pound (as of October 1975). This is the most economical fiber now for the higher performance applications requiring a moving flywheel for transportation, aerospace and military. Since S-2 is produced in limited quantities the economies of scale have not yet been achieved. Our cost studies for S-2 projected into the millions of pounds indicate the possibility of roughly halving the current prices (in 1975 constant dollars).

S901, the OCF aerospace grade roving, currently sells for close to \$8 per pound and is proposed for only the highest performance application where the best available glass fiber (shear strength) is desired. Volume in the millions of pounds would most likely result in a significantly lower price here, too (in 1975 constant dollars).

TABLE II

MATERIAL	COMPOSITE OR METAL MAXIMUM TENSILE STRENGTH, PSI	APPROX. COST, \$/LB.	COMPOSITE OR METAL DENSITY, ³ LBS./IN.	APPROX. COST, \$/1000 PSI	APPROX. STORAGE WATT-HRS/LB.	STATIONARY FLYWHEEL MATERIALS COST, \$/WATT HR.	MOVING FLYWHEEL RELATIVE MATERIALS COST
Composite E-glass (Epoxy) ¹							
Rm. Temp.	250,000	1.00	0.078	0.031	53	.019	1.0
-40°F	370,000	1.00	0.078	0.021	78	.013	0.68
-154°F	387,000	1.00	0.078	0.020	81	.012	0.63
-374°F	410,000	1.00	0.078	0.019	87	.011	0.58
Carbon Fiber Composite ²							
	200,000	30.00	0.059	0.89	52	0.58	23.1
S-2/S-glass Composite ³							
	350,000	1.85	0.077	0.041	70	0.026	1.3
Kevlar Composite ⁴							
	220,000	6.60	0.051	0.15	66	0.10	3.4
Aluminum Alloy ⁵	80,000	2.50	0.100	0.31	26	0.08	6.4
Maraging Steel ⁶	400,000	5.00	0.289	0.36	44	0.11	22.5

ASSUMPTIONS:

- 1 - E-glass at \$0.40 per lb. fiber cost, with \$0.60 per lb. fabrication cost (mass-produced simple shape with epoxy resin).
- 2 - Carbon Fiber at \$20 per lb. fiber cost, with same fabrication cost as E-glass. Rough estimate pricing at high volume.
- 3 - S-2 glass at \$1.25 per lb. fiber cost, with same fabrication cost as E-glass. Rough estimate pricing at high volume.
- 4 - Kevlar at \$6.00 per lb. fiber cost, with same fabrication cost as E-glass. Rough estimate pricing at high volume.
- 5 - Cost estimate from Air Force Materials Lab. Fabricated cost.
- 6 - Rolston cost estimate (verified elsewhere). Fabricated cost.

Storage - Peak storage capability at failure--no derating factors shown.

J.A. Rolston
S.N. Loud 11/1/75

FLYWHEEL SYSTEM OBJECTIVES

We are told that one of the great unanswered questions is which materials system will work in flywheels. The target for these materials is a practical and usable 25 - 50 watt-hour per pound flywheel system capability. Such a system would make the electric car feasible. We think that glass fiber should be continually considered by all as one of the best choices available in achieving this objective.

PLANS

We at OCF plan to continue materials development in current and new fibers. We also will probably study several resin systems, since we are one of the largest producers of polyesters. In the past we have fabricated prototype composites where we saw that we could make a contribution. For materials screening purposes we are studying the possibility of a spin testing capability to test composites to ultimate, to aid in finding better fibers, resins and processes. Owens-Corning Fiberglas has the experience over 36 years and hundreds of millions of pounds of glass fiber production experience to have the know-how and interest to work in support of these programs.

WHAT'S NEEDED:

A. Don't discount any of the various fiber alternatives (including graphite and aramid) too early in the game. Too little is known about performance of the materials systems under flywheel operating conditions.

B. Test various resin systems - Epoxies have an excellent history, but perhaps resins developed or selected for dynamic composite stress will be better. (This proved critical in FRP pressure pipe.)

C. Determine whether hybrids of various fibers have a place.

D. Quantify the importance of cost-effectiveness of tensile versus modulus versus shear versus even impact. Thoroughly characterize and prioritize the actual needs for composite performance.

E. Test all composites under high stress and dynamic fatigue, plus in vacuum and cold conditions.

F. Develop reliable test methods to stress composites under high speed rotating conditions to aid in screening new development materials and find methods which can be standardized for use by many suppliers.

G. Study composites produced by several processes - filament wound (wet), prepreg tape wound, pultruded strand (wound rim or brush).

H. Gather and disseminate information regularly to interested parties through forums such as this symposium or through newsletters. Keep the information flowing to all of the materials companies so that they can develop the programs needed to pursue the identified areas of missing information.

FINAL COMMENT

Remember that when you need help in glass fiber, that Owens-Corning is Fiberglass.

References

1. Plastec - Plastics Technical Evaluation Center - Picatinny Arsenal, Dover, New Jersey.
2. Properties - Materials Engineering - Selector '76 - 9/75.
3. Chiao, T. T. et al, "Stress-Rupture of Simple S-Glass/Epoxy Composites," Journal of Composite Materials, July, 1972, pp. 358-370.
4. Otto, W. H. "The Effects of Moisture on the Strength of Glass Fibers - A Literature Review," NTIS-AD 629370, June 1965.
5. Lindsay, E. M. and Hood, J. C., "Final Report on Glass Reinforcements for Filament Wound Composites," Air Force Systems Command, AFML-TR-64-8-104, December 1963.
6. Post, R. F., "Multi-Ring Fiber Composite Flywheels for Large-Scale Energy Storage," from paper presented in October 1974 in Germany.

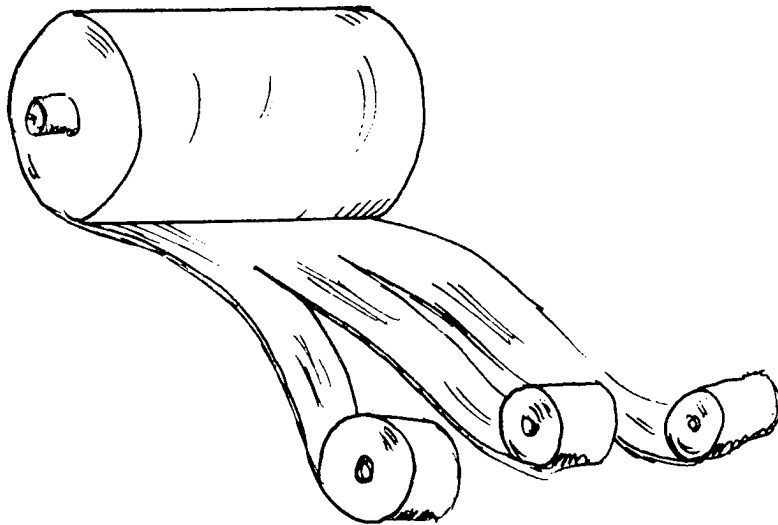
"SCOTCHPLY" PREPREGS FOR FLYWHEEL APPLICATIONS

J. B. Snell and J. N. Schurb
3M Company
3M Center, Building 230-IF
St. Paul, Minnesota 55101

ABSTRACT

"Scotchply" prepreg is a ready-to-mold combination of epoxy resin, latent curing agent and continuous reinforcing fibers in a convenient roll form. It is available with glass, graphite, boron or Kevlar reinforcement and can be purchased in unidirectional, cross ply or isotropic (0° , $\pm 60^\circ$) orientations. It has particular advantages in large volume applications where fabrication speed and controlled quality is of importance. The accompanying tables show the properties of three glass-reinforced prepregs and the mechanical properties of cured laminates molded from these prepregs. Tensile properties of the resin matrix materials are also shown. Some advanced composite prepregs are described. Transverse tensile properties of experimental glass-reinforced laminates were correlated with resin matrix properties, in regard to potential flywheel applications. Transverse modulus of the laminates was much more dependent on fiber volume than on modulus of the resin matrix.

FIGURE I
"SCOTCHPLY" PREPREG



WHAT A PREPREG IS :

- * READY-TO-MOLD COMBINATION OF LATENT EPOXY RESIN SYSTEM AND CONTINUOUS REINFORCING FIBERS IN A CONVENIENT ROLL FORM.

ADVANTAGES OF SCOTCHPLY PREPREG :

- * AVOIDS MESSY "WET" LAYUP AND WINDING OPERATIONS.
- * TAKES RESIN FORMULATION OUT OF PRODUCTION.
- * PROVIDES LOW TOXICITY RESINS.
- * AVAILABLE IN UNIDIRECTIONAL AND ANGLE PLY ORIENTATIONS .
- * CAN BE TAPE WOUND OR SHEET LAMINATED.
- * CONSISTENT AND REPRODUCIBLE QUALITY .
- * PRE-ENGINEERED BY MATERIAL EXPERTS .

"SCOTCHPLY" GLASS REINFORCED PREPREGS

<u>TYPE</u>	<u>RESIN CONTENT</u>	<u>FIBER VOLUME</u>	<u>CURING TEMPERATURE</u>	<u>APPLICATIONS</u>
1002	36%	45.6 %	330 ⁰ F.	HELICOPTER BLADES ELECTRICAL MACHINERY SPRINGS INSULATED RAILJOINTS
1009-26	26 %	57.3 %	325 ⁰ F.	MILITARY AND ELECTRICAL HIGH FIBER VOLUME APPLICATIONS
S P 250	36 %	45.6 %	250 ⁰ F.	HELICOPTER BLADES ELECTRICAL MACHINERY SPORTING GOODS

"SCOTCHPLY" GLASS REINFORCED LAMINATE
MECHANICAL PROPERTIES

<u>TYPE</u>	<u>0⁰ TENSILE STRENGTH</u>	<u>MODULUS OF ELASTICITY</u>	<u>ULTIMATE ELONG.</u>	<u>COMPRESSION STRENGTH</u>	<u>FLEX. STR.</u>	<u>FLEX. MOD.</u>	<u>BEAM SHEAR STR.</u>	<u>SPECIFIC GRAVITY</u>	<u>FIBER VOLUME</u>
1002	150,000	5.7 x 10 ⁶	2.6 %	90,000	165,000	5.3 x 10 ⁶	8.9 (8/1)	1.8	50 %
1009-26	185,000	7.4 x 10 ⁶	2.5 %	90,000	200,000	7.0 x 10 ⁶	8.5 (8/1)	2.0	65 %
SP-250	150,000	5.7 x 10 ⁶	2.6 %	90,000	165,000	5.3 x 10 ⁶	9.450 (8/1)	1.8	50 %

RESIN CASTINGS

<u>RESIN</u>	<u>TENSILE STRENGTH</u>	<u>TENSILE MODULUS</u>	<u>ELONGATION</u>
1002	10,500	422,000	2.8 %
1009-26	8,640	427,000	2.3 %
SP 250	5,600	570,000	1.1 %

"SCOTCHPLY" ADVANCED COMPOSITE PREPREGS

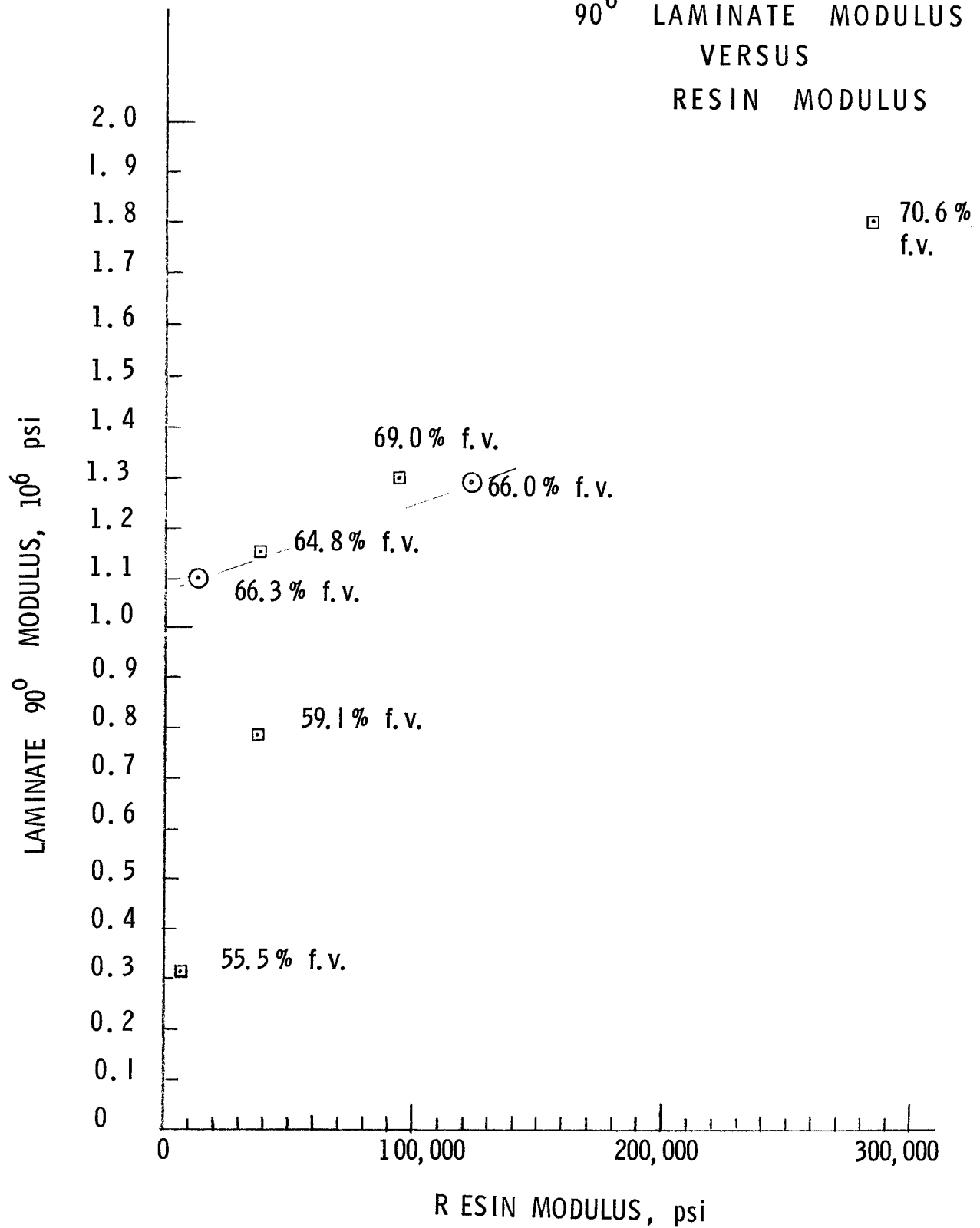
<u>NO.</u>	<u>RE INFORCEMENT</u>	<u>RESIN</u>	<u>CURE TEMP.</u>	<u>APPLICATIONS</u>
SP 290	BORON	PR 287	350 ⁰ F.	F-14 HORIZONTAL STABILIZER
SP 296	BORON	PR 286	350 ⁰ F.	F-15 HORIZONTAL STABILIZER
SP 288	GRAPHITE	PR 288	275 ⁰ F.	FAN BLADES, AIR FRAME STRUCTURES, SPORTING GOODS
SP 313	GRAPHITE	PR 313	350 ⁰ F.	AIR FRAME STRUCTURES
SP 308	KEVLAR	PR 288	275 ⁰ F.	SPORTING GOODS

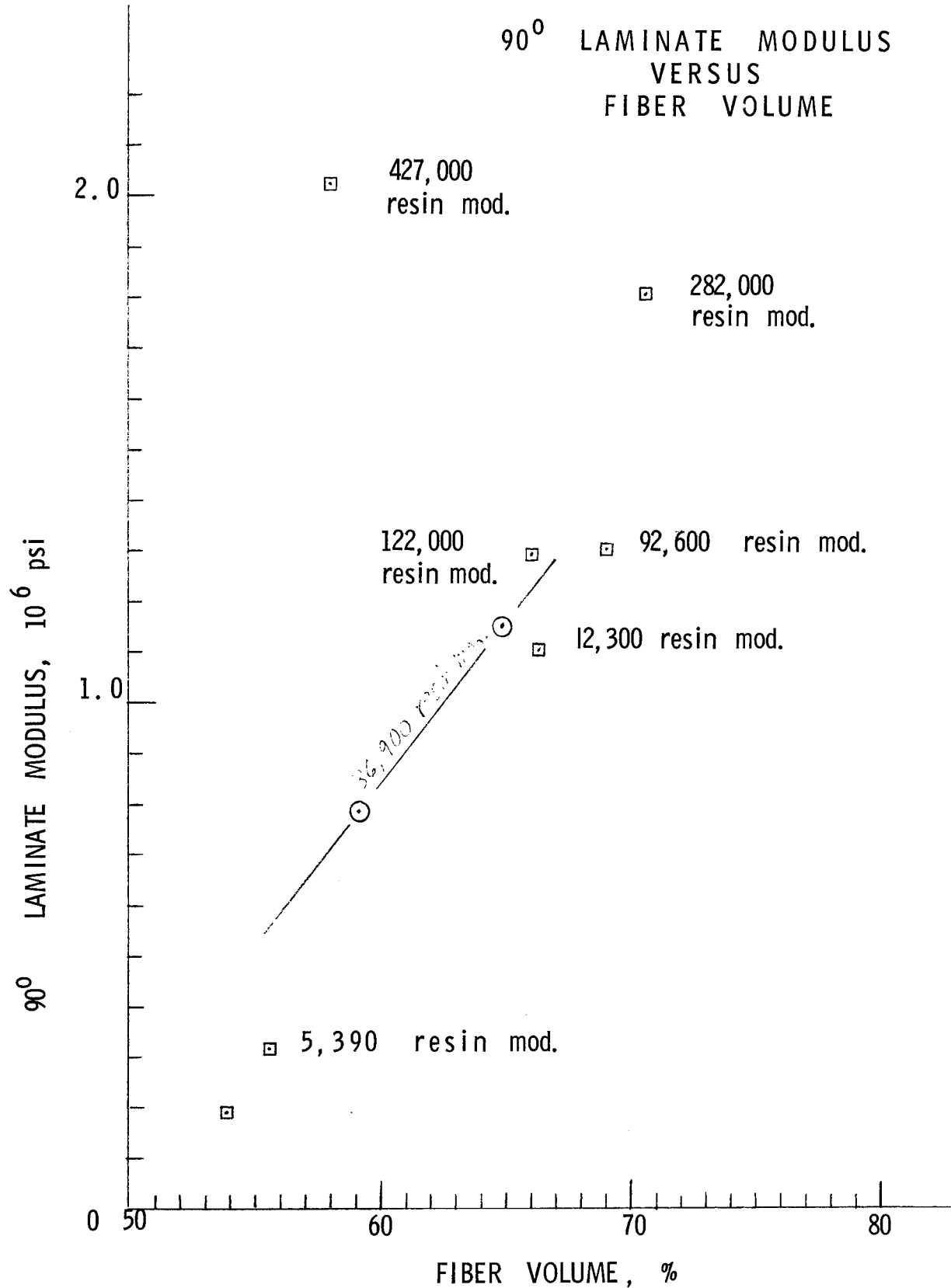
RESIN CASTING AND LAMINATE 90° PROPERTIES

NO.	RESIN CASTINGS		90° UNIDIRECTIONAL GLASS REINFORCED LAMINATES			
	TENSILE STRENGTH	TENSILE MODULUS	FIBER VOLUME	TENSILE STRENGTH	TENSILE MODULUS	ULTIMATE ELONGATION
1009-26	8,640	427,000	58.1 %	4,390	2.02×10^6	2.5 %
2	4,380	92,600	69.0 %	5,290	1.3×10^6	--
4	3,240	36,900	64.8 %	4,930	1.15×10^6	--
			59.1 %	4,090	0.786×10^6	--
5	2,980	122,000	66.0 %	4,640	1.29×10^6	--
6	6,980	282,000	70.6 %	5,170	1.8×10^6	--
7	2,590	12,300	66.3 %	4,340	1.1×10^6	--
8	1,850	5,390	55.5 %	2,410	0.314×10^6	3.4 %
9	---	---	53.8 %	1,770	0.190×10^6	3.3 %

NOTES : (1) "E" GLASS USED IN 1009-26, 2, and 6. "S" GLASS USED IN ALL OTHERS.
(2) MODULUS QUOTED FOR CASTINGS IS SECANT MODULUS, EXCEPT FOR 1009-26.

90° LAMINATE MODULUS VERSUS RESIN MODULUS





POTENTIAL ADVANTAGES OF KEVLAR^R 49 IN FLYWHEEL APPLICATIONS

D. L. G. Sturgeon
Textile Fibers Department, Building 262
E. I. du Pont de Nemours and Company
Wilmington, Delaware 19898

ABSTRACT

Various physical properties of Kevlar^R yarns and Kevlar^R composites that are important to flywheel applications are presented graphically. Properties exhibited are tensile, compressive and impact strengths; tensile modulus and tensile strength as functions of temperature; stress concentration; failure stress and fracture toughness as functions of notch length; and failure in tension at constant load.

INTRODUCTION

The purpose of this presentation is to review the properties of Kevlar^R 49 aramid fiber that make it useful as a rotor material for advanced flywheels.

KEVLAR 49 PROPERTIES

Table I lists the properties of Kevlar 49, beginning with those most familiar to this audience: its high tensile strength, its low density and its potentially low cost.

This high performance aramid fiber has several properties that add to its value in flywheel applications. Kevlar 49 retains the processability normally associated with more conventional textiles. It has good impact strength, and it is the material of choice in high performance ballistic applications. Its fracture toughness is higher than for glass and graphite fiber-reinforced resins. Its combination of low creep and excellent creep rupture characteristics are important when one considers that many high performance flywheel designs require reinforcing fibers to operate at high percentages of their ultimate tensile strength. The excellent fatigue performance of these composites is also noted.

Figure 1 contrasts the almost linear stress-strain curves of Kevlar^R 29 and Kevlar^R 49 with the yielding behavior of conventional nylon and polyester yarns. The tensile stress-strain curve of galvanized improved plow steel wire is shown for comparison. It is evident that Kevlar^R

is more like wire than conventional textiles in its stress-strain behavior.

Figure 2 displays the specific tensile strength and tensile modulus of Kevlar^R 29 and Kevlar^R 49 fibers measured according to the ASTM D2343-67 strand method compared to other reinforcing fibers. The high strength (525×10^3 psi) and low density (1.45 g/cc) result in these fibers having the highest specific tensile strength of commercially available materials. Their specific tensile modulus, however, is intermediate between those of glass and the graphite fibers. This very high specific strength makes Kevlar^R 49/epoxy filament wound composites the materials of choice in high performance, internally-pressurized vessels.

Because high performance aramid fibers are not ceramic, their strength and modulus decrease with temperature, as shown in Figures 3 and 4. However, they outperform heretofore available organic fibers. The effect of prolonged heating of Kevlar^R on its retained tensile strength at room temperature suggests that 160°C should be the maximum long-term in-service temperature (Figure 5). This temperature capability is in excess of that anticipated for most flywheel applications.

The ability of lightweight Kevlar^R 49 fabrics, felts and composites to absorb large amounts of energy is displayed in Figure 6. Data by J. H. Gerstle of Boeing Commercial Aircraft Co., Seattle, Washington, shows the effectiveness of Kevlar^R in defeating high energy fragment

particles that simulate an engine burst condition. The effectiveness of Kevlar^R 49 as lightweight armor around high performance flywheels is obvious. The fracture toughness of Kevlar^R compared to E-glass in both tape and fabric form are shown in Figures 7, 8, 9 and 10. The relative ability of different composite materials to withstand holes, cut-outs, and cracks will become an increasingly important design consideration as the technology of flywheels advances. The advantage of high performance aramid fibers is expected to be substantial.

The stress rupture characteristics of unidirectional fiber-reinforced composites will undoubtedly influence the relative merits of competing fiber-reinforced materials. To the extent that high performance flywheels are expected to operate at high fractions of their ultimate tensile strength, stress rupture properties, rather than instantaneous ultimate tensile strength, may become the guiding criteria for selection (Figure 11). In this regard, careful work on the stress rupture of glass fiber and Kevlar^R 49 has been done by T. T. Chiao (Ref. 1). Comparatively less information exists on the creep rupture behavior of Kevlar^R 29.

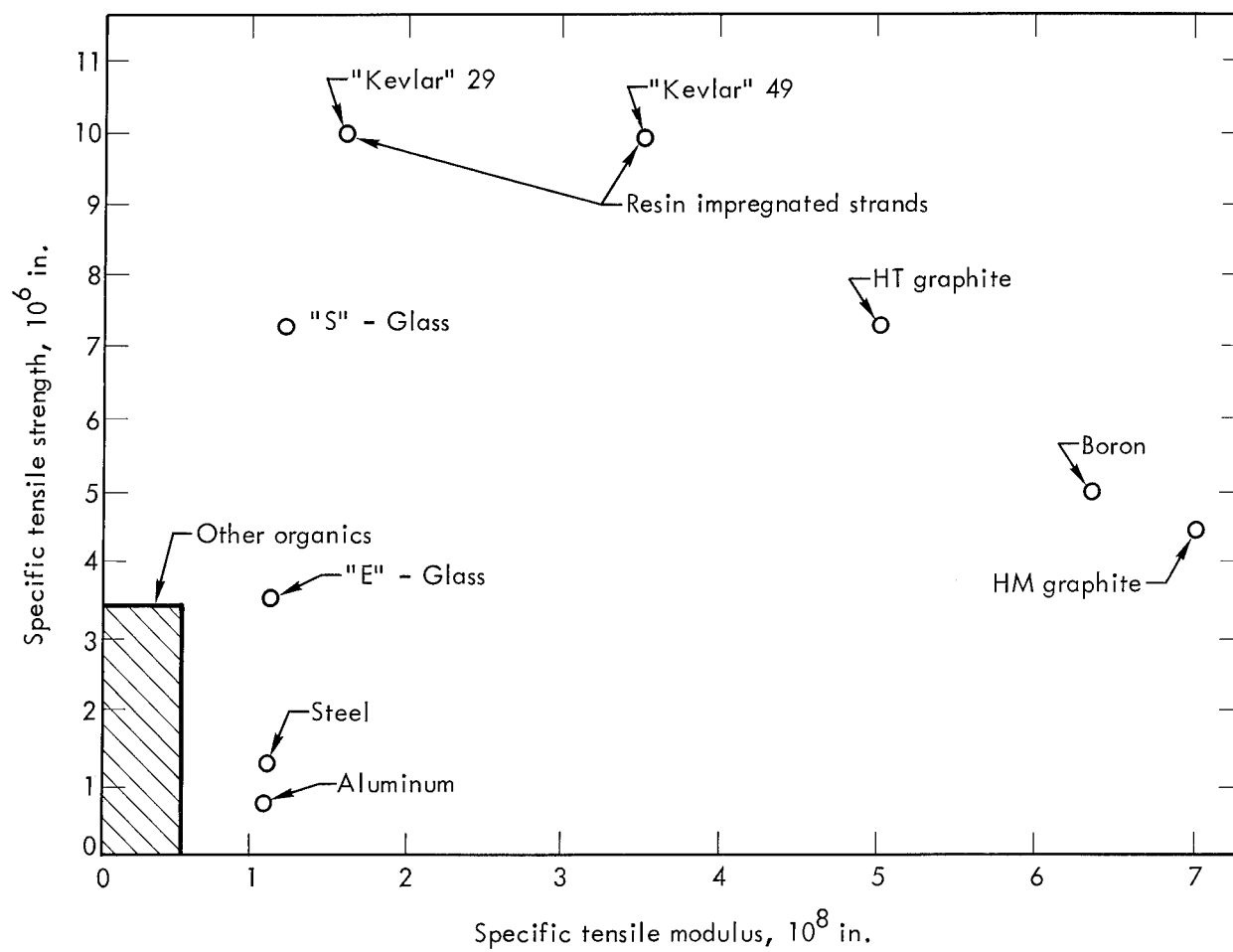
The final two charts show the fatigue performance of both Kevlar^R 49 composites (Figures 12) and Kevlar^R 49 yarns and strands (Figure 13), compared to the other materials. Advantages for Kevlar^R over S-glass and improved plow steel are indicated.

CONCLUSIONS

Kevlar^R 49 aramid fiber provides high specific strength, as well as a combination of properties (e.g., textile processability, impact strength, fracture toughness, good creep rupture and excellent fatigue) that make it a leading contender as a reinforcement for high performance flywheels. This set of properties, combined with attractive economics, suggests profitable further development work with Kevlar^R 49 composites in the area of flywheels as energy storage devices for transportation vehicles.

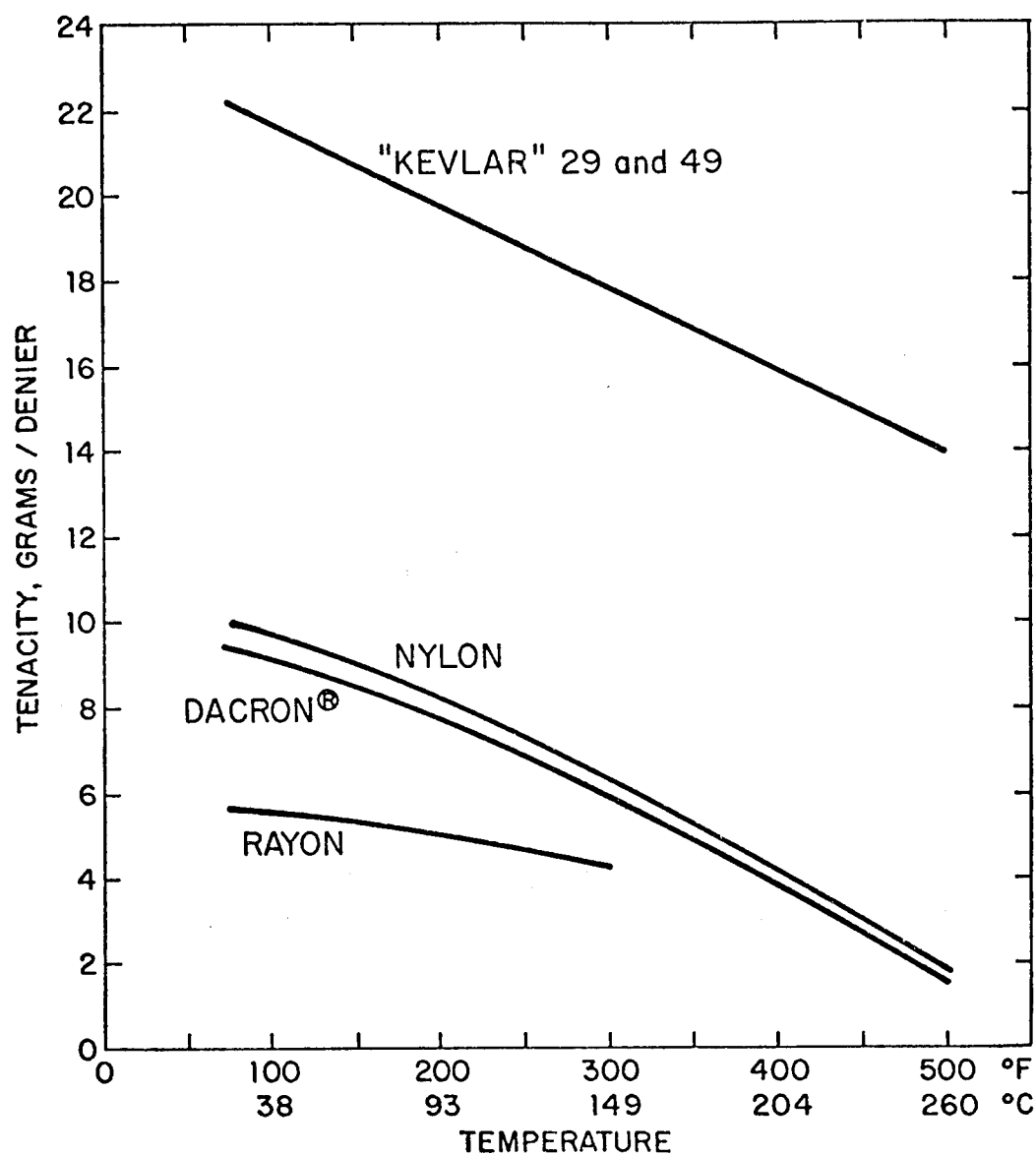
Reference

1. Chiao, T. T., "Filament-Wound Kevlar^R 49/Epoxy Pressure Vessels," November 9, 1973, Lawrence Livermore Laboratory, Report No. NASA CR-134506, UCRL-51466.



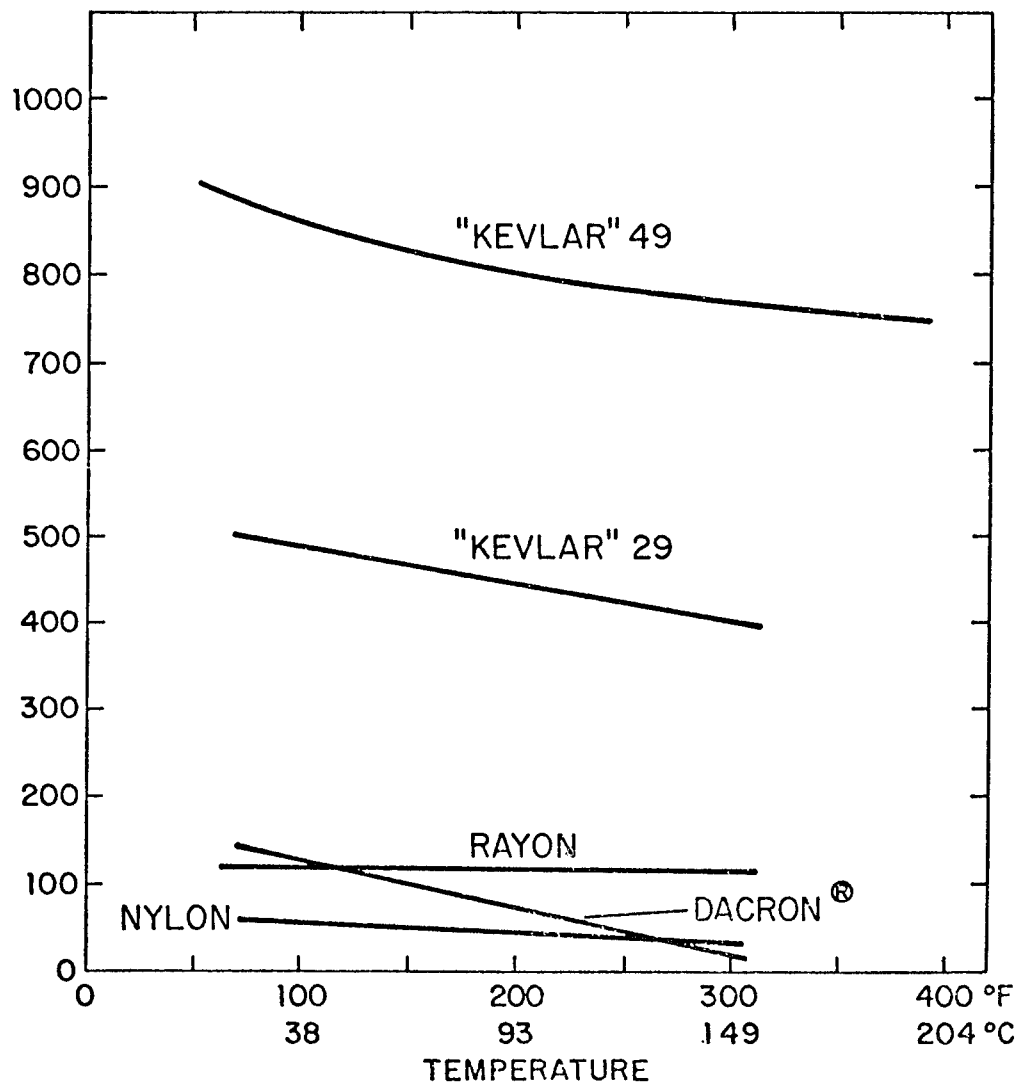
EFFECT OF TEMPERATURE ON YARN TENSILE STRENGTH

TESTED AT TEMPERATURE AFTER 5 MINUTE EXPOSURE IN AIR

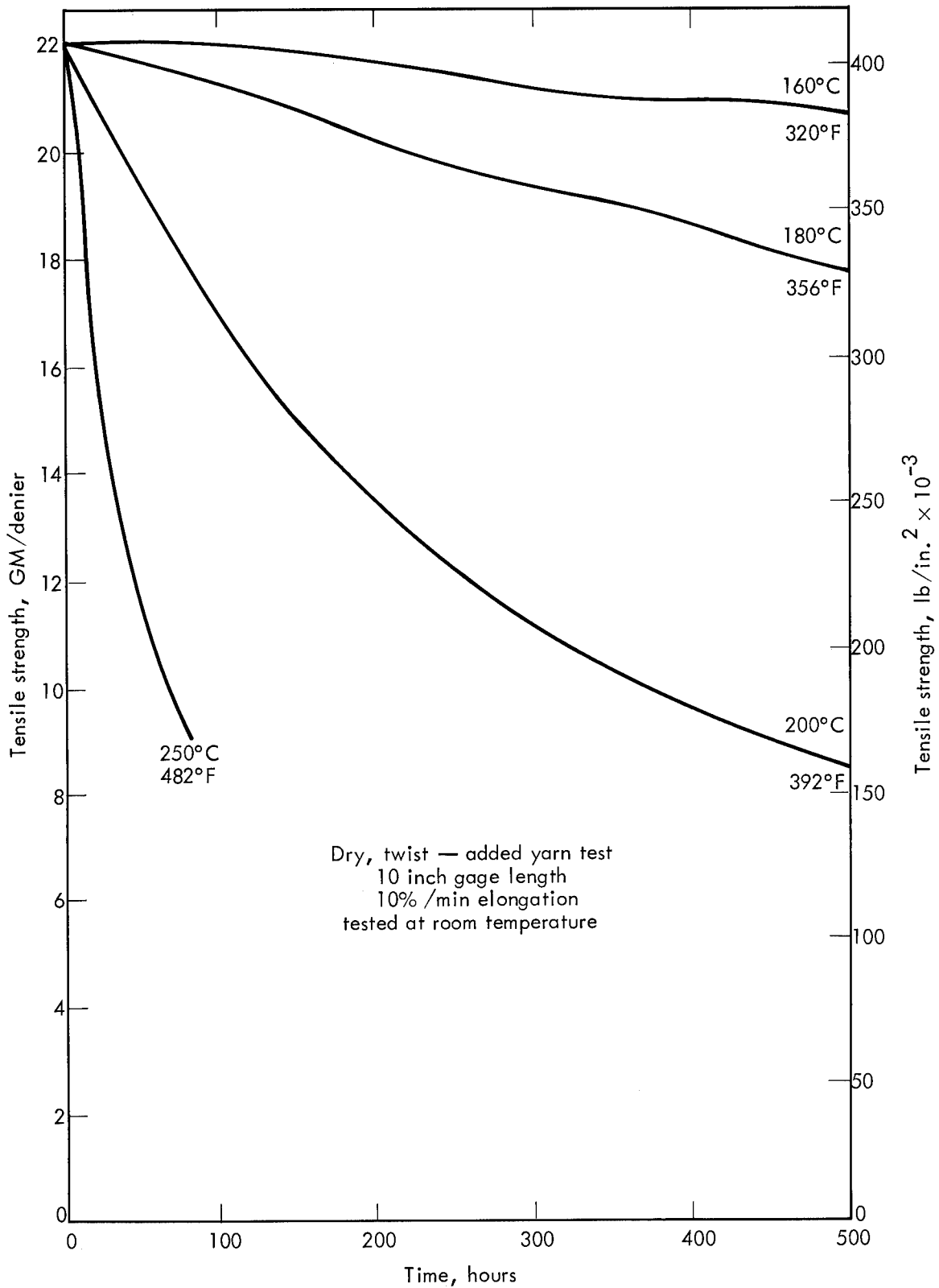


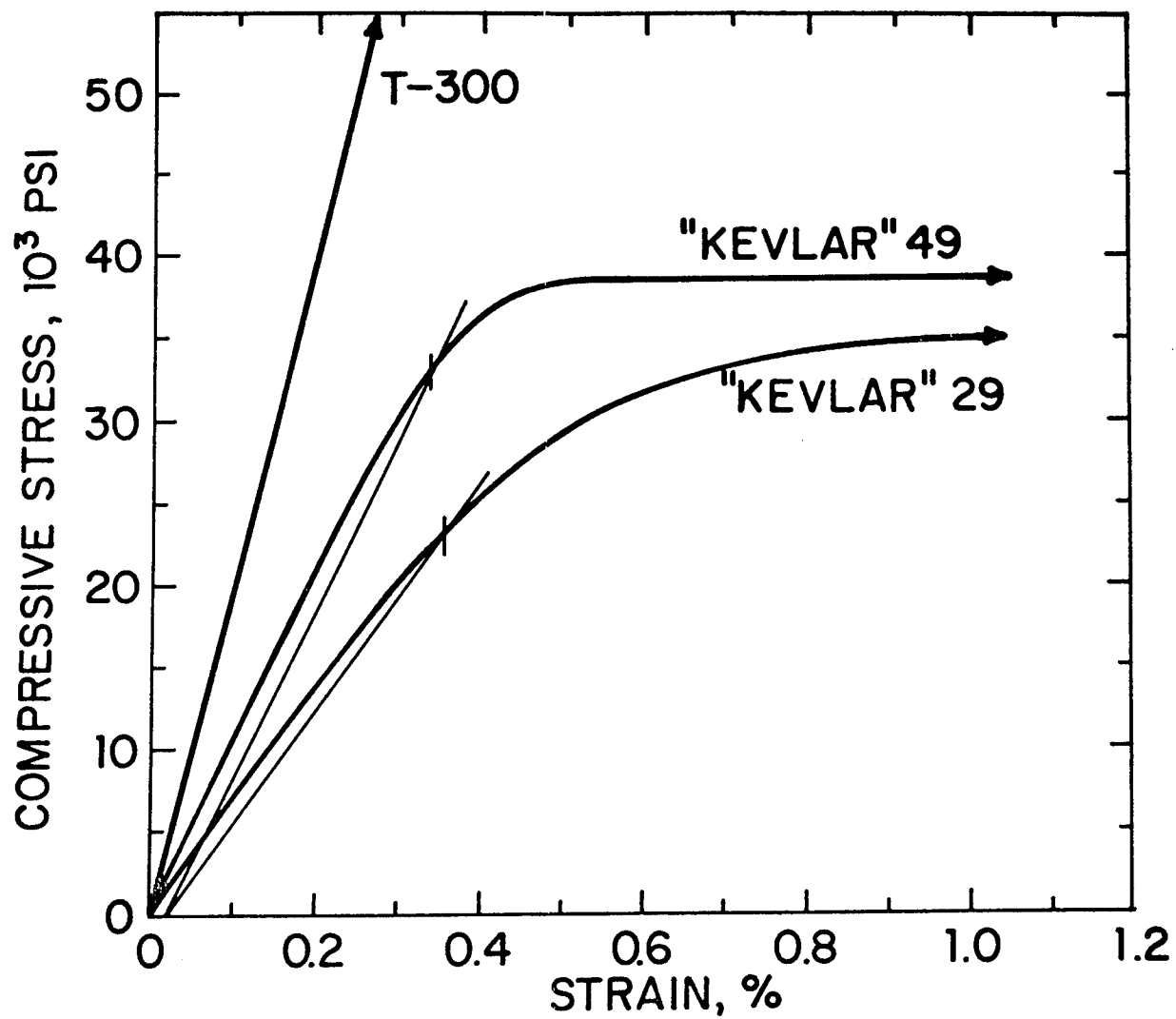
EFFECT OF TEMPERATURE ON YARN TENSILE MODULUS

TESTED AT TEMPERATURE AFTER 5 MINUTE EXPOSURE IN AIR

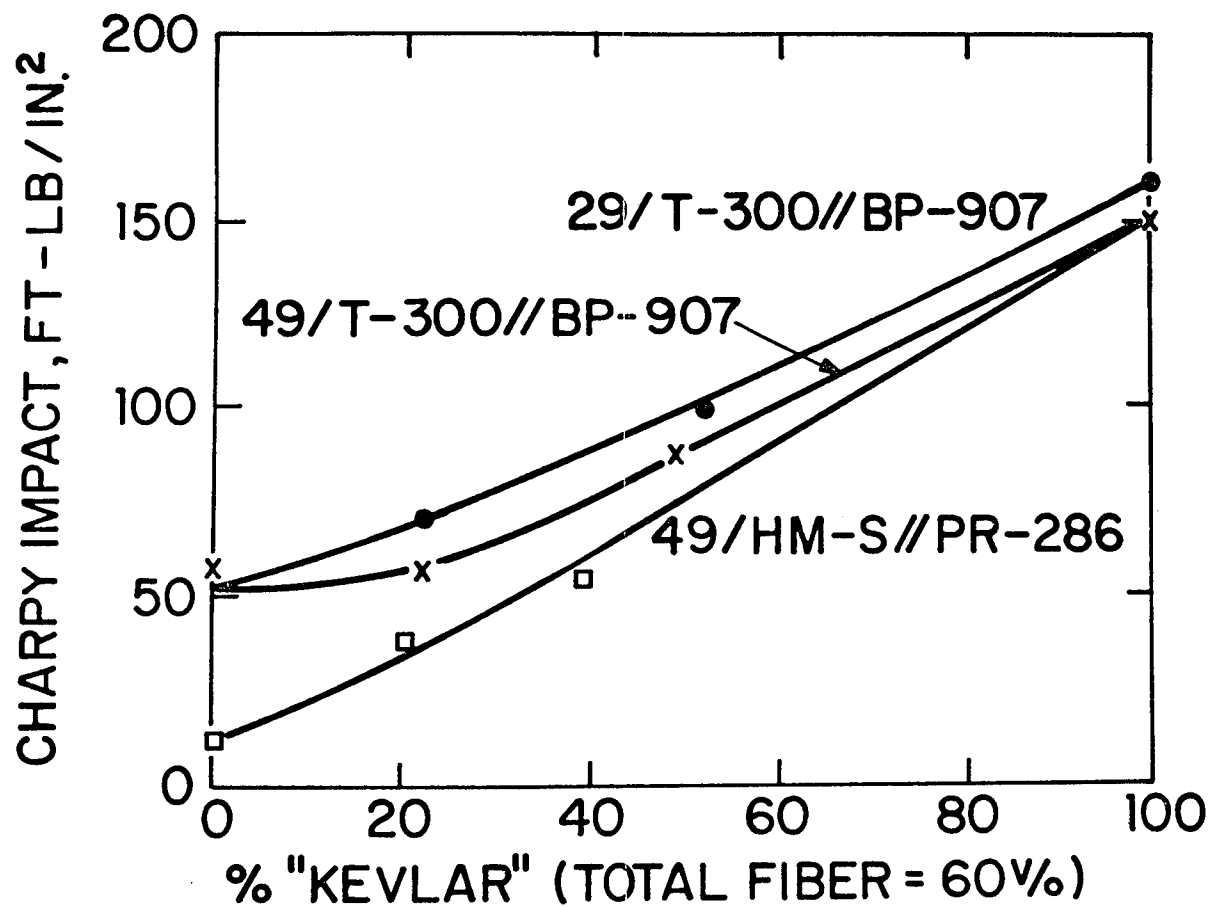


The effect of temperature on
the tensile strength of "Kevlar" 29

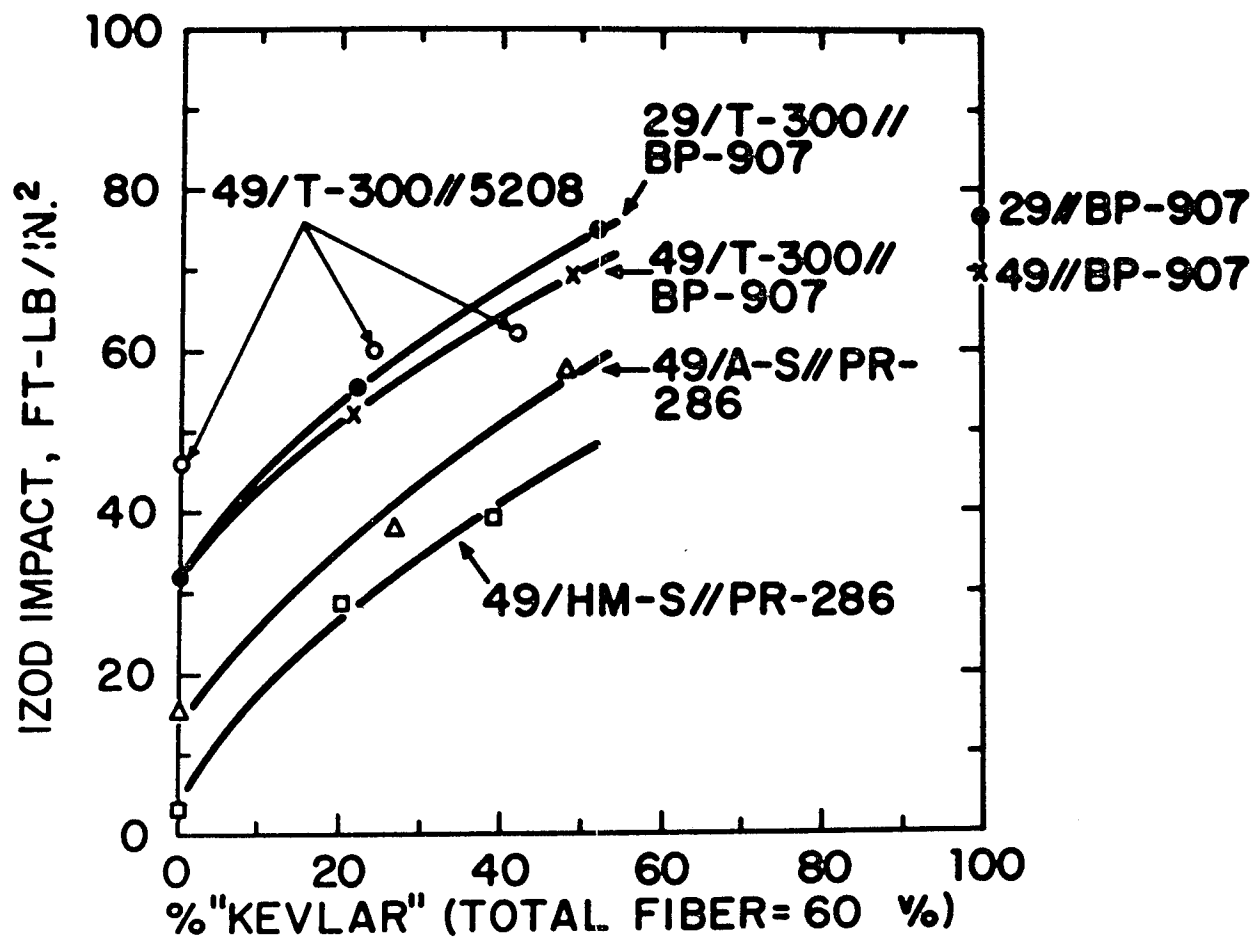




COMPRESSIVE STRESS-STRAIN CURVES FOR
UNIDIRECTIONAL 60 V/O KEVLAR® 29, KEVLAR® 49,
AND "THORNEL" 300 GRAPHITE COMPOSITES



CHARPY IMPACT STRENGTH OF UNIDIRECTIONAL
KEVLAR® 29 AND KEVLAR® 49 HYBRID COMPOSITES



IZOD IMPACT STRENGTH OF UNIDIRECTIONAL
KEVLAR® 29 AND KEVLAR® 49 COMPOSITES

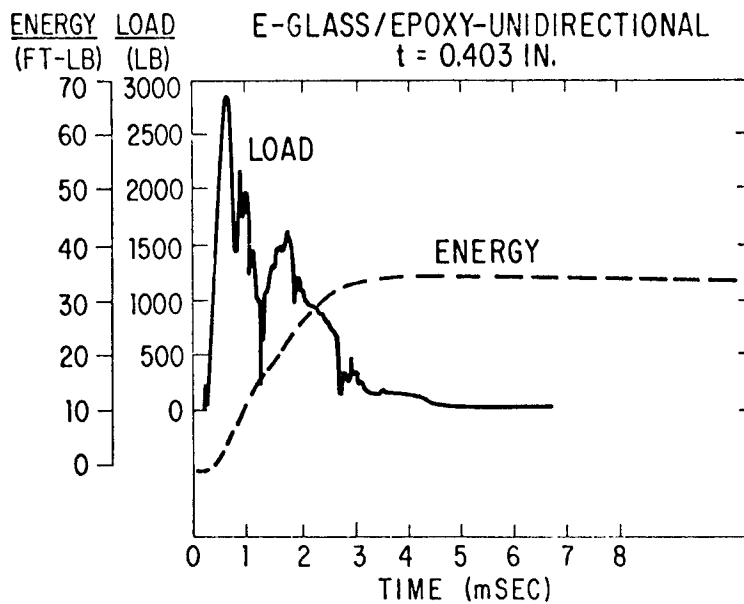


Fig. 8 - Load history of Charpy Impact Test E-Glass/Epoxy Unidirectional $t = 0.403$ in

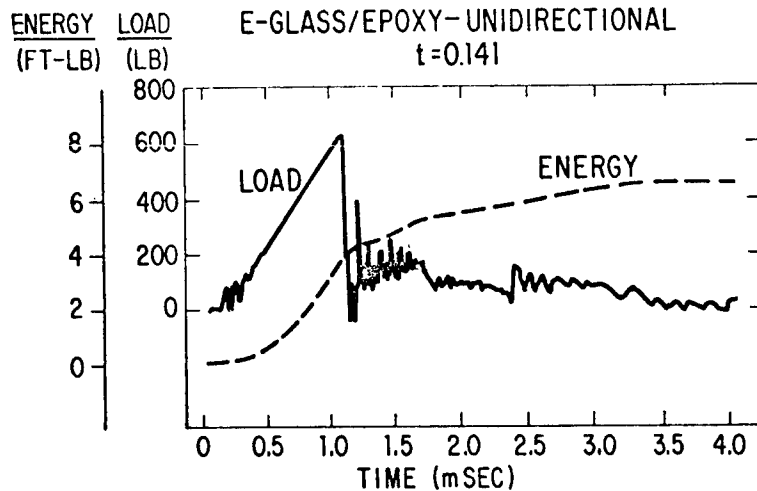


Fig. 9 - Load history of Charpy Impact Test E-Glass/Epoxy Unidirectional $t = 0.141$

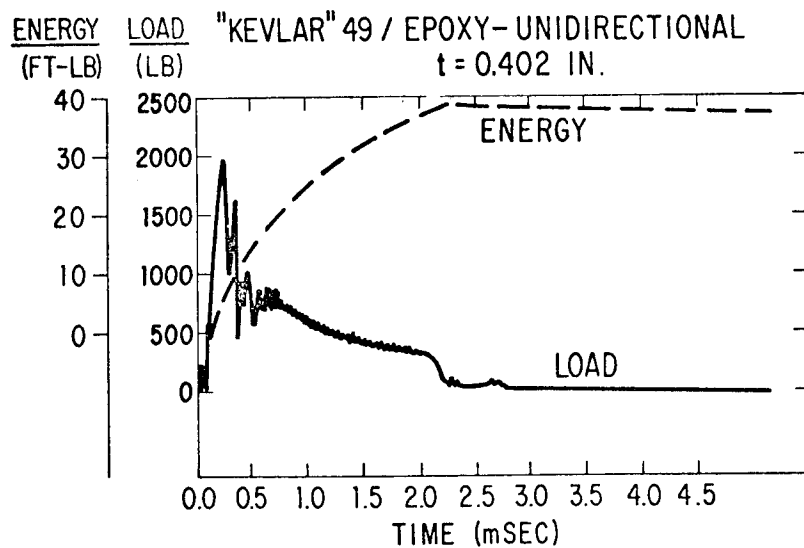


Fig. 10 - Load history of Charpy Impact Test "Kevlar" 49/Epoxy Uni-
directional $t = 0.402$ in

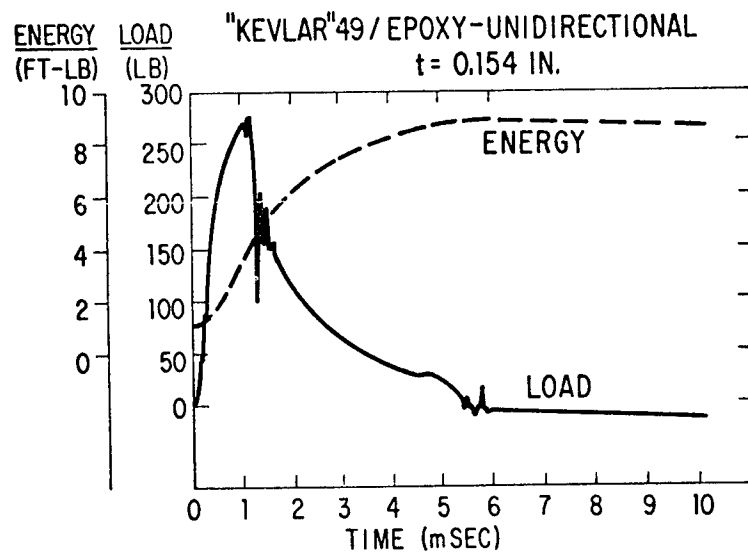
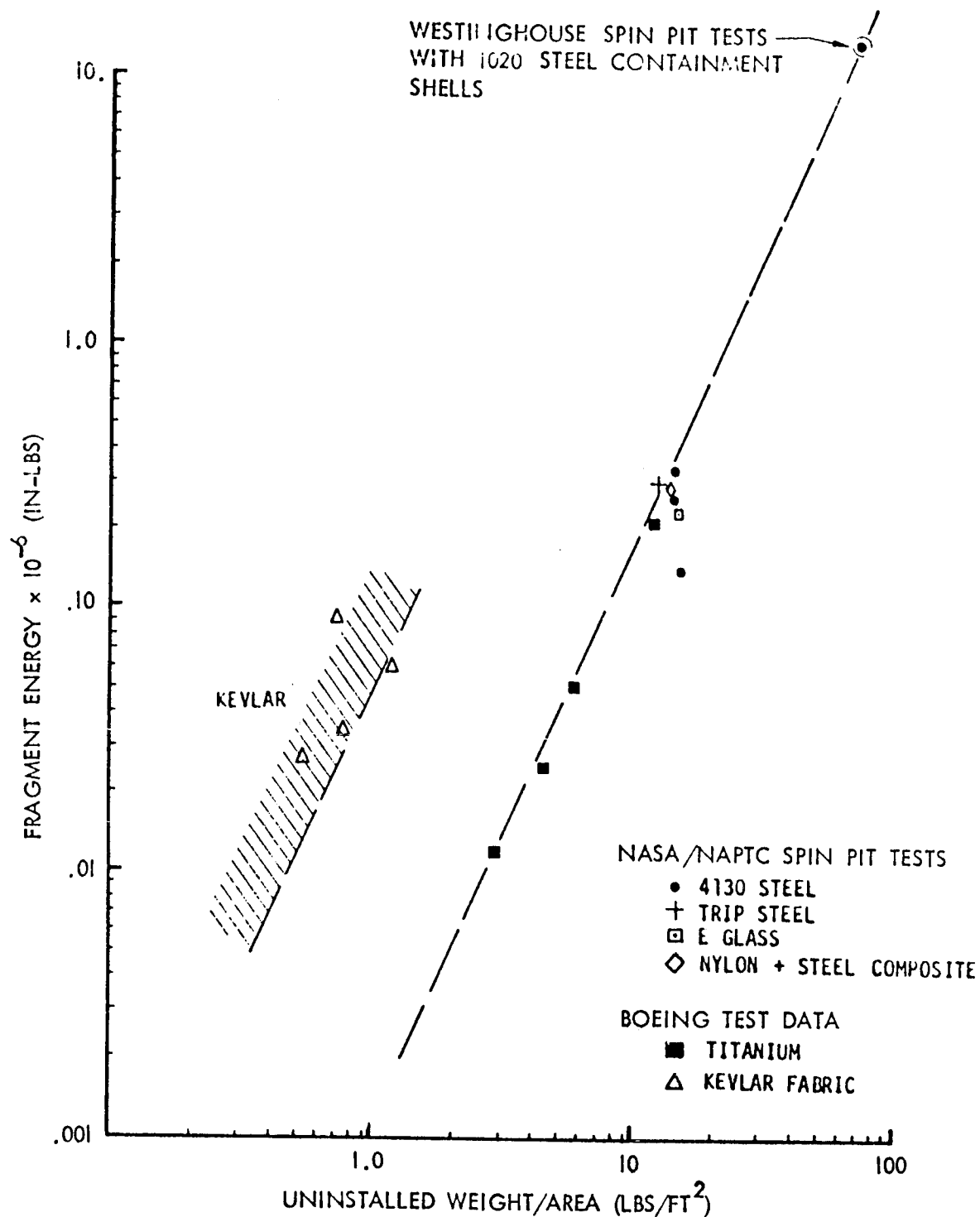
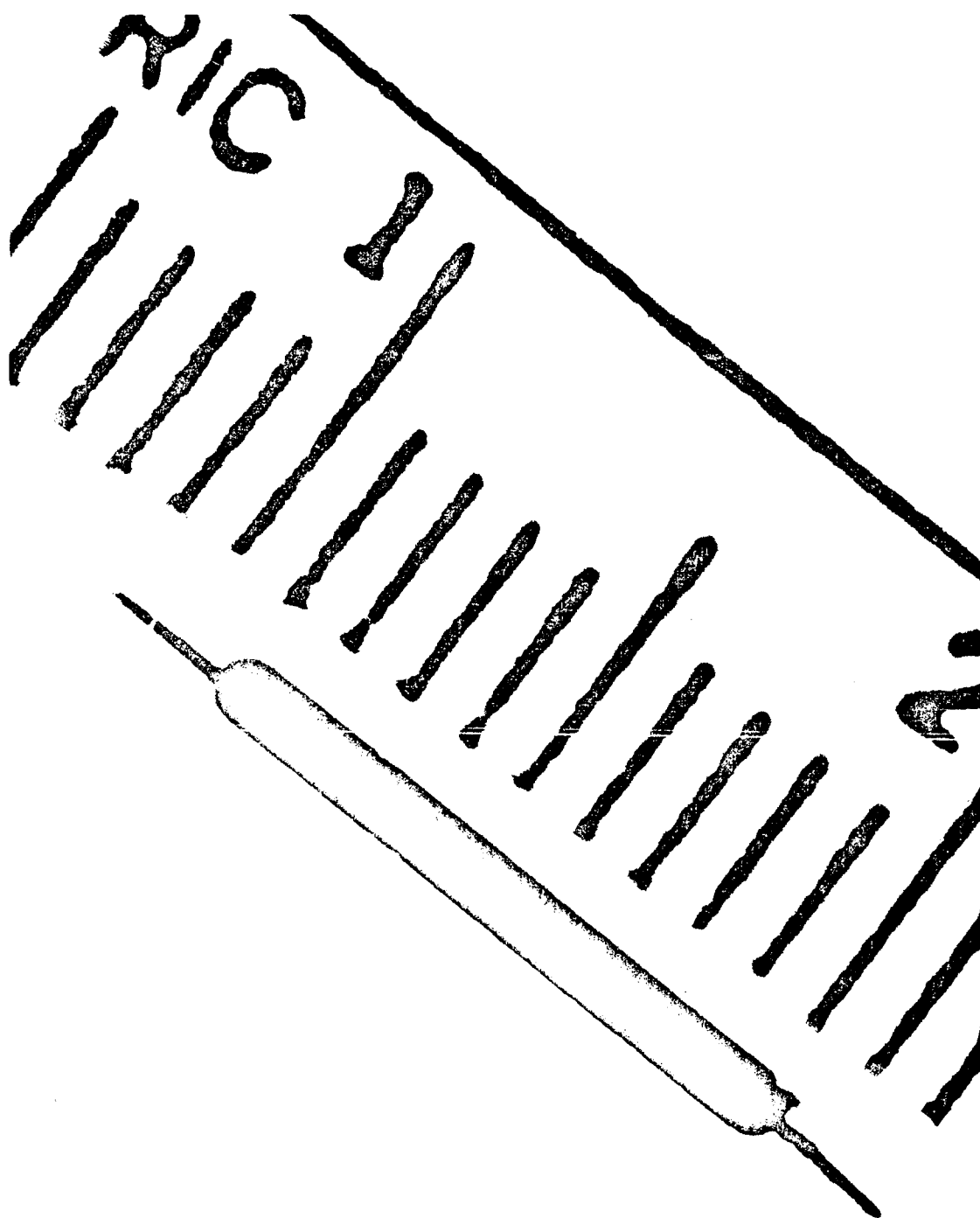
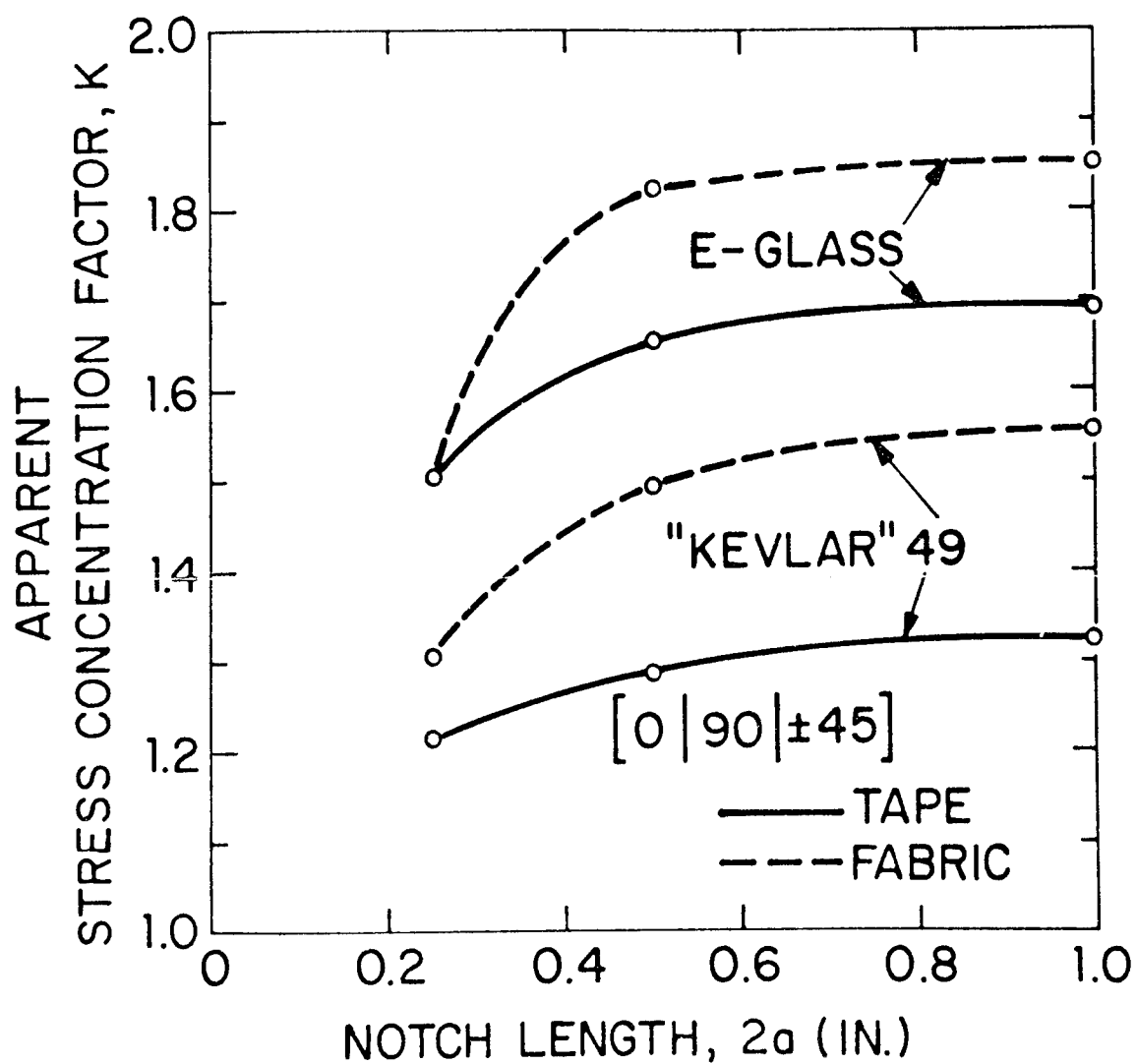


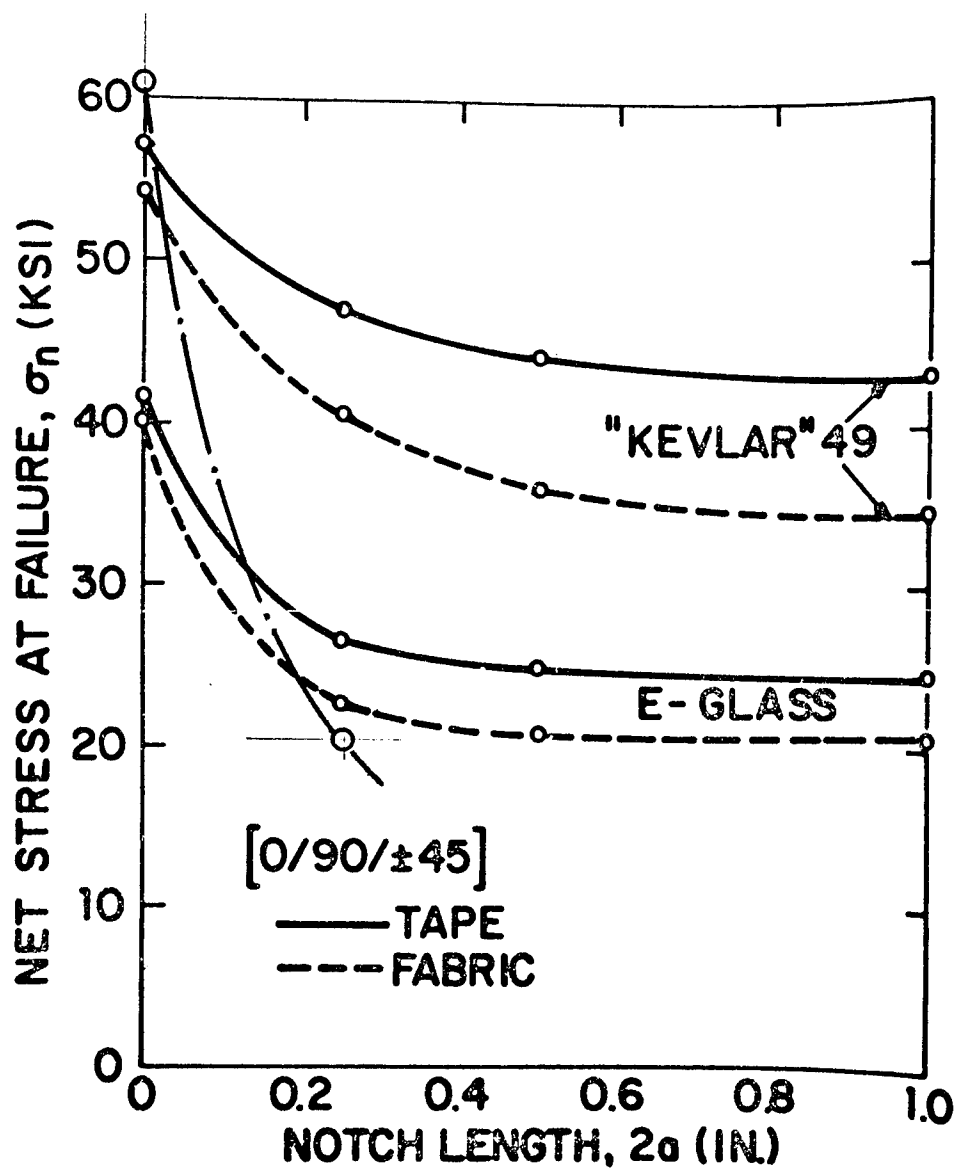
Fig. 11 - Load history of Charpy Impact Test "Kevlar" 49/Epoxy Uni-
directional $t = 0.154$ in



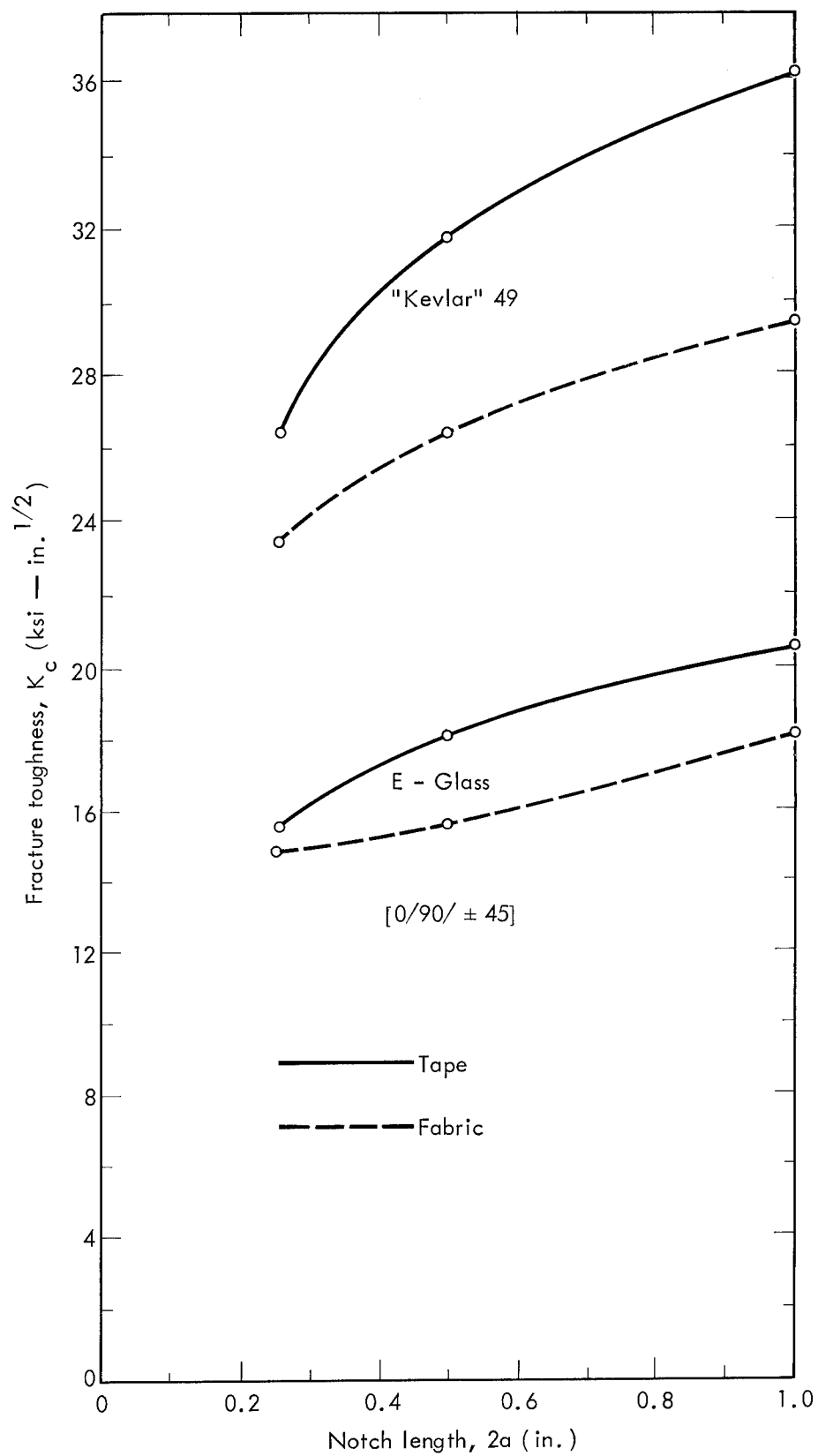




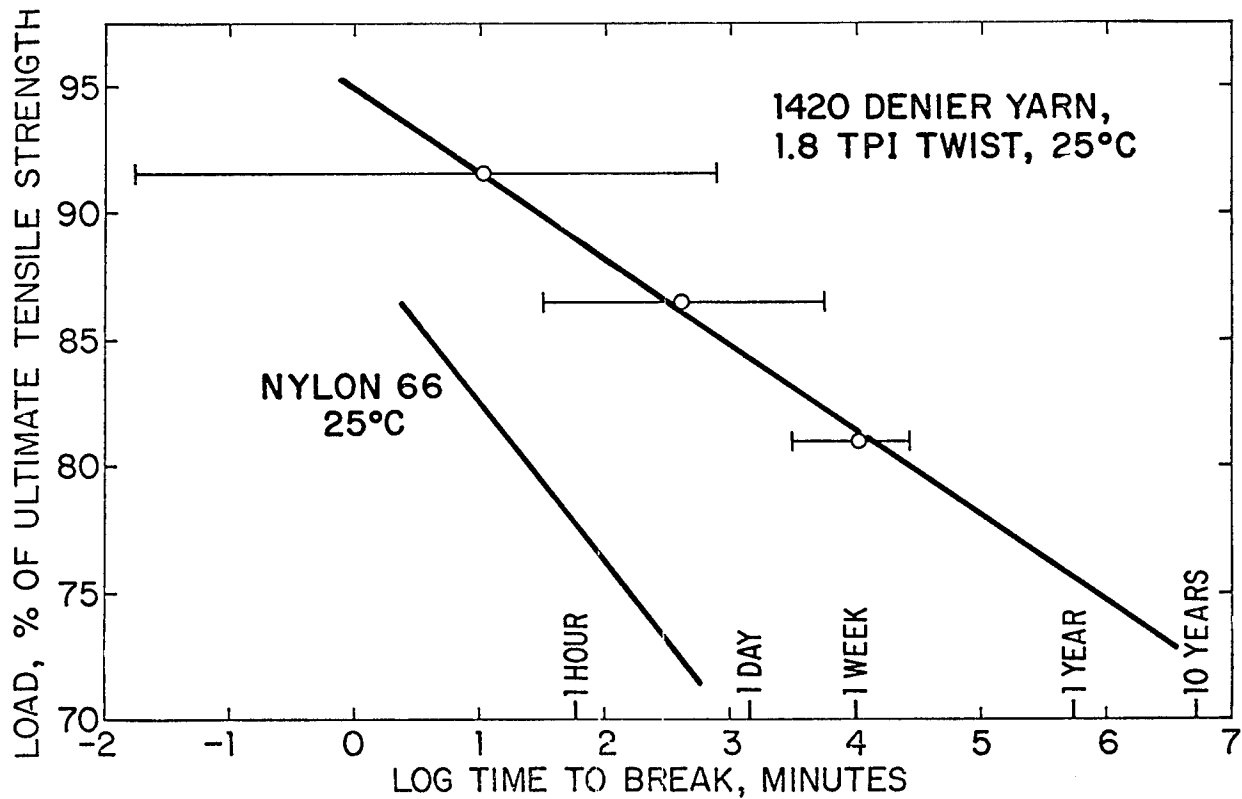
Apparent Stress Concentration Factor vs. Notch Length for "Kevlar" 49 and E-Glass Quasi-Isotropic Laminates



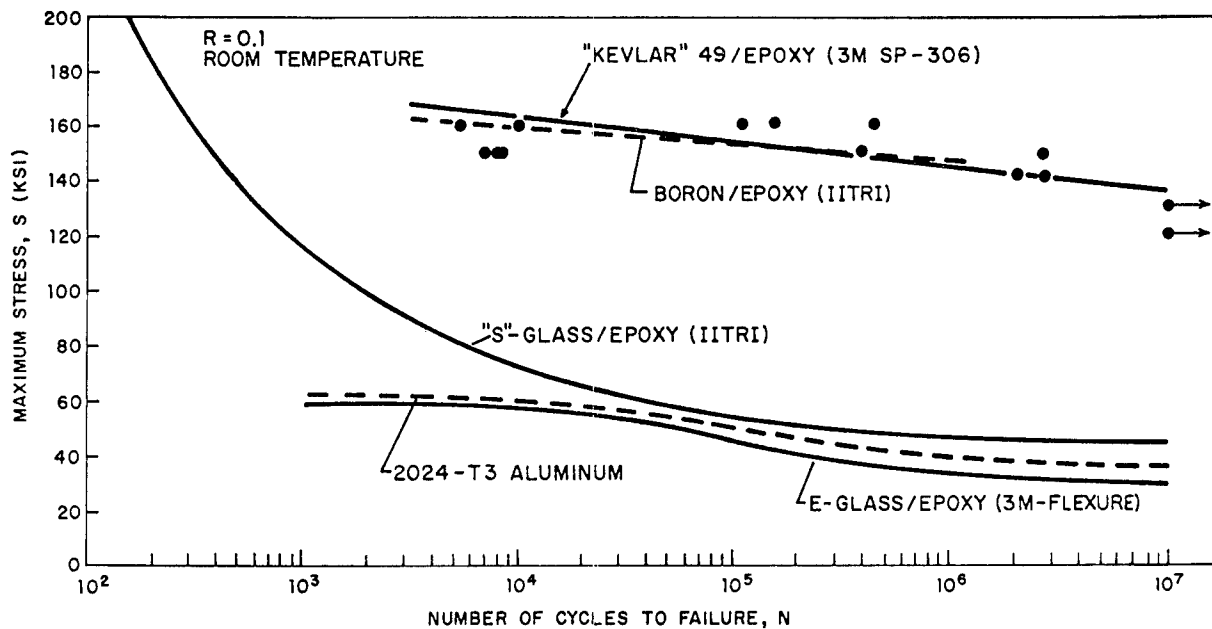
Net Failure Stress vs. Notch Length for "Kevlar" 49 and E-Glass Quasi-Isotropic Laminates

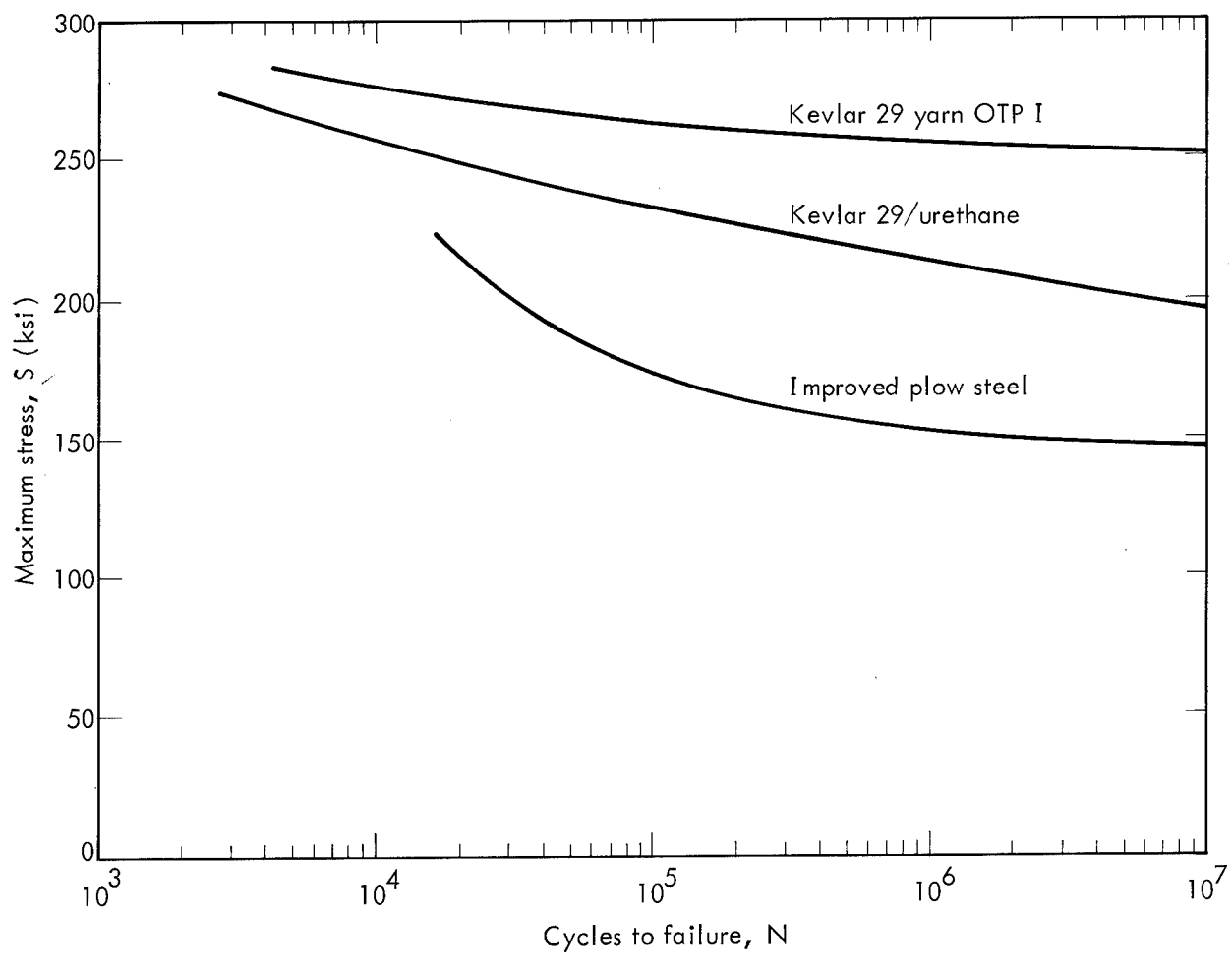


STRESS-RUPTURE OF "KEVLAR" 49 YARN TIME TO FAILURE UNDER CONTINUOUS STATIC LOAD



TENSION-TENSION FATIGUE BEHAVIOR OF UNIDIRECTIONAL COMPOSITES AND ALUMINUM





ENGINEERING DESIGN DATA FOR COMPOSITE MATERIALS*

Linda L. Clements

Lawrence Livermore Laboratory, University of California

Livermore, California 94550

ABSTRACT

LLL has been studying some basic mechanical properties of filament-wound composites. These include elastic and ultimate properties in tension and compression for both longitudinal and transverse modes as well as $\pm 45^\circ$ -tensile shear properties.

Measurements of the properties of composites of Kevlar 49 in an epoxy matrix are complete and are reported here, along with limited comparative data from Kevlar 49 in a second epoxy matrix. Some preliminary data from measurements of E-glass/epoxy specimens are also included.

INTRODUCTION

Designing a flywheel requires a certain, important minimum of realistic engineering data. Chiao and Hamstad¹ concluded that for filament-wound composites the minimum should include both elastic and ultimate properties in tension and compression for both longitudinal and transverse modes, as well as in-plane shear data.

Recent studies at LLL have concentrated on measuring these properties for composites of Kevlar 49** and E-glass fibers in an epoxy matrix. Table 1 lists the three composite systems studied.

TEST DATA FROM THE KEVLAR 49/EPOXY A COMPOSITE

For Kevlar 49 in epoxy A, all of the above mechanical characterization tests have been completed. Figure 1 compares the resulting stress-strain curves schematically. As can be seen in Figure 2, in which the data are normalized to 65 vol% fiber, properties in tension and compression differ considerably. The

ultimate stress and strain values obtained from elongated-ring longitudinal-tensile tests (1500 ± 230 MPa, $1.71\% \pm 0.25\%$)[†] are several times greater than those from flat-plate "Celanese" longitudinal compression tests (254.6 ± 3.5 MPa, $0.478\% \pm 0.026\%$). Furthermore, the elastic modulus in compression (73 ± 8 GPa) is significantly less than that in tension (87.6 ± 3.2 GPa), although the Poisson's ratio for compression (0.44 ± 0.09) is comparable to the tension result (0.39 ± 0.12). We feel that refinement of the compression test is necessary in order to verify these results.

As shown in Fig. 3, transverse properties of flat-plate specimens also differ, depending on whether they are measured in tension or compression. Here, however, the Celanese compression ultimate (53.0 ± 3.4 MPa, $1.41\% \pm 0.12\%$) are several times greater than the tension results (12.35 ± 0.38 MPa, $0.283\% \pm 0.011\%$). However, the secant moduli at 0.1% strain for tension (4.65 ± 0.17 GPa) and compression (4.5 ± 0.6 GPa) are comparable. Again, compression-test refinement is necessary.

*This work was performed under the auspices of the U. S. Energy Research & Development Administration under contract No. W-7405-Eng-48.

**Reference to a company or product name does not imply approval or recommendation of the product by the University of California or the U. S. Energy Research and Development Administration to the exclusion of others that may be suitable.

[†]All limits are 95% confidence limits.

Table 1. Composite Systems Studied.

Fiber	Nominal vol% fiber	Resin	Cure
Kevlar 49 - 1420 denier	65%	Epoxy A: Dow XD7818/ Jeffamine T403 (100/49)	16 h at 60°C 3 h at 90°C
Kevlar 49 - 1420 denier	65%	Epoxy B: Dow DER332/ Jeffamine T403 (100/39)	24 h at 60°C
E-glass - Type 30	70%	Epoxy B: Dow DER332/ Jeffamine T403 (100/45)	24 h at 60°C

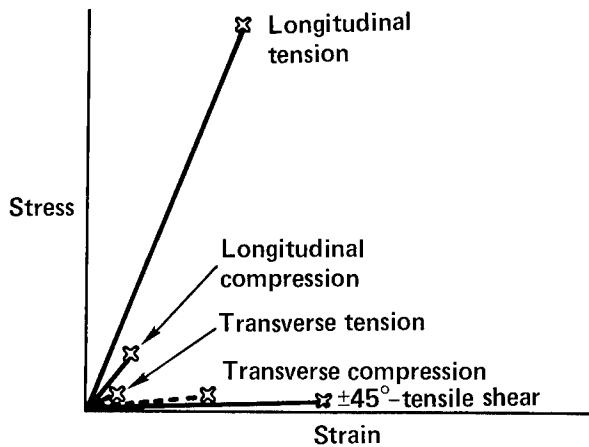


Fig. 1. Schematic comparison of various stress-strain curves obtained for Kevlar 49 in epoxy A.

Shear properties were obtained from the $\pm 45^\circ$ -laminate tensile test. While the exact significance of the ultimate properties measured in this type of test has not been established, the test does give good comparative values for different composite systems.² As shown in Fig. 4, the shear modulus obtained for a 58.3 vol%-fiber composite is 1.877 ± 0.028 GPa, and the $\pm 45^\circ$ -shear ultimates (taken at the inflection of the stress-strain curve) are 37.96 ± 0.36 MPa and $2.56\% \pm 0.06\%$.

KEVLAR 49/EPOXY B COMPOSITE

Limited data for comparison only was obtained for Kevlar 49 in epoxy B. Table 2 shows the ultimate strengths of elongated rings of Kevlar 49 in epoxy A and epoxy B. The epoxy B matrix seems to produce a composite with higher ultimate strength.

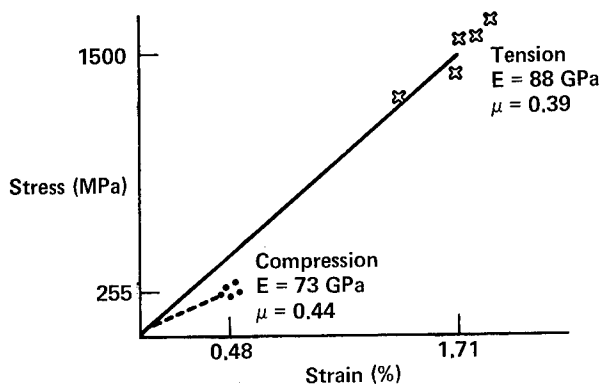


Fig. 2. Longitudinal properties in tension and compression for 65 vol% Kevlar 49 in epoxy A.

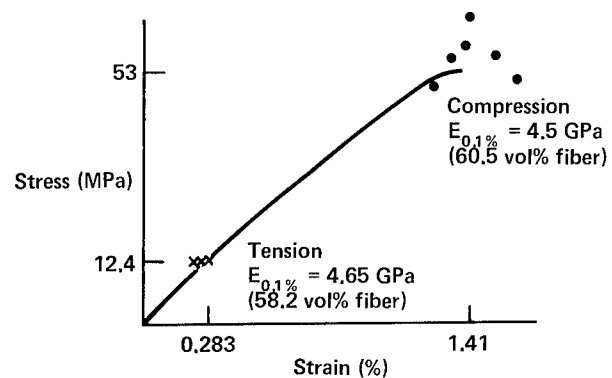


Fig. 3. Transverse properties in tension and compression for Kevlar 49 in epoxy A.

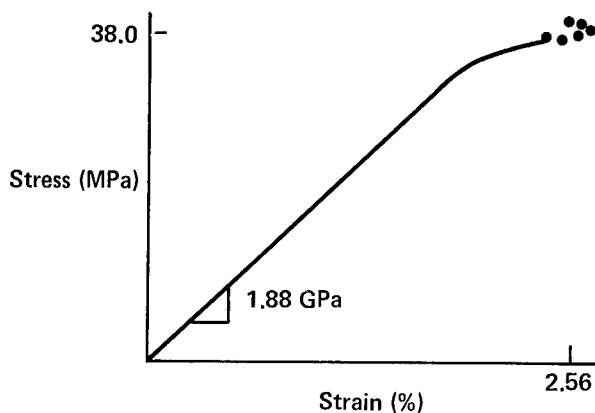


Fig. 4. Shear properties from $\pm 45^\circ$ -tensile specimen for 58.3 vol% Kevlar 49 in epoxy A.

The $\pm 45^\circ$ -tensile shear properties of the two composites are compared in Fig. 5. Although the shear modulus for the epoxy B composite (1.85 ± 0.12 GPa) is comparable to that for the epoxy A composite, the ultimate stress and strain for the epoxy B matrix (31.5 ± 1.1 MPa, $1.94 \pm 0.09\%$) are significantly less.

E GLASS/EPOXY B COMPOSITE DATA

Only preliminary results are available for E-glass in epoxy B. However, as shown in Fig. 6, these include almost the entire spectrum of test modes. Figure 7 presents the longitudinal properties, normalized to a 70-vol%-fiber composite. We see that the ultimate strengths in elongated-ring tensile tests (1240 ± 80 MPa, $2.30\% \pm 0.16\%$) are about twice those measured in compression (570 ± 120 MPa, $1.11\% \pm 0.27\%$). The tensile modulus (69 ± 11 GPa) is greater than that in compression (53.5 ± 4.3 GPa).

Figure 8 gives the transverse tensile properties. The secant modulus values are high (16.5 ± 4.9 GPa), but the ultimate stress and strain are extremely low (5.9 ± 1.0 MPa, $0.040\% \pm 0.018\%$). Since the

Table 2. Longitudinal tensile strengths of 65 vol% Kevlar 49 in two different matrices.

Matrix	Ultimate stress (MPa)
Epoxy A: XD7818/T403	1500 ± 230
Epoxy B: DER332/T403	1760 ± 110

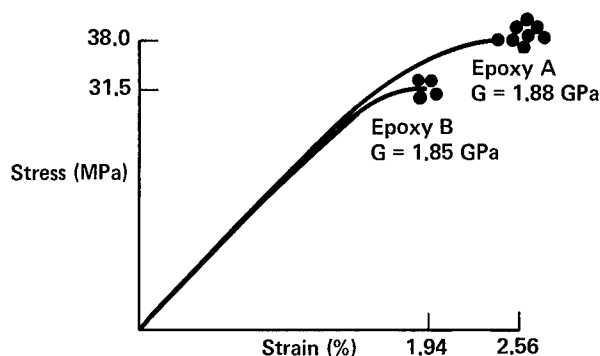


Fig. 5. Shear properties from $\pm 45^\circ$ -tensile specimen for Kevlar 49 in epoxy A and epoxy B.

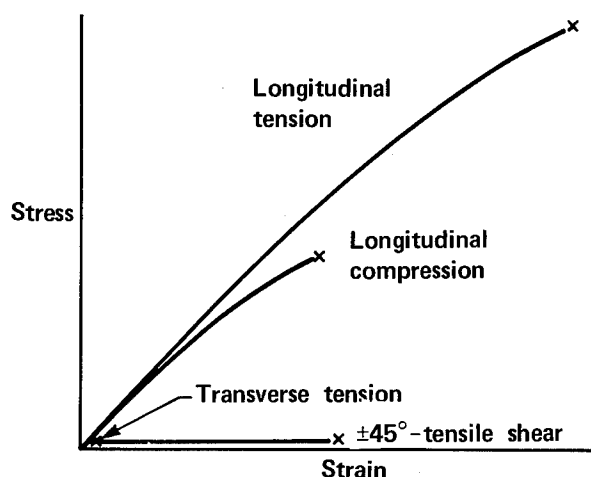


Fig. 6. Schematic comparison of various stress-strain curves obtained for E-glass in epoxy B.

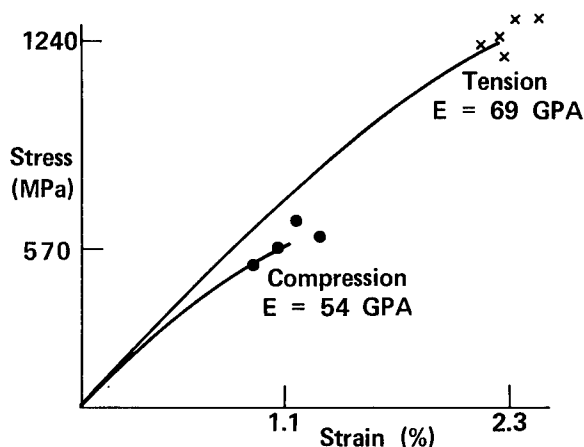


Fig. 7. Longitudinal properties in tension and compression for 70 vol% E-glass in epoxy B.

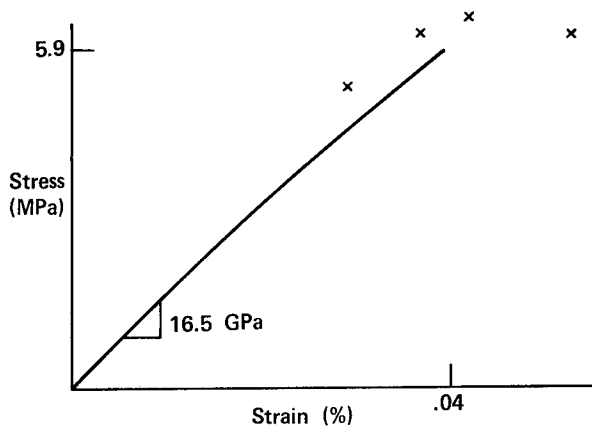


Fig. 8. Transverse tensile properties for 67.6 vol% E-glass in epoxy B.

transverse tensile test is extremely sensitive to edge effects, the low values could be caused by an edge problem in the flat-plate specimen configuration. Additional transverse tensile measurements of filament-wound tubes will be made to verify these results.

Shear properties from $\pm 45^\circ$ -tensile specimens of E-glass in epoxy B are shown in Fig. 9. The shear modulus (8.0 ± 0.9 GPa) is quite high, compared to the Kevlar 49 composites. The ultimate stress and strain values in Fig. 9 require further refinement.

SUMMARY AND FUTURE PLANS

In summary, mechanical characterization data for engineering design were obtained in detail for Kevlar 49 in epoxy A. Limited work was done on

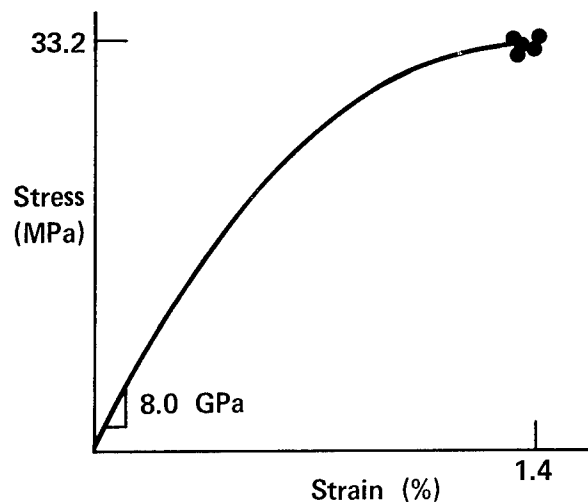


Fig. 9. Shear properties from $\pm 45^\circ$ -tensile specimen for 69 vol% E-glass in epoxy B.

Kevlar 49 in epoxy B, but only preliminary for flywheel will include:

- Continuation of E-glass work, including more study of the 70-vol% fiber composite, study of 65- and 75-vol%-fiber composites, and determination of physical properties.
- Both mechanical and physical characterization of composites of other fibers (i.e., S2-glass, Kevlar 29) and other resins (i.e., more flexible resin).
- Study and refinement of test techniques, particularly those used for compression testing.

REFERENCES

1. T. T. Chiao and M. A. Hamstad, "Testing of Fiber Composite Materials," Lawrence Livermore Laboratory, UCRL-76365, Livermore, CA, Jan. 9, 1975.
2. C. C. Chiao, R. L. Moore, and T. T. Chiao; to be published.

FRACTURE MECHANICS ASPECTS OF FILAMENTARY COMPOSITE FLYWHEELS

G. A. Vroman
Rocketdyne Division
Rockwell International
Canoga Park, California 91304

ABSTRACT

Application of the knowledge of fracture mechanics to the design of composite flywheels can improve their performance and safety. Fracture toughness, for example, is an indicator of composite material tolerance of its inherent defects, such as broken fibers, inhomogeneity, voids in the matrix material or lack of filament to matrix bonding. Toughness data can be used to select appropriate materials of construction. Crack growth rates are also important, since they may indicate voids or poor filament to matrix bonding. Extensive crack branching under very high stresses may be desirable for flywheel safety if such branching absorbs energy during rupture and causes many small particles rather than a few large ones to form.

INTRODUCTION

Flywheel materials must function under very difficult conditions. As an energy storage device the material is subjected to very high stress levels. In most applications, many loadings (and unloadings) will be encountered that have high stress durations of a few minutes to many hours. The material stress state will vary from plane stress in the rim where the loading is near uniaxial to plane strain in the hub region where the stresses are triaxial. If the flywheel is designed to operate in a vacuum, problems associated with moisture in the flywheel material itself are largely eliminated. Without a near-perfect vacuum, there may be an aerodynamic heating effect that significantly raises the flywheel operating temperature. Also, there will be a heat input from the support bearings and material hysteresis energy losses, all of which may raise operating temperatures well above room temperature.

DISCUSSION

Filamentary composites have both advantages and disadvantages. Their principal advantage is in a high strength-to-density ratio. Another benefit is that their mechanical properties can be varied for different loading directions to optimize the material usage. Variables such as fiber volume density, filament weave, matrix material, and laminate ply angles

can be used to tailor the mechanical properties to the specific application.

One of the disadvantages of filamentary composites is that of service life, which is largely controlled by inherent defects. Broken fibers, voids in the matrix material, lack of bond between the fiber bundle and the matrix material, inhomogeneity--all are found in typical composites even before service loading. Initially, these defects are small and do not have a great effect on the tensile strength. However, during repeated loadings additional fibers are broken, and crack-like voids grow in the matrix material, resulting in a degradation of strength.

Figure 1 illustrates evidence of inherent defects. C. K. H. Dharan showed that defective fibers fractured at relatively low loading and that the fiber crack extended to form a penny-shaped crack in the matrix material (Ref. 1). He also observed that when the load was removed the matrix crack closed up, leaving only the fiber fracture as visible evidence of a defect. He points out that the matrix cracking in the composite occurs at strain levels much less than that indicated by testing only matrix material. This can be seen in Figure 1 by comparing the strain to initiate composite matrix microcracks (0.01 in./in.) with the strain survived by the matrix material only (0.03 in./in.).

Additional evidence of defects can be seen in Figure 2. This information was extracted from Ref. 2; it illustrates the degradation of S-Glass composites occurring under cyclic loading. The decrease in stiffness is attributable to the growing of defects by additional fiber failure and/or crack growth in the matrix.

The study of fracture mechanics provides a means for evaluating the effect of defects in composite materials. Since fracture toughness is an indicator of material tolerance of defects, it provides an index by which to select materials. An example of fracture toughness is shown in Figure 3, which was extracted from Ref. 3. In this figure the fracture stress data obtained from flawed specimens are mostly bounded by the two lines of constant stress intensity, 75 and 112 ksi $\sqrt{\text{in.}}$. Additional fracture toughness data, shown in Figure 4, were obtained from Ref. 4. Here it can be seen that the glass-epoxy composite systems vary in fracture toughness by a factor of almost five from the high to the low (1520/320). All other factors being equal, the composite with the highest fracture toughness should be selected for design. Since fracture mechanics analysis predicts that the fracture stress for a given defect size is directly proportional to the fracture toughness, composite No. 2 would have five times the fracture stress of composite No. 5 for a given defect size.

Crack growth rate data can be used either to select the best material or to improve a given material. The crack growth rate data shown in Figure 5 were extracted from Ref. 5, in which P. A. Thornton reported that a lot of otherwise identical material showing a high crack growth rate was found to have a lack of bonding (poor wetting) of some of the filaments to the matrix material, as well as air voids in the matrix material from which cracks were generated.

Perhaps the most serious concern in flywheel design is the danger of releasing high-energy projectiles as a result of structural failure. Filamentary composites are expected to be better than solid metals in this regard, but a significant danger still exists. It would be desirable to develop a material that fractures in a manner similar to automobile safety glass. Figure 6 illustrates how a standard fracture mechanics test specimen can be utilized to develop such a material.

Two benefits can be gained by controlling the frangibility. First, the branching of cracks results in a greater energy dissipation during rupture, and second, the smaller particles released during failure are less damaging upon impact. It is very possible that composite materials can be developed that have the desired frangibility characteristics while still meeting the other requirements.

Fracture mechanics material testing can provide valuable information to aid in the development of filamentary composite flywheels. However, it is very important that the test conditions closely simulate the design conditions or misleading results will be obtained. The load-time relationship should simulate the strain rate during spin-up, the load-holding duration, and the strain rate during spin-down. All of these do not have to be investigated with a single group of specimens. It may be practical to simulate the strain rates in one group of specimens and the load-holding times in another group, varying the number of specimens in each group. It is also important to simulate the design environment during testing. Vacuum may effect the fracture toughness of resins containing volatiles. Flywheel temperature extremes may cause significantly different material properties than the room temperature values from which the initial design analysis was made.

This presentation can be summarized by listing the two messages it was intended to convey:

1. The design capability of filamentary composite flywheels is largely determined by inherent defects.

2. Fracture mechanics provides a means of improving flywheel design.

References

1. Dharan, C. K. H.: "Fatigue Failure Mechanisms in a Unidirectionally Reinforced Composite Material," Fatigue of Composite Materials, ASTM STP 569, American Society for Testing and Materials, 1975, pp. 171-188.
2. Durchlaub, E., and P. Sacca: Fracture Mechanics and Damage Tolerance of S-Glass Composites, Technical Report AFFDL-TR-72-82, Air Force Flight Dynamics Laboratory, August 1972.

3. Jaques, W. J.: Soft Body Impact Damage Effects on Boron-Aluminum Composites, GAW/MC/74-13, Air Force Institute of Technology, March 1974.
4. Sanford, R. J., and F. R. Stonesifer: Fracture Toughness of Filament-Wound Composites, NRL Report 7112, Naval Research Laboratory, July 1970.
5. Thornton, P. A.: "Fatigue Crack Propagation in a Discontinuous Composite," Journal of Composite Materials, January 1972, pp. 147-151.

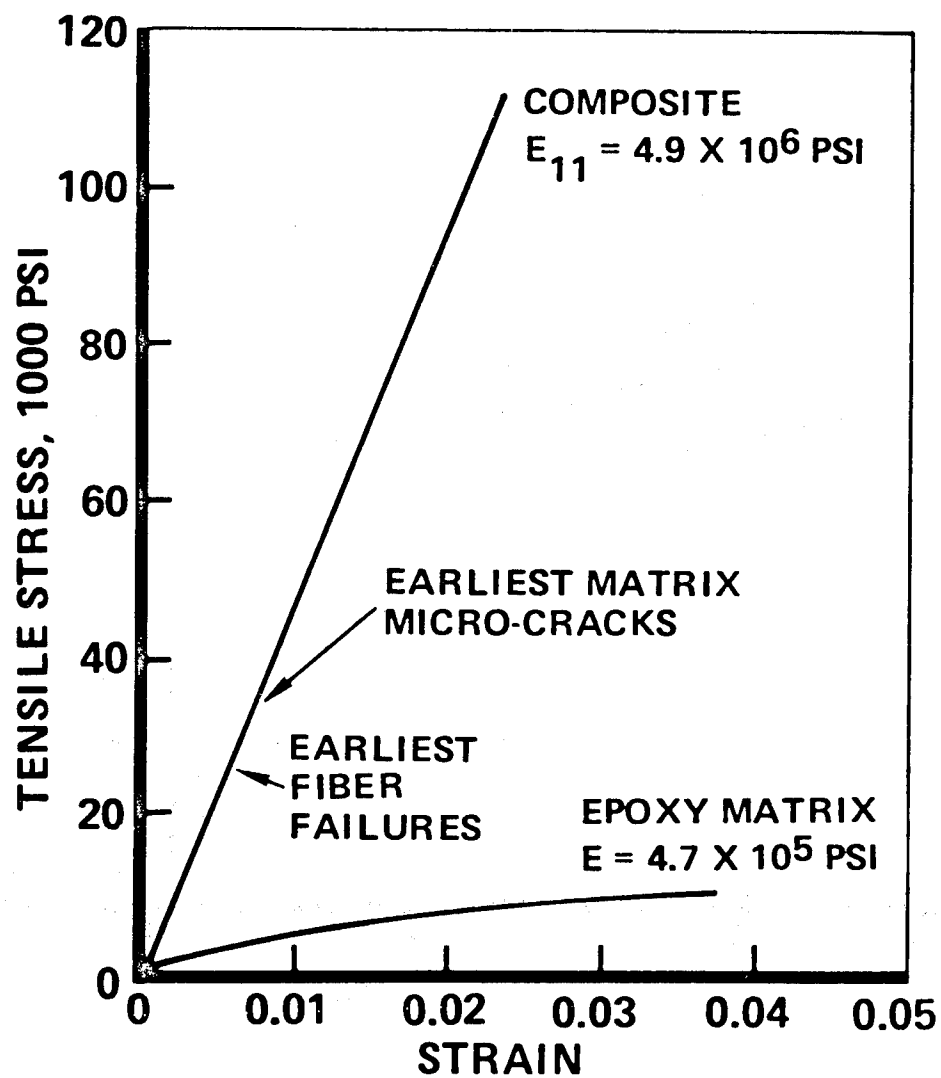


Figure 1. Evidence of Inherent Defects

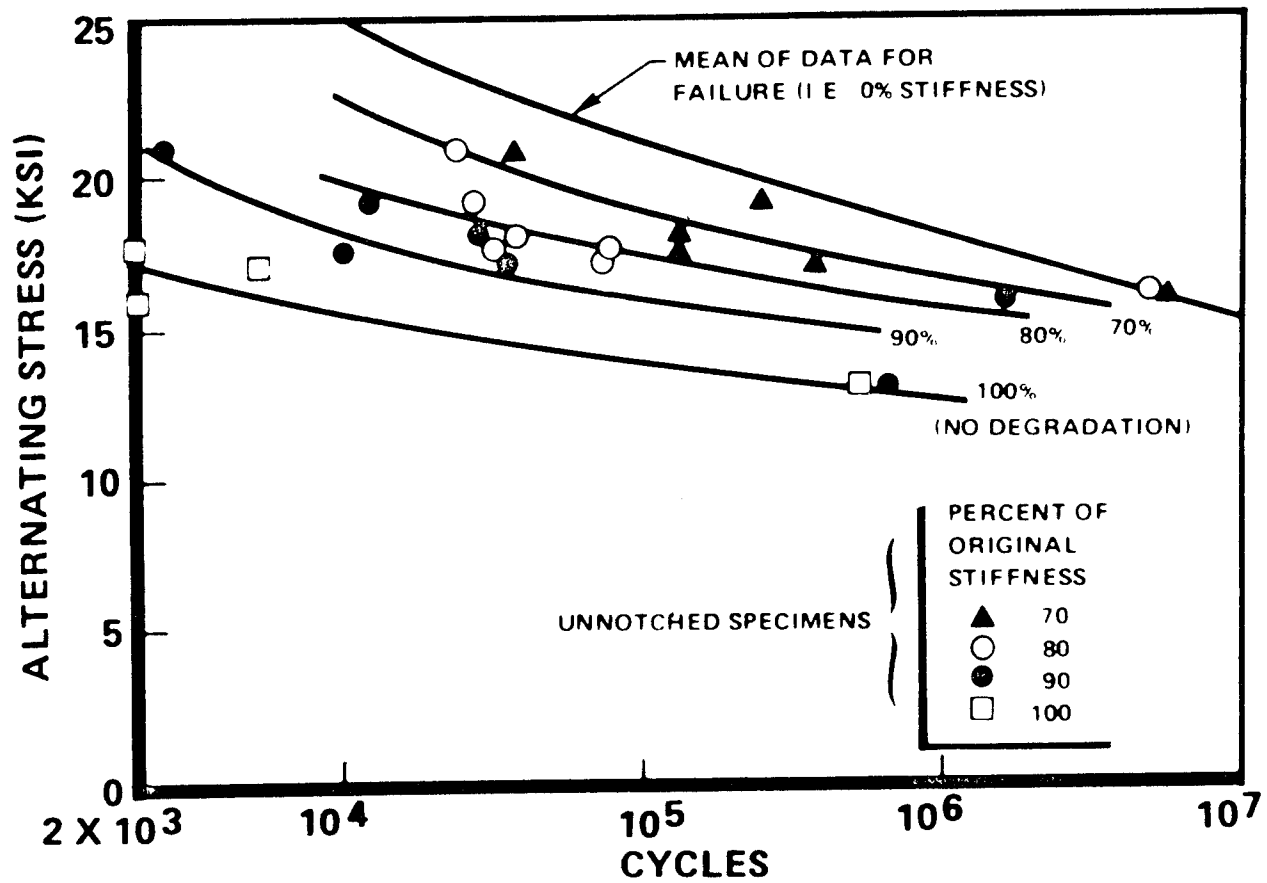


Figure 2. Evidence of Growing Defects

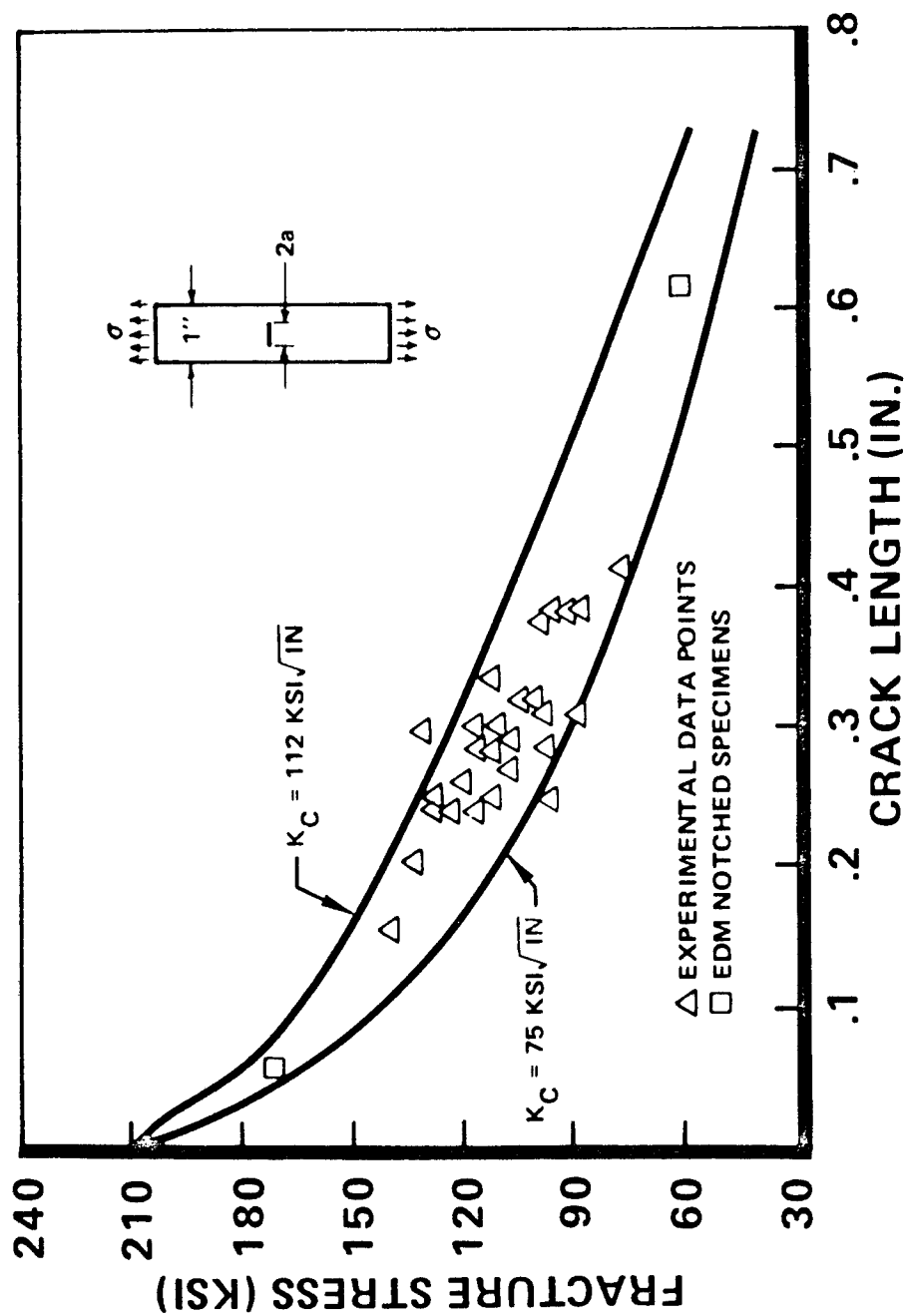


Figure 3. Fracture Toughness of a Boron-Aluminum Composite

NO	RESIN SYSTEM		GLASS TYPE	SINGLE EDGE NOTCHED SPECIMEN		DOUBLE EDGE NOTCHED SPECIMEN	
				K_{Ic}'	G_c'	K_{Ic}'	G_c'
	SOURCE	TYPE		PSI $\sqrt{IN.}$	LB/IN.	PSI $\sqrt{IN.}$	LB/IN.
1	SHELL	EPON 826/CL	S-HTS	1270	0.9	1080	1.0
2	UNION CARBIDE	ERL 2256/0820	E-HTS	1520	1.2	1310	1.3
3	SHELL	EPON 826/CL	E-HTS	1340	1.6	1100	1.1
4	UNION	ERL 2256/0820	E-HTS	1030	0.3	850	0.3
5	SHELL	EPON 826/CL (B-STAGE ONLY)	S-HTS	320	0.5	270	0.3

Figure 4. Fracture Toughness of Glass-Epoxy Composites

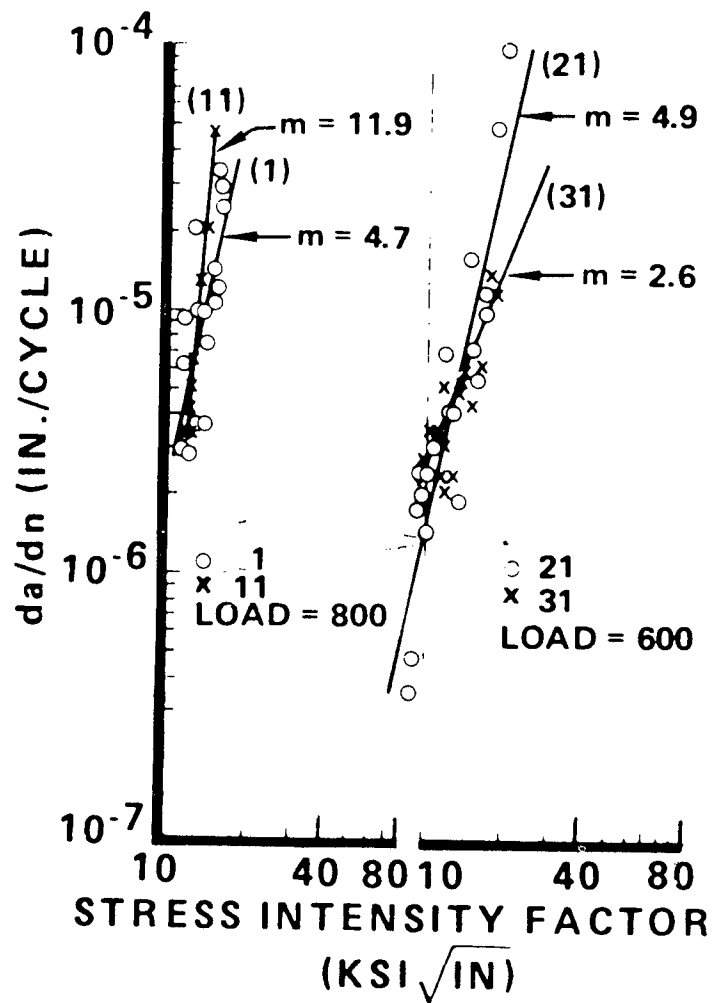


Figure 5. Crack Growth Rate of an Aluminum Epoxy Composite

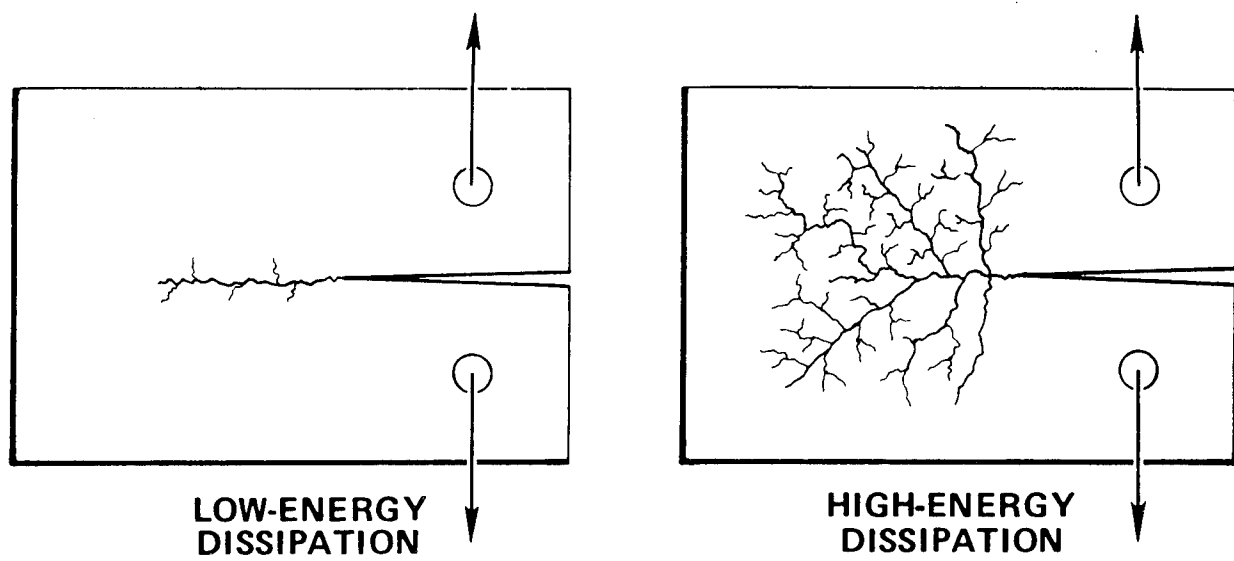


Figure 6. Fracture Mechanics Development of Frangible Material

TRANSFER MATRIX ANALYSIS OF COMPOSITE FLYWHEELS WITH RELIABILITY APPLICATIONS

Richard H. Toland
Department of Mechanical Engineering and Mechanics
Drexel University
Philadelphia, Pennsylvania 19104

ABSTRACT

The author is undertaking a study of several aspects of the reliability of selected composite flywheel design concepts. As a first step, analytical models suitable for describing the steady-state behavior of wide disks, thin rims and modular ring concepts are developed and presented herein. Orthotropic material properties are incorporated. The transfer matrix method is shown to be a flexible and computationally concise scheme well suited for simulation methods of reliability assessment.

INTRODUCTION

An important part of the development of a high performance product is an early assessment of the reliability of the concept designs, their ability to achieve a reasonable design life and their expected operational maintenance requirements. These aspects of product design should be incorporated into the early stages of the development process.

In cooperation with Lawrence Livermore Laboratory the author has begun a program that will address various aspects of the reliability of selected composite flywheel design concepts subject to realistic service environments. Principal failure modes will be identified and their interdependency established by a Fault Tree Analysis leading to a prediction of the probability of failure, P_f , of a flywheel.

The analytical problem of reliability seeks a probabilistic statement of a design's survival, $P_S = (1 - P_f)$, subject to a given environment, system variability, and with known failure modes and established failure criteria. Mathematical reliability theory is a well-developed tool used in many engineering disciplines (1, 2, 3, many other references). For a composite flywheel, the theory will be used to address reliability as the prediction of the probability of survival to a specified time t , and the prediction of the hazard function as the probability of failure in the interval $t, t + \Delta t$ given the survival to time t . Additionally, it is intended to use these methods to provide direction

to cost effective quality control of the fabrication process (4), proof testing requirements and maintenance inspection intervals (5).

In applying reliability theory to physical systems, analytical models of these systems must be developed which relate the requisite top events as a function of their variables, both deterministic and random. Some analytical models are explicitly formulated in concise mathematical expressions. These frequently permit the analyst to develop "true" analytical statements of the reliability and hazard functions. Other models involve great complexity in the functional relation of the top event with its variables. The solution to these problems is often sought by simulation methods (4), such as Monte Carlo Simulation, MCS. Coupled with a sensitivity analysis, simulation can prove a powerful tool to examine otherwise intractable problems of reliability prediction. Both classes of problems are expected to appear in this study of composite flywheel reliability.

OBJECTIVES

The first six weeks of this study had as its general objective the development of analytical models suitable for examining a wide class of flywheel design concepts. It was decided that a basic prerequisite for any model must be good computational efficiency suitable for simulation studies. Mechanics studies of flywheels can be grouped into the three physical categories: steady-state behavior (constant rotational velocity), transient

behavior (run-up, run-down) and critical speeds (whirling). Mathematically, these are boundary-value, initial-value and eigen-value problems. A total analysis must examine all areas defining all design requirements, failure modes and ultimately addressing reliability and design optimization.

For this study, it was decided to model and study the steady-state behavior of:

- (a) solid disk flywheels of orthotropic materials,
- (b) thin rim flywheels and
- (c) modular ring composite flywheels.

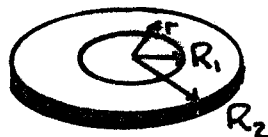
The specific objectives are:

- (a) to build the necessary analytical models,
- (b) to perform parametric studies to better understand flywheel behavior,
- (c) to develop feasible concept designs and
- (d) to examine reliability for select failure modes.

ANALYTICAL MODELS

ORTHOTROPIC WIDE DISKS AND THIN RIMS

The plane stress 2-D elasticity solution for a constant thickness disk, Figure 1, with orthotropic properties was formulated. For traction-free inner and



$$\sigma_r(R_1) = \sigma_r(R_2) = 0$$

Figure 1. Constant thickness disk.

outer edges, the analytical expressions for radial and hoop stresses and radial displacement are as follows:

$$\sigma_r = \rho \omega^2 R_2^2 \left(\frac{3 + \nu_{\theta r}}{9 - \nu_{\theta r}/\nu_{r\theta}} \right) \left[\left(\frac{b^{3-n} - b^{-2n}}{1 - b^{-2n}} \right) a^{n-1} - \left(\frac{b^{3-n} - 1}{1 - b^{-2n}} \right) a^{-n-1} - a^2 \right]$$

$$\sigma_{\theta} = \rho \omega^2 R_2^2 \left(\frac{3 + \nu_{\theta r}}{9 - \nu_{\theta r}/\nu_{r\theta}} \right) \left[\left(\frac{b^{3-n} - b^{-2n}}{1 - b^{-2n}} \right) n a^{n-1} + \left(\frac{b^{3-n} - 1}{1 - b^{-2n}} \right) n a^{-n-1} - \left(\frac{3\nu_{\theta r} + \nu_{\theta r}/\nu_{r\theta}}{3 + \nu_{\theta r}} \right) a^2 \right]$$

where

$$n = \sqrt{\nu_{\theta r}/\nu_{r\theta}} = \sqrt{E_{\theta}/E_r}$$

$$b = R_1/R_2, \quad a = r/R_2$$

also

$$U = \frac{(\sigma_{\theta} - \nu_{\theta r} \sigma_r) a R_2}{E_{\theta}}$$

These expressions were evaluated for many values of disk width, b , and material orthotropy ratio E_{θ}/E_r ($\nu_{\theta r}/\nu_{r\theta}$). This ratio was varied from 0.1, stiffer in radial direction, to 25, stiffer in the hoop direction. The latter case is representative of filament wound composite flywheels. The nondimensionalized stresses for two cases with orthotropy ratios of 1.0 (isotropic) and 10.0 (typical of Kevlar 49 composite system) are presented in Figures 2 and 3.

Several important observations can be made if one examines the hoop stress distributions for the wide rim disks, $b = 0.1$. For the isotropic case, the peak hoop stress is at the inner radius, $a = 0.1$, while for the orthotropic case the peak hoop stress is outward near $a = 0.8$. For a constant stress design (varying thickness) the isotropic flywheel is thicker at the hub and the orthotropic flywheel is thicker outboard. The latter is more efficient for energy storage. However, variable thickness flywheels should generally be treated as a 3-D elasticity problem since a τ_{rz} shear stress is introduced. For a filament-wound composite design, this is an interlaminar shear with possible design limiting significance.

Further insight is obtained if one examines the ratio of maximum radial and hoop stresses for a wide rim disk, $b = 0.1$. For the isotropic and orthotropic cases, these are approximately 0.4 and 0.18 respectively. A low ratio is desired for filament-wound composite designs, since the radial stress corresponds to a transverse tensile stress in a unidirectional composite. The higher orthotropy ratios result in lower values of this stress ratio, but within the limits of practical materials, do not lower it sufficiently. This results from a recognition that the ratio of allowable strengths corresponding to the fiber and transverse direction is typically of the order of 0.03 to 0.05 ($\ll 0.18$). Filament wound wide disk designs would appear to be inefficient, since the fibers could not be highly stressed.

Some other important observations are made if one examines the stresses for a thin rim wheel, $b = 0.9$. The radial stresses are effectively zero for both cases, but the hoop stresses are identical for both. The thin rim design is effectively in a membrane state of stress, i.e., the stresses are independent of material properties and only the displacements and strains are material dependent. The thin-rim, filament-wound composite flywheel is attractive from a stress viewpoint. Variations of a single ring design include nested thin rings and the modular ring concept.

This plane stress analytical model will be used for the study of thin-rim, flywheel design concepts. Another promising concept appears to be the modular ring (6) where relatively thin composite rings

are nested and bonded together by an elastomeric material, Figure 4. This system can be modelled by several methods, including finite elements, F.E. The F.E. methods, however, are generally computationally time consuming, which is a drawback for a simulation approach to reliability studies. For this reason, this class of flywheel system was modelled by the transfer matrix method (7).

TRANSFER MATRIX ANALYSIS

The transfer matrix method can be applied to a broad class of flywheel designs and analytical problems. It is also an efficient computational scheme. Figure 5 illustrates a modular ring flywheel where the parameter r_i defines the radial position of any station of interest through the flywheel width. This may include the interface between two materials or a position within a given ring. The previously derived, plane stress solution for a rotating orthotropic disk is recast into the following transfer matrix form.

$$\begin{Bmatrix} \sigma_r \\ U \\ 1 \end{Bmatrix}_i = \begin{bmatrix} C_{11} & C_{12} & C_{13} \\ C_{21} & C_{22} & C_{23} \\ 0 & 0 & 1 \end{bmatrix}_i \begin{Bmatrix} \sigma_r \\ U \\ 1 \end{Bmatrix}_{i-1}$$

\uparrow State Vector at r_i \uparrow Transfer Matrix for i^{th} layer \uparrow State Vector at r_{i-1}

r_i - Radial Stress at r_i

U_i - Radial Displacement at r_i

Also

$$\sigma_{\theta i} = \left\{ \begin{matrix} E_{\theta i} \\ E_{\theta i-1} \end{matrix} \right\} \frac{U_i}{r_i} + \left\{ \begin{matrix} \nu_{\theta r i} \\ \nu_{\theta r i-1} \end{matrix} \right\} \sigma_{r i}$$

Hoop Stress at r_i

The stresses and displacements (state vector) at a given station r_i are related to the same quantities at a previous station r_{i-1} by a transfer matrix, $(C)_i$, developed from the plane stress solution.

The terms in (C) are lengthy and are not written out here. The expression for hoop stress was written to allow for a jump across an interface of two materials.

The state vector for any general position may be related to the state vector at r_0 , the inner boundary, by simple matrix multiplication as follows

$$\begin{Bmatrix} \sigma_r \\ U \\ 1 \end{Bmatrix}_1 = (C)_1 \begin{Bmatrix} \sigma_r \\ U \\ 1 \end{Bmatrix}_0$$

$$\begin{Bmatrix} \sigma_r \\ U \\ 1 \end{Bmatrix}_2 = (C)_2 \begin{Bmatrix} \sigma_r \\ U \\ 1 \end{Bmatrix}_1 = (C)_2 (C)_1 \begin{Bmatrix} \sigma_r \\ U \\ 1 \end{Bmatrix}_0$$

$$\begin{Bmatrix} \sigma_r \\ U \\ 1 \end{Bmatrix}_N = (C)_N \dots (C)_2 (C)_1 \begin{Bmatrix} \sigma_r \\ U \\ 1 \end{Bmatrix}_0$$

or

$$\begin{Bmatrix} \sigma_r \\ U \\ 1 \end{Bmatrix}_i = (P)_i \begin{Bmatrix} \sigma_r \\ U \\ 1 \end{Bmatrix}_0$$

The boundary conditions are routinely incorporated as illustrated in the following example

$$\begin{Bmatrix} \sigma_r \\ U \\ 1 \end{Bmatrix}_N = \begin{bmatrix} P_{11} & P_{12} & P_{13} \\ P_{21} & P_{22} & P_{23} \\ 0 & 0 & 1 \end{bmatrix}_N \begin{Bmatrix} \sigma_r \\ U \\ 1 \end{Bmatrix}_0$$

or

$$\sigma_N = P_{11}\sigma_0 + P_{12}U_0 + P_{13}$$

$$U_N = P_{21}\sigma_0 + P_{22}U_0 + P_{23}$$

if

$$U_0 = \sigma_N = 0$$

$$\sigma_0 = -P_{13}/P_{11}$$

$$U_N = P_{23} - P_{13}P_{21}/P_{11}$$

The hoop stresses at the inner and outer edges can also be computed now. Then we have defined the state vectors at r_0 and r_N .

$$\begin{Bmatrix} \sigma_r \\ U \\ \sigma_\theta \end{Bmatrix}_0 \quad \& \quad \begin{Bmatrix} \sigma_r \\ U \\ \sigma_\theta \end{Bmatrix}_N$$

We can now calculate the state vector at all intermediate stations as

$$\begin{Bmatrix} \sigma_r \\ U \end{Bmatrix}_i = \begin{bmatrix} P_{11} & P_{12} & P_{13} \\ P_{21} & P_{22} & P_{23} \end{bmatrix}_i \begin{Bmatrix} \sigma_r \\ U \\ 1 \end{Bmatrix}_0$$

$$i = 1 \text{ to } N-1$$

Also

$$\sigma_{\theta_i} \quad (\text{Right \& Left})$$

Other boundary conditions can be prescribed including elastic constraints.

The scheme was checked in three ways. First, the basic expression for the transfer matrix was reduced to the isotropic case and compared to the cataloged expression found in Pestel and Leckie (7). Second, the solution for a solid orthotropic disk was computed and compared to the results of the previous section. Finally, a trial design of the modular ring construction similar to that of Figure 4 was investigated. A radius of 12 inches and a rotation velocity of 3000 radians per second were chosen such that the peak hoop stress in a Kevlar 49 ring would be somewhat less than 150 ksi. The resulting hoop and radial stress distributions are shown in Figures 6 and 7. The peak hoop stress is approximately 136 ksi while the inner Kevlar rings are understressed. The jump in hoop stress across the Kevlar/elastomer interface is obvious. The peak radial stress in Kevlar is above 10 ksi. This is not desirable and indicated either the need for a greater number of thinner Kevlar rings or choice of another elastomeric material, or both. The high radial stress in the steel ring at the inner hub results from the boundary constraint of zero radial displacement.

Considerable confidence in the model was gained from these three checks. An undocumented Fortran program is listed in Appendix A. The advantages of the method include the following items.

(a) It provides an "exact" solution within the assumptions of 2-D elasticity theory.

(b) It addresses routinely problems with layers made of different materials. The materials can be orthotropic or isotropic in elastic moduli. The method can be readily generalized to include orthotropic thermal expansion coefficients to study thermal and residual stresses. It can also be generalized to account for flywheels of varying thickness. The latter solution is approximate since an average layer thickness is used. Also the τ_{rz} and σ_z stresses are not accounted for.

(c) The scheme is computationally concise. A typical CPU time for the example problem is 0.05 sec on an IBM 370-165 system, level H.

SIMULATION APPROACH TO RELIABILITY

The conciseness of the above analytical scheme allows the practical application of simulation methods. Inherent to this approach is the necessity of making many (say 10,000) individual sample runs. Monte Carlo Simulation coupled with a sensitivity analysis has seen many systems applications including the design and reliability assessment of composite structures (4). Briefly, in this method one must:

(a) define fixed variables

(b) define random variables and their probability distributions (ex. material properties, geometry, loads and history)

(c) define constraints on system performance

(d) define failure mode criterion as a function of the random variables $Z = f(\bar{x})$ (ex. allowable strength - design stress)

(e) sample from each random variables population according to the MCS format and compute a value of Z. Perform sufficient number of replications and form a histogram of probability distribution of Z. Assess reliability of system for this failure mode.

(f) use sensitivity analysis methods to determine the percent variation of Z caused by each x_i .

The necessary number of replications is controlled by practical criteria, which can be found in advanced references. High reliability requirements require high numbers of replications, since the problem is addressing the extreme values in the tail of the Z distribution. The incorporation of a proof test is an excellent control on these extreme values with corresponding improvement in the reliability assessment.

A sample histogram excerpted from (4) is reproduced as Figure 8. Negative values of the random variable correspond to failure. The corresponding area under the curve enclosing the histogram is the probability of failure. The complimentary area is the probability of survival.

FAILURE MODES OF COMPOSITE FLYWHEELS

Consideration will be given to a wide variety of plausible failure modes including maximum stress states, fracture, static fatigue (stress rupture) and cyclic fatigue. The variability in material properties will be considered as will realistic load history.

CONCLUSIONS

Efficient analytical models suitable for the reliability assessment of several composite flywheel design concepts have been presented. The transfer matrix method is shown to be well-suited for simulation studies of complex flywheel designs such as the modular ring. Future studies will implement these tools in describing the mathematical reliability of selected concept designs and the failure modes.

References

1. M. L. Shooman, Probabilistic Reliability: An Engineering Approach, McGraw-Hill, 1968.
2. R. M. Stark and R. L. Nicholls, Mathematical Foundations for Design: Civil Engineering Systems, McGraw-Hill, 1972.
3. F. Moses and D. E. Kinser, "Optimum Structural Design with Failure Probability Constraints", AIAA J., Vol. 5, No. 6, June 1967, pp. 1152-1158.
4. R. E. Maxwell, R. H. Toland and C. W. Johnson, "Probabilistic Design of Composite Structures", ASTM STP 580 Composite Reliability, 1975.
5. J. N. Yang and W. J. Trapp, "Reliability Analysis of Aircraft Structures Under Random Loading and Periodic Inspection", AIAA J., Vol. 12, Dec. 1974, pp. 1623-1630.
6. R. F. Post and S. F. Post, "Flywheels", Scientific American, Vol. 299, No. 6, Dec. 1973, pp. 17-23.
7. E. C. Pestel and F. A. Leckie, Matrix Methods in Elastomechanics, McGraw-Hill, 1963.

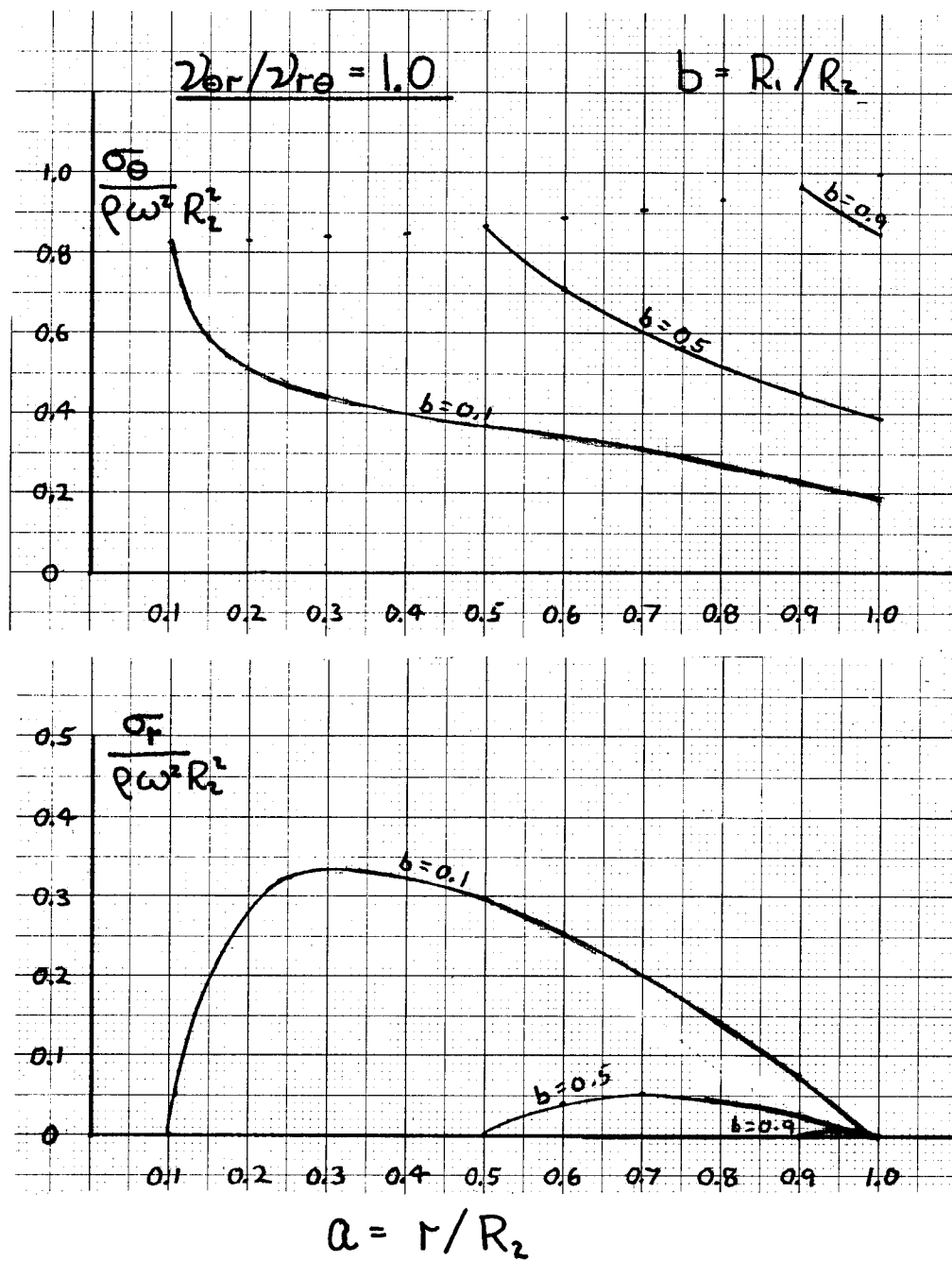


Fig. 2. Nondimensionalized hoop and radial stresses for a class of isotropic flywheels of varying width, b , but constant thickness.

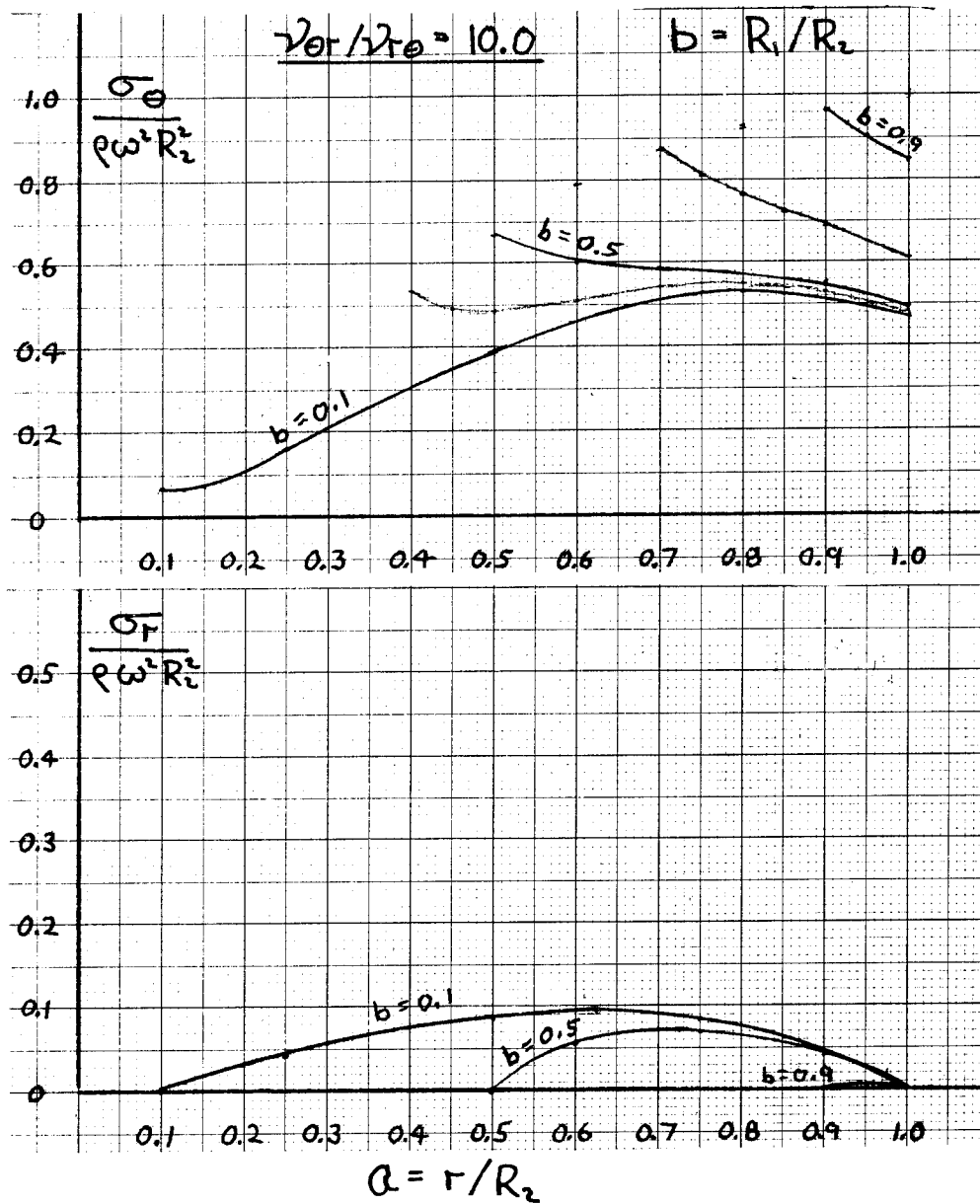


Fig. 3. Nondimensionalized hoop and radial stresses for a class of orthotropic ($E_{\theta}/E_r = 10$) flywheels of varying width, b , but constant thickness.

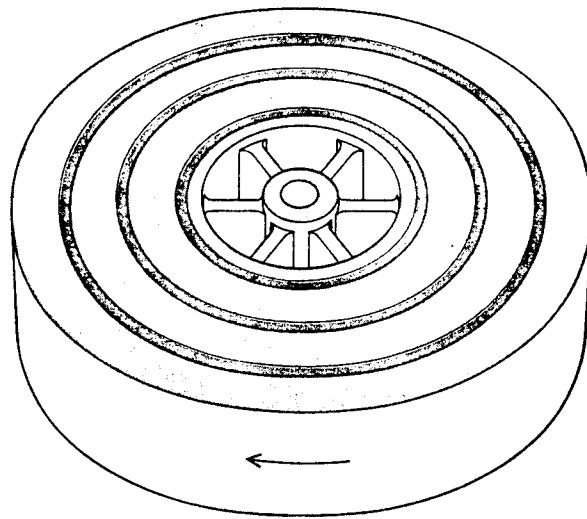
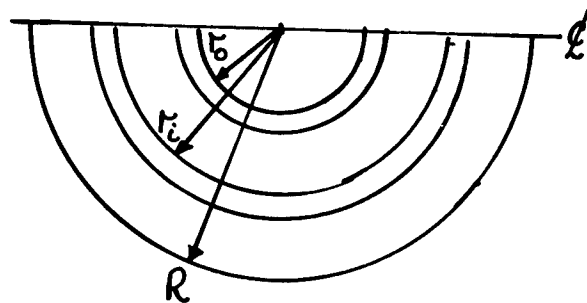


Fig. 4. Modular ring flywheel concept, [6].



$$\begin{aligned} r_i &= a_i R \\ r_n &= R \\ r_0 &= a_0 R \end{aligned}$$

Fig. 5. Transfer matrix parameters for a flywheel.

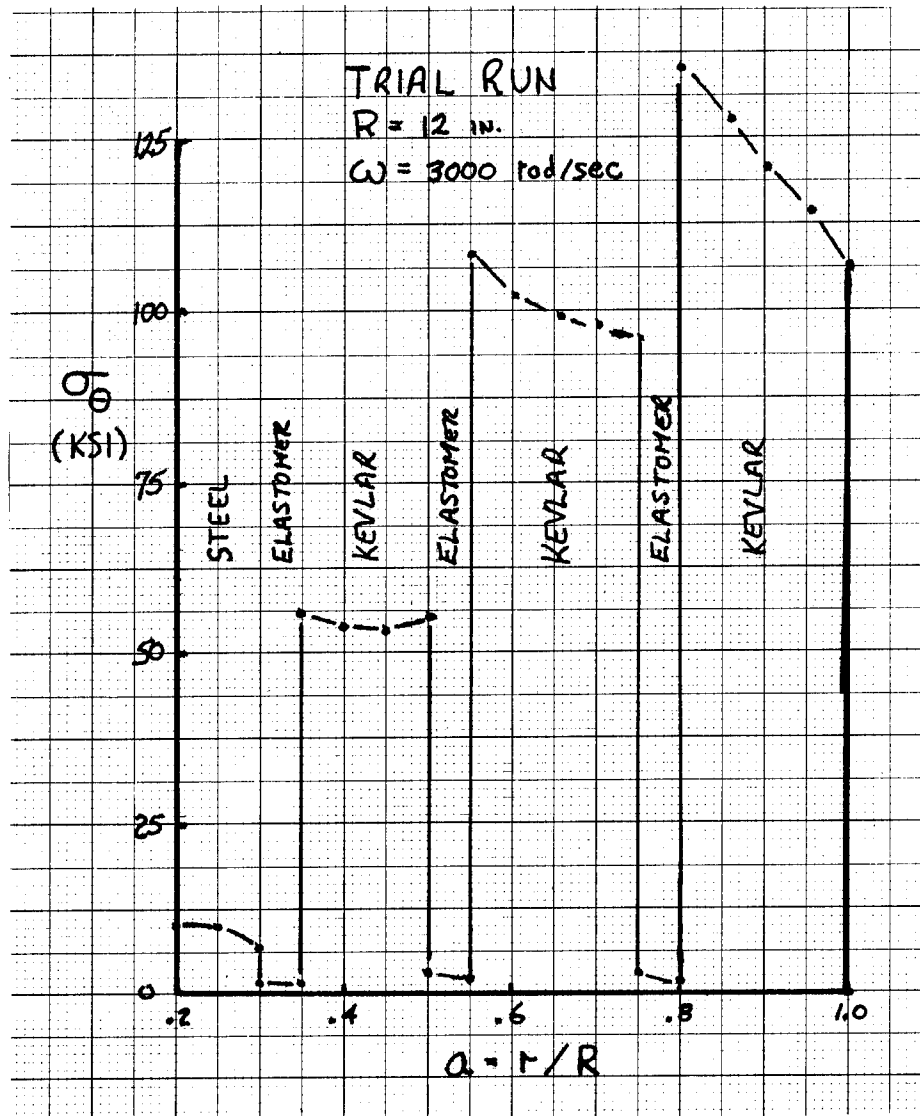


Fig. 6. Hoop stresses in a modular ring flywheel concept design computed by transfer matrix analysis.

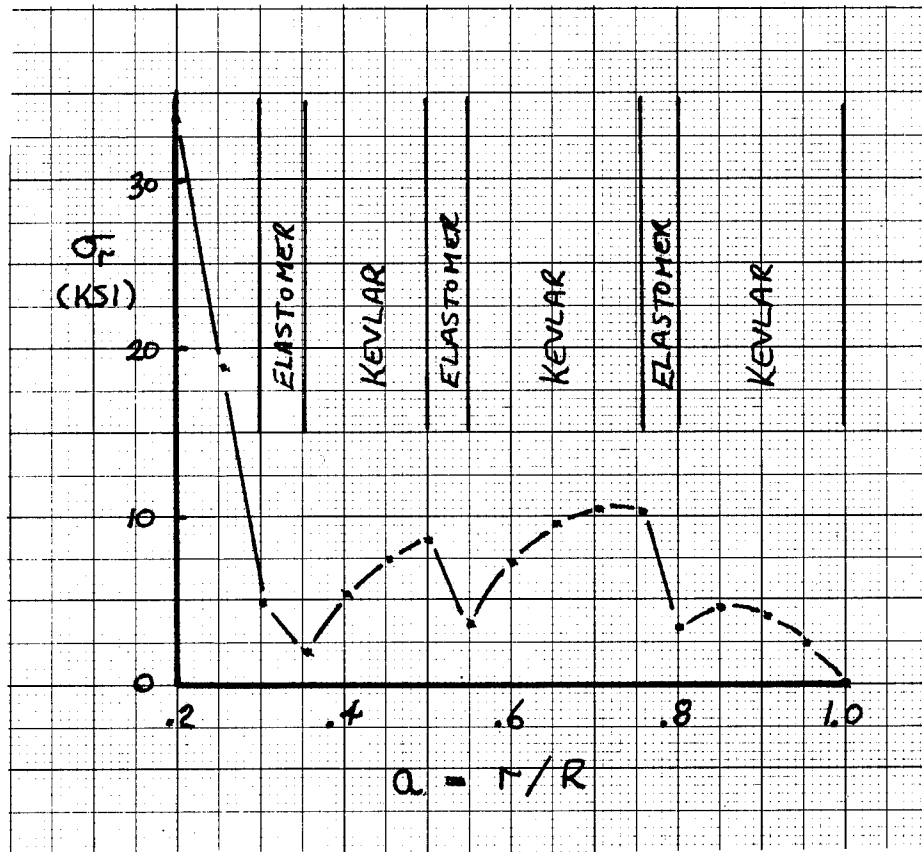


Fig. 7. Radial stresses in a modular ring flywheel concept design computed by transfer matrix analysis.

HISTOGRAM - MONTE CARLO SIMULATION

INITIAL TRUSS PROBABILITY OF FAILURE

RANDOM VARIABLE	SUMMED DENSITY FUNCTION	DENSITY	
-2708.494			
-2650.902	0.00031	0.00031	+
-2275.715	0.00145	0.00114	++
-2100.528	0.00386	0.00242	+++
-1825.341	0.00712	0.00326	++++
-1550.153	0.01044	0.00332	++++
-1274.956	0.01692	0.00648	++++++
-999.7788	0.02647	0.00955	++++++
-724.5916	0.03289	0.01343	++++++
-449.4043	0.05629	0.01640	++++++
-174.2172	0.07701	0.02072	++++++
100.9701	0.10149	0.02448	++++++
376.1572	0.12303	0.02154	++++++
651.3445	0.17017	0.03714	++++++
926.5317	0.21203	0.04186	++++++
1201.719	0.25992	0.04789	++++++
1476.906	0.30531	0.04538	++++++
1752.094	0.35466	0.04936	++++++
2027.281	0.40551	0.05084	++++++
2302.468	0.45755	0.05205	++++++
2577.655	0.50874	0.05119	++++++
2852.843	0.55048	0.04973	++++++
3128.030	0.61160	0.05312	++++++
3403.217	0.66201	0.05040	++++++
3678.404	0.70752	0.04552	++++++
3953.592	0.75280	0.04527	++++++
4228.777	0.79242	0.03963	++++++
4503.961	0.82808	0.03566	++++++
4779.145	0.86180	0.03372	++++++
5054.328	0.89133	0.02953	++++++
5329.512	0.91712	0.02580	++++++
5604.695	0.93597	0.01865	++++++
5879.879	0.95217	0.01619	++++++
6155.063	0.96472	0.01255	++++++
6430.246	0.97562	0.01090	++++++
6705.430	0.98402	0.00839	++++++
6980.613	0.98965	0.00563	++++++
7255.797	0.99323	0.00358	++++
7530.980	0.99570	0.00247	+++
7806.164	0.99767	0.00197	+++
8081.348	0.99853	0.00086	++
8356.531	0.99891	0.00038	+
8631.715	0.99924	0.00033	+
8906.898	0.99980	0.00057	++
9182.082	0.99992	0.00012	+
9457.266	1.00000	0.00007	+
9594.859			
MEAN=XB = 2710.40 XB+3S = 8541.52 XB-3S = -3120.71			
STANDARD DEVIATION=S = 1943.71 RANGE = 12383.4			
% NEGATIVE 7.9600 FROM EXTRAPOLATED NORMAL 0.81591D-01 CV(%) 71.713			
TOTAL SAMPLE SIZE = 10000			
CHI-SQUARE FOR NORMALITY = 96.2119 POS = 1.00000			
CORRELATION WITH NORMAL DISTRIBUTION = 0.992813			
% OF VARIATION EXPLAINED BY NORMAL DIST = 98.56779			

Fig. 8. Representative histogram of a failure probability by simulation methods, [4].

APPENDIX A

```

                                START OF
DIMENSION A(20),PHU(20),EHUOP(20),PR(20),RATIO(20),P11(20),P12(20)
1,P13(20),P21(20),P22(20),P23(20),U(20),SIGR(20),SIGH1(20),SIGH2(20)
1),AMASS(20),ERTIA(20),ENER(20)
READ(5,101)N,R,RV,H,G
101 FORMAT(I5,4F10.3)
READ(5,102)(A(I),I=1,N+1)
102 FORMAT(10F8.0)
DO 100 I=1,N
READ(5,103)PHU(I),EHUOP(I),PR(I),RATIO(I)
103 FORMAT(2E10.0,2F8.0)
A1=A(I)
A2=A(I+1)
AMASS(I)=PHU(I)*3.1416*H*((A2*R)**2.-(A1*R)**2.)*G
ERTIA(I)=0.5*AMASS(I)*((A2*R)**2.+(A1*R)**2.)
ENER(I)=0.5*ERTIA(I)*RV**2.
C1=SQRT(RATIO(I))
B1=(C1+PR(I))/(2.*C1)
B2=(C1-PR(I))/(2.*C1)
B3=EHUOP(I)/(2.*C1)
B4=(-(3.+PR(I))/(9.-RATIO(I))
B5=(RATIO(I)+3.*C1+3.*PR(I)+PR(I)*C1)/((9.-RATIO(I))*2.*C1)
B6=(3.*C1-3.*PR(I)+PR(I)*C1-RATIO(I))/(9.-RATIO(I))*2.*C1)
B7=(RATIO(I)-PR(I)**2.)/(2.*C1*EHUOP(I))
B8=(PR(I)**2.-RATIO(I))/(9.-RATIO(I))*EHUOP(I))
B9=(C1*RATIO(I)+3.*RATIO(I)-C1*PR(I)**2.-3.*PR(I)**2.)/(9.-RATIO(I))
1I))*2.*C1*EHUOP(I))
B10=(C1*RATIO(I)-3.*RATIO(I)-C1*PR(I)**2.+3.*PR(I)**2.)/(9.-
1RATIO(I))*2.*C1*EHUOP(I))
C11=B1*A1**((1.-C1)*A2**C1-1.)+B2*A1**((1.+C1)*A2**(-C1-1.))
C12=B3*(A1**(-C1)*A2**C1-1.)-A1**C1*A2**(-C1-1.)/R
C13=PHU(I)*(RV**2.)*(B4*A2**2.+B5*A1**3.-C1)*A2**C1-1.))+B6*
1A1**3.+C1)*A2**(-C1-1.))
C21=B7*R*(A1**((1.-C1)*A2**C1-1.)+B2*A1**((1.+C1)*A2**(-C1-1.))
C22=B1*A1**C1*A2**(-C1)+B2*A1**(-C1)*A2**C1
C23=PHU(I)*RV**2.*R**3.*(B8*A2**3.+B9*A1**3.-C1)*A2**C1+B10*A1**C
13.+C1)*A2**(-C1))
IF(I.GT.1) GO TO 10
P11(1)=C11
P12(1)=C12
P13(1)=C13
P21(1)=C21
P22(1)=C22
P23(1)=C23
GO TO 100
10 P11(I)=C11*P11(I-1)+C12*P21(I-1)
P12(I)=C11*P12(I-1)+C12*P22(I-1)
P13(I)=C11*P13(I-1)+C12*P23(I-1)+C13
P21(I)=C21*P11(I-1)+C22*P21(I-1)
P22(I)=C21*P12(I-1)+C22*P22(I-1)
P23(I)=C21*P13(I-1)+C22*P23(I-1)+C23
100 CONTINUE
SIGR0=-P13(N)/P11(N)
UN=P23(N)-P21(N)*P13(N)/P11(N)
SIGH0=PR(1)*SIGR0

```

```

      SIGHN=EHOOP(N)*UN/R
      DO 200 I=1,N-1
      SIGR(I)=P11(I)*SIGR0+P13(I)
      U(I)=P21(I)*SIGR0+P23(I)
      SIGH1(I)=EHOOP(I)*U(I)/(A(I+1)*R)+PR(I)*SIGR(I)
      SIGH2(I)=EHOOP(I+1)*U(I)/(A(I+1)*R)+PR(I+1)*SIGR(I)
200  CONTINUE
      WRITE(6,111)SIGR0,SIGH0
      WRITE(6,112)(SIGR(I),SIGH1(I),SIGH2(I),U(I),I=1,N-1)
      WRITE(6,113)SIGHN,UN
111  FORMAT(1X,E10.4,10X,E10.4,4X3H0.0)
112  FORMAT(1X,3E10.4,E10.4)
113  FORMAT(5X6H0.0 ,E10.4,10X,E10.4//)
      TMASS=0.
      TERTIA=0.
      TENER=0.
      DO 300 I=1,N
      TMASS=TMASS+AMASS(I)
      TERTIA=TERTIA+ERTIA(I)
      TENER=TENER+ENER(I)
300  CONTINUE
      WRITE(6,114)(AMASS(I),ERTIA(I),ENER(I),I=1,N)
      WRITE(6,115)TMASS,TERTIA,TENER
114  FORMAT(1X,3E10.4)
115  FORMAT(1X//1X,3E10.4)
      STOP
      END

```

Input

RHO - mass density
 EHOOP - E_{θ}
 PR - $\frac{\tau_{r\theta}}{E_r}$
 RATIO - E_{θ}/E_r
 A(I) - $a_i = r_i/R$

N - no. of layers
 R - outer radius
 RV - rotational velocity (rad/sec)
 H - thickness
 G - gravitational constant
 (set 1)

HYBRID CAR PROJECT BY LEMMENS ENTERPRISES

Joseph Lemmens
Lemmens Enterprises
248 Mayrand Street
St. Jean, Prov. Quebec
Canada

ABSTRACT

- I. Previous Study and New Concept I.V.T.
- II. Infinitely Variable Transmission.
- III. Lemmens Single Hybrid Transmission with Dual Function.
- IV. Specific Data About the Lemmens Hybrid Transmission.
- V. Conclusion.

PREVIOUS STUDY AND NEW CONCEPT I.V.T.

Lemmens Enterprises has been working in research, technical innovation and prototype building for the last ten years.

The different inventions that resulted were called the Infinitely Variable Transmissions and Hybrid Systems. Both systems use the well known continuously variable transmission (CVT) V-Belt and Pulleys.

Why the choice of V-Belt and Pulleys as C.V.T.?

V-Belts and Pulleys have proved their durability, capability, reliability and low cost.

1. In automotive application in the last years, Dof, even in racing in formula III.
2. In many manufacturing applications, harvester machines and farm equipment.
3. In snowmobiles, more than 1,000,000 (V-Belts and Pulleys) transmissions are King. No other C.V.T. manual or automatic transmission will be able to compete against them.

4. It is also the only C.V.T. that has rotating parts that cut the flywheel air drag by 50%. Ours will be the first practical hybrid car that does not need vacuum, pump, shield, special bearing and seals.

INFINITELY VARIABLE TRANSMISSION

OR

Dual power paths transmission using a direct drive, a C.V.T. drive, differential gearing in a new configuration that has a dynamic neutral like the Stroboscopic effect and an infinite variation of speed between maximum reverse speed and maximum forward speed.

Intensive tests led to the discovery of three main types of transmissions with characteristics suitable for the hybrid car project.

1. Medium torque increased at near stall speed: 2.5
2. High efficiency mid-to-top range speed: 90%
3. High horsepower capability: 150 to 200 H.P. with a C.V.T. Drive (V-Belt and Pulleys) weighing 60 pounds and industrial H.P. rating.

LEMMENS SINGLE HYBRID TRANSMISSION WITH DUAL FUNCTION

Intensive study and tests of three types of hybrid flywheel heat engine systems gave us:

1. A dual transmission hybrid configuration using only C.V.T. (V-Belt and Pulleys) is easy to build, but for a family car it needs a high volume (4 C.V.T.) and has high cost and complexity.
2. Dual transmission hybrid configuration using 2 Infinitely Variable Transmissions in the same configuration as the Hybrid Car by Lockheed (Popular Science, August 1973). This system is easy to build but also has a high volume, high cost and complexity.
3. Single Hybrid Transmission with dual function. The use of one Infinitely Variable Transmission with the flywheel fixed to the member of the C.V.T. varies speed inversely with the output shaft speed.

SPECIFIC DATA OF THE LEMMENS HYBRID TRANSMISSION

EFFICIENCY DATA

1. Actual known art; C.V.T. (V-Belt and Pulleys): 85% efficiency.
2. Single unit Lemmens I.V.T.: 90% efficiency.
3. Dual transmission flywheel hybrid round trip efficiency (RTE): $(90\%)^2 \times (90\%)^2 = 65\%$.
4. Single transmission flywheel hybrid RTE better than dual configuration: 65% to 75%.
5. Practical tests conducted with the S.T.F.H. dual function transmission gave:

(a) Input torque as high as 200 foot-pounds at 5,000 rpm.

(b) Output torque of 400 foot-pounds with a 30 H.P. engine at 2,000 rpm input speed. (Future possibility is 800 foot-pounds of torque with dual speed output shaft; maximum output shaft speed 5,000 rpm)

(c) Power density test: a test of extractive power on several occasions showed 7,000 to 3,000 rpm at the transmission flywheel weighing 150 pounds, 18" diam., in time ranging from 10 to 20 sec.

(d) Spindown tests: spindown test was conducted by running the engine at 2,000 rpm at the same time that the transmission spun the flywheel to 6,600 rpm. By uncoupling the engine and letting the flywheel rotate at atm. pressure, 7 minutes were required to dissipate the kinetic energy of the flywheel.

Kinetic energy store: around 300,000 foot-pounds.

Duration: 7 minutes or 420 sec.

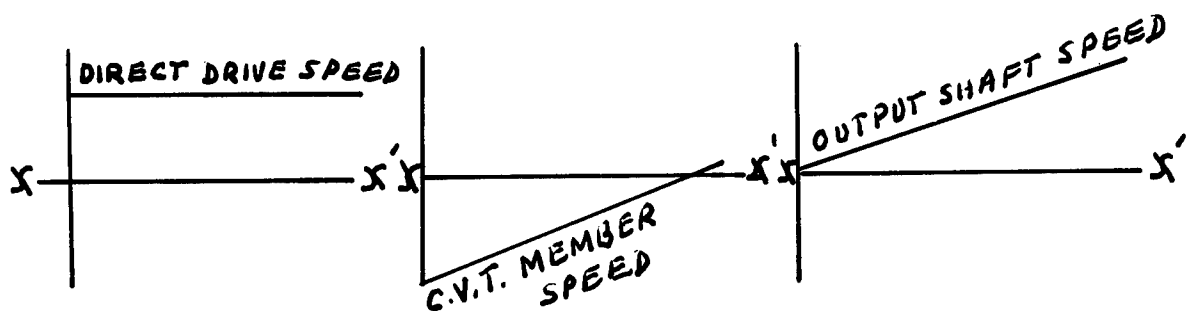
Horsepower loss in air-drag flywheel and transmission drag: less than 1 1/2 H.P. average.

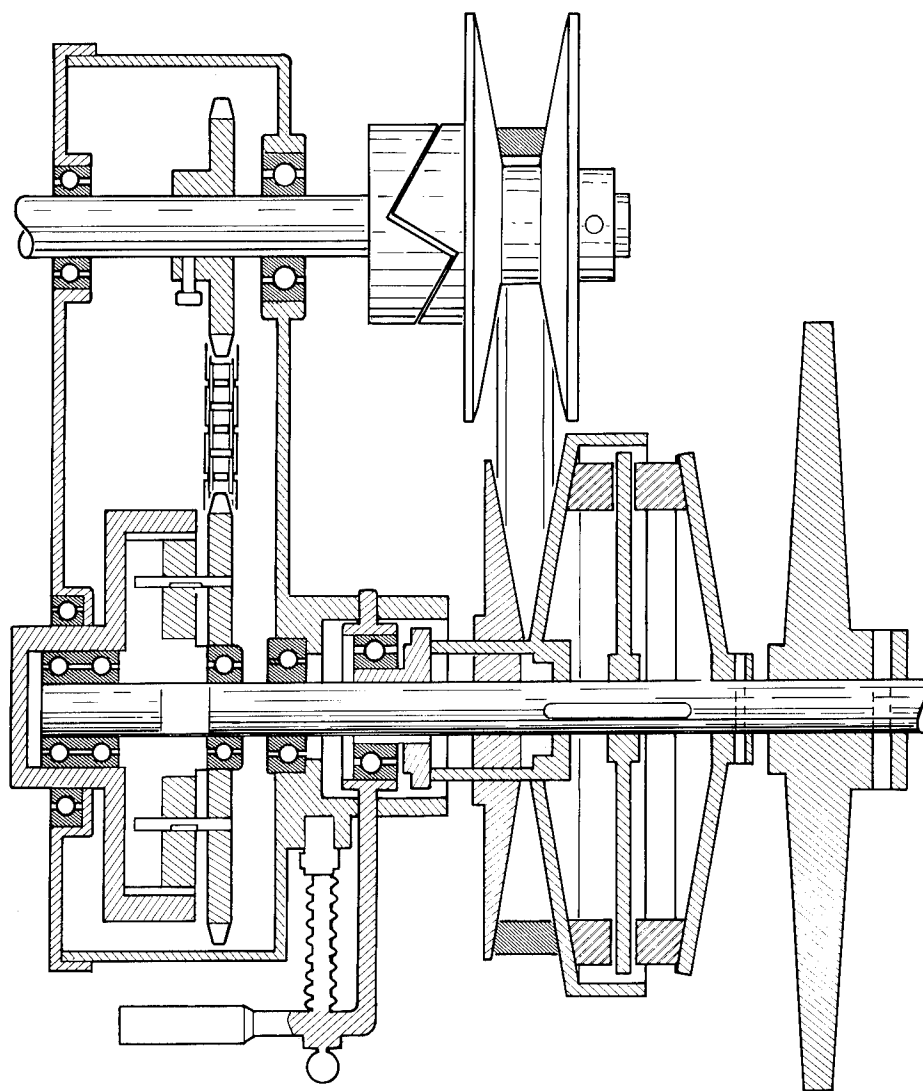
CONCLUSIONS

The single transmission hybrid:

1. Is already compact enough to fit under a family car hood.
2. Has an output capability of 200 H.P.
3. Will be ready to sell for specific utilization in 1976.
4. Does not change the weight of the car or the driver's habits and "feel".
5. Cost will be competitive with 4 speed and transmissions with lock-up system.
6. Techniques are much easier than actual automatic transmissions, considering that the whole system has only 100 or fewer parts, instead of the usual 300 to 400.
7. A fuel improvement of 200%, which means \$300 gas saving when driving 15,000 miles a year.
8. Gives a pollution decrease of 400% due to the steady running of the engine; a 200% decrease in pollution and the 200% improvement in fuel consumption add up to a fantastic 400% improvement.

SCHEMATIC EXAMPLE OF THE SINGLE HYBRID TRANSMISSION IN RELATION TO THE CONTROL POSITION





FABRICATION AND THERMAL STRESS IN COMPOSITE FLYWHEELS*

Robert C. Reuter, Jr.
Sandia Laboratories, Advanced Energy Projects
P. O. Box 5800
Albuquerque, New Mexico 87115

ABSTRACT

This paper analyzes the stresses that can occur in fiber composites, particularly Kevlar 49/epoxy composites, suitable for flywheels. Fabrication stresses are characterized by analytical modeling of four fabrication phases: winding, heating to cure temperature, heating at cure temperature and cooling. The final state of stress depends on winding tension, cure temperature and the properties and dimensions of the mandrel, fiber and matrix. Thermal stresses related to changes in service temperature are treated in terms of geometry, mechanical and thermal orthotropy and Poisson effects.

INTRODUCTION

Energy storage performance of composite flywheels could be seriously limited by stresses in the wheel due to fabrication and temperature variations. It is very important that the effects of parameter changes on fabrication and thermal stresses be fully understood so that optimizations can be performed and efficient flywheels designed.

DISCUSSION

Composite materials have been suggested for flywheel applications because of certain advantages they have over their isotropic counterparts. These advantages include high specific strength, ease of fabrication and the ability to fail gracefully. These are strong and important advantages, and they should continue to provide an impetus for advanced composites development for flywheels.

There is a class of composite flywheels that can be treated as a multiply-connected continuum for analytical purposes and that possess cylindrical orthotropy. These composites include those fabricated by winding continuous wet or preimpregnated filaments over an elastic mandrel under some prescribed winding tension. While it is this type of composite flywheel which will be addressed most directly, the analytical tools developed for this study are also applicable to arbitrarily laminated rings and polar weave composites.

In addition to the advantages that composites register for flywheel applications, they also possess features which could be considered liabilities. These features are: 1) the general inability of the above class of composites to withstand a uniform temperature change without generating internal stresses, and 2) the general inability to fabricate composites of this class without building in fabrication, or residual, stresses.

Fabrication stresses are characterized through analytical modeling of four fabrication phases. The first is the winding phase, where continuous filaments are wound under tension over a mandrel until the final thickness is achieved. The matrix material is assumed to have no load carrying capability during this process. The winding process creates a general state of radial compression throughout the cylinder, or disc, and also generates either tension or compression in the circumferential direction, depending on the winding tensions. It is possible that overwrapping internal layers causes them to lose their original winding tension and drives them into compression. This could lead to local buckling of the fibers.

The second process is that of heating the composite to its cure temperature. Differential thermal expansion at the mandrel and thermal anisotropy of the composite cause a redistribution of stresses that existed after winding. The matrix

*This work was supported by the United States Energy Research and Development Administration.

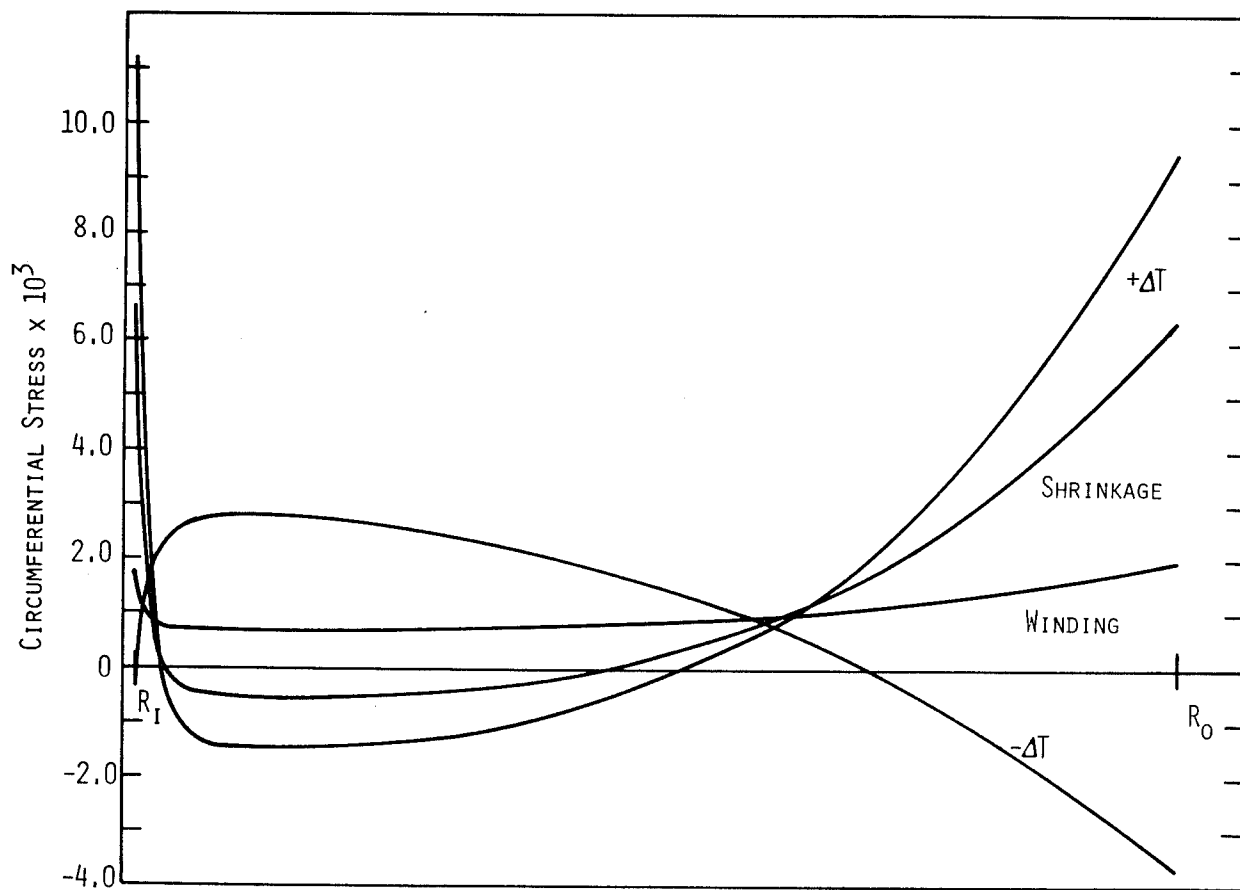
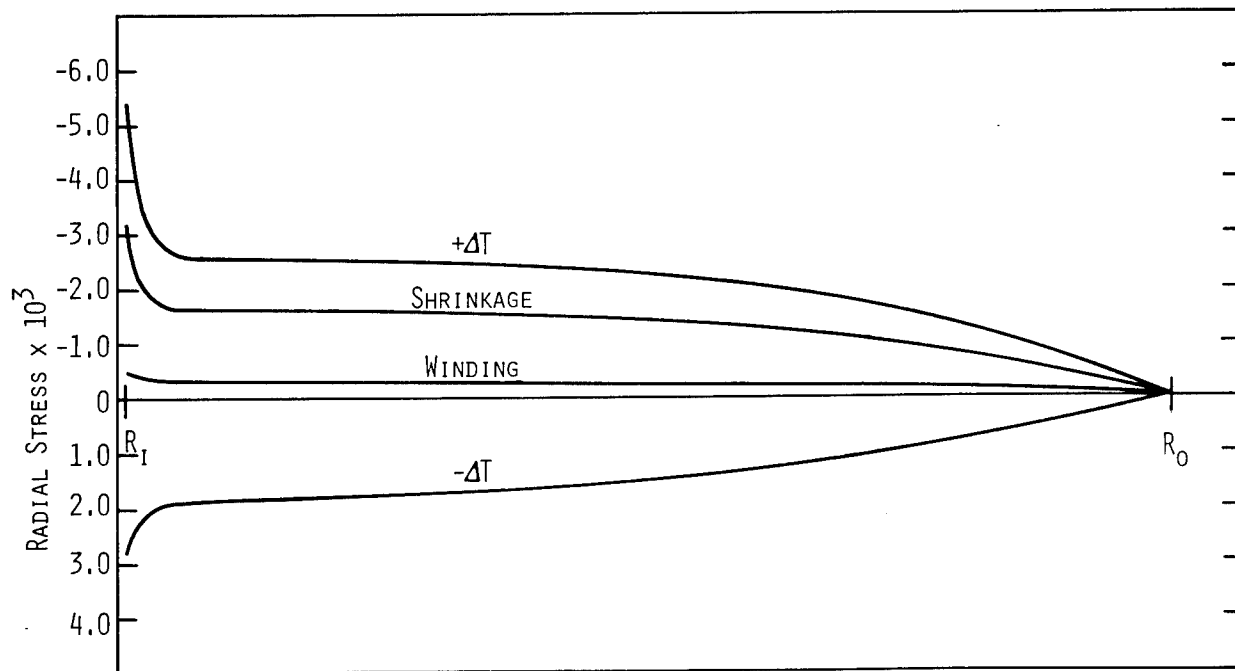
material still carries no load. The third process is that of allowing the matrix material to shrink and cure to its final properties, thus causing another redistribution of stress. Finally, the cured composite is allowed to return to room temperature. This also causes a redistribution of stress. The final state of stress can be quite varied, depending on winding tension patterns, cure temperatures, the dimensions and material properties of the mandrel, fibers and matrix of composites. Final stress can, however, be tensile stress in the radial direction, which reduces the performance capability of the flywheel.

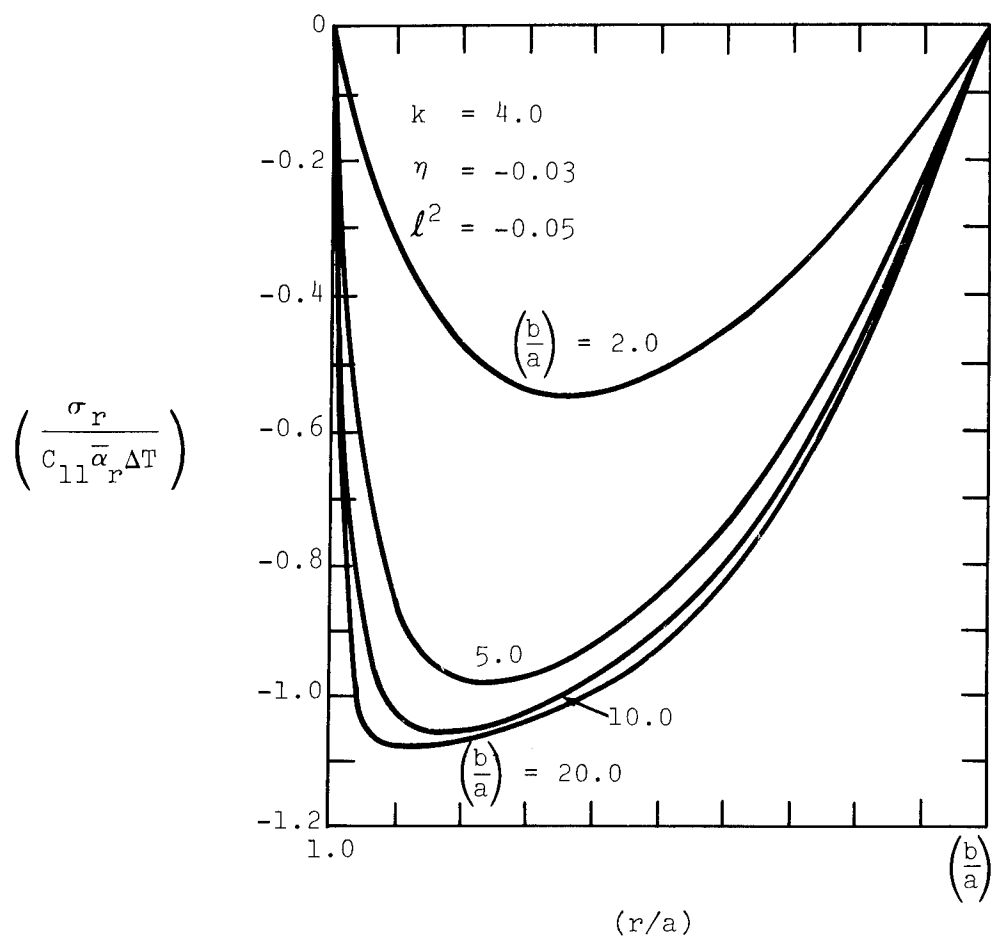
Thermal stresses also occur as service temperatures change. Four independent parameters are all that are required to characterize the thermal stresses due to uniform temperature changes in the subject class of composites. They are

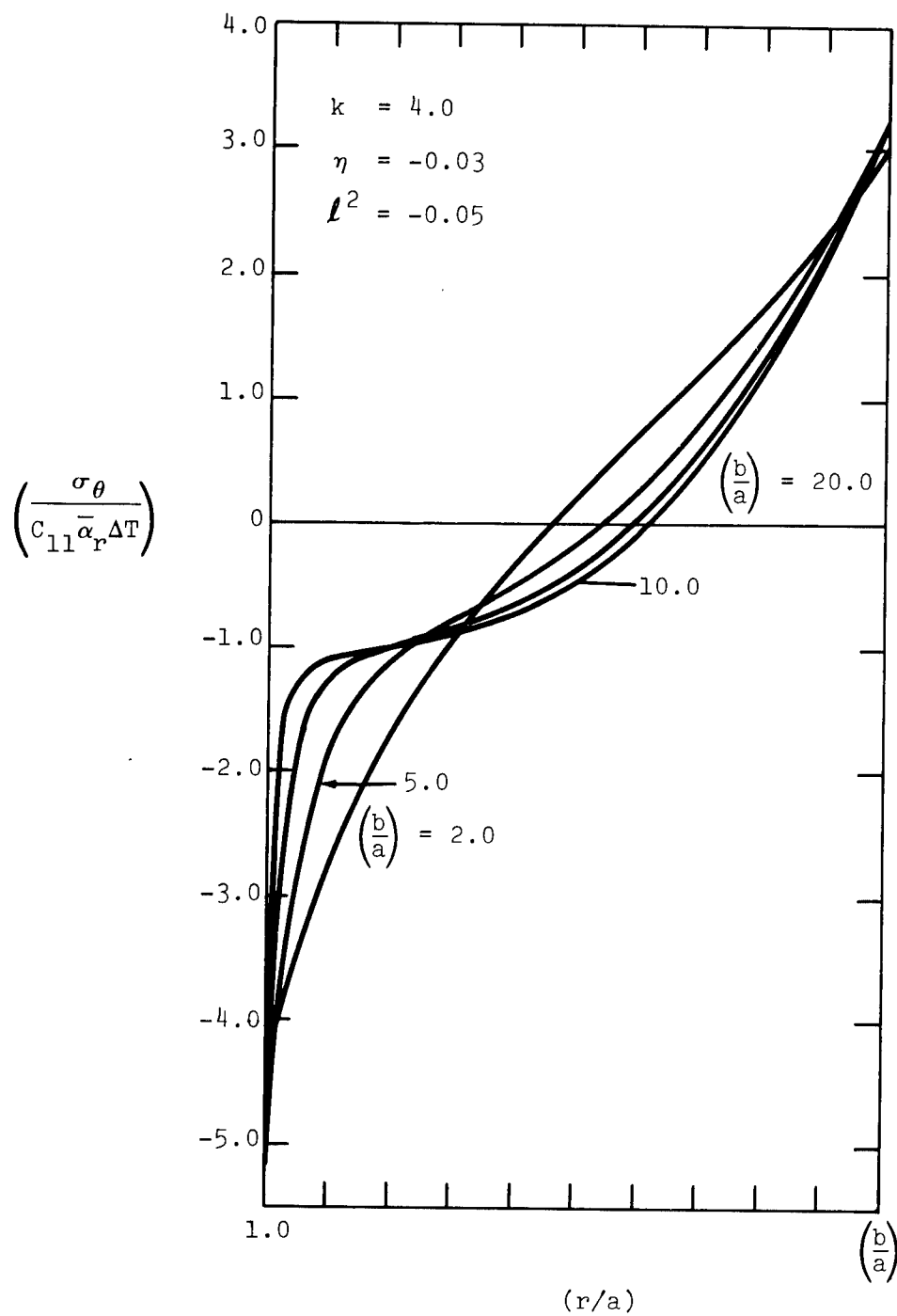
<u>Parameter</u>	<u>Which Characterizes</u>
(b/a)	Geometry
k	Mechanical Orthotropy
ν^2	Poisson Effects
n	Thermal Orthotropy

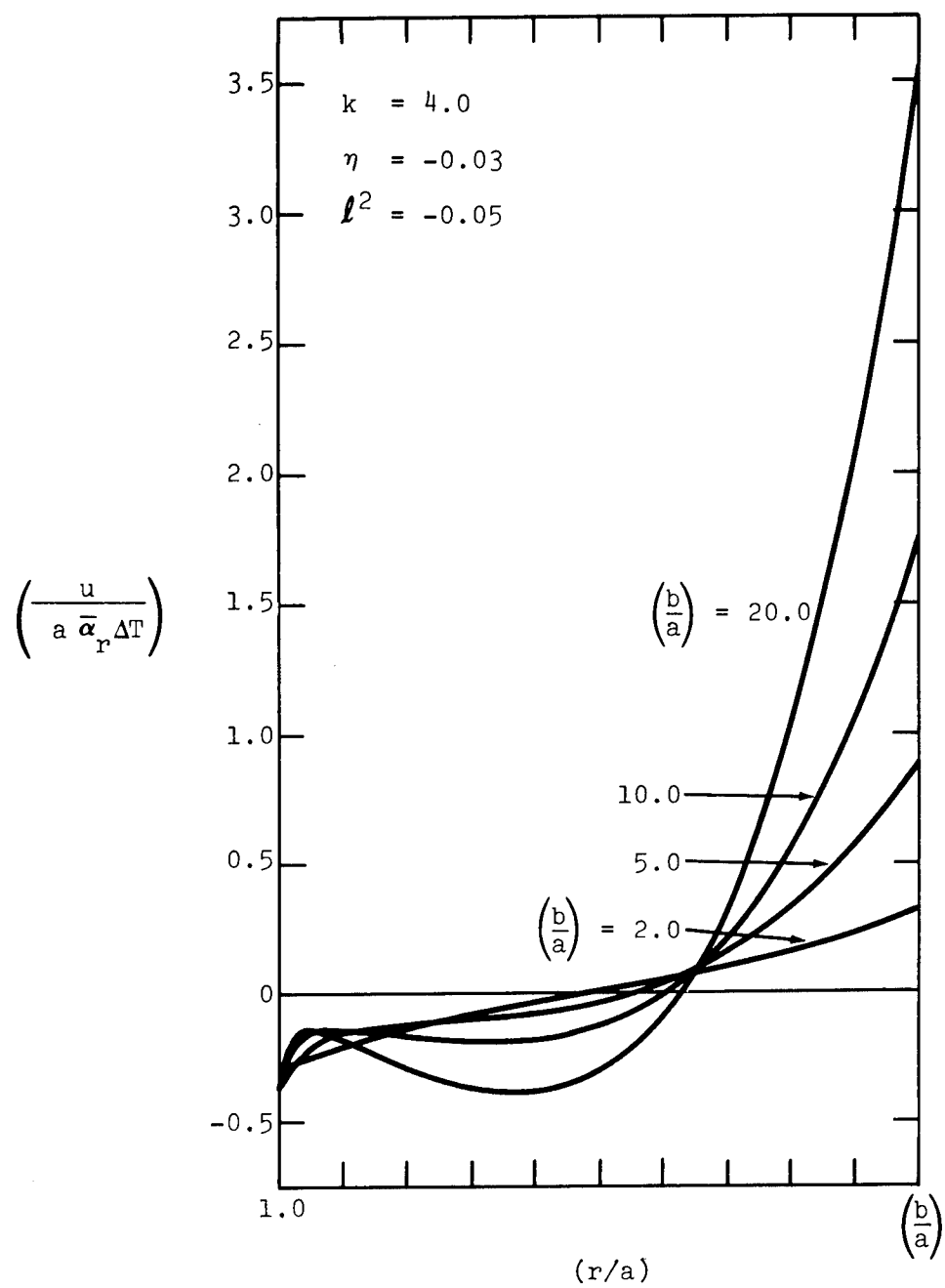
Numerical results for thermal stresses attributable to variations in the above parameters are presented. In most cases the properties of a Kevlar 49/epoxy resin composite are used. For flywheels with (b/a) of about 20, radial tensile stresses of about 30 psi/°F are possible after cooling to room temperature. This is significant compared to strengths in this direction of the order of 2000-3000 psi.

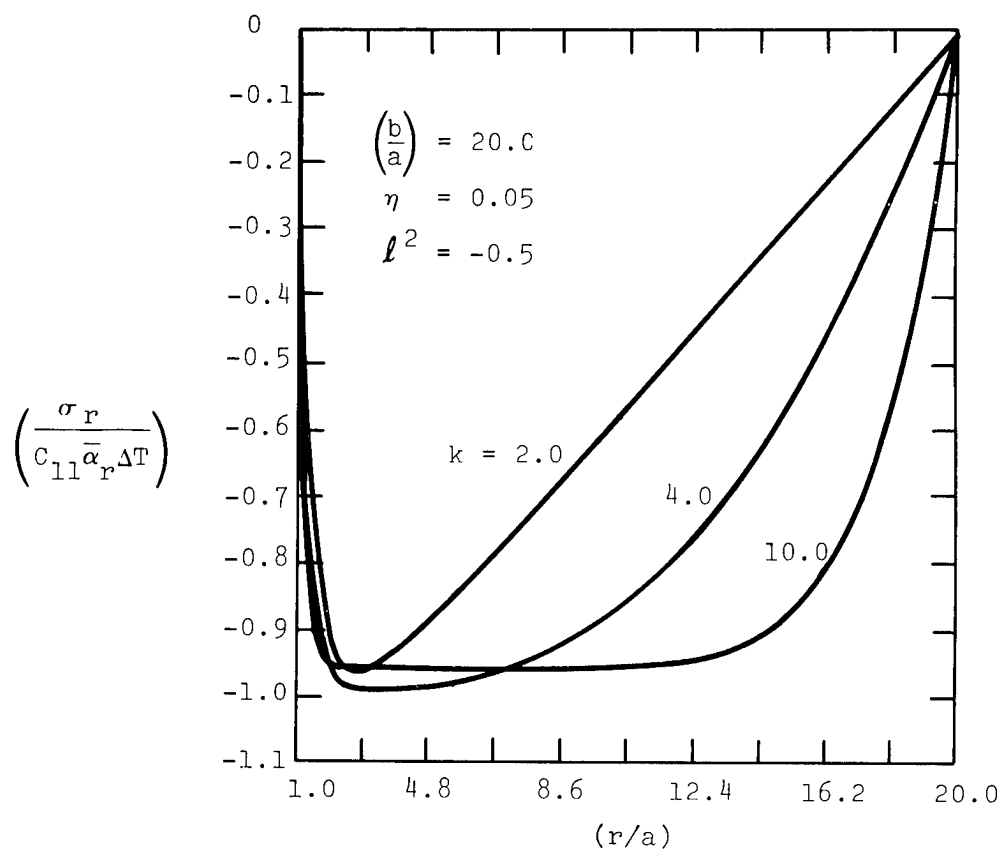
Fabrication stresses of Kevlar composites are shown in the figures below. These results should be added to those of the thermal stress problem to obtain total stress states.

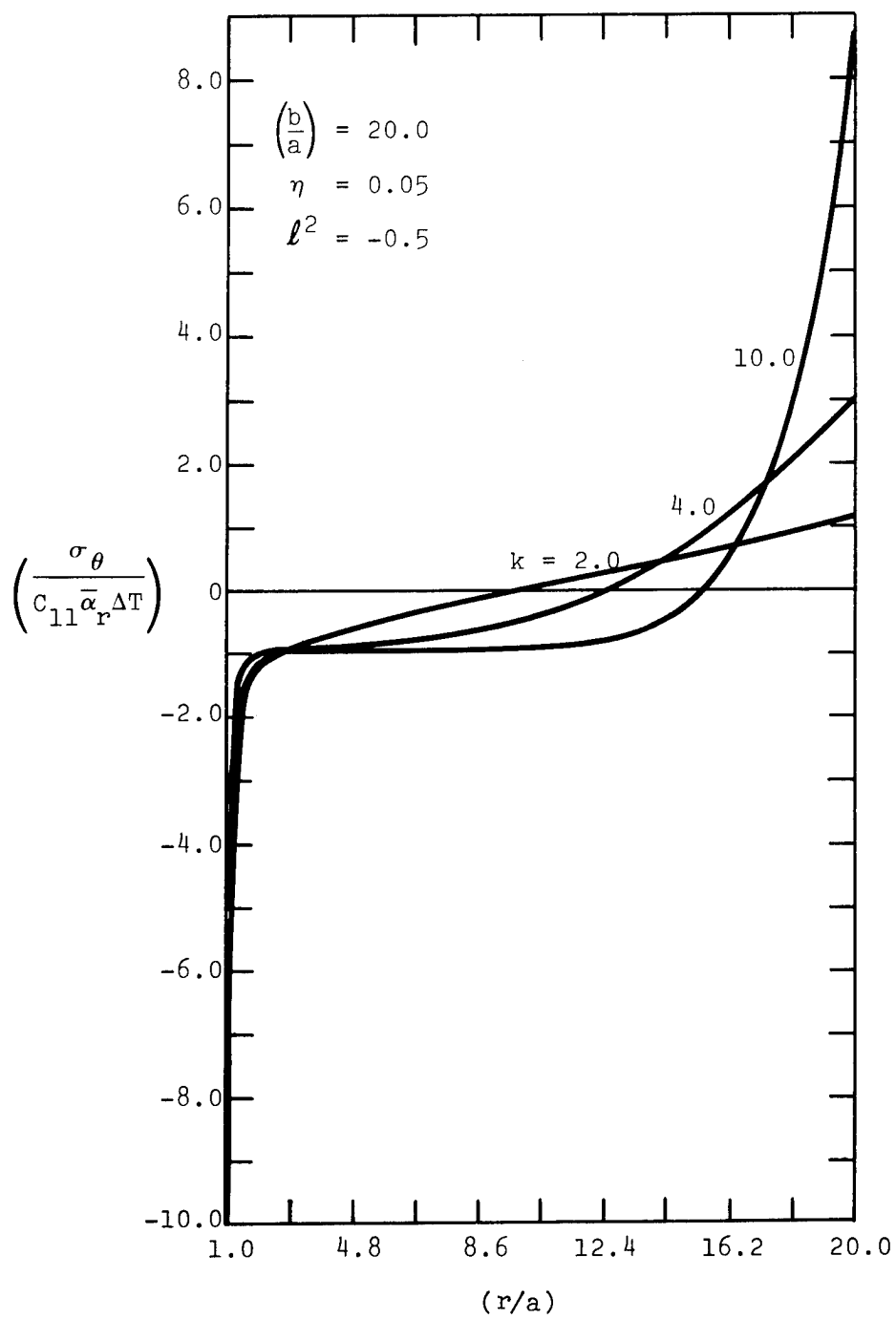


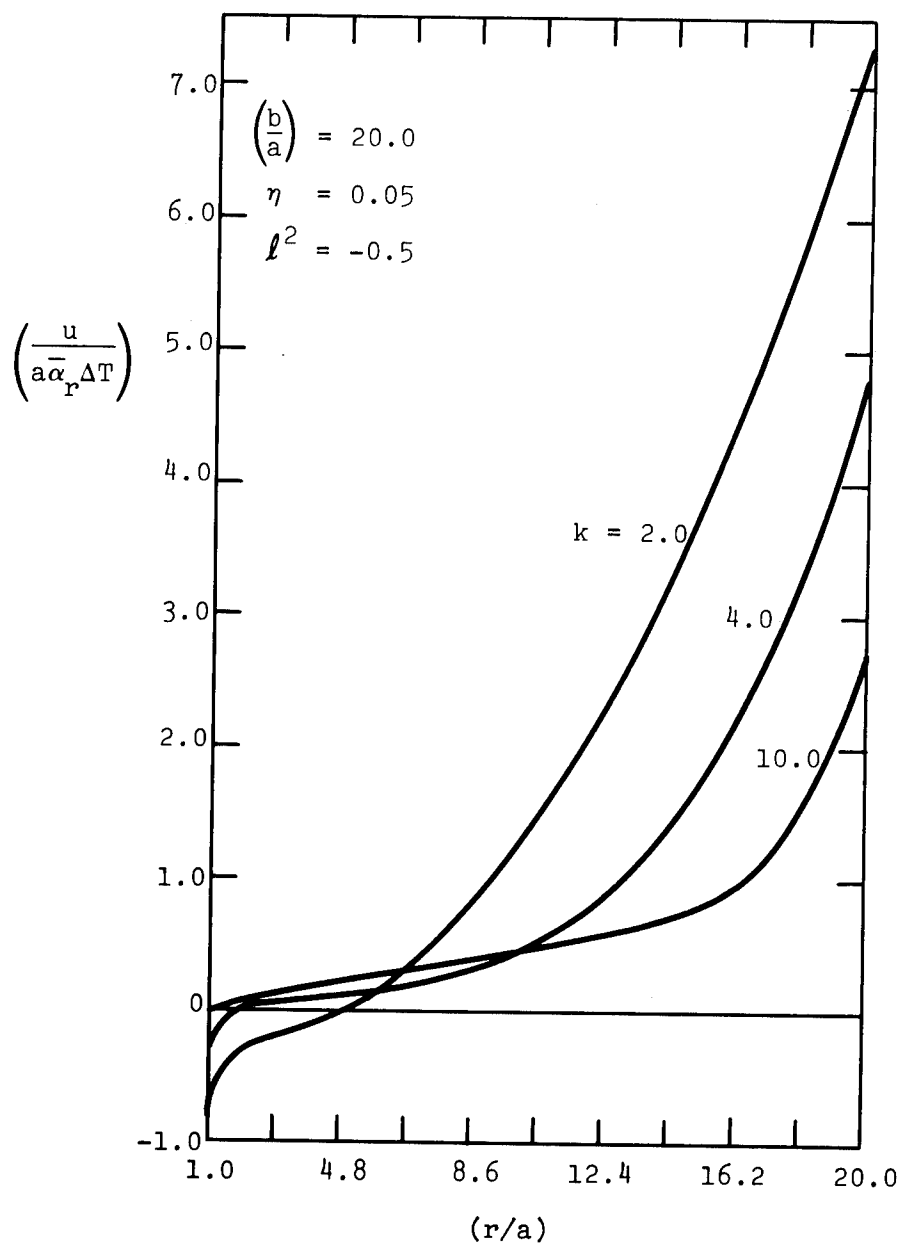


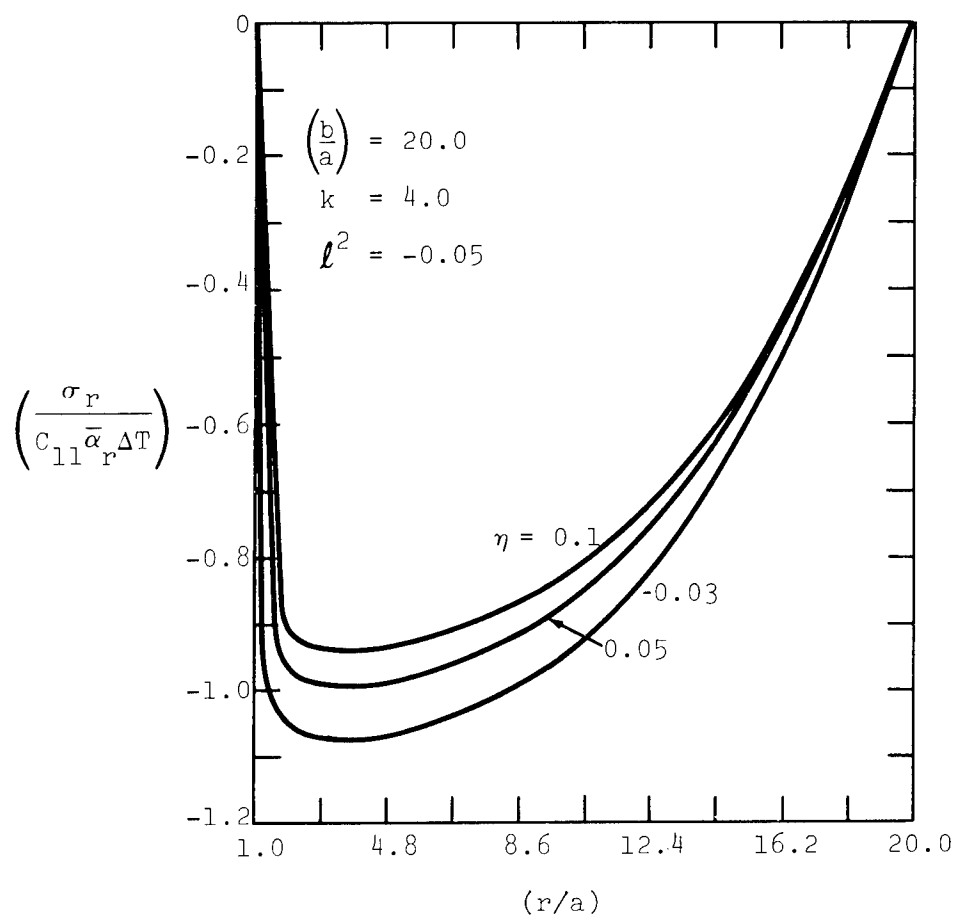


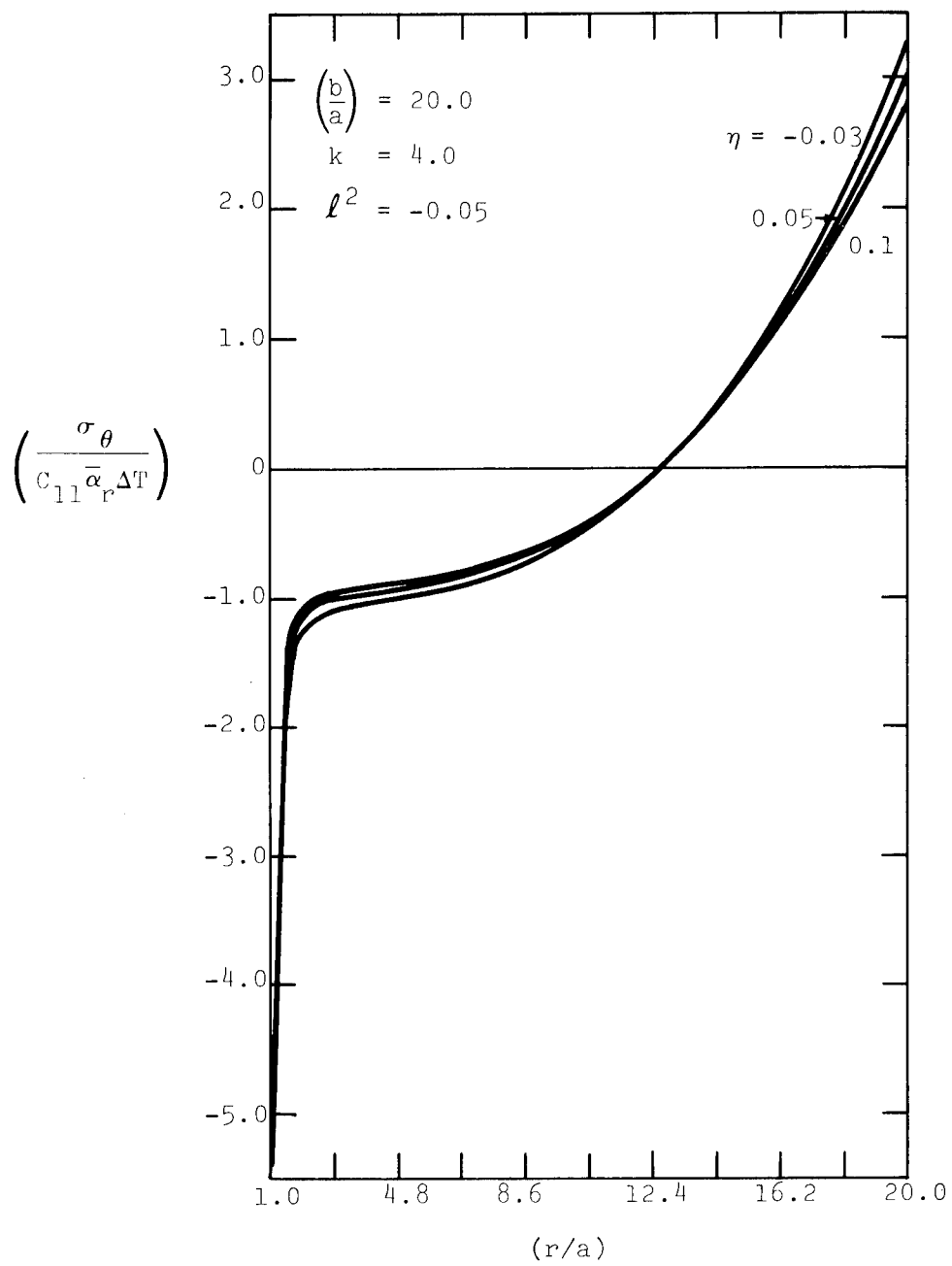


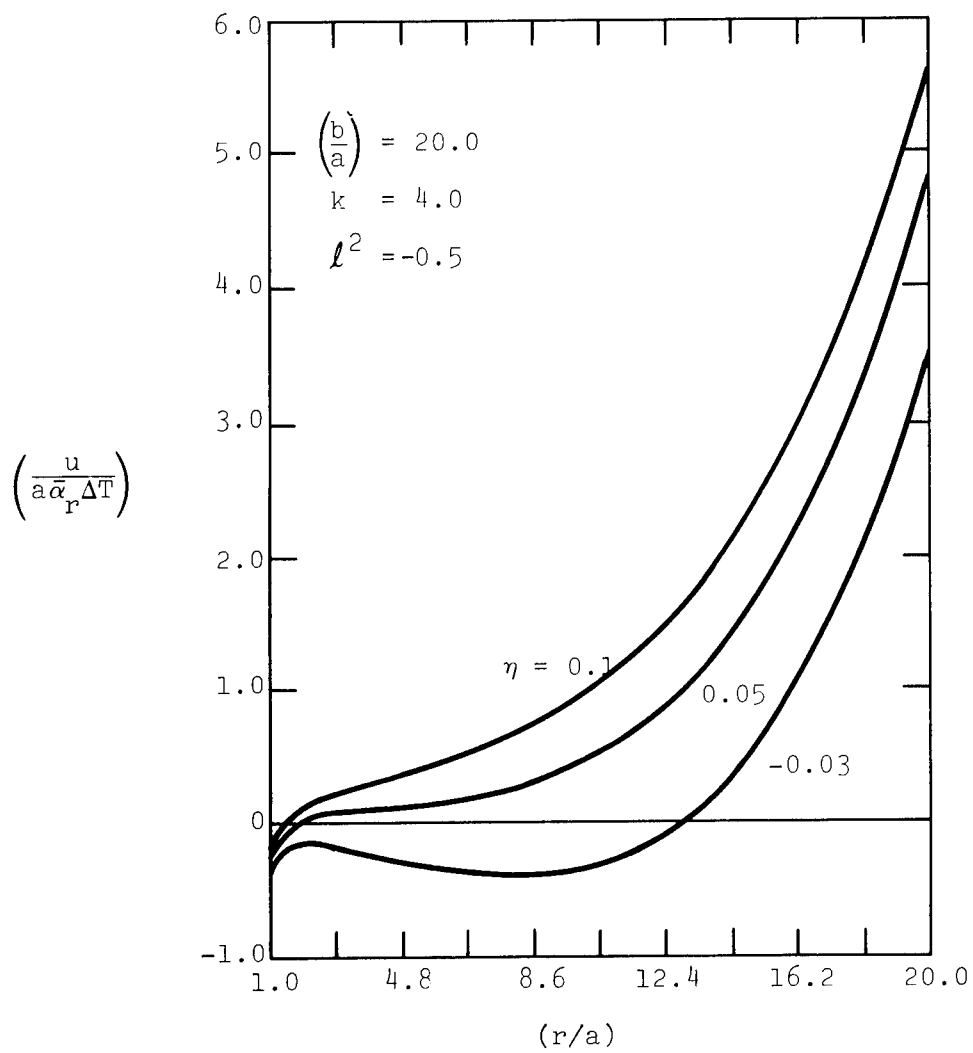


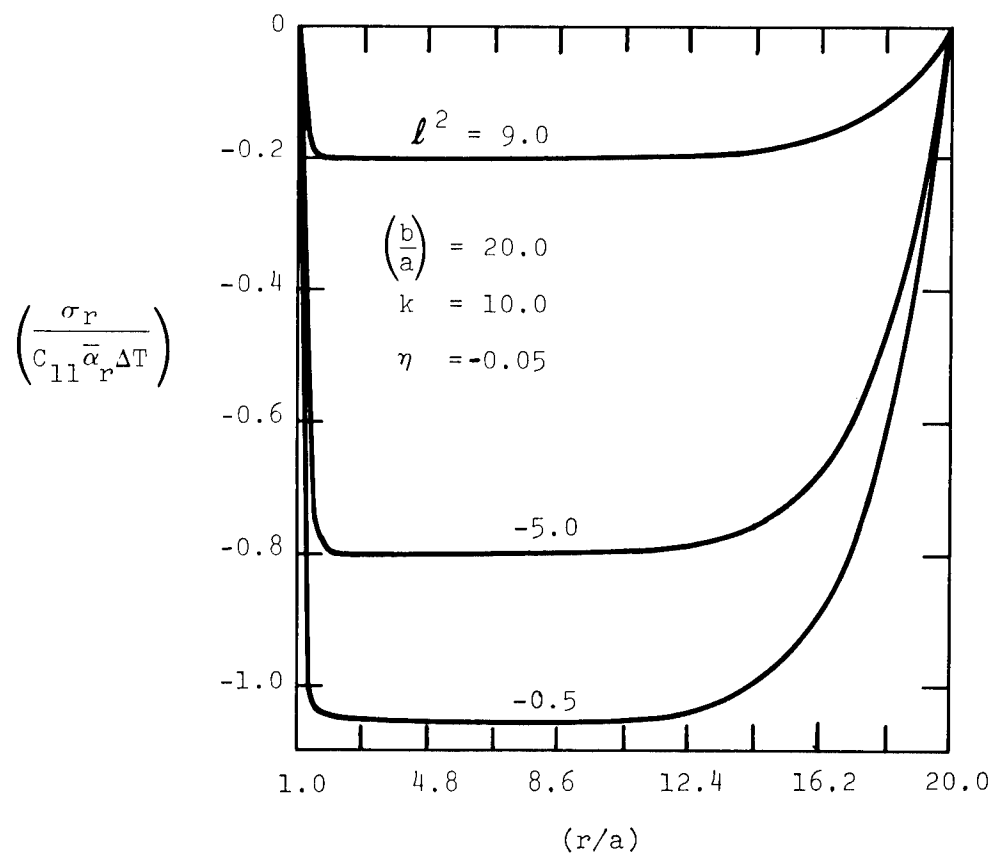


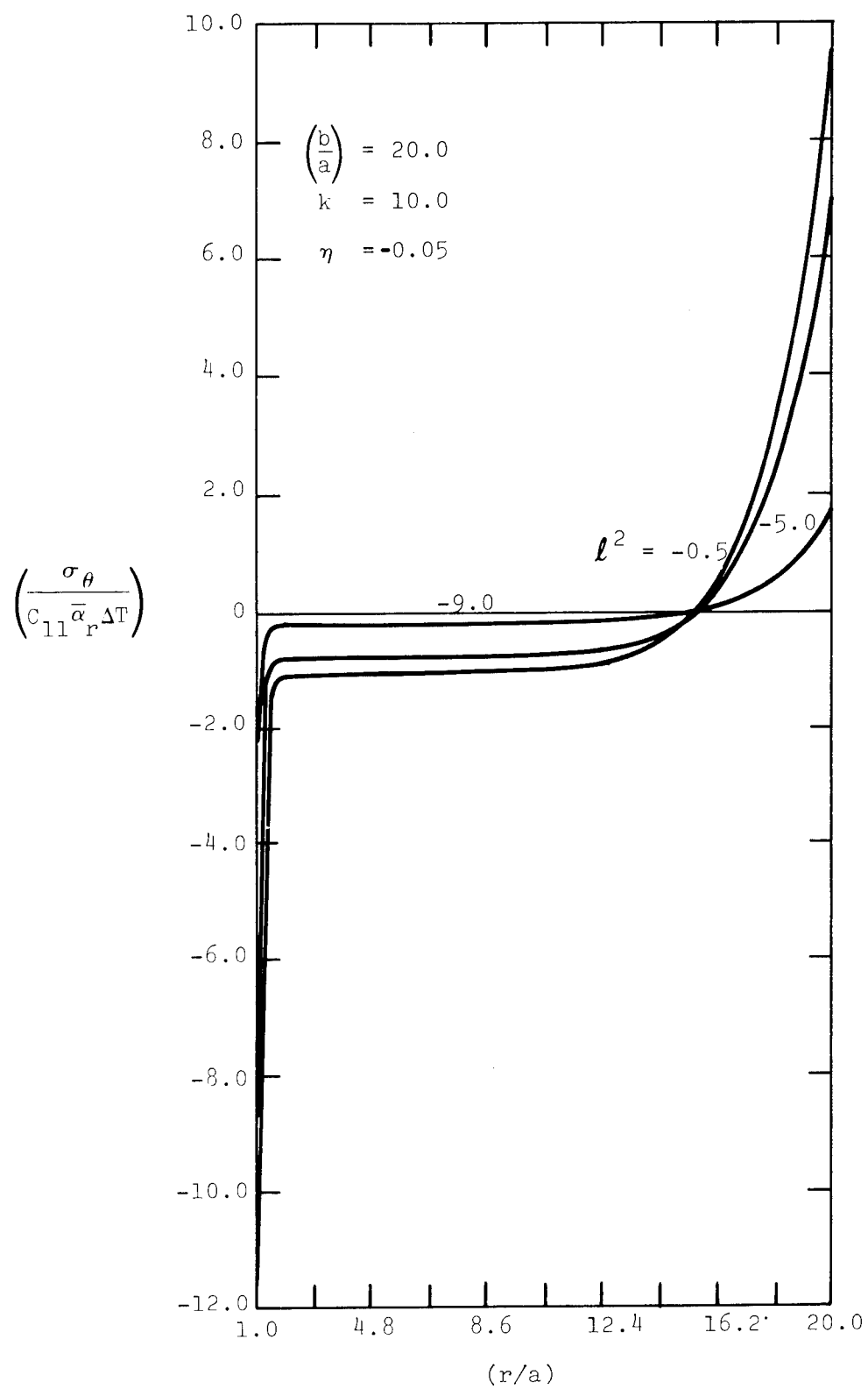


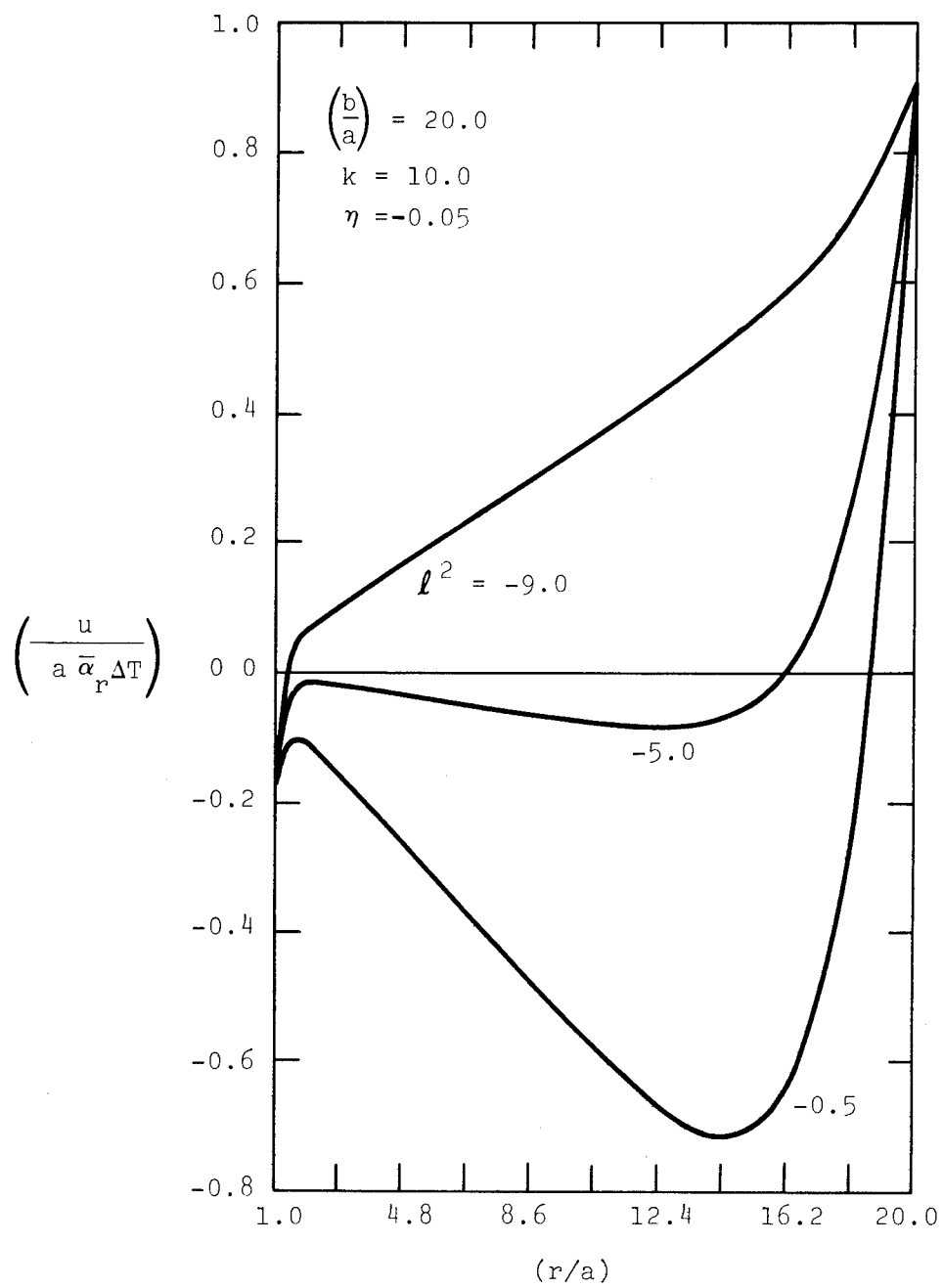












DESIGN AND MANUFACTURING CONSIDERATIONS FOR COMPOSITE FLYWHEELS

William E. Dick
Senior Design Engineer
Defense Products Division
Brunswick Corporation
4300 Industrial Avenue
Lincoln, Nebraska 68504

ABSTRACT

Important design and manufacturing variables for composite flywheels are considered. A computer analysis of the inertial stress distribution in two flywheel designs is presented, and theoretical and experimental results of a thermal stress study for Kevlar/epoxy flywheels are discussed.

INTRODUCTION

Much has been written and said about the energy storage potential of composite flywheels. It is well known that, due to their high specific strength, high performance fiber-composites offer a significant advantage over other materials such as steel.

Flywheel efficiency can be stated as "energy storage potential per swept volume" and is defined by:

$$E_v = K_s \frac{\sigma}{\rho},$$

where σ/ρ is the specific strength of the material and K_s is a function of the flywheel geometry. For fiber-composites, σ/ρ is high only in the direction of the fibers, so that fiber orientation is an important design consideration.

Many design concepts have been proposed which attempt to make optimum use of composite properties. Shape factors (K_s) for several flywheel geometries are given in Table 1. Basically they can be placed in two groups. One group is the brush or rod type which orients the fibers in the radial direction. The other is the filament wound type which orients the fiber in the circumferential direction. Included in the second category are flat discs, concentric rings, thin rings, and flared discs. From the viewpoint of shape factor and producibility, the filament wound flywheels seem to offer the most advantages. A shape factor of 0.3 to 0.4 in non-balanced wheels is readily attainable. Filament winding technology of pressure vessels and rocket motor cases can, with some work, be extended to flywheels. This report is limited to filament wound flywheels.

TABLE 1

SHAPE FACTORS FOR VARIOUS FLYWHEEL GEOMETRIES

GEOMETRY	K_s
Layup Or Pultrude	
Thin Rod	0.05
Brush Type	0.1
Filament Wound	
Thin Ring	0.05
Flat Disc	0.3
Flared Disc	0.4
Concentric Rings	0.3-0.4

INERTIAL STRESS EFFECTS

Much of the published analytical work on flywheel stresses has concerned itself with inertial loading. Computer programs have been developed by Brunswick and others which predict the stresses, strains and deflections in any circumferentially wound flywheel design. Details of the analysis will not be covered here, but a brief summary of the stress distribution in two different designs will be presented.

Flat Disc. The flat disc is the most elementary form of filament wound flywheel, and all other designs can be considered as a variation on it. Because of this, it is a useful analytical tool and the results can be extended to other de-

TABLE 2

PROCESSING VARIABLES

<u>VARIABLE</u>	<u>EFFECTS/POTENTIAL PROBLEMS</u>	<u>CONTROLS</u>
Winding Tension	Residual Fiber Stress Fiber Volume Composite Uniformity	Programmed Winding Tension Uniform Band Tension
Cure Schedule	Thermal Stress Cure Shrinkage	Low Or Room Tempera- ture Cure Resin Systems Stepped Cure (Or B-Stage)
Band Width	Composite Uniformity Winding Angle Production Rate	Optimize For Particu- lar Design
Laydown Reversals/ Cut Fibers (Layer Termination)	Surface Uniformity Mechanical Properties Near The Surface	Programmed Laydown Gel Coats
Other Considerations	Vacuum Winding For Void Free Composite Kevlar Affected By Rela- tive Humidity Wetwinding Vs Pre-Impregnation Etc.	Depends On Specific Design And Pro- cessing Require- ments

signs. In Figure 1 is a plot of the hoop and radial stress distribution for a sixteen-inch diameter Kevlar*/epoxy flywheel at 40,000 rpm. Two radial moduli (E_r) are shown to illustrate the strong effect of resin modulus. For most Kevlar composites, the transverse tensile strength is in the range of 4000 to 5000 psi, while the maximum working stress in the fiber direction is around 280 ksi. A radial modulus of 10^6 psi can be achieved with resin systems commonly used in filament winding but, for the design illustrated, results in excessively high radial stress. A speed of 40,000 rpm can be realized with a radial modulus of 0.256×10^6 psi; however, the design is still critical with respect to radial stress. Obviously, a refinement in the design is necessary to achieve a 280 ksi composite hoop stress prior to failure in the transverse (radial) direction.

Concentric Rings. One variation on the flat disc geometry is the concentric ring design. In Figure 2, one of the discs from Figure 1 is divided into four concentric rings and separated by a low modulus (10^3 psi) material 0.13 inch thick. The effect on the radial stress is dramatic. However, care must be taken in the design of the system for attaching the rings to each other in order to avoid fatigue and vibrational problems. Further optimization of this design can be accomplished by varying the ring thickness and the material properties through the wheel.

MANUFACTURING CONSIDERATIONS

Processing is as important to flywheel performance as design. However, there has been very little published work on manufacturing considerations. Perhaps this is because a filament wound flywheel appears deceptively easy to produce. There are, however, many processing variables which must be understood and controlled to produce a flywheel that meets its performance potential. Several of the more important variables are summarized in Table 2 along with some of the effects they can have on a flywheel. Only two, winding tension and cure schedule, will be discussed in detail. Obviously other processing variables such as band width, layer termination, winding environment and special material handling procedures must be considered in the actual production of a flywheel.

Winding Tension. For any filament wound composite part, accurate and uniform winding tension control is necessary to produce a uniform composite. Uniformity is especially critical for flywheel balance.

One major effect of winding tension is fiber volume. A high winding tension results in a high fiber volume, which in turn leads to a higher specific strength in the fiber direction but, in general, poorer transverse properties. Thus, a trade-off must be considered by the designer.

Finally, an obvious effect of winding tension is the residual fiber stress in the finished part. Excessive residual tensile stresses reduce the effective maximum operating hoop stress of the flywheel. Compressive fiber stress can lead to fiber buckling and in some cases matrix cracking. In thick composites such as occur with most flywheel designs, compressive stress can be a significant problem. It results from the inward radial deflection of a layer due to the pressure of succeeding layers and is a function of winding tension, of anisotropy and of resin migration of the uncured composite. An example of the effect of winding tension on compressive radial stresses is shown in Figure 3. Two identical E-glass/epoxy flat discs were wound--one with a constant ten pounds tension and the other with a programmed decreasing tension. The fiber buckling evident in the constant tension wheel is completely eliminated with programmed tension.

Cure Schedule. To a great extent, the composite cure schedule is determined by the resin system selected for the part. In the case of flywheels, their thick sections demand that careful attention be paid to the effect of the cure cycle on the finished wheel. In particular, the thermal stresses generated by elevated cure temperatures can be significant. In Figure 4 are positive prints of X-ray photographs of two flywheels cured at 130°F and 300°F, respectively. The photographs show clearly the potential effect of a high cure temperature resin system on a Kevlar/epoxy flywheel. In Figure 5 are the results of a thermal stress computer program for a filament wound Kevlar/epoxy disc, which show radial tensile strain due to a 50°F reduction in tempera-

*DuPont Kevlar^R Aramid Fiber, Type 969

ture. The experimental results in this figure show good agreement with theory. This effect not only applies to cool down during the cure cycle but can also result from environmental temperature changes after the flywheel is in operation.

An experimental study performed by the Brunswick Corporation confirmed these analytical predictions. The X-ray photographs shown in Figures 6 and 7 indicate the effects of cooling on the residual radial stress of Kevlar/epoxy discs. After initial strain gage measurements, the discs were progressively cooled from 100°F in 25°F decrements and strain gage data was reported. After each temperature decrement, the discs were also X-rayed. Figures 6 and 7 are the X-ray photographs taken at 50°F, 25°F, 0°F and -25°F. They show that a single circumferential crack occurred between 50°F and 25°F at approximately one-third the distance from the inner to the outer diameter. Two more cracks appeared between 0°F and -25°F. The location of the cracks is significant, because they occurred at regions of maximum radial stress, as predicted by analysis and confirmed by strain gage readings.

The strain gage results taken at each temperature level are plotted in Figure 8. Here the strain levels shown are the difference between the radial strain gage reading and the amount the composite wants to strain due to its radial coefficient of thermal expansion. This differential strain is indicative of the radial stress, (i.e., for an isotropic material ϵ_g would equal $\alpha_R \Delta T$ and there would be no stress.). The increasing tensile stress, with decreasing temperature, is evident until the first crack appears at 25°.

The location of the delamination corresponds to the region of maximum tensile strain. The crack acts as a stress relief mechanism and the tensile strain decreases on either side of the crack. This process continues as the composite is progressively cooled. Obviously these cure-related thermal stresses must be controlled. A room-temperature cure resin system or a carefully controlled stepped cure program are two methods which can be used for this purpose.

Resin shrinkage during cure has an effect similar to thermal stress, since it leads to residual radial tensile stress. The cure schedule can also be used to control, to some extent, the effect of resin

shrinkage and resin migration. By step curing or step B-staging the composite, some of the resin shrinkage of the inner layers is allowed to take place prior to winding subsequent layers. This reduces one significant source of compressive hoop and tensile radial residual stresses.

CONCLUSION

The technology of composite flywheels is still in its infancy, and there is a great deal of work yet to be done. Most of the work done has treated design and configuration, and it appears that the tools do exist for selecting and optimizing a flywheel design. But effort cannot stop there, because it is equally important to have a complete understanding and adequate control of processing variables. Without them, the full design potential of the "super-flywheel" cannot be realized.

FIGURE 1

STRESS DISTRIBUTION IN A FILAMENT WOUND FLAT DISC KEVLAR/EPOXY FLYWHEEL

COMPOSITE HOOP MODULUS (E_θ) = 12.8×10^6 psi, ω = 40,000 RPM

OUTSIDE DIAMETER = 16 INCHES, INSIDE DIAMETER = 6.4 INCHES

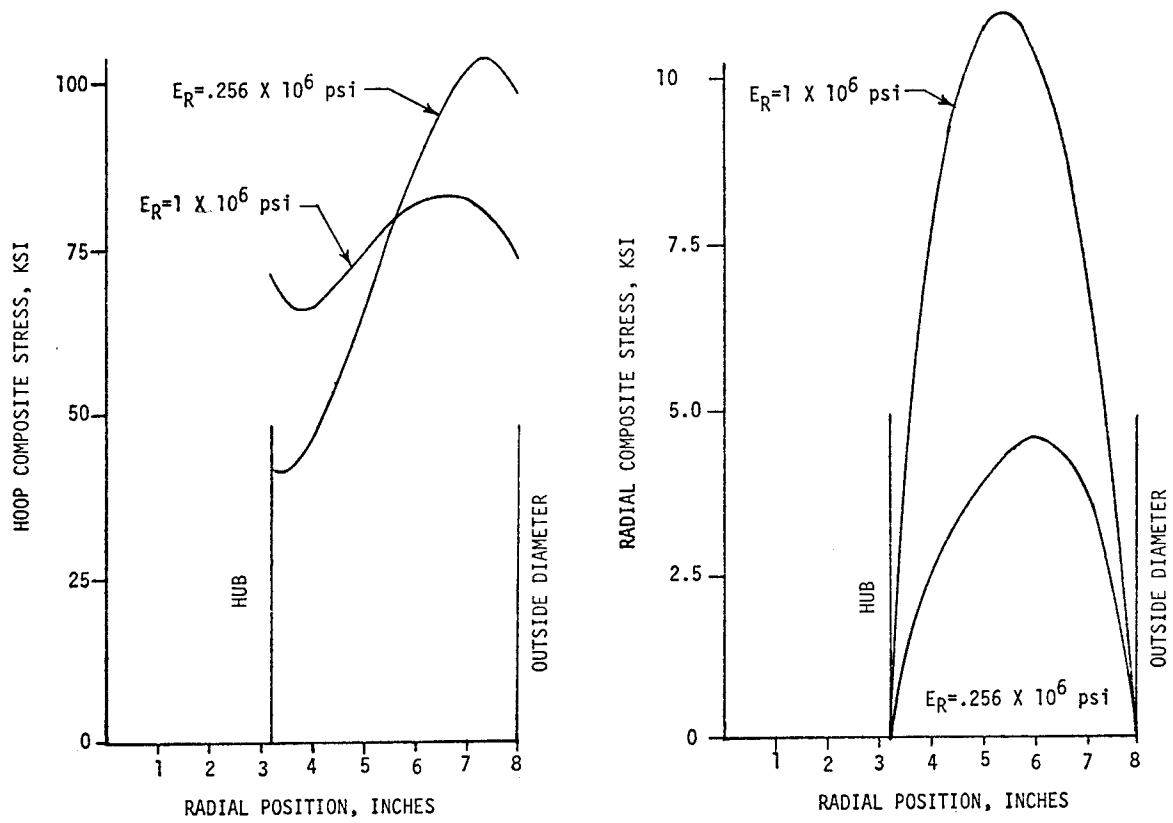
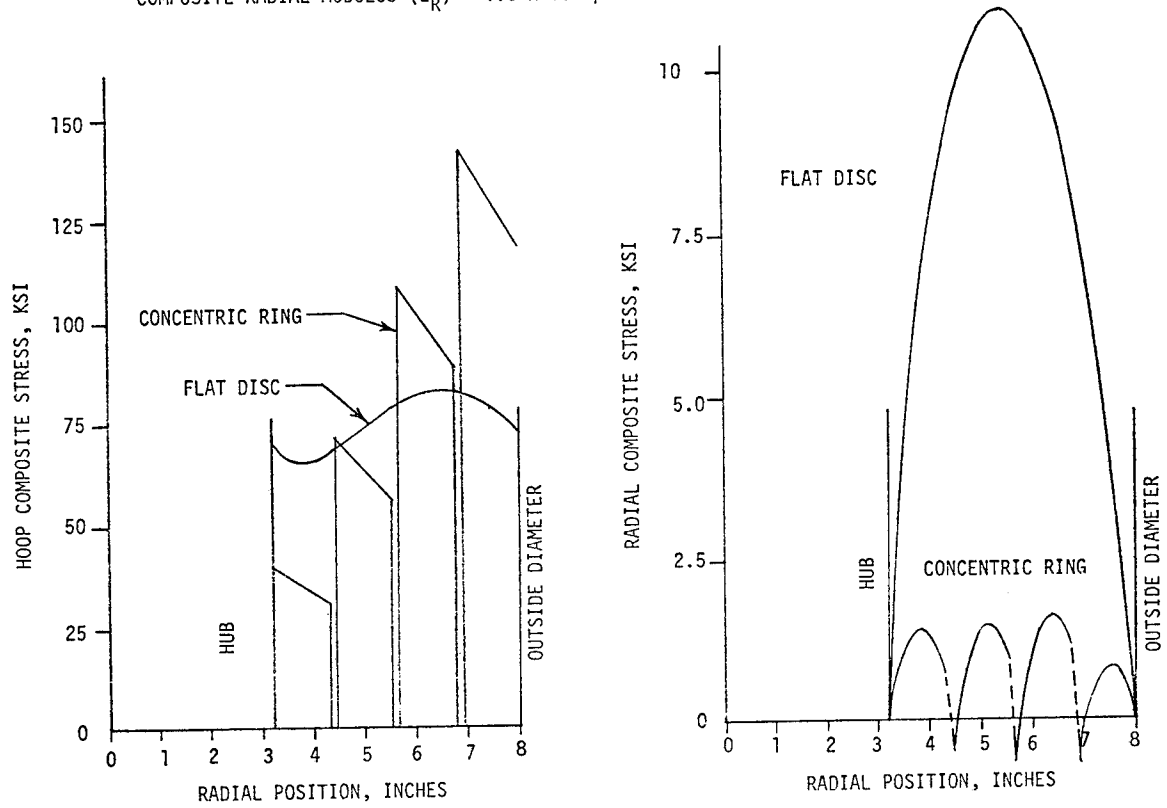


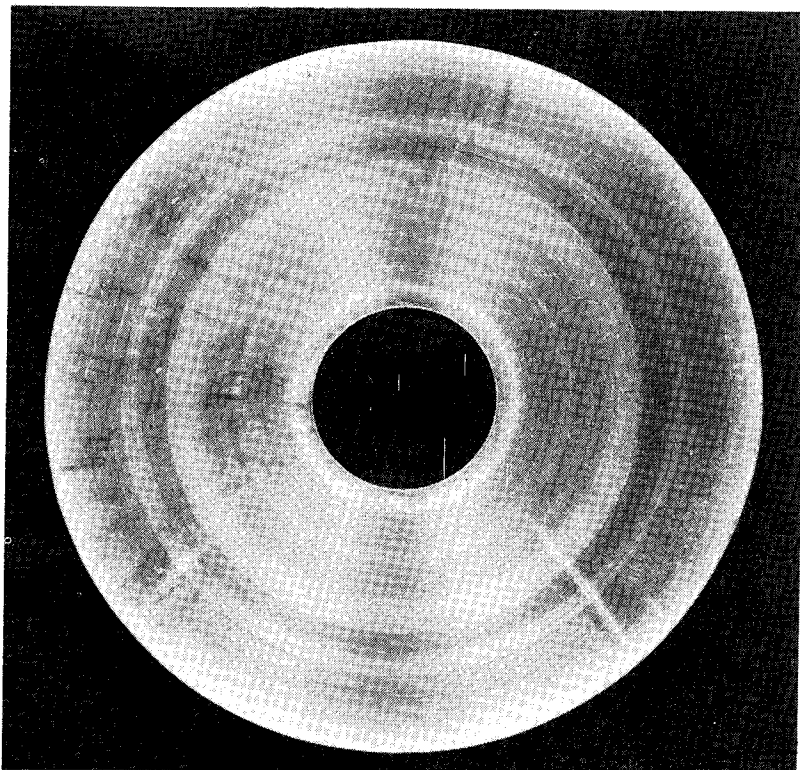
FIGURE 2

COMPARISON OF THE STRESS DISTRIBUTION IN A FLAT DISC AND CONCENTRIC RING FLYWHEELS

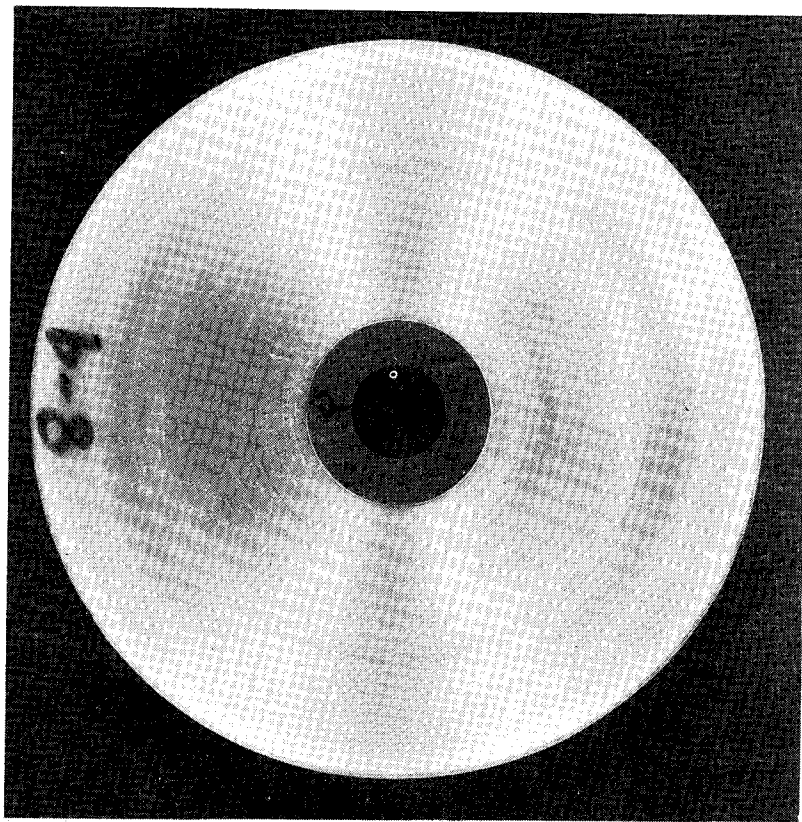
COMPOSITE HOOP MODULUS (E_θ) = 12.8×10^6 psi, $\omega = 40,000$ RPM

COMPOSITE RADIAL MODULUS (E_R) = 1.0×10^6 psi



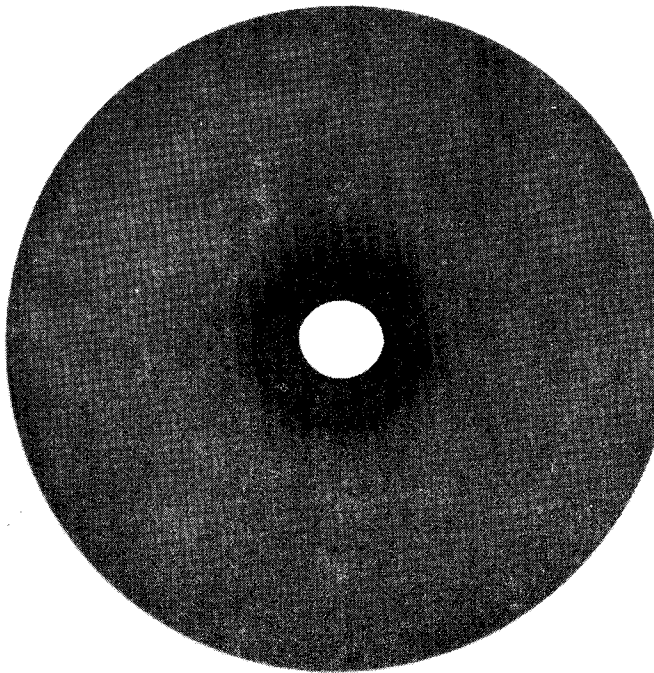


HOOP WOUND GLASS/EPOXY DISCS
CONSTANT WINDING TENSION

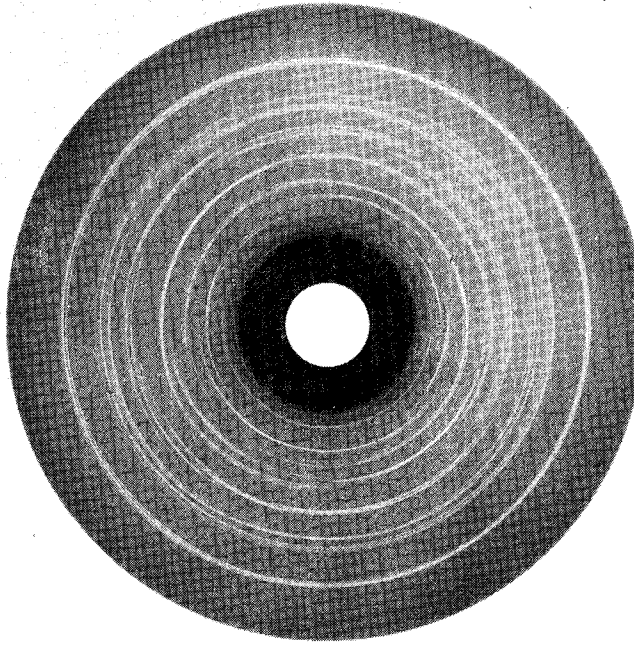


HOOP WOUND GLASS/EPOXY DISCS
PROGRAMMED WINDING TENSION

FIGURE 3. EFFECT OF WINDING TENSION ON FIBER BUCKLING
DUE TO COMPRESSIVE RESIDUAL HOOP STRESS



FLAT HOOP WOUND KEVLAR/EPOXY DISC
XRAY TAKEN AT ROOM TEMPERATURE
CURE TEMPERATURE: 130° F



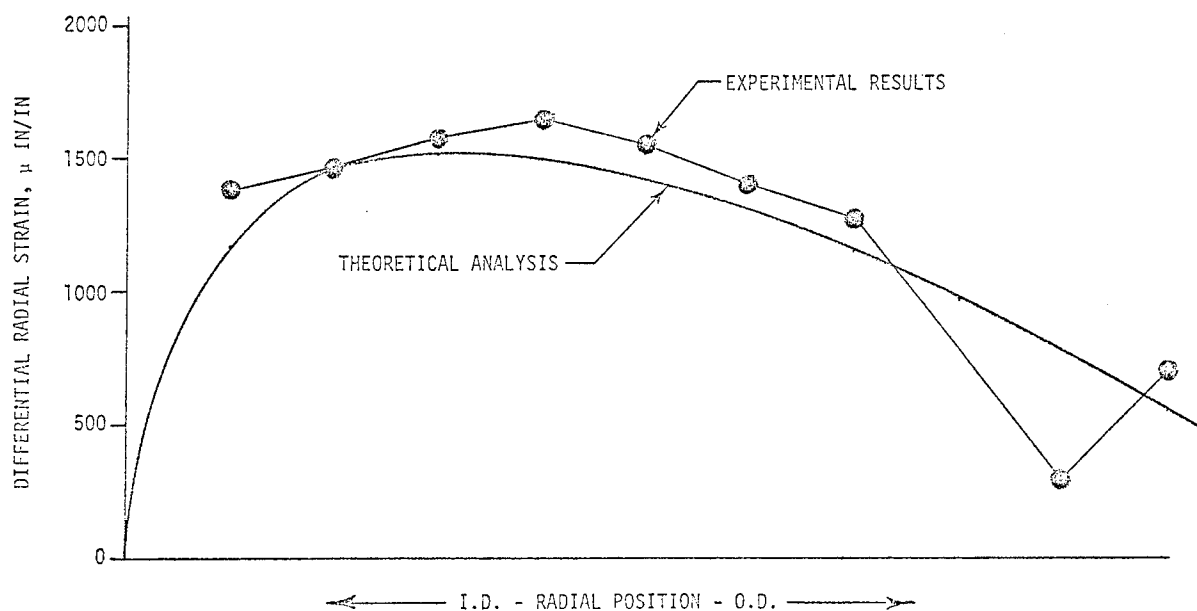
FLAT HOOP WOUND KEVLAR/EPOXY DISC
XRAY TAKEN AT ROOM TEMPERATURE
CURE TEMPERATURE: 300° F

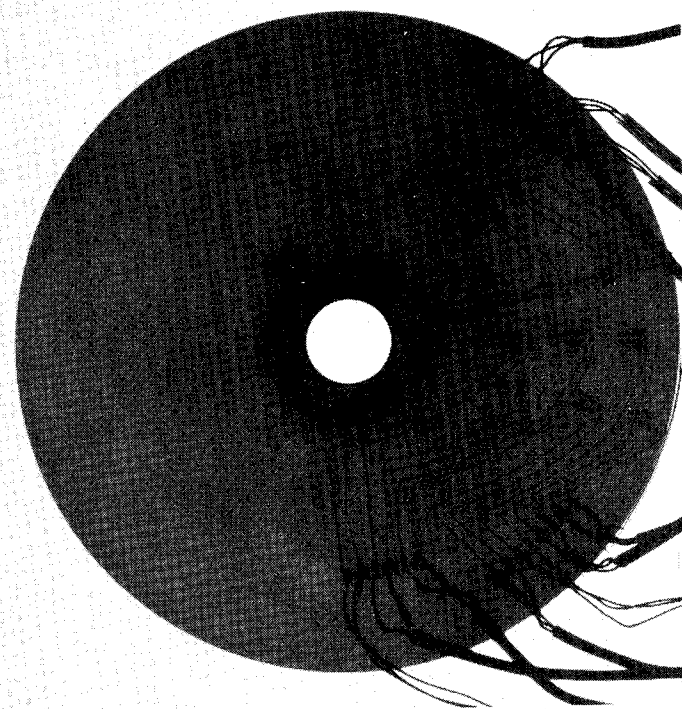
FIGURE 4. EFFECT OF CURE TEMPERATURE ON
RESIDUAL RADIAL STRESS

FIGURE 5. DIFFERENTIAL THERMAL STRAIN ($\Delta\epsilon_T$) VS
POSITION FOR A KEVLAR/EPOXY FLAT DISC
O.D. = 7.96 INCHES, I.D. = 2.0 INCHES

$$\Delta\epsilon_T = \epsilon_g - \alpha_R \Delta T$$

ϵ_g = ACTUAL STRAIN
 α_R = RADIAL COEFFICIENT OF THERMAL EXPANSION
 ΔT = -50°F

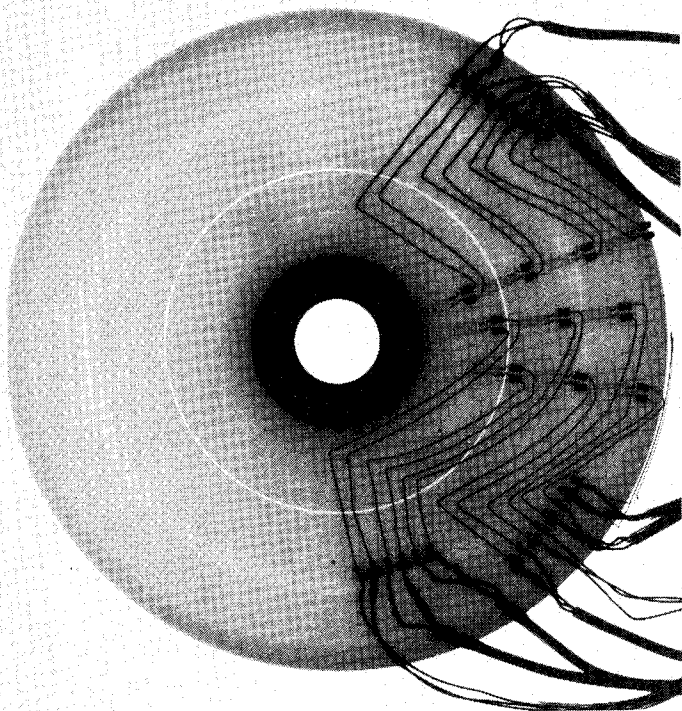




FLAT HOOP WOUND KEVLAR/EPOXY DISC

XRAY TAKEN AT 50° F

CURE TEMPERATURE: 130° F

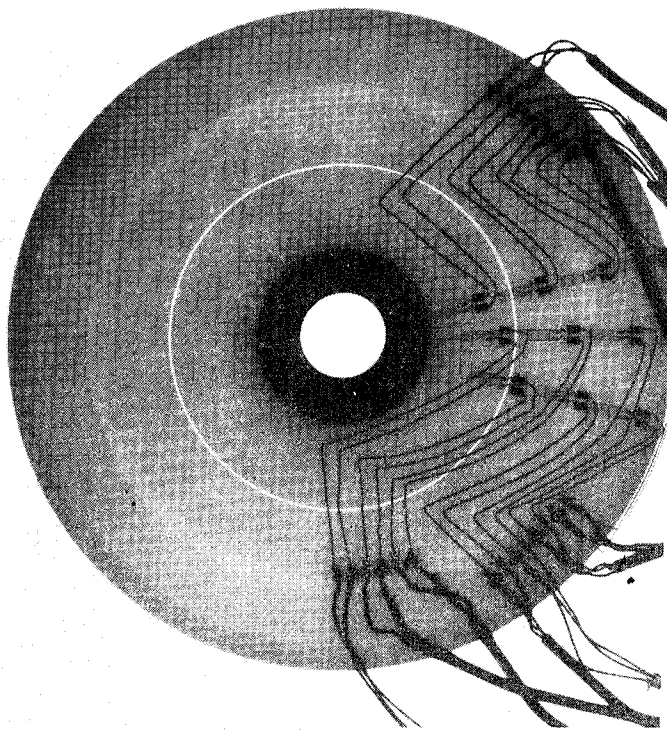


FLAT HOOP WOUND KEVLAR/EPOXY DISC

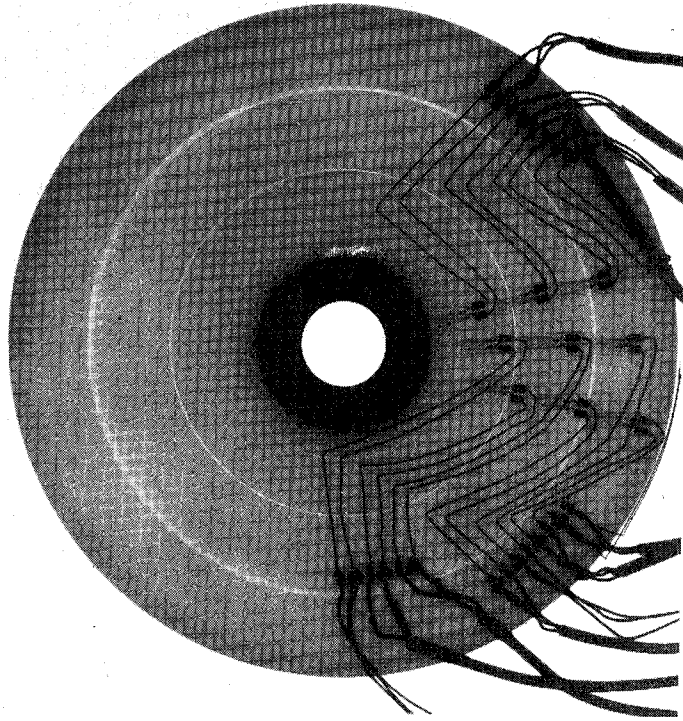
XRAY TAKEN AT 25° F

CURE TEMPERATURE: 130° F

FIGURE 6. EFFECT OF COOLING ON RESIDUAL RADIAL STRESS



FLAT HOOP WOUND KEVLAR/EPOXY DISCS
XRAY TAKEN AT 0° F
CURE TEMPERATURE: 130° F



FLAT HOOP WOUND KEVLAR/EPOXY DISCS
XRAY TAKEN AT -25° F
CURE TEMPERATURE: 130° F

FIGURE 7. EFFECT OF COOLING ON RESIDUAL RADIAL STRESS

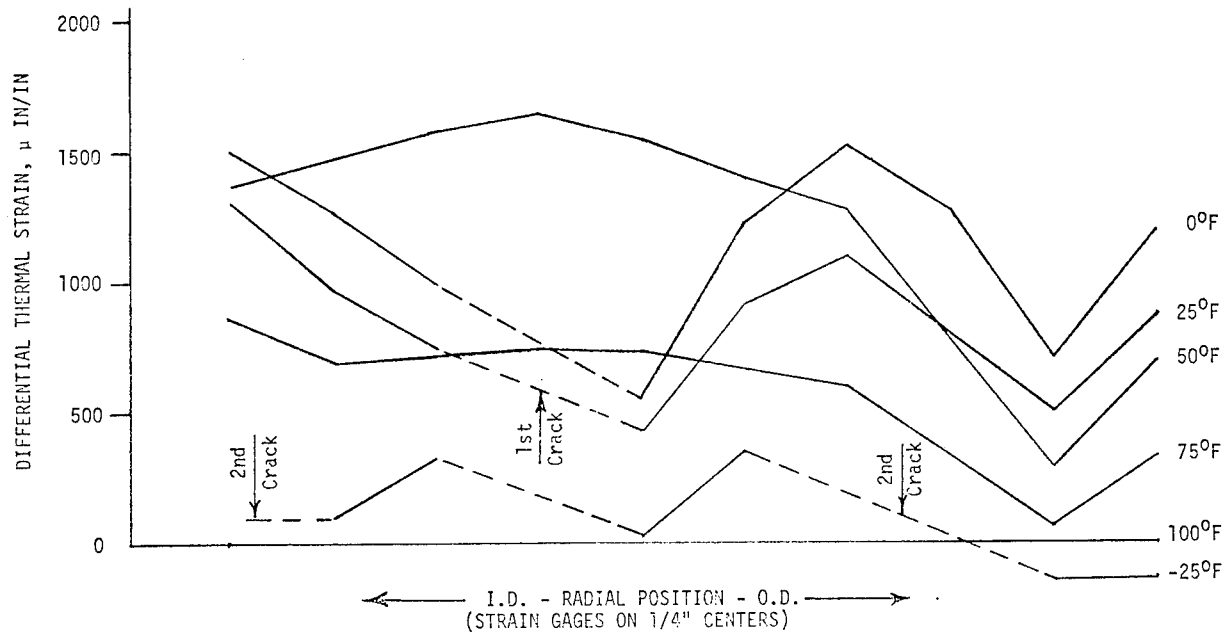
FIGURE 8. DIFFERENTIAL THERMAL STRAIN ($\Delta\epsilon_T$) IN A
CIRCUMFERENTIALLY WOUND KEVLAR/EPOXY DISC

O.D. = 8 INCHES, I.D. = 2 INCHES

$$\Delta\epsilon_T = \epsilon_g - \alpha_R \Delta T$$

ϵ_g = STRAIN GAGE MEASUREMENT

α_R = RADIAL COEFFICIENT OF THERMAL EXPANSION



PANEL DISCUSSION

At the end of the Flywheel Technology Symposium, there was a one-hour panel discussion to summarize the preceding two days' activities, to exchange ideas on what should be done next, and to clarify any points of confusion. The following is a brief summary of these discussions.

To start the discussion off, the question was asked, "What research should be started first?" One answer was that we needed to get hardware on the road and do more research in the area of design and manufacturing of hardware. It was pointed out that DOT has hardware in service now in the form of the R-32 cars in the NY subways and these cars are demonstrating efficiencies and energy conservation. Also, DOT has a new RFP out for another large system. This moved the discussion into the area of funding for small companies vs large companies. The need for funding of small companies was mentioned by several individuals.

In answer to a question on total U. S. funding for flywheel research, estimates were made ranging from \$1 - 6.5 million this year. About 90% of this money comes directly or indirectly from U. S. government funds.

Considerable discussion centered around questions of when the next flywheel symposium should be held, what its structure should be, who should sponsor it, and what types of papers should be presented. Some of the suggestions were: hold the next meeting within one year, have a hardware exhibition, have workshops to discuss different areas of flywheel development. People would like to see papers presented in areas of (1) impact of flywheel systems on fuel consumption, (2) what flywheels can do for our economy, (3) more systems designs and analysis, (4) bearing systems, including magnetic systems, constant frequency generators, infinitely variable speed transmissions, etc. Also, the suggestion was made to form a flywheel association.

One important question discussed was: when will flywheel transportation systems be available; in two or ten years? The point was made that low energy density systems (5 watt-h/lb) are possible now; they can be on the road within the next two years. However, higher energy density

systems, especially those containing fiber composite flywheels, require more research and may require up to ten years for development. One company already has four flywheel-containing cars on the road.

The comment was made there had not been a good case presented at the flywheel meeting for flywheel systems in competition with other energy storage systems, i.e., batteries, etc. Someone mentioned that the Rockwell Study does contain this information; it should be available early in 1976 (January). This study answers questions about the technical and economic feasibility of flywheels for transportation, utilities, and other applications. It shows that flywheel technology is not yet truly competitive with the internal combustion engine as a primary propulsion system. The San Francisco Muni Railway is planning to convert several hundred of their buses to flywheels for short-term energy storage (0-3 miles operation).

Copies of ERDA reports (Rockwell Study) can be obtained from ERDA Technical Information Center, Oak Ridge, TN 37830.

The suggestion was made that a competition be held among colleges for the best flywheel car. By offering a prize of from \$10-50,000, a large amount of work will be done per dollar spent, and also a large amount of publicity will be generated.

Two extensive areas were discussed in which knowledge is thin about composite materials in flywheel applications. These areas are: (1) dynamic fatigue of composites under stress in flywheel environments, particularly in cold and vacuum; and (2) the safety factor needed for composites in flywheel applications or reliability of various composite materials in flywheel designs.

LIST OF ATTENDEES AND SPEAKERS

K. Aaland
Lawrence Livermore Laboratory
P. O. Box 808
Livermore, CA 94550

W. D. Allan
Narmco Materials, Inc.
600 Victoria Street
Costa Mesa, CA 92627

R. E. Allred
Sandia Laboratories
Division 5844
Kirtland AFB East
Albuquerque, NM 87115

G. B. Andeen
Stanford Research Institute
Menlo Park, CA 94025

M. Audette
DOT/Canada/TDA
1000 Sherbrooke W.
CP549
Montreal Quebec H3A2R3

D. W. Bareis
Agbabian Associates
250 N. Nash Street
El Segundo, CA 90245

W. R. Benn
Great Lakes Carbon Corporation
299 Park Avenue
New York, NY 10017

N. Bennett
Sperry Flight Systems
21111 N. 19th Avenue
Phoenix, AZ 85036

M. J. Bergen
Pacific Missile Test Center
Pt. Mugu, CA 93042

J. F. Biehl
Brunswick Corporation
1620 S. Lewis Street
Anaheim, CA 92803

J. G. Bitterly
U.S. Flywheels, Inc.
P. O. Box 306
San Juan Capistrano, CA 92675

Alexander Blake
Lawrence Livermore Laboratory
P. O. Box 808
Livermore, CA 94550

W. M. Brobeck
Wm. M. Brobeck & Assoc.
1011 Gilman Street
Berkeley, CA 94710

E. A. Brock
Fiberglass Design Research
2555 Pacheco Boulevard
Martinez, CA 94553

G. R. Brown
Hexcel
11711 Dublin Boulevard
Dublin, CA 94566

E. J. Brunelle
Rensselaer Polytechnic Institute
Department of Mechanics
Room 304, Troy Building
Troy, NY 12181

A. F. Burke
Aerospace Corporation
2350 E. El Segundo Boulevard
Los Angeles, CA 90009

Christine M. Calhoun
Dow Chemical U.S.A.
Texas Division
Building B-1603
Freeport, TX 77541

J. F. Campbell
DOT, Room 6104F
2100 Second Street, S.W.
Washington, D.C. 20590

C. C. Chamis
NASA-Lewis Research Center
21000 Brookpark Road
Cleveland, OH 44135

G. Chang
U.S.E.R.D.A.
20 Massachusetts Avenue, N.W.
Washington, D.C. 20545

J. Chi
National Bureau of Standards
Gaithersburg, MD 20234

C. C. Chiao
Lawrence Livermore Laboratory
P. O. Box 808
Livermore, CA 94550

T. T. Chiao
Lawrence Livermore Laboratory
P. O. Box 808
Livermore, CA 94550

R. Christensen
Washington University
Department of M.E.
Lindell and Skinker Boulevards
St. Louis, MO 63130

Linda Clements
Lawrence Livermore Laboratory
P. O. Box 808
Livermore, CA 94550

A. A. G. Cooper
Babcock & Wilcox
P. O. Box 419
Alliance, OH 44601

T. D. Cooper
U.S.A. MERDC
Ft. Belvoir, VA

J. D. Cyrus
Division 5715
Sandia Laboratories
Albuquerque, NM 87115

T. Dannevig
Boeing Company
5112 - 14th Place, S.E.
Bellevue, Washington

D. E. Davis
Rockwell International
Rocketdyne Division
6633 Canoga Avenue
Canoga Park, CA 91304

W. E. Dick
Brunswick Corporation
4300 Industrial Avenue
Lincoln, NB 68504

F. W. Flowers, Jr.
General Engines Company, Inc.
Route 130
Thorofare, NJ 08086

F. W. Flowers, Sr.
General Engines Company, Inc.
Route 130
Thorofare, NJ 08086

P. B. Ford
Terracraft International
3190 Airport Loop Drive
Building D
Costa Mesa, CA 92626

Mrs. P. B. Ford
Terracraft International
3190 Airport Loop Drive
Building D
Costa Mesa, CA 92626

E. L. Foster
Institute for Defense Analyses
400 Army-Navy Drive
Arlington, VA 22202

A. Frank
University of Wisconsin
Department of Elect. & Computer
Engineering
909 Engineering Research Building
Madison, Wisconsin 53706

J. A. Friedericy
Garrett AiResearch
2525 W. 190th Street
Torrance, CA 90509

B. L. Friedman
Office of Naval Research (Code 221)
800 Quincy Street
Arlington, VA 22217

A. M. Garber
General Electric
P. O. Box 8555
Philadelphia, PA 19101

F. Gerstle, Jr.
Composite Materials Development
Division 5844
Sandia Laboratories
Albuquerque, NM 87115

J. Glaser
Garrett Corporation
2525 W. 190th Street
Torrance, CA 90509

H. S. Gordon
Wm. M. Brobeck & Assoc.
1011 Gilman Street
Berkeley, CA 94710

M. Hamstad
Lawrence Livermore Laboratory
P. O. Box 808
Livermore, CA 94550

J. E. Harrison
Sperry Flight Systems
21111 N. 19th Avenue
Phoenix, AZ 85036

B. D. Hatch
General Electric
Corporate Research & Development
Building 37, Room 380
P. O. Box 43
Schenectady, NY 12301

C. W. Helsley, Jr.
Rockwell International LAAD
Los Angeles International Airport
Los Angeles, CA 90009

J. Henderson
Henderson Engineering Company, Inc.
701 Factory Road
Addison, Illinois 60101

P. W. Hill
Hercules Incorporated
P. O. Box 210
Cumberland, MD 21502

W. B. Hillig
General Electric
Research & Development Center
P. O. Box 8
Schenectady, NY 12301

O. Hoffman
Lockheed Missiles & Space
Lockheed Palo Alto Research Laboratory
Org. 52-33, Building 205
3251 Hanover Street
Palo Alto, CA 94304

W. E. Hull
U.S. Postal Service
11711 Parklawn Drive
Rockville, MD 20852

P. Huntley
Orshansky Transmission Corporation
Santa Fe Street
San Diego, CA

J. S. Jones
Rockwell International
Space Division
Downey, CA

J. P. Joyce
NASA Lewis Research Center
21000 Brookpark Road
Cleveland, OH 44135

C. E. Knight, Jr.
Union Carbide Nuclear Division
P. O. Box Y, Building 9998
Oak Ridge, Tennessee

K. G. Konieczny
Dow Chemical
Drawer H
Walnut Creek, CA 94596

J. Koper
DOT/Federal Railroad Administration
Office of Research & Development
2100 - 2nd Street, S.W. /RRD-12
Washington, D. C. 20590

J. H. Laakso
Boeing Aerospace Company
Mail Stop 8C-43
P. O. Box 3999
Seattle, Washington 98124

G. Larson
DOT Transportation Systems Center
Kendall Square
Cambridge, Massachusetts

A. T. Kaskaris
AVCO Corporation
Systems Division
Lowell Industrial Park
Lowell, Massachusetts 01851

L. J. Lawson
AiResearch Manufacturing Company
2525 W. 190th Street
Torrance, CA 90509

J. Lemmens
Lemmens Enterprises
248 Mayrand Street
St. Jean, P. Quebec
Canada

E. M. Lenoe
AMMRC
Watertown, Massachusetts 02172

A. F. Lewis
Lord Corporation
2000 West Grandview
Erie, PA 16509

R. W. Lewis
Union Carbide Corporation
270 Park Avenue
New York, NY

A. Levy
Grumman Aerospace Corporation
Bethpage, NY 11714

W. G. Lionetta, Jr.
Army Materials & Mechanics Research
Center
Composites Division
Arsenal Street
Watertown, MA 02172

W. V. Loscutoff
Battelle Pac. N.W.
Richland, Washington 99352

S. N. Loud
Owens Corning Fiberglas
Fiberglas Tower - 7
Toledo, OH 43659

E. L. Lustenader
General Electric
P. O. Box 43
Building 37, Room 311
Schenectady, NY 12301

F. E. Mack
Rockwell International
Seal Beach, CA

W. P. Manger
RCA Astro-Electronics
P. O. Box 800
Princeton, NJ 08540

H. K. Marshall
Kinergy Research & Development
Division of Marshall Oil
P. O. Box 1128
820 South Main Street
Wake Forest, NC 27587

J. L. Mason
Garrett Corporation
9851 Sepulveda Boulevard
Los Angeles, CA 90009

M. W. Matsler
School of Oceanography
Oregon State University
Corvallis, OR 97331

R. A. McCoy
U.S. Naval Academy
Annapolis, MD 21402

R. Medick
Ferro Corporation
3512-3520 Helms Avenue
Culver City, CA

E. Mones
Lawrence Livermore Laboratory
P. O. Box 808
Livermore, CA 94550

Richard Moore
Lawrence Livermore Laboratory
P. O. Box 808
Livermore, CA 94550

R. J. Moulton
Hexcel Corporation
11711 Dublin Boulevard
Dublin, CA 94566

K. H. Muller
AFWAL
Wright Patterson AFB
Dayton, Ohio 45431

D. M. C. Narasimhan
Strength Physics Department
Materials Research Center
P. O. Box 1021R
Allied Chemical
Morristown, NJ 07960

P. M. Newgaard
Stanford Research Institute
Menlo Park, CA 94025

R. B. Northup
Owens Corning Fiberglas Corporation
5933 Telegraph Road
Los Angeles, CA 90040

T. A. Norman
U.S. Postal Service
11711 Parklawn Drive
Rockville, MD 20852

J. E. Notti
Rockwell International
Downey, CA 90241

L. L. Omohundro
Kinergy Research & Development
Division of Marshall Oil
P. O. Box 1128
820 South Main Street
Wake Forest, NC 27587

R. L. Page
Kelsey-Hayes Company
2054 Della Lane
Anaheim, CA 92802

C. Pax
U.S.E.R.D.A.
20 Massachusetts Avenue
Washington, D.C. 20545

L. Penn
Lawrence Livermore Laboratory
P. O. Box 808
Livermore, CA 94550

J. W. Pepper
EPRI
P. O. Box 10412
Palo Alto, CA 94303

D. W. Rabenhorst
Applied Physics Laboratory
Johns Hopkins University
Johns Hopkins Road
Laurel, MD 20810

A. E. Raynard
Garrett AiResearch
2525 W. 190th Street
Torrance, CA 90509

M. M. Reddi
Franklin Institute
20th & Race Streets
Philadelphia, PA 19103

T. J. Reinhart, Jr.
AFMC/ABC
Wright Patterson AFB
Ohio 45419

R. C. Reuter, Jr.
Sandia Laboratories
Advanced Energy Projects
Division 5715
P. O. Box 5800
Albuquerque, NM 87115

J. Rexer
Battelle Geneva
Ch 1227 Carouge
Geneva, Switzerland

J. Rinde
Lawrence Livermore Laboratory
P. O. Box 808
Livermore, CA 94550

H. F. Rizzo
Lawrence Livermore Laboratory
P. O. Box 808
Livermore, CA 94550

A. Rolston
Owens Corning

E. Rottmayer
Goodyear Aerospace Corporation
1210 Massillon Road
Akron, OH 44315

A. D. Sapowith
AVCO
Lowell Industrial Park
Lowell, Massachusetts 01851

R. Sarson
Brunswick Corporation
2000 Brunswick Lane
DeLand, FLA 32720

E. W. Schlieben
RCA
Box 800
Princeton, NJ 08540

J. N. Schurb
3M Company
3M Center, Building 230-1F
St. Paul, Minnesota 55101

D. M. Schuster
Sandia Laboratories
Albuquerque, NM 87115

R. D. Scott
RCA
Box 887
Camden, NJ 08101

D. W. Sheddon
Union Carbide Corporation
270 Park Avenue, 25th Floor
New York, NY 10017

R. J. Sherry
Lawrence Livermore Laboratory
P. O. Box 808
Livermore, CA 94550

J. A. Sivak
Carnegie-Mellon University
5125 Margaret Morrison Street
Pittsburgh, PA 15213

T. R. Small
Applied Physics Laboratory
Johns Hopkins University
Johns Hopkins Road
Laurel, MD 20810

G. Smit
Borg Warner Corporation
Wolf & Algonquin Roads
Des Plaines, Illinois 60018

L. I. Smith
European Aerospace Corporation
1101 - 15th Street, N.W.
Washington, D. C. 20005

John B. Snell
3M Company
Building 230-1, 3M Center
St. Paul, Minnesota 55101

G. Souva
Garrett Corporation
9851 Sepulveda Boulevard
Los Angeles, CA 90009

R. R. Spencer
Kelley Hayes Company
1205 W. Columbia
Springfield, Ohio

R. G. Stone
Lawrence Livermore Laboratory
P. O. Box 808
Livermore, CA 94550

P. Straus
San Francisco Muni Railway
949 Presidio Avenue
San Francisco, CA 94114

K. Street
Lawrence Livermore Laboratory
P. O. Box 808
Livermore, CA 94550

D. L. G. Sturgeon
E. I. du Pont de Nemours and Company
Textile Fibers Department
Building 262
Wilmington, DEL 19898

P. G. Sullivan
NETCO
110 Pine Avenue #906
Long Beach, CA 90802

B. E. Swartout
U.S. Flywheels, Inc.
P. O. Box 306
San Juan Capistrano, CA 92675

W. D. Timmons
Celanese Corporation
Box 1000
Summit, NJ 07901

R. Toland
Drexel University

K. Tolk
Energy Storage Group
University of Texas
Taylor Hall - M. E. Department
Austin, TX 78712

Rene Torossian
Aerospatiale
78 Lesmureaux
France

D. Ullman
Ohio State University
Department of Mechanical Engineering
206 West 18th
Columbus, OH 43210

M. Vagins
Battelle N.W. Laboratories
Battelle Boulevard
Richland, Washington 99352

A. F. Veneruso
Sandia Laboratories
Division 5715
P. O. Box 5800
Albuquerque, NM 87115

R. D. Vergara
Battelle Columbus Laboratories
505 King Avenue
Columbus, OH 43201

F. Von Musser
U.S. Flywheels, Inc.
P. O. Box 306
San Juan Capistrano, CA 92675

G. Vroman
Rockwell International
Rocketdyne
Canoga Park, CA 91304

A. Vroman
Sperry Flight Systems
21111 North 19th
Phoenix, AZ 85036

L. H. Wald
Lockheed
679 Tiffany Court
Sunnyvale, CA 94087

A. E. Wetherbee, Jr.
Power Systems Division
United Technologies Corporation
1690 New Britain Avenue
Farmington, Connecticut 06032

D. Wildermuth
Lear Motors Corporation
P. O. Box 60000
Reno, NV 89506

E. Wu
University of Washington
1420 Silver Leaf Lane
St. Louis, MO 63141

F. C. Younger
Wm. M. Brobeck & Assoc.
1011 Gilman Street
Berkeley, CA 94710

C. G. Zlomke
Brunswick Corporation
4300 Industrial Avenue
Lincoln, NB 68504

J. E. Zweig
Benet Weapons Laboratory
Watervliet Arsenal
Watervliet, NY 12189

F. A. Zylus
Rockwell International
Space Division
12214 Lakewood Boulevard
Downey, CA 90241

R. Kiang
Stanford Research Institute
Menlo Park, CA 94025

G. Pezdirtz
U.S.E.R.D.A., Washington, D.C. 20545